

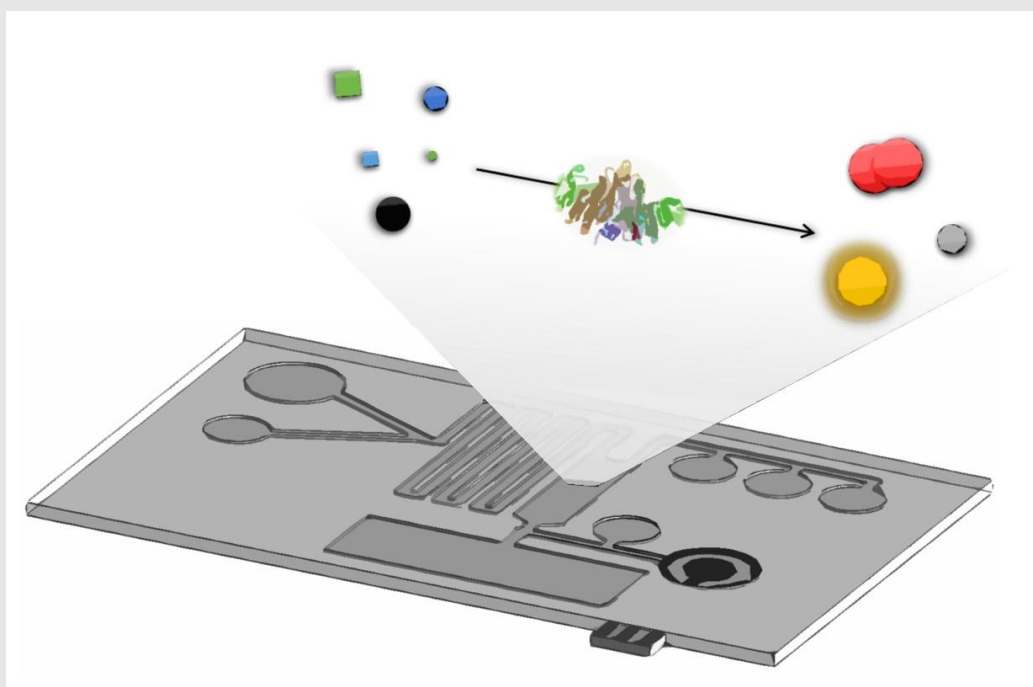
eman ta zabal zazu



Universidad  
del País Vasco

Euskal Herriko  
Unibertsitatea

# ENZYMATIC MODULATION OF NANOMATERIALS AND ITS APPLICATION TO BIOSENSING



**Beatriz Díez Buitrago**

Donostia – San Sebastián, 2020



# ENZYMATIC MODULATION OF NANOMATERIALS AND ITS APPLICATION TO BIOSENSING

To obtain the degree of PhD in  
Applied Chemistry and Polymeric Materials  
at the University of the Basque Country  
(UPV/EHU)

**Beatriz Díez Buitrago**

Donostia – San Sebastián, 2020



**Thesis Supervisors:**

**Dra. Nerea Briz**

Biomaterials Group, Tecnalia, Basque Research and Technology Alliance (BRTA)  
Donostia-San Sebastián (Spain)

**Dr. Valery Pavlov**

Biosensing Lab., CIC biomaGUNE, Donostia-San Sebastián (Spain)

**University tutor:**

**Prof. Dr. Antxon Santamaría**

Department of Polymer Science and Technology , Faculty of Chemistry, University of  
the Basque Country (UPV/EHU), Donostia-San Sebastián (Spain)



# Table of contents

<b>Abstract</b> .....	1
<b>Resumen</b> .....	3
<b>Chapter 1: General introduction</b> .....	11
<b>Chapter 2: Motivation and objectives</b> .....	51
<b>Chapter 3: Enzymatic growth of nanoparticles and applications</b>	
• Specific bioanalytical optical and photoelectrochemical assays for detection of methanol in alcoholic beverages .....	59
• Facile synthesis and characterization of Ag/Ag <sub>2</sub> S nanoparticles enzymatically grown in situ and their application to the colorimetric detection of glucose oxidase .....	85
• Development of portable CdS screen printed carbon electrode platform for electrochemiluminescence measurements and bioanalytical applications .....	111
<b>Chapter 4: Design and development of a Lab-on-a-Chip</b>	
• Modification of chlorosulfonated polystyrene substrates for bioanalytical applications .....	137
• Design of a photoelectrochemical lab-on-a-chip immunosensor based on enzymatic production of quantum dots in situ .....	156
<b>Chapter 5: General conclusions</b> .....	175
<b>Publications</b> .....	181
<b>CV</b> .....	185
<b>Acknowledgements</b> .....	189





## Abstract

The growing demand for in situ detection and monitoring of (bio)chemical compounds has led to a great increase in research and development of portable, sensitive and reliable devices to satisfy current and new necessities of analysis. Biosensors emerged as versatile and convenient tools with excellent features and broad variety of possible applications. Within the medical sector, biosensors are mainly used in clinical and diagnostics, with major interest in point-of-care testing. Particularly, methodologies based on immunoassays provide high sensitivity and selectivity towards most biomarkers with medical relevance. However, the miniaturization and integration in portable platforms is still a challenging task. This problematic inspired us to design and develop an electrochemical immunosensing platform with improved characteristics owing to the signal amplification methods and immobilization techniques. Enzymatic amplification has provided outstanding improvements in signal detection and amplification when combined with the modulation of nanomaterials' properties. This strategy was applied to the detection of analytes with analytical interest by the in situ enzymatic growth or blocking of metal nanostructures such as Ag/Ag<sub>2</sub>S and CdS nanoparticles and/or quantum dots by products of enzymatic reactions. The biocatalytical activity was measured by optical and electrochemical readout techniques, the latter showed better performance and suitability for integration in lab-on-a-chip platforms. Parallely, we investigated the improvement of immobilization techniques on polystyrene surfaces. Chlorosulfonation process enabled the activation of the surface and subsequent introduction of several functional groups such as amines or acids. This methodology allowed for the fabrication of a broad library of functionalities available for antibody immobilization through covalent links or physical adsorption. Finally, the combination of enzymatic detection and signal amplification with improved orientation of antibodies resulted in the development of a photoelectrochemical immunosensor lab-on-a-chip with potential analytical applications.



## Resumen

La sociedad actual se encuentra muy influenciada por los continuos avances tecnológicos en prácticamente todos los ámbitos de la vida cotidiana. La rapidez con la que se producen estos cambios hace indispensable la labor de investigación y desarrollo de nuevos dispositivos que cubran las necesidades emergentes. En concreto, una de las principales demandas en la mayoría de los sectores es la de herramientas de detección y/o cuantificación de sustancias (bio)químicas empleadas en un amplio abanico de aplicaciones. Para satisfacer estas necesidades, uno de los instrumentos más potentes y eficaces son los biosensores, dispositivos capaces de solucionar los problemas existentes y de adaptarse a las exigencias futuras.

Los biosensores son instrumentos analíticos integrados por un elemento de biorreconocimiento y un transductor, que transforma los procesos biológicos en señales cuantificables y proporcionales a la concentración del analito a detectar. Desde los primeros diseños fabricados a mediados del siglo XX para la detección de oxígeno y la comercialización del primer biosensor de glucosa en años posteriores, la investigación y desarrollo en esta área ha crecido exponencialmente hasta nuestros días. En los últimos años, sus aplicaciones se han multiplicado en todas las áreas de interés analítico como en el sector salud, la industria agroalimentaria, el sector medioambiental, la seguridad y la defensa. Su éxito se basa en los progresos obtenidos en los campos de la biotecnología, nanociencia y microfabricación, que posibilitan el diseño y la producción de aparatos portátiles, de lectura rápida, sensibles y de fácil manejo.

En la actualidad, las aplicaciones biomédicas lideran el mercado de los biosensores, sobre todo para su empleo en la detección y monitorización de analitos de interés como la glucosa, marcadores de cáncer, medicamentos y otros metabolitos. Esta tendencia se justifica por la creciente demanda de dispositivos rápidos, robustos y de alta precisión y sensibilidad para su uso en diagnóstico y seguimiento rutinario de enfermedades, fundamentalmente. Dentro de la amplia gama de los diferentes instrumentos, el mayor porcentaje de dispositivos comercializados está representado por biosensores para aplicaciones en puntos de cuidado o lugares de atención al paciente (*point-of-care*, POC). Estos dispositivos son portables, automáticos, permiten la descentralización de las medidas a tiempo real y son fácilmente manejables por personal no cualificado. Para cumplir con estas características generalmente se requiere de la tecnología Lab-on-a-Chip (LOC), que integra los conocimientos de las ramas de

## Resumen

la química, física, biología e ingeniería para llevar la investigación técnica y básica a aplicaciones reales.

Una plataforma LOC incorpora una o varias tareas de laboratorio en un único dispositivo de pequeño tamaño, normalmente de milímetros a centímetros cuadrados. Estos sistemas miniaturizados permiten la reducción de los volúmenes de muestreo y reactivos requeridos, minimizan la manipulación de materiales peligrosos, permiten la detección de múltiples analitos y mejoran la detección. Estas propiedades se ven incrementadas cuando se combina con tecnologías como la nanotecnología y la microfluídica. La integración de nanomateriales en sistemas LOC aporta una ventaja adicional en cuanto a sensibilidad y miniaturización, además de la versatilidad en cuanto a diseño y aplicaciones. Por otro lado, la microfluídica permite abordar problemáticas tales como el transporte y la mezcla de muestra y de reactivos en sistemas miniaturizados. Todo esto hace del LOC el candidato más adecuado para aplicaciones POC.

Como biosensor, estos dispositivos responden a la concentración de un analito de interés en la muestra analizada. En el caso del diagnóstico médico, este analito generalmente se llama biomarcador, y está relacionado con el estado médico del paciente. De entre los biomarcadores de interés, los más utilizados son las proteínas porque son las que normalmente están asociadas a las enfermedades más recurrentes. Hoy en día, la metodología más extendida para la detección de proteínas es el inmunoensayo. El uso de anticuerpos aporta ventajas adicionales como es la alta selectividad con el antígeno (la proteína) y la amplia variedad de anticuerpos disponibles. Actualmente, los inmunoensayos para POC con más presencia en el mercado están basados en ensayos de flujo lateral. Esta tecnología es rápida, barata y de lectura óptica, pero solo es eficaz cuando el analito se encuentra en grandes cantidades. Por otro lado, en laboratorios de rutina, la técnica más empleada para la detección de una gran cantidad de biomarcadores es el ensayo por inmunoabsorción ligado a enzimas (ELISA). A pesar de la alta sensibilidad de esta metodología, aún es minoritario el número de productos en el mercado que integren estos ensayos en sistemas portables debido al elevado número de etapas de su protocolo y a la detección óptica, que implica sistemas de lectura poco portables y más caros que, por ejemplo, los electroquímicos.

Adicionalmente, existen varias estrategias para mejorar la detección y la sensibilidad de los procesos ELISA adaptados a sistemas miniaturizados: por un lado, el incremento del número de anticuerpos disponibles para el biorreconocimiento (técnicas de inmovilización) y, por otro lado, amplificación de la señal generada. Esta última metodología permite aumentar la señal producida como consecuencia del proceso bioquímico mediante la incorporación de

compuestos o estructuras adicionales. En el caso de los inmunoensayos, la técnica más empleada es el uso de anticuerpos marcados con enzimas. Estas son elementos ampliamente utilizados en bioanálisis ya que presentan una gran especificidad y una alta actividad enzimática lo que implica una amplificación de la señal. Además, recientemente se ha comprobado que los enzimas son capaces de modular el tamaño de ciertos nanomateriales mediante su actividad, lo que aumenta la variabilidad en la detección (fluorescencia, fotoelectroquímica) respetando la amplificación mediante cascada enzimática, que es fundamental para mantener límites de detección bajos en los inmunoensayos.

Para abordar estas cuestiones, la presente tesis se centra en el estudio de la modulación enzimática de nanopartículas para su aplicación como estrategia de amplificación de señal en biosensores y su adaptación e integración en una plataforma LOC para el desarrollo de un inmunosensor electroquímico. Para el diseño de este último se plantearon dos puntos clave a considerar: el incremento de la sensibilidad del inmunoensayo mediante estrategias de inmovilización y amplificación de la señal; y la miniaturización y adaptación a un sistema microfluídico. De esta forma, la tesis está estructurada en un primer capítulo de introducción a los biosensores haciendo hincapié en los inmunosensores electroquímicos para aplicaciones POC e integración en sistemas LOC (capítulo 1). A continuación, dentro de la parte experimental, en el primer bloque se han estudiado diferentes técnicas de amplificación de la señal mediante el uso de anticuerpos marcados con enzimas para la modulación enzimática de nanopartículas (capítulo 3). El segundo bloque se ha centrado en la mejora del proceso de inmovilización de anticuerpos y la miniaturización del proceso electroquímico para su integración en un LOC (capítulo 4).

Dentro del capítulo 3 se han llevado a cabo tres estrategias diferentes para la modulación enzimática de nanopartículas.

La primera parte titulada *“Specific bioanalytical optical and photoelectrochemical assays for detection of methanol in alcoholic beverages”* describe la síntesis enzimática de puntos cuánticos (quantum dots, QDs) y su aplicación en la detección de metanol en bebidas alcohólicas por espectroscopia de fluorescencia y por fotoelectroquímica (proceso en el cual algunos nanomateriales absorben un fotón de luz y tras su excitación y recombinación generan electrones que pueden ser detectados electroquímicamente). La síntesis de estos QDs de CdS se llevó a cabo en presencia de iones  $S^{2-}$  y  $Cd^{2+}$ , y cisteína, que actúa como estabilizante y favorece el efecto de confinamiento cuántico gracias a su grupo tiol que se une fácilmente a las nanopartículas semiconductoras. Sin embargo, la cisteína se oxida fácilmente a cistina en presencia de agentes oxidantes como el agua oxigenada ( $H_2O_2$ ), perdiendo sus propiedades de

## Resumen

agente estabilizante. Este proceso se utilizó para la modulación del crecimiento in situ de QDs de CdS gracias a la actividad enzimática de la alcohol oxidasa (AOx) que es capaz de generar  $H_2O_2$  a través de la oxidación de metanol. De esta forma, se pudo relacionar la cantidad de metanol en la muestra con la disminución en la cantidad de QDs de CdS. Además, se estudió la posible interferencia de etanol en el proceso y se comprobó que la enzima es selectiva solo para el metanol como sustrato. Para la detección de estos QDs se utilizaron dos técnicas: la espectroscopía de fluorescencia y la fotoelectroquímica. En ambos casos se optimizaron los parámetros de medida, se realizaron sendos calibrados y se determinaron los límites de detección en  $0.21 \text{ mg L}^{-1}$  y  $0.16 \text{ mg L}^{-1}$ . Se comprobó que los dos protocolos propuestos son más sensibles que otras técnicas como la cromatografía y amperometría, incluso en presencia de los dos alcoholes. Para la validación de estos dos métodos se analizaron muestras de bebidas alcohólicas reales (vodka y sidra) y en ambos casos se obtuvieron resultados satisfactorios y en concordancia con los valores estipulados en la legislación vigente.

La segunda parte se titula "*Facile synthesis and characterization of Ag/Ag<sub>2</sub>S nanoparticles enzymatically grown in situ and their application to the colorimetric detection of glucose oxidase*" y presenta la síntesis enzimática in situ de nanopartículas de plata y azufre (Ag/Ag<sub>2</sub>S NPs) para su detección por colorimetría. En este caso, la síntesis de estas NPs se produjo por la fuerte interacción entre los iones  $S^{2-}$  y  $Ag^+$  en presencia de ácido cítrico como estabilizante. Debido a la baja constante de solubilidad de este compuesto el proceso es muy selectivo e inmediato en medio acuoso. El control del crecimiento de estas estructuras se consiguió mediante la actividad enzimática de la glucosa oxidasa (GOx), que al oxidar la tioglucosa genera los iones  $S^{2-}$  necesarios para la formación de Ag/Ag<sub>2</sub>S NPs en presencia de plata. Estas presentan un color amarillo y se torna oscuro incluso marrón al aumentar la cantidad de las mismas en disolución. Mediante colorimetría se pudo seguir la actividad de la enzima y se pudieron determinar sus parámetros analíticos. Adicionalmente se validó este mecanismo a través de un ensayo competitivo del sustrato artificial y la glucosa natural. Aquí, la presencia de la glucosa disminuye la cantidad de  $S^{2-}$  y con ella la señal detectada. Este protocolo presentó un límite de detección de  $176.21 \mu\text{M}$  para la glucosa. Conociendo sus propiedades analíticas se aplicó a la detección de glucosa en suero humano por la metodología de adiciones estándar. El valor obtenido de glucosa en suero correspondió a los valores normales (entre 2.8 y 7 mM), por lo que de esta forma pudimos comprobar su eficacia en muestras reales.

La tercera y última parte de este bloque "*Development of portable CdS screen printed carbon electrode platform for electrochemiluminescence measurements and bioanalytical applications*" está enfocada al uso de productos enzimáticos para la modulación de la señal

electroquimioluminiscente (ECL) de las NPs de CdS. La ECL es una técnica donde la excitación de las NPs se realiza electroquímicamente y la detección de la señal generada, mediante técnicas ópticas. Gracias al empleo de diferentes fuentes de excitación y detección es muy sensible, ya que permite anular la señal de interferencia de fondo, además de presentar las ventajas inherentes de los sistemas electroquímicos. La fase sensora constó de un electrodo serigrafiado de carbono modificado con NPs de CdS generadas químicamente por interacción de iones  $S^{2-}$  y  $Cd^{2+}$  en tampón tris-HCl. Al prescindir de agente estabilizante la estructura generada es una red de núcleos de CdS de 3.89 nm de diámetro con propiedades fluorescentes y electroquimioluminiscentes. A fin de poder llevar a cabo el proceso ECL, es necesario el uso de un cofactor que sea capaz de reducir las NPs de CdS electroquímicamente excitadas para producir la señal ECL como, por ejemplo, el  $H_2O_2$ . Este compuesto se produce de manera natural en muchas reacciones bioquímicas, por lo que pudimos combinar esta metodología con la reacción enzimática de la alcohol oxidasa y el metanol. De esta manera, se estudiaron los parámetros analíticos (límite de detección  $61.46 \mu g L^{-1}$ ) y se validó el sistema para la detección de metanol en vodka. Se utilizó la técnica de adiciones estándar en la muestra y se comprobó que el nivel de metanol en vodka estaba dentro de los rangos normales. Por añadidura, se estudió otro sistema enzimático para comprobar la aplicabilidad de nuestro sistema: producción de  $H_2O_2$  por acción enzimática de la glucosa oxidasa. Se comprobó que solo en presencia de la enzima y el sustrato se obtenía señal ECL.

Otra estrategia para la modulación de la señal ECL es el uso de ciertos productos enzimáticos para el bloqueo de la superficie y la inhibición del proceso ECL. Los tioles presentan una gran afinidad por la superficie de las NPs de CdS y pueden ser generados enzimáticamente, por ejemplo, por la actividad enzimática de la acetilcolinesterasa con acetiltiocolina. De esta forma, al aumentar la concentración de sustrato aumenta la cantidad de tioles y disminuye la señal ECL de las NPs de CdS. Este proceso se validó con la detección de la enzima en suero humano con la metodología de adiciones estándar, pudiendo detectar un valor normal de la misma en la muestra real sin necesidad de realizar un pretratamiento. Por último, se estudió la posibilidad de detectar inhibidores de la enzima como el 1,5-bis-(4-allyldimethylammonium-phenyl)pentan-3-one dibromide (BW284c51). Este inhibidor bloquea la actividad enzimática de la acetilcolinesterasa y por lo tanto la producción de tioles, incrementando la señal ECL. Esta metodología presentó un límite de detección para este inhibidor de 79.22 nM, similar a otros métodos más convencionales (fibra óptica o fluorogénicos).

En este primer bloque pudimos demostrar la variabilidad y aplicabilidad de la modulación enzimática de nanopartículas como estrategia de amplificación de señal. Se estudiaron

## Resumen

diferentes técnicas de detección y se seleccionó la fotoelectroquímica como la más idónea para su integración en plataformas LOC. Por un lado, es una técnica muy sensible que permite trabajar sin interferencias de fondo debido a la diferente naturaleza de las fuentes de excitación y emisión, y por otro lado la detección es electroquímica, lo que permite una mayor facilidad de miniaturización e integración en sistemas portables a bajo coste.

El segundo bloque de la parte experimental (capítulo 4) está centrado en el diseño y desarrollo de un inmunosensor fotoelectroquímico integrando la parte de amplificación de señal enzimática estudiada en el capítulo 3.

La primera parte se titula "*Modification of chlorosulfonated polystyrene substrates for bioanalytical applications*" y aquí se estudiaron diferentes técnicas de inmovilización de anticuerpos en superficies de poliestireno. Este trabajo se realizó porque además de la mejora en la sensibilidad por técnicas de amplificación de señal, también es importante aportar estabilidad para favorecer el proceso de biorreconocimiento, por ejemplo, mediante la correcta inmovilización y orientación de los anticuerpos a los soportes utilizados. Normalmente los anticuerpos se inmovilizan por enlaces covalentes o por adsorción física asegurando por un lado la conservación la estructura del anticuerpo para evitar pérdidas de actividad y, por otro lado, la correcta orientación para permitir su interacción con el antígeno. En el método propuesto se modificaron sustratos de poliestireno con ácido clorosulfónico para la introducción de grupos reactivos fácilmente convertibles en otros grupos funcionales. De esta forma se puede obtener una amplia librería de sustratos con diferentes propiedades de hidrofobicidad y biocompatibilidad para cada anticuerpo. Se compararon las dos estrategias de inmovilización y su aplicabilidad frente a un kit comercial para albumina de suero humana (HSA). Se comprobó que el uso de poliestireno aminado para la adsorción física de anticuerpos proporcionaba una mejora en el límite de detección frente al kit comercial. Se validó así el protocolo propuesto de fabricación de sustratos de poliestireno funcionalizados para la correcta inmovilización de anticuerpos con potenciales aplicaciones en sistemas LOC.

La segunda parte "*Design of a photoelectrochemical lab-on-a-chip immunosensor*" integra los resultados obtenidos en el capítulo 1 (amplificación de la señal) y en la primera parte del capítulo 4 (inmovilización de anticuerpos) para el diseño y desarrollo de un inmunosensor fotoelectroquímico. De cara al diseño de dispositivos POC se requieren procesos rápidos, sencillos y ausencia de reactivos costosos y condiciones de reacción difíciles de conseguir en el punto de medida. Por ello, primero se estudió la miniaturización del inmunoensayo y su adecuación a las exigencias establecidas, es decir, la reducción de volúmenes, tiempos y etapas de reacción, así como la adaptación del proceso enzimático a condiciones ambientales.



A continuación, se validaron los electrodos seleccionados para su impresión en el sustrato del chip. Seguidamente, se diseñó la plataforma microfluídica integrando el poliestireno modificado y los electrodos serigrafiados. Finalmente, se validó el chip final comprobando su aplicabilidad para la detección de HSA fotoelectroquímicamente, obteniendo mejores resultados que el kit comercial en menor tiempo y de manera portable.

Como conclusión, durante los trabajos realizados a lo largo de esta tesis se ha podido comprobar las ventajas de aplicar la actividad enzimática para la modulación de nanopartículas como estrategia de amplificación de señal para su integración en el proceso de detección en biosensores. Además, se ha establecido la clorosulfonación de poliestireno como una metodología versátil y eficiente en la inmovilización de anticuerpos, mejorando el proceso de biorreconocimiento y así, la sensibilidad del sistema. Finalmente, se ha logrado integrar ambas estrategias en una plataforma sensora obteniendo un inmunosensor fotoelectroquímico con potenciales aplicaciones bioanalíticas. Aunque el trabajo de esta tesis concluye con la demostración y validación del chip, la investigación continuará en esta línea para su optimización y aplicación en procesos reales.



## **CHAPTER 1: GENERAL INTRODUCTION**

---



## 1. BIOSENSORS

A biosensor is an analytical device incorporating a biological sensing element that detects biological or chemical reactions by generating signals proportional to the concentration of an analyte.<sup>1</sup> This concept of biosensor has evolved over the last century. At the beginning of this research activity, some authors considered the biosensor as an independent device able to respond to the concentration of a chemical species in biological samples. This concept didn't refer to any biological active material involved in the device and thus, a simple physical or chemical sensor operating in biological samples was considered a biosensor. Nowadays it is accepted that biosensors integrate a biological sensing material and a transducer in a unique platform. Even now, the concept continues evolving and recent studies were reported in which biosensors were manufactured by replacing or mimicking the biological material with synthetic chemical compounds such as metal/metal oxides or smart polymers.

The first "true" biosensor was conceived by Leyland C. Clark and co-workers in 1965 when they proposed to immobilize enzymes on electrodes to form "enzyme electrodes" for glucose detection.<sup>2</sup> This discovery was followed by a large amount of research works until the first commercial biosensor for glucose detection was released in 1975 by Yellow Spring Instruments (YSI).<sup>3</sup> Two decades later, optical transducers laid the establishment of a new line of investigation and since then, remarkable progress has been achieved in the field of biosensors thanks to the continuous technological breakthroughs. This field is now a multidisciplinary area where basic science meets with cutting-edge technologies resulting in a constant development and progress of the sector. In the present, the market of biosensors is continuously growing with a current turnover in excess of US\$ 18 billion<sup>4,5</sup> and an indexation in the database "Web of Knowledge" of more than 46000 reports on the topic "biosensor" in the last 10 years.

The study of biosensors has always been motivated by a strong practical interest. Government agencies, private companies and public initiatives aim to drive the global market through the investment in R&D activities. The high demand for sensible and multi-detection devices, the rapid technological advances and the growing scope of applications explain the ongoing growth of the biosensor market. Key applications segments include industry, healthcare/medical (e.g., point-of-care, home diagnosis), monitoring of food toxicity, water quality, air composition, environment, agriculture, security and others.<sup>5</sup> In present, much effort is invested in the development and discovering of non-invasive, miniaturized and affordable devices based on biosensing technologies. Within the biosensor market, current

trends face these demands mostly towards home and real-time monitoring to make them more accessible both for patients and general consumers.

### 1.1. Structure and classification

Biosensors typically consist of a biorecognition component for the selective or specific recognition of analytes and a transducer component for the conversion of the biochemical process to a measurable electric signal (Figure 1). The biological material can be, for instance, an enzyme, nucleic acid, cell, or antibodies that interact specifically with the target analyte to produce a physical, chemical or electrical signal. These readout signals are transformed into a more easily measurable and quantifiable electrical signal through the transducer and finally, collected and interpreted with the reader device.

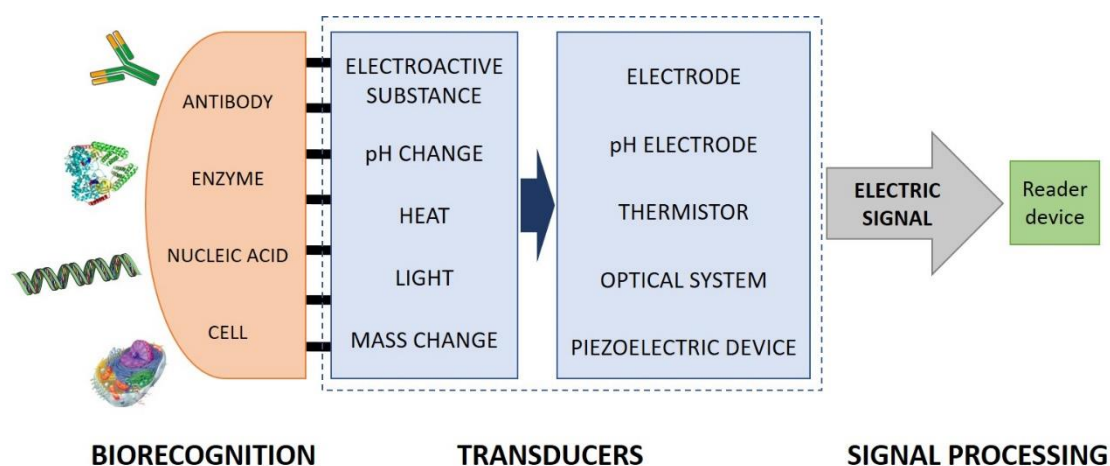


**Figure 1.** General schematic representation of a biosensor.

The biochemical layer provides specific binding sites for the interaction with the analyte of interest giving sensitivity and selectivity to the biorecognition event. The development on the design of the receptive layer allows to improve the recognition process by using molecular or biomolecular recognition such as antigen-antibody binding,<sup>6</sup> self-assembled monolayers<sup>7</sup> or polymer coatings.<sup>8</sup> Although notably advances have been made, there is still much work to do, especially to avoid non-specific interactions and improve the immobilization of the sensing component on the transducer surface. The transducer is in contact with the biological sensitive material and permits the interpretation of the biological process. The physical transducer often determines the limit of attainable detection seeking of new strategies for a better performance is constantly stimulated. Therefore, the development of outstanding materials to improve both biorecognition and transduction processes is key in manufacturing more sensitive, selective, rapid and detection devices with low limits of.<sup>9</sup>

As an analytical tool, biosensors must be validated to ensure their performance and demonstrate their reliability. This can be done by specifying their figures of merits.<sup>10,11</sup> For biosensors, we can highlight the following points:

- Selectivity: is the capability to select and measure only the analyte of interest without or minimal interference from the rest of species in the sample. This feature is the main consideration when choosing the bioreceptor for a biosensor.
- Sensitivity (limit of detection): is the minimum amount of analyte that can be detected. This is an important property because in a number of applications the concentration of the analytes is in the range of  $\text{ng mL}^{-1}$  or  $\text{fg mL}^{-1}$ .
- Reproducibility and repeatability: according to the IUPAC, they refer to the agreement between the results of successive measurements carried out in the same (repeatability) or different (reproducibility) conditions related to operator, apparatus and laboratories. They are characterised by the precision and accuracy of the transducer and electronics in the biosensor. Precision is the ability to provide equal results every time the biosensor makes a measurement. Accuracy indicates how close to the true values are the results measured by the biosensor when detection is carried out several times.
- Stability: characterizes the change in its baseline of sensitivity over a fixed period of time. It is also the degree of susceptibility to ambient disturbances that can cause drift in the output signals. This is the most important property to take into account when working with biosensors that requires long incubation times or in continuous monitoring. Furthermore, to ensure a high stability it is important to ensure a permanent strong interaction of the analyte with the bioreceptor as well as a low degradation of the bioreceptor over a period of time.
- Linearity: also called dynamic range, is the concentration range over which the sensor reliably detects a perturbation in concentration of the analyte of interest. It is also an attribute that shows the accuracy of the measured response with respect to a straight line, usually represented as  $y = mc$ , where  $y$  is the output signal,  $m$  is the sensitivity and  $c$  is the concentration of the analyte.
- Lifetime: is the time period over which the biosensor can be used without significant deterioration of properties and performance characteristics. It is dependent on the method of immobilization of the biosensing element.

- **Response time:** is the time required to indicate 63% of its final response due to a step change in analyte concentration. This feature is determined by the kinetics of the reaction.

The vast amount of biosensors comes from the diverse possibilities available considering the different combinations of the sensing element and transducer (Figure 1). They can be generally divided regarding the detection technology into label-free and label-based biosensors (Figure 2).<sup>12</sup> Moreover, according to the structure of the biosensors they can also be classified on the basis of the nature of the biological entity used as the bioreceptor and by to the type of transducer employed.<sup>11,13</sup>

### 1.1.1. Classification by labelling

Label-based approaches rely on the specific properties of the labels used to mark the target analyte. These technologies use “tags” to detect the specific target against other species in the sample matrix. The most popular techniques are fluorescence,<sup>14,15</sup> chemiluminescence<sup>16,17</sup> and radioactivity.<sup>18</sup> The labelling and purification processes often lead to a loss of sample, becoming critical when sample test quantity is limited. Moreover, there is frequently a lack in stability and functionality of final labels, especially of proteins and other biopolymers. Label-free detection techniques can overcome these disadvantages due to the absence of labels. These techniques are suitable for the target molecules that are not labelled or the screening of analytes which are not easy to tag. Some label-free techniques are mass spectrometry,<sup>19</sup> surface plasmon resonance<sup>20,21</sup> and optical methods.<sup>22,23</sup>

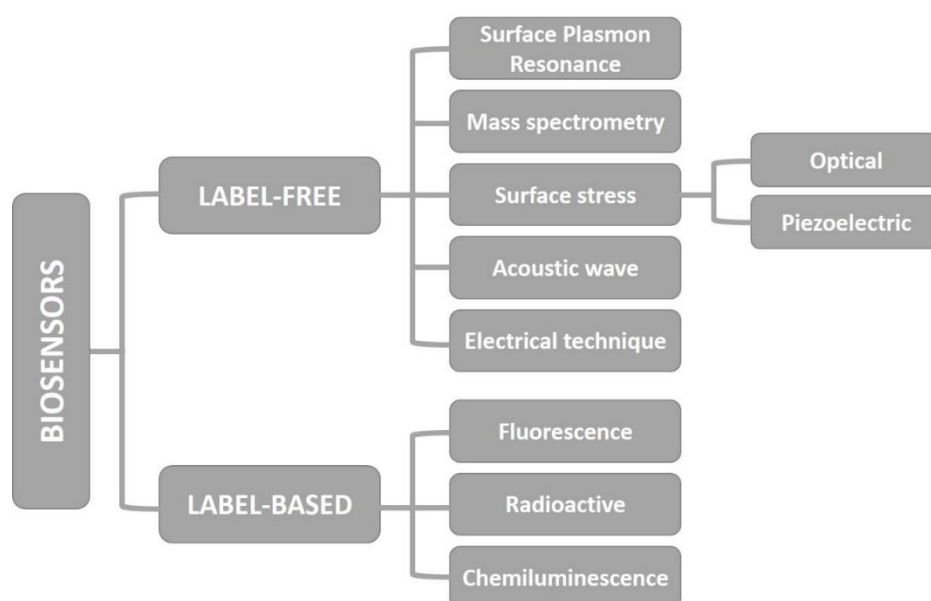


**Figure 2.** Classification of biosensors by labelling technique.



### 1.1.2. Classification by type of bioreceptor

Taking into account the wide range of possibilities, the choice of the recognition element depends exclusively on the target analyte. The interaction bioreceptor-analyte should be selective, with a high binding affinity and high stability. Classical recognition elements (enzymes, antibodies, nucleic acids) are most commonly used for designing a biosensor. Nevertheless, other bioreceptors such as phages, molecular imprinted polymers (MIPs) and affibodies have recently attracted the attention of scientific researchers due to their improved analytical performance regarding their rapid synthesis and easy integration with the transducers.<sup>24-26</sup> Moreover, the combination of classical and modern sensing elements is getting interest for the improvement of the biosensors performance (e.g., antibodies linked to nanoparticles).

- Enzymes

Enzymes are proteins which show catalytic activity, so they are biocatalysts that catalyze chemical reactions. Enzymatic biosensors are based on the highly selective interaction between the enzyme and its substrate (analyte in the sample) generating a product that is afterwards directly determined by the transducer. Detection mechanism of enzyme-based biosensors is based on the activation or inhibition of their activity as a response towards the target analyte. This can be done by one of two ways: the enzyme catalyses the reaction with the substrate so that the signal measured is proportional to the catalytic transformation, or the analyte inhibits the enzyme so that the signal decrease with the decrease in its activity (decrease in product formation).

- Antibodies

Antibodies are the most popular affinity recognition elements used in biosensing. They are glycoproteins produced by the immune system in response to a foreign substance (antigen). These bioreceptors interact in a selective way with their specific antigen forming stable antigen-antibody complexes. Among the variety of antibodies, the monoclonal ones only bind to a unique epitope (binding site) on a specific antigen, whereas the polyclonal antibodies present affinity for various binding sites, therefore, the binding is stronger but can suffer from cross-reactivity. This biomolecular interaction provides a high selectivity and specificity and can be additionally improved in affinity and selectivity by designing new recombinant antibodies with genetic engineering.

- Nucleic acids

DNA/RNA probes for detection of analyte DNA/RNA gain their sensitivity and specificity from the very strong base pair affinity between complementary bases in the nucleotide strands through stable hydrogen bonds. Moreover, recent works employed DNA/RNA-aptamers, defined as small single-stranded DNA or RNA sequences used as an alternative to antibodies due to their high stability, specificity, low cost and simpler detection strategies. In this case, the specific interaction with the target molecules is caused by hydrogen bonding between DNA/RNA bases and target molecules.

- Cells

Cells express a wide variety of molecules (receptors) in different proportions, so they can not only yield quantitative response of specific stimuli, but they can also help in analysing more than one analyte at the same time. They provide a natural amplification of the signal due to the optimal activity and specificity of their enzymes and other molecules that are present in their native environment.

- Phages

Phages, or bacteriophages, are viruses that infect bacteria and display peptides or proteins on their surface, so they are employed as biorecognition elements to detect pathogens. They are environmentally more robust and can be stored for longer times, so longer shelf life times, with minimal loss of binding affinity.

- Molecular Imprinted Polymers (MIPs)

MIPs are synthetic cross-linked materials with artificially generated recognition sites with a performance similar to the antibodies. They are synthesized by polymerization of functional monomers in a mixture with cross-linkers and template molecules that are the target analytes. After the removal of the templates, chemically-selective recognition sites are created in the matrix complementary in shape, size and functional groups to the template molecules (target analyte). This sensing elements have gained much popularity as affinity-based bioreceptors due to their high selectivity, stability, short time of synthesis, high thermostability and cost effectiveness.

- Affibodies

Affibodies are small robust three-helical peptide, made up of few amino acids with no disulphide bonds in their structure. They are a new class of engineered affinity proteins that can reach considerable selectivity and affinity. Although they have been commonly used in imaging, diagnosis and therapeutics, their role as bioreceptors in biosensors is becoming a relevant strategy and has increased potential.

### 1.1.3. Classification by type of transducer

Biosensors can be also classified according to the principle used in the signal transduction: electrochemical, optical, piezoelectric and thermal.<sup>11,13,27</sup> The selection of the transducer in the design of the biosensor is a key step that must consider some features such as the interaction between the analyte and receptor, the final application of the biosensor and the manufacturing cost of the device.

- Electrochemical

Electrochemical biosensors have been the most widely studied and utilized since the first enzymatic biosensor was produced in 1962. They present some outstanding advantages such as their cost-effectiveness, portability, high sensitivity and compatibility with modern microfabrication technologies. They are based on the basic principle that the biochemical interaction between the analyte and the bioreceptor involves the production or consumption of electrons that in turn produce some change in the electrical current or potential. The transducer detects these changes and generates an electrochemical signal proportional to the analyte concentration in the sample. A further classification can be done according to the type of measured signal. *Potentiometric biosensors* measure the difference in potential between the working and reference electrodes at a virtually zero current flow. They are based on the use of ion-selective electrode (ISE) where the electrodes are covered with an ion-selective membrane that selectively interacts with the target analyte resulting in a change in potential corresponding to the concentration of the analyte. *Amperometric biosensors* measure the current of the system during the oxidation or reduction of the electroactive reactant or product. The resulting current is directly correlated to the concentration of the electroactive species (production or consumption). They are more sensitive faster and more suitable for mass production than potentiometric ones. *Conductometric biosensors* measure the electrical conductivity of the solution between two electrodes. The ability of the analyte under study to conduct

electrical current is detected with this type of transducer. They are less commonly used in biosensing and they usually employ enzymes as bioreceptors. *Transducers based on field-effect transistors (ISFET)* measure the change in the potential caused by the activity of the target ion in the sample. They are in essence a potentiometric system but with input transistor transposed into the solution. This increases the resolving power of the transducer and thus, the sensitivity of the biosensor.

- Optical

Optical biosensors are able to detect optical changes in the input light as a consequence of the presence of the analyte. The analyte-bioreceptor interaction produces a change in the light that can be quantified through its intensity or amplitude, which is correlated to the concentration of the analyte in the sample. They are characterized by their rapid detection, sensitivity, robustness and ability to detect multiple analytes. One of the most used technique is the *surface plasmon resonance (SPR)*, which is able to detect changes in the refractive index as result of the analyte concentration, without the use of labelled molecules. Other techniques require employment of a label. *Absorbance biosensors* are simple and inexpensive and allow the direct detection of the analytes regarding their intrinsic absorption at a certain wavelength of light. *Fluorescence biosensors* detect the change in frequency of electromagnetic radiation emission caused by previous absorption of radiation and generation of excited states. *Luminescence biosensors* measure the light emitted spontaneously in a biochemical reaction as a consequence of the components excitation and return to the ground state. They are usually called chemiluminescent biosensors or bioluminescent biosensors when this process occurs within a biological organism.

- Piezoelectric

Piezoelectric biosensors, or mass-based biosensors, produce an electrical signal when a mechanical force is applied. In these biosensors the bioreceptor is coupled to a piezoelectric component, usually a quartz-crystal. The operation of this type of biosensors is based on the ability of the piezoelectric material to change its frequency of oscillation with the increase/decrease in mass due to the interaction of the bioreceptor on their surface with the analyte in the sample.

- Thermometric

Thermal biosensors are also known as calorimetric or thermometric biosensors. They are able to measure the change in temperature resulting from the interaction between the bioreceptor and the analyte. They present some advantages such as no need of labelled reactants, robustness and no disturbances by electrical or optical properties of the sample. Although they are not very common and their use is limited, most of them are based on enzymatic reactions with a thermistor to detect the change in temperatures.

## 1.2. Biosensor applications on the market

Since the first advent of the first glucose biosensor on the market in 1975, the trade of these devices has exponentially growing up with a turnover of more than 18 billion US\$ worldwide and it is expected to increase in revenues to reach 31 billion by the end of 2023.<sup>28</sup> With around 45 years of development, biosensors have evolved towards smart devices with great applicability in our daily life.

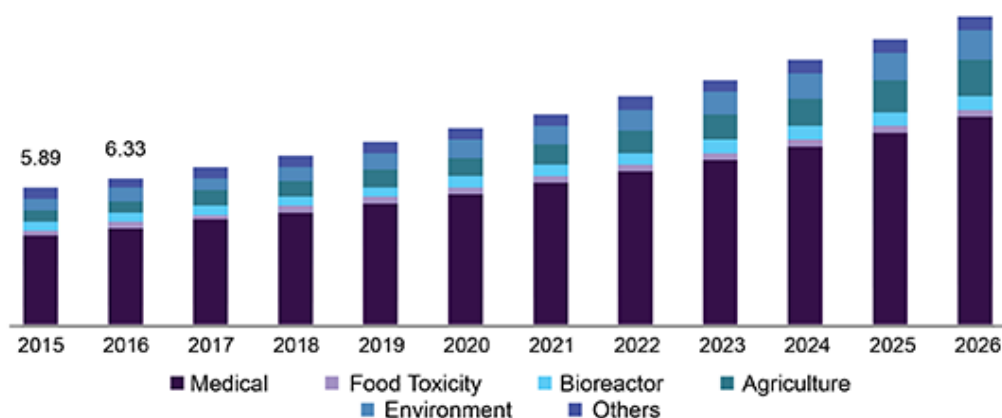


**Figure 3.** North America biosensors market size by application 2015-2026 (USD Million), from [www.grandviewresearch.com](http://www.grandviewresearch.com).

Biosensors on the market can be classified by their application into medical, food analysis/toxicity, agriculture, industrial process control, environmental monitoring, defense and others.<sup>3,5</sup> In the last years, medical applications have led the market where biosensors are considered an essential tool in the detection and monitoring of relevant analytes such as cancer markers, glucose, drugs and other metabolites (Figure 3).<sup>29</sup> Their superior market presence is explained by the increasing demand for rapid, accurate and reliable devices mainly for clinical applications. Although much effort has been put into improving their performance, few biosensors show a real presence on the market. The most commonly known biosensing device is commercialized mostly as an enzymatic amperometric biosensor for glucose

## Chapter 1

detection.<sup>30-32</sup> Other biosensors on the market with clinical applications are the human chorionic gonadotrophin (hCG) biosensor, also known as pregnancy test,<sup>33</sup> biosensors for cholesterol,<sup>34</sup> influenza A and B viruses,<sup>35</sup> *Helicobacter pylori*,<sup>36</sup> human immunodeficiency virus (HIV),<sup>37</sup> tuberculosis<sup>38</sup> or malaria.<sup>39</sup>

Despite the inherent difficulties associated with the diverse types of samples having variable compositions in food industry, the implementation of advanced biosensors in this field has increased considerably. The principal aim in the design and development of these devices is to ensure a good quality control and safety of the products that is achieved in two ways: the detection of the components (food analysis) and the presence of microorganisms.<sup>40</sup> Biosensors for food analysis are mainly based on enzymes or antibodies that confer a high selectivity and specificity for the analyte/microorganism of interest.<sup>41</sup> They are used to guarantee an optimal status of the products as well as a proper control of the freshness and stability. Besides, it is important to ensure the safety of the products regarding the possible contamination with some microorganisms potentially harmful for humans and animals. Some examples of the most utilized biosensors are those for the detection of some pathogens like *Escherichia coli*,<sup>42</sup> pesticides<sup>43</sup> or drug residues such as antibiotics.<sup>44</sup>

Additionally, there has been a growing interest and development in other fields like agriculture, where the fast growth is associated with the technological improvement that provides rapid and specific devices for the detection of soil nutrients, moisture or nitrogen as well as fungi and plagues, avoiding the livestock and crops loss.<sup>45</sup> Within the military sector there is a need for the design and application of biosensors in the field of defense. Some bacterial/viral agents, other organisms or toxins are considered biological warfare agents (BWA) that can be used as weapons in bioterrorism. The main value of these devices is the ability to selectively, sensitively and rapidly detect and identify BWAs in real time in order to avoid poison threat. Most of these biosensors are based on molecular techniques to recognize chemical markers from BWAs like biological entities such as Hepatitis C or Ebola viruses combined with different transducers (e.g., electrochemical, optical).<sup>46-48</sup> Finally, environmental sector employs biosensors in the monitoring and detection of some pollutants and harmful chemicals present in soil, air and specially in water.<sup>49</sup> Some of the most dangerous products are pesticides, herbicides, heavy metals and some pathogens. There is an extensive literature data regarding the design and development of biosensors with environmental applications, but only a small part of them have reached the market. Biological oxygen demand (BOD) is known as the amount of oxygen that aerobic organisms require in the presence of pollutants during de biochemical degradation of organic matter in water and wastewater. This

parameter is the most widely utilized in environmental applications and this is why the research and development of such devices are so advanced.<sup>50</sup>

Attending to the end use of biosensors, their classification includes mainly point-of-care testing, home healthcare diagnostics, research laboratories, food industry and others, such as security and bio-defense. As can be seen in Figure 4, point-of-care (POC) testing represents almost half of the global market share by end use. These instruments enable real-time and remote health monitoring while keeping the inherent advantages of a classical biosensor. Some requirements to fulfil by POC systems are the high speed in giving the results, high accuracy and sensitivity comparable to bench-top analysers used in central laboratories, and easy-handling to ensure their use by non-trained personnel.

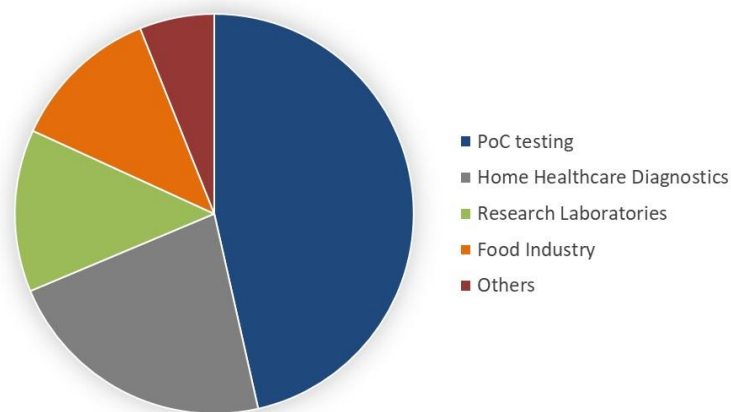


**Figure 4.** Global biosensors market share by end use in 2018 (%). Source, Frost & Sullivan.

The increased demand of POC testing devices relies on the need of rapid, reliable and easy-to-use instrumentation for the detection and monitoring of several analytes of interest in biological fluids such as sweat, blood, saliva and urine. These platforms are aimed to be used as a complete diagnostic tool, although they are often considered as a fast and simple pre-screening methodology, reducing considerably the cost of monitoring programs. Thanks to the technological advances in this field, some of the most common, costly and preventable health problems can be nowadays followed and monitored with POC systems (e.g., type 2 diabetes, obesity, cancer, stroke, heart diseases or arthritis).

POC testing offers an affordable alternative to diagnostic platforms of centralized laboratories that can be used in the doctor's offices, hospitals and patient's homes by non-professionally trained individuals. While in developed countries both POC and sophisticated equipment are present in daily life, in developing countries there is still lack of equipment and laboratory infrastructure, trained personnel and state of the art apparatus, so the need of portable and reliable systems with medical/food/agriculture applications is yet a challenge to deal with.

Nevertheless, even in developed countries there is still a high demand for POC devices due to the need of accurate and rapid responses to new diseases/pathogens, regular monitoring or early diagnostics.

POC systems present several benefits compared to bench-top laboratory facilities such as portability, automation, shorter response time and reduced cost. These features can only be improved by the strong collaboration among researchers from chemistry, physics, biology and engineering. Moreover, the current growth trend of POC devices is only possible thanks to the Lab-on-a-Chip (LOC) technology that brings the technical research to life applications.

## 2. Lab-on-a-Chip technology

A Lab-on-a-Chip (LOC) is a miniaturized device that integrates one or several laboratory functions on a single compact platform, usually ranged from millimetres to a few square centimetres in size (Figure 5).<sup>51,52</sup> The main objective of these devices is to automatize standard and routine laboratory procedures and to conduct chemical and biochemical analysis in a miniaturized system. They present some advantages such as high throughput, cost-efficiency, high sensitivity, lack of cross-contamination and multi-detection of analytes. Moreover, miniaturized LOC systems facilitate the use of reduced volumes, minimize the manipulation of dangerous materials and allow minute reagent and sample consumption as well as less waste generation.

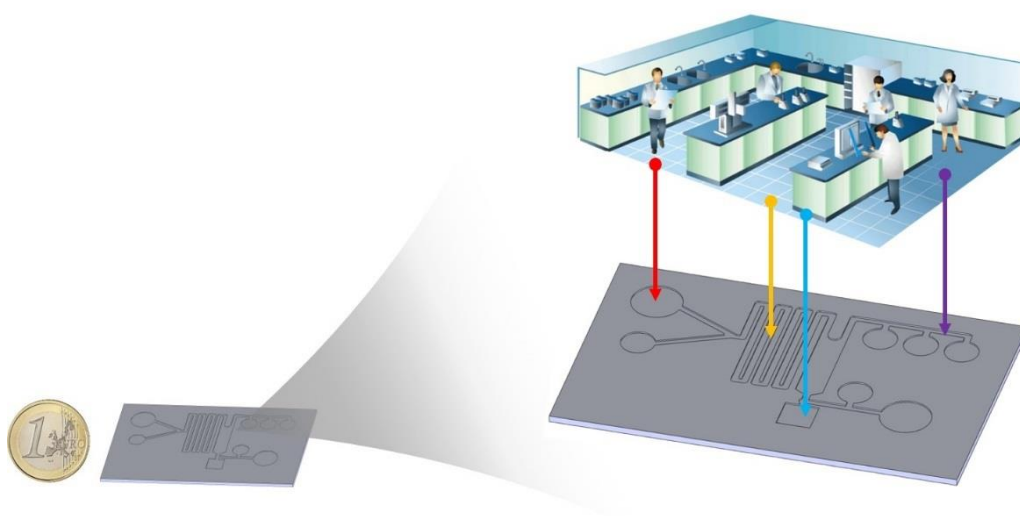


**Figure 5.** Representative scheme of a lab on a chip device.



The history of LOC is intrinsically linked to microfluidics, that is, the science and technology of systems that manipulate and control small amounts of fluids ( $10^{-9}$  to  $10^{-18}$  litres) using networks of channels with dimensions from tens to hundreds of micrometres.<sup>53</sup> From the late 1950s, miniaturization techniques have been continuously shaping the microelectronic and microfluidic technologies in the search for smaller, faster and more efficient systems for a wide range of applications. In the early 1970s it was possible to fabricate the first microsensor in silicon which opened up a new field in material science called micro-electro-mechanical systems (MEMs).<sup>54</sup> Thanks to the developments in these fabrication techniques, the first real LOC device for gas chromatography was created in 1979 by S. C. Terry at Stanford University.<sup>55</sup> However, it was not until the beginning of the 1990s when this technology started to grow and gain popularity among the scientific community. New concepts and functional elements were discovered and described including micro-pumps, switchers, valves, actuators, mixers, filters, separators, heaters, dispensers, etc. These elements were used in the adaptation of microfabrication processes for the production of polymer-based LOC. That was the time when Manz et al. established the concept of Micro Total Analysis System ( $\mu$ TAS).<sup>56</sup> In this work they described a revolutionary instrument consisted of a silicon chip analyser that included the sample pretreatment, separation and detection in a single microfluidic platform. This technology set the basis of miniaturized systems that integrated all the laboratory steps towards the chemical/biochemical analysis, from the sample collection to its separation and final determination.<sup>57,58</sup>

In the subsequent years, a major effort was undertaken in microfabrication and development of new materials to cover a broader range of applications resulting in a new field in fabrication processes named soft-lithography.<sup>59</sup> Thanks to the improvement of these techniques, in 1998 a rapid prototyping of microfluidic system in polydimethylsiloxane (PDMS) was released by Professor George Whitesides.<sup>60</sup> This work proposed a fast and easy design and fabrication of microfluidic chips in a transparent material by using the photolithography technique. It had a great impact and pushed the development of more sophisticated techniques such as molding and self-assembly procedures, microcontact printing, paper-based fabrication method or 3D printing technology.<sup>61-64</sup> All of these techniques were conceived and designed to fulfil the requirements for LOCs devices, basically with commercial purposes, that are: disposability, easiness to fabricate and low price per unit. This is the reason why special production processes and materials need to support mass manufacturing which means that thermoplastics should be used instead of glass and easy to scale methods like injection molding are preferably selected rather than microproduction processes.

## Chapter 1

Although first LOC devices didn't achieve an important relevance, the need for rapid, small and versatile platforms to deal with new demands caused the rapid rise of this technology. Nowadays, the continuous technological advances are reflected by the increasing number of publications and patents of LOC devices with high impact in the scientific community as well as in the industrial sector with USA in the head of the countries with major influence.<sup>65,66</sup> The multiple advantages of microfluidics applied to LOC devices has increased the growth of this market globally. In the beginning, the development of LOC devices was applied to genomics (capillary electrophoresis and DNA microarrays) and military defense (portable chemical and biochemical warfare detection systems),<sup>57</sup> but the huge potential of LOCs resulted in their application to other fields. In the present, most LOCs are developed within the biomedical field, from basic research to commercial applications (e.g., drug delivery, immunoassays, DNA amplification, neuron manipulation, single cell analysis, tissue engineering).<sup>52</sup>

The key biomedical market segments for LOC applications are:

- Diagnostics and patient monitoring

The miniaturization and adaptation of microfluidics to LOCs makes them suitable for clinical diagnostics and “near to patient” or “point of care” (POC) testing. This is considered one of the highly competitive markets and it is expected lead the segment globally during the next forecast period owing to the growing demand for portable, fast and sensible diagnostics. As the global population grows, the number of patients with diseases increases as well as the demand for diagnosis and treatment of those diseases. POC systems provides instant and accurate detection of diseases helping in taking precautionary measures and thus, reducing the number of patients in the hospital. Not only should they give quick results, but they should also be easy to use, with no need of external equipment and no specific requirement of trained personnel. Many useful POC devices are already on the market with relevant improvement of the public healthcare: glucose testing, pregnancy tests, blood analysis, urine test, bacteria screening or HIV testing.<sup>68</sup> Portability of POC devices provides a great advantage over classical benchtop technologies (e.g. core laboratory in a hospital) regarding the decentralization of medical testing. POC devices help doctors to provide results at a faster and more efficient rate, allowing them to aid the patients wherever and whenever it is needed. Some applications include the monitoring of regular metabolic parameters, e.g. glucose, or other more specific substances such as chemotherapeutic markers in cancer patients.

- Drug discovery

LOCs are widely used in pharmaceutical industry in the development of new drugs and the improvement of their therapeutic effects. This is the second largest segment in the biomedical field market. Their principal application is the screening of drugs during the manufacturing process for their further validation.<sup>69</sup>

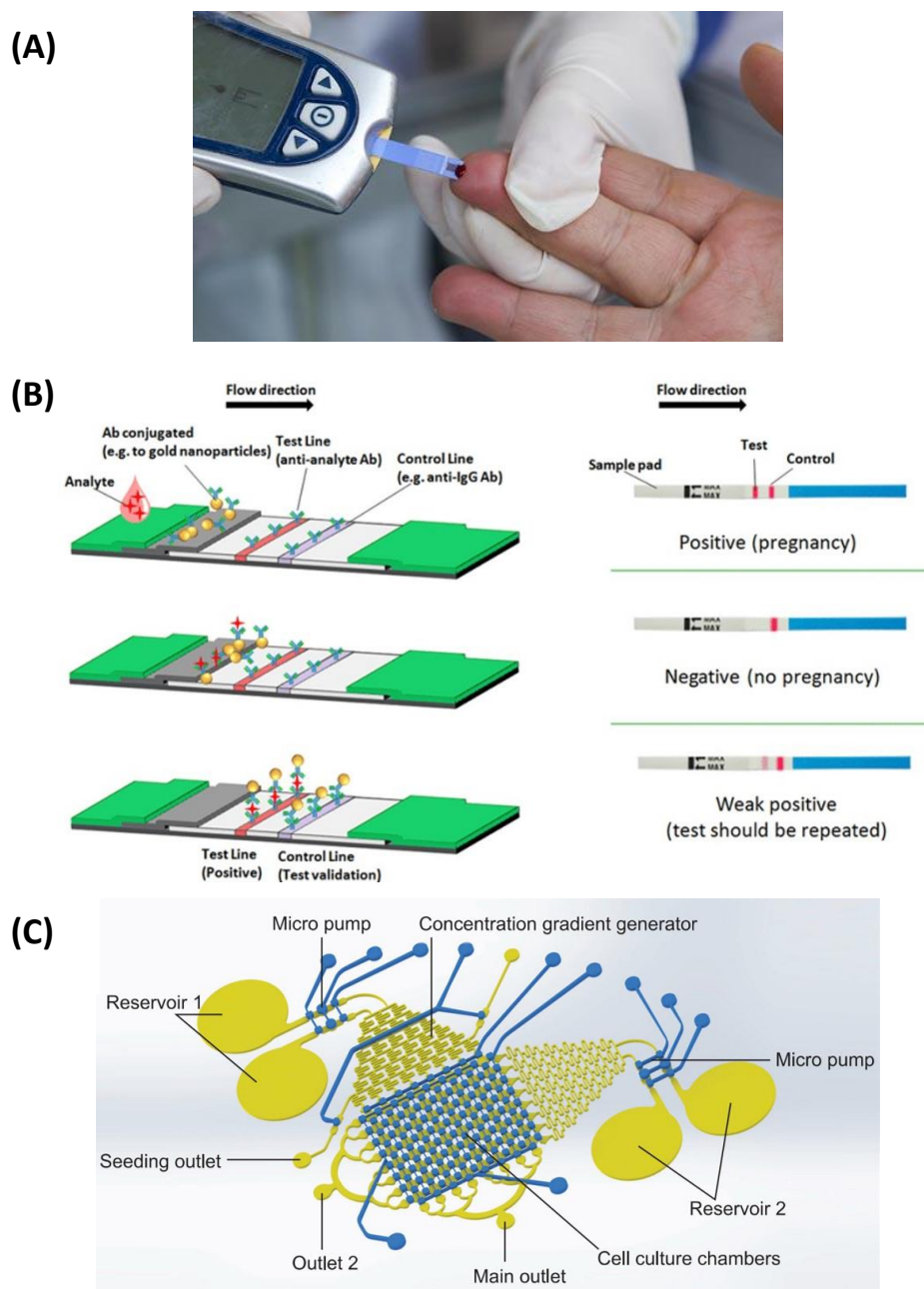


**Figure 6.** Examples of some representative LOC: (A) commercial POC testing for whole blood profile, (B) lateral flow immunoassay of a pregnancy test: schematic representation of the assay's mechanism and hCG strips with possible results,<sup>70</sup> (C) scheme of a microfluidic array for drug screening: different concentrations of sensitizer and drug are generated in the diffusive gradient mixers sequentially to perfuse cells cultured in downstream microchambers, subsequently dyes are added to differentiate live/dead cells.<sup>71</sup>

## Chapter 1

Focusing on diagnostics, POC testing devices present the most attractive and suitable technology to “bring the doctor to the patient”. These devices must fulfil some requirements such as a) high throughput in data generation to improve the response time; b) accuracy and sensitivity; and c) ease of handling by non-trained personnel, with minimum user interventions. Moreover, in the case of biomedical applications, POC systems must integrate the biosensor in its platform, which is achieved thanks to the new developments in material science, microfluidics and microelectronics. As a biosensor, POC systems respond to the concentration of the analyte of interest in the sample. When using POC for diagnostics, this analyte is normally called biomarker and refers to an objective indicator of the medical state of the patient.<sup>72</sup> Usually, these are biomarkers from protein, cells, nucleic acids or metabolites and each of them will require different diagnostic principles, assays and operating systems.

Among them, proteins are the most commonly used in POC testing because they often reveal the presence or status of diseases that are typically monitored or treated. For successful clinical applications, POC testing needs to be accurate for usual levels of protein as well as at elevated/reduced concentrations and they must be resistant to interference from nontargeted proteins. Today, most protein determination methods for POC are based on antibody assays due to the extensive library of antibodies against most proteins and the high selectivity of the immunoassay process.<sup>73</sup> The best and well-known immunoassay widely used for protein detection is the enzyme-linked immunosorbent assay (ELISA). Although this technique is frequently used in diagnostic and hospital laboratories, there are very few examples of successful adaptations to POC platforms. On the other hand, most of the portable immunoassays on the market are based on the lateral flow technology that is able to provide results in a fast, low-cost and simple manner. Such immunoassays are very popular and are broadly used for several applications in biomedicine, but they require relatively high concentrations of the biomarker to be able to give an accurate result.<sup>70</sup> On the other hand, ELISA protocols are more sensitive, even more when combined with other techniques to amplify the signal (e.g., enzymatic amplification).

Regarding the transducer, POC immunoassays are usually optical or electrochemical. Lateral flow assays rely on the optical readout because this method is simpler and easier for integration into the biosensors. They are commonly called “dipsticks” and we can find them available on the market for a wide range of biomarkers (e.g., pregnancy hormones, cardiac markers, infectious diseases, etc.). However, electrochemical immunoassays have demonstrated a superior performance in terms of sensitivity and easier integration in LOC platforms because of its simpler miniaturization, economical production and lower power consumption.<sup>74</sup>

## Electrochemical immunosensors

Immunoassays represent one of the most selective and sensitive methodologies for the detection and quantification of pathogens, toxic elements, contaminants and metabolic analytes with a critical role in medical sector, and more precisely, with relevant interest in healthcare. Briefly, an immunoassay is a technique that employs antibodies to detect a specific antigen, generating a detectable signal that is afterwards quantified.<sup>75</sup> To follow the reaction, either the antibody or the antigen should be properly labelled in order to provide a stable easily traceable signal. In the beginning, the antibodies were modified with a radioactive label (radioimmunoassays) because of the high sensitivity of radiation detection. Later, the use of radioisotopes was restricted, and new labels were introduced such as enzymes, chemiluminescent compounds and fluorophores. Among these, enzymes are the most widely used to label antibodies because of the variety of chemical reactions that they are able to catalyze producing generally optical or electroactive species that can be afterwards be detected and quantified.

Electrochemical immunosensors use this enzymatic activity to detect the analytes of interest in the sample by measuring the electrical signal resulting from the binding event between the antibody and the antigen (Figure 7).<sup>76</sup> The electrochemical procedure provides great advantages such as easiness of operation, possibility to miniaturize, use of reduced sample volumes, good performance and high sensitivity. In a standard protocol, the immunoassay is performed on the surface of the electrode and the last step involves the incubation of the enzyme with its substrate to produce the electroactive product that generates the electrical signal proportional to the analyte in the sample.

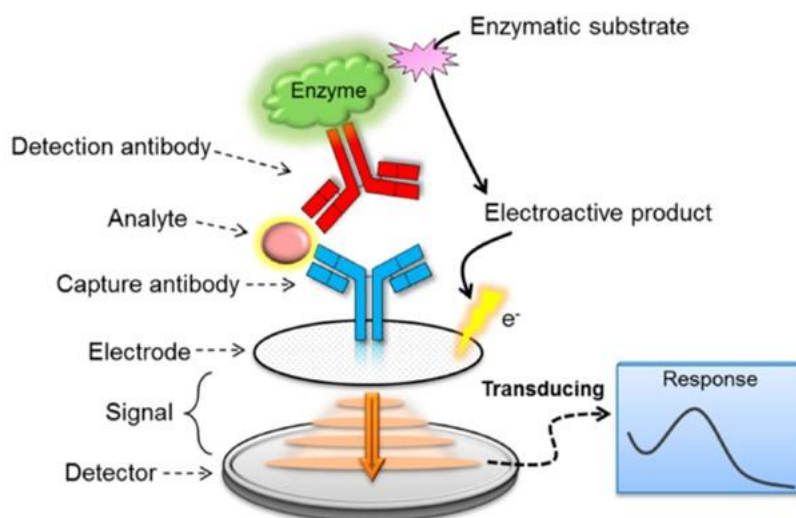


**Figure 7.** Scheme of the basic components of an electrochemical immunosensor.

Since the first electrochemical biosensor for glucose released in 1962, research and development in the field has grown at a remarkable rate and it is expected to continue evolving in the next years towards the construction of more efficient devices. Initially, a variety of catalytic electrochemical biosensors based on the same principle as the glucose one (enzymatic process) were developed aimed at exploiting the specificity of the reaction between the enzyme and its substrate. These enzymatic biosensors were able to detect particular analytes in the sample by their specific and selective interaction with the enzyme immobilized on the surface of the electrode.<sup>77</sup> In 1985, electrochemical immunoassays were first described by Heineman and Halsall.<sup>78</sup> They employed voltammetric and amperometric techniques to detect and measure small molecules such as hormones via competitive and sandwich-type immunoassays. A few years later, in 1995, the description of the first electrochemical immunosensor where the antibodies were immobilized on the surface of the electrode was published.<sup>79</sup> In the last years, trends in the field are moving beyond these technologies and new directions are being explored in the use of nanomaterials to amplify the signal, to seek for more efficient protocols to immobilize the antibodies, as well as the use of new capture agents such as aptamers or affibodies to simplify the detection schemes.<sup>80</sup>

All of these technological advances can be applied to the design and fabrication of LOC devices for POC applications such as diagnostics. In order to obtain a suitable POC for diagnostics, there are several demands to be satisfied, among them, two key points to achieve a good sensitivity are: the correct immobilization of the recognition element and the amplification of the electrochemical signal.

### **a) Immobilization procedures**

In electrochemical immunosensors, the electrochemical reaction is in general carried out with three-electrode system and the biorecognition element is immobilized on the surface of working electrode. The immobilization procedure plays a critical role in the achievement of a high performance of an immunoassay through the facilitation of the interactions between the antibody and the analyte. Immobilization strategies are focused on the seek of strong anchoring of the antibodies to the surface while preserving their activity.<sup>81</sup> Selecting the proper immobilization approach is fundamental in the design of the immunosensor because it defines the stability and sensitivity of the biosensor (Figure 8).

- Physical adsorption

It is the most common, simplest and easiest method for immobilization of antibodies on the selected surface. The physical immobilization is achieved by non-covalent interactions (electrostatic forces, ionic bonds or hydrophobic interactions) or by the physical entrapment of the proteins. Some examples are the direct immobilization on the carbon/graphene working electrode surface, on intermediate structures such as gold nanoparticles or on thin films or polymeric matrices to entrap the antibodies<sup>82-85</sup>. Although this is an easy and cheap way to immobilize the bioreceptor, it sometimes lacks stability, reproducibility or homogeneity.

- Covalent binding

This is another well-known technique based on the formation of covalent bonds between the antibody and the electrode surface. The covalent attachment provides a strong immobilization and high stability, even although in some cases they can modify the structure of the antibody leading to a loss of activity. Generally, electrode surfaces are not suitable for covalent bonding, so it is necessary to premodify them by introducing a specific functional group able to interact with some moiety of the antibody. For this purpose, some reagents such as glutaraldehyde, N-hydroxysuccinimide, carbodiimide succinimide ester or maleinimide can be used as crosslinkers, molecules that can react as bi-functional reagents connecting the surface of the electrode and the antibody.<sup>86,87</sup> Moreover, some works propose the use of an intermediate structure, for instance, a self-assembled monolayer (SAM), gold nanoparticles or even polymers such as cellulose. These structures enable stable surface modification and allow for the introduction of a wide range of functionalities, which extend the possibilities for interaction with the different antibodies.<sup>88-90</sup>

- Affinity immobilization techniques

This approach is based on different bioaffinity interactions and is a promising strategy for obtaining high capture efficiency and well orientated antibodies. A number of affinity systems have been reported such as lectin-sugar, protein A or G, biotin-streptavidin interactions, His-Tag system, DNA-directed immobilization or affinity capture ligand system.<sup>91-96</sup> All of these protocols increase the stability and orientation of the antibodies, while maintaining their activity, but they are often sensitive to the procedure conditions.

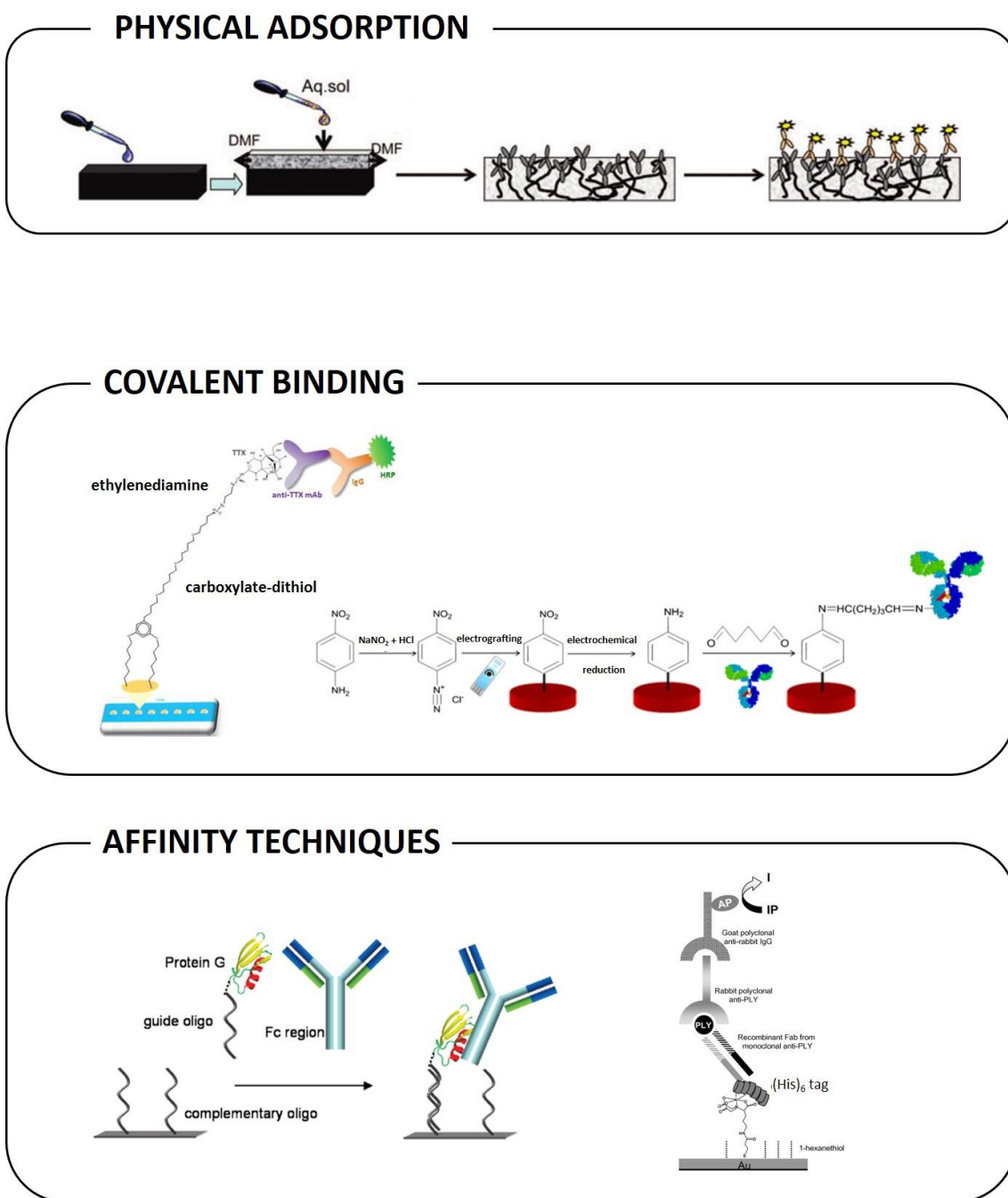


**Figure 8.** Classification of different antibody immobilization techniques (A) physical adsorption by antibody entrapment on polymer/thin film matrices,<sup>84,85</sup> (B) covalent binding through introduction of crosslinkers such as glutaraldehyde<sup>86</sup> or SAMs<sup>88</sup> and (C) affinity techniques based on affinity processes by using His-Tag<sup>96</sup> and DNA-directed immobilization procedures.<sup>95</sup>



## b) Signal amplification

In most cases the interaction between the antibody and its antigen doesn't produce any detectable signal thus quantification of the process requires an extra compound/structure to produce a detectable signal and transform into an amplified electrochemical signal. The amplification strategies can be classified into two mayor sections. The first one employs innovative materials with improved properties as electrodes or supporting matrices. The second strategy includes a labelling step to introduce the appropriate compound to produce a detectable response proportional to the concentration of the analyte.

- Functional materials as sensing platforms

The choice of the electrode material is crucial when designing an electrochemical immunosensor because of it defines sensitivity, cost of the assay and the possibility to perform immobilization procedures.<sup>97</sup> The electrode acts as a solid support for the immunoassay as well as the sensing part for the electrons produced in the course of the biological reaction. Generally, solid electrodes are made of inert metals such as gold and platinum and several forms of carbon including glassy carbon or graphene.<sup>98</sup> Although the good performance and the wide application of these electrodes, they are not suitable for electrochemical immunosensing due to the large volumes required to perform the measurement and their production cost. Screen-printed electrodes (SPE) present a promising alternative in terms of cost-efficiency, use of low volumes (microliters), easy modification, mass production and better integration to LOC devices.

Several types of inks are available on the market along with customized structures and geometries designed and selected for each application. In terms of electrochemical immunosensors, the electrodes should fulfil some requirements such as excellent biocompatibility with biomolecules, sufficient electro-catalytic activity and acceptable electron transfer ability. **Nanomaterials** are materials with dimensions in the nanoscale range (1-100 nm) that present unique optical and electrical properties and a high surface/size ratio what means higher surface reaction activity and more conformational freedom for protein immobilization.<sup>99</sup> Over the past decade, they have been incorporated in biosensor configurations providing an improvement in their limit of detection, sensitivity and reducing matrix effect. Furthermore, some nanomaterials present interesting properties of biocompatibility, conductivity, catalytic properties and good stability that make them an appropriate tool to increase the signal amplification as well as the electron transfer process.<sup>100</sup>

*Metal nanomaterials* are commonly used to increase the electron transfer and the effective electrode surface for the antibodies immobilization. Gold nanoparticles (AuNPs) are mostly commonly used in the field of electrochemical immunosensors. A simple and direct approach consists in the immobilization of AuNPs on the electrode surface for their further use as sensing platform. Besides, these nanoparticles can be modified in a previous step with proteins or combined with other materials to improve the electron transfer rate (e.g., graphene, carbon nanotubes).<sup>101–103</sup> Other strategies employ nanoparticles such of silver, zirconia or IrO<sub>2</sub>.<sup>84,104,105</sup> Although these nanomaterials demonstrate good properties, sometimes they are not suitable for high-performance analysis, so eventually they need to be combined with other structures forming nanocomposites. These structures improve the immobilization procedure and the long-term stability. Recently, several works have demonstrated the high performance of biosensors using polymers to entrap NPs in sol-gel, chitosan or dendrimers.<sup>106–108</sup>

*Carbon nanomaterials* present unique physical and chemical properties such as excellent electrical conductivity, ultra-lightweight, highly ordered structures and high mechanical strength and surface area. These features are responsible for the increasing interest in their incorporation into electrochemical immunosensors. Carbon nanotubes (CNTs), graphene, carbon nanospheres (CNSs) or fullerenes are some carbon nanomaterials with different shapes used in the fabrication of these devices. Two strategies are generally followed for the introduction of these nanomaterials, the first one consists of the direct electrode modification with these structures by simple adsorption or through a covalent link. Herein, they act as the supporting platform for protein immobilization, for instance, CNTs or graphene modified with specific functionalities compatible with those from the F<sub>c</sub> part from the antibodies.<sup>109,110</sup> They can also be doped with metal nanoparticles such as AuNPs or metal oxide nanoparticles as electrocatalysts to enhance the sensing and biosensing performance for biomedical applications.<sup>111–113</sup> The other strategy relies on the assembly of such nanomaterials with polymeric matrices like chitosan,<sup>114,115</sup> (polyamidoamine) dendrimers<sup>116</sup> or nafion polymer.<sup>117</sup>

*Magnetic nanoparticles*, commonly called magnetic beads (MBs), ranging in size from nm to μm are made of a paramagnetic or superparamagnetic core, mainly Fe<sub>2</sub>O<sub>3</sub> or Fe<sub>3</sub>O<sub>4</sub>, covered with a thin shell of polymer that serves as the basis for further modifications.<sup>100</sup> They are biocompatible, with high surface area but their mayor advantage over other nanomaterials is the possibility to control their transporting by using a magnetic field. These structures provide an increase in the antibody loading per bead, reaching lower

detection limits, and a simpler manipulation during the immunoassay, reducing volumes and matrix effect. Moreover, they permit to amplify the signal by selectively concentrating the MBs on the surface of the electrode. MB are commercially available (functionalized or not-functionalized) and have been increasingly used in recent works for the development of electrochemical (magneto)immunosensors. Normally, MBs are used as supports in enzyme-labelled assays for the concentration of the biorecognition elements on the electrode surface and thus, the electrochemical signal.<sup>118,119</sup>

*Conducting polymers* are convenient components to form an appropriate environment for protein immobilization while interacting with the electrode surface. They are generally electrodeposited on the top of the electrode surface and can be doped with metal nanoparticles to achieve better sensitivities. Most frequently used are polypyrrole, polythiol, polyaniline and PEDOT polymers.<sup>120-123</sup>

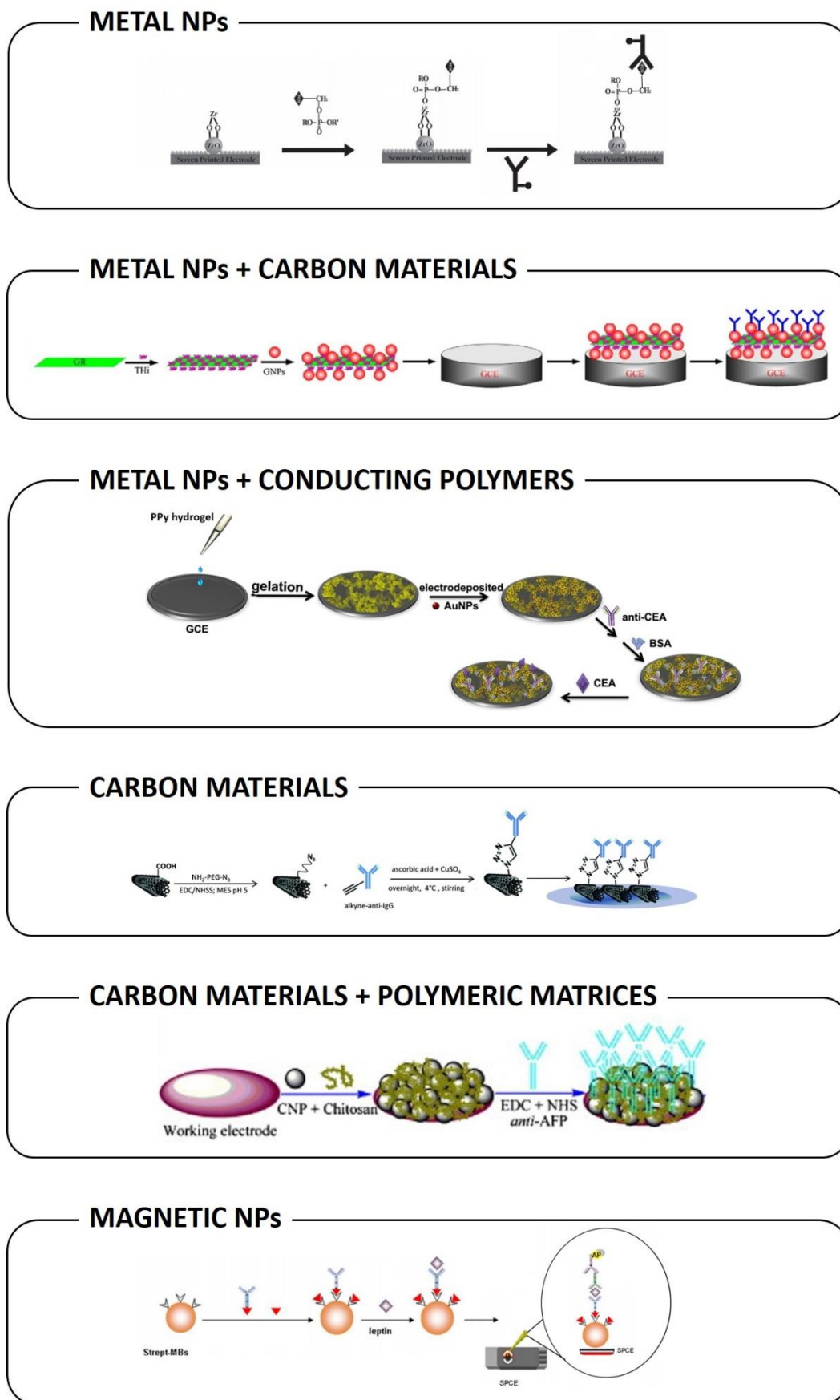


Figure 9. Different strategies of signal amplification based on the use of nanomaterials as sensing platform.<sup>103,104,110,114,118,120</sup>

- Labelling techniques

Despite the importance of molecular orientation and immobilization strategies in signal amplification, a labelling approach based on various bioconjugation techniques can have a great influence on improved sensitivity. The vast majority of electrochemical immunosensors are based on the sandwich-type methodology: capture antibody is immobilised on the substrate and interacts with the antigen. Afterwards, a second antibody tagged with a signalling element binds to the captured antigen. Since immunoassays are usually applied to the detection of ultra-low analyte concentrations, few number of labels are captured per biorecognition event, resulting in low sensitivity. Thus, signal amplification by labelling techniques have attracted much attention in order to achieve better sensitivities and lower detection limits. Among the various signalling elements utilized in the last years, **enzymes** are still the most broadly employed biocatalyst to fabricate enzyme-labelled-based immunosensors.<sup>124</sup> Enzymes are pivotal elements in bioanalysis due to their extremely high catalytic activity. In enzyme-labelled electrochemical immunosensors, the choice of enzymatic substrate is a key step when designing the assay because either the substrate or the product should trigger a traceable electrochemical signal. Popular enzymes are the horse-radish peroxidase (HRP) and the alkaline phosphatase (ALP) that can be easily found conjugated to a wide range of commercial antibodies. These enzymes are able to convert the biorecognition process into an electrochemical signal by two main ways. The first one is based on the use of natural or artificial redox species as an electron-transfer mediators. *Redox mediators* are electroactive compounds that facilitate the electron transfer between the enzyme and the electrode and thereby they can enhance the electrochemical response. Within this type of reagents, reversible redox species are able to carry out oxidation and reduction processes in a repetitive way with no loss of reactivity, so they are used in the so-called “*redox cycling*”. Some examples of cycling amplification are the oxidation of p-aminophenyl by ALP with NADH as reductor, or the use of  $\text{Ru}(\text{NH}_3)_6^{3+}$  complex as redox mediator in the glucose oxidation by using glucose oxidase.<sup>125,126</sup> HRP is able to catalyze the oxidation of these compounds in presence of hydrogen peroxide yielding oxidized mediators that are afterwards electrochemically reduced on the surface of the electrode (e.g., TMB).<sup>127</sup> The second way involves the conversion of electrochemically inactive compounds into a detectable electroactive products. ALP is one of the enzymes with such capabilities, one of the most common reactions is the conversion from p-aminophenyl to p-aminophenol that can be oxidized on the surface of the electrode.<sup>128</sup> Other strategies

involve the conversion of 1-naphthyl phosphate to 1-naphthol and direct detection using differential pulse voltammetry.<sup>129</sup>

Conventional enzymatic labels (HRP, ALP) have been used in electrochemical immunosensors over the years providing good performance and sensitivity. However, they are not suitable enough for ultrasensitive detection; therefore, they need to be coupled to some amplification techniques.

**Nanomaterials** also present outstanding properties that make them a convenient choice for antibody labelling. The seek for more sensitive systems has led to the use of these structures due to their high stability and their efficiency because of their higher redox active sites-to-volume ratio.<sup>130</sup> *Inorganic nanomaterials* such as AuNPs or Quantum dots (QDs) has proven their exceptional behaviour as electrochemical labels in a great range of applications.<sup>131,132</sup> Direct measurement of inorganic labels are usually carried out by square wave voltammetry where the metal oxidation and reduction is measured on the surface of the electrode yielding a signal proportional to the amount of nanoparticles linked to the antibodies. Moreover, some structures present catalytic properties similar to the enzymes such as the nanostructure made of cuprous oxide nanowires functionalized with silver nanoparticles.<sup>133</sup> Additionally, different nanomaterials have been used as *nanovehicles or nanocarriers* including AuNP, carbon nanotubes (CNT), graphene, liposome and their composites. Thanks to their large surface area they can be loaded with a higher amount of antibodies and signal tracers. This coimmobilization allows to increase the amount of sensing labels on the surface of the electrode resulting in a highly sensitive detection. AuNP, graphene and CNT can act as nanocarriers by themselves, but they can be also be combined in the same structure (e.g., CNT or graphene functionalized with AuNPs).<sup>114,134,135</sup> Liposome is a unique nanocarrier capable of transporting different agents in their aqueous cavities.<sup>136</sup> Nano-composites are also employed for signal amplification by combining nanoparticles with polymer nanospheres or even mesoporous silica nanoparticles.<sup>137–139</sup>

Recently, the combination of **enzymes and nanoparticles** have attracted much attention as signal amplification strategy. Biosensing strategies based on enzymatic reactions and NPs provide highly sensitive and versatile approaches with enormous possibilities for electrochemical immunosensors. NPs properties strongly depend on their size that can be modulated by their physical and chemical environment. The products of enzymatic reactions can interact with them, resulting in modification of their measurable

properties.<sup>140</sup> There are three principal ways to carry out these modifications: enzymatic growth or etching of NPs and interference by the products of enzymatic reactions.

*Enzymatic growth of NPs* is based on the formation of NPs or QDs by using particular enzymatic product precursors and an additional reagent or seed. One example is the in situ formation of CdS QDs through the catalytic generation of  $\text{PO}_4^{3-}$  and  $\text{S}^{2-}$  using ALP for their further photoelectrochemical detection on carbon electrodes.<sup>141</sup> On the other hand, AgNPs have been enlarged via deposition of Ag reduced by ascorbic acid resulting from the ALP reaction with ascorbic acid 2-phosphate using stripping voltammetry detection.<sup>142</sup> This methodology improves and decreases cost of procedure since no previous NPs synthesis is required. Moreover, it simplifies the overall process reducing assay steps and allows for the direct measurement of NPs grown in situ.

*Enzymatic etching of NPs*, on the contrary, employs the enzymatic reactions to etch NPs or nanostructures contained in the system. Some enzymes generate oxidant products (e.g.,  $\text{H}_2\text{O}_2$ ) that can be employed in the NPs degradation leading to a change in their physicochemical properties. Glucose oxidase enzyme generate  $\text{H}_2\text{O}_2$  in nature, so it has been employed in immunoassays for the etching of NPs other nanostructures, for example, the reducing/etching of  $\text{MnO}_2$  nanosheets doped with CdS QDs producing the reduction in photocurrent.<sup>143</sup>

*Enzymatic product interference* strategy involves the use of enzymatic products in the modification and/or passivation of the NPs surface. As an example, HRP is able to catalyze the oxidation of 4-chloro-1-naphthol to produce a layer of insoluble precipitate and thus, causing a change in the impedance of the system.<sup>144</sup> Besides, HRP can also induce biocatalytic precipitation of blocking species on CdS nanocrystals immobilised on carbon electrodes reducing the electrochemiluminescence signal.<sup>145</sup>

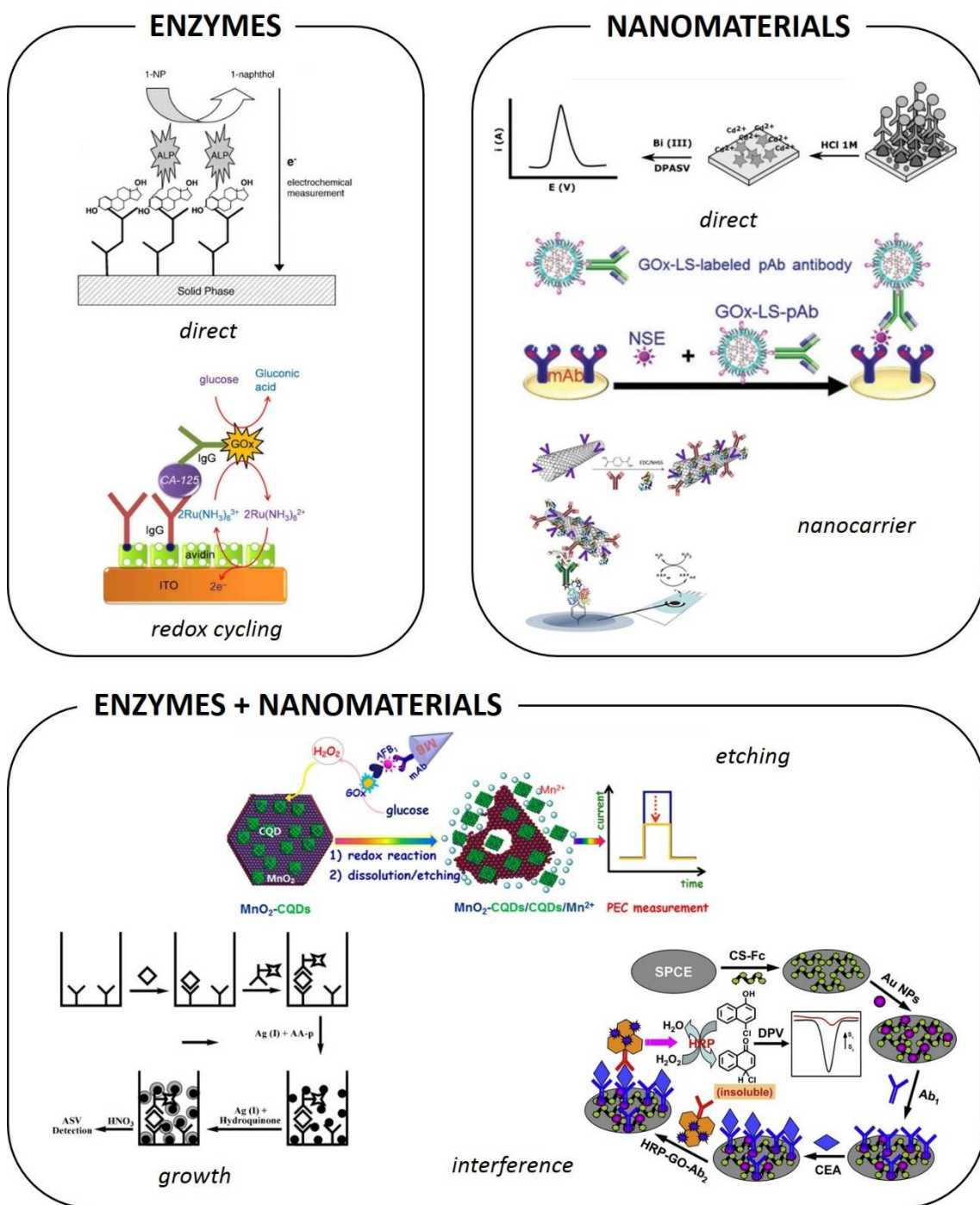


Figure 10. Labelling techniques for signal amplification based on the use of enzymes,<sup>126,129</sup> nanomaterials<sup>132,134,136</sup> and enzymatic modulation of NPs.<sup>146–148</sup>



## References

- (1) Turner, A. P. F.; Karube, I.; Wilson, G. S.; Worsfold, P. J. *Biosensors: Fundamentals and Applications*; 1987; Vol. 201.
- (2) Clark Jr., L. C.; Lyons, C. ELECTRODE SYSTEMS FOR CONTINUOUS MONITORING IN CARDIOVASCULAR SURGERY. *Ann. N. Y. Acad. Sci.* **1962**, *102* (1), 29–45.
- (3) Lee, T. M. H. Over-the-Counter Biosensors: Past, Present, and Future. *Sensors* **2008**, *8* (9), 5535–5559.
- (4) Turner, A. Biosensors: Then and Now. *Trends Biotechnol.* **2013**, *31* (3), 119–120.
- (5) Grand View Research. *Biosensors Market Size, Share & Trends Analysis Report By Application (Agriculture, Medical) By Technology (Thermal, Electrochemical, Optical), By End Use (PoC Testing, Food Industry), And Segment Forecasts, 2019 - 2026*; 2017.
- (6) Hock, B.; Seifert, M.; Kramer, K. Engineering Receptors and Antibodies for Biosensors. *Biosens. Bioelectron.* **2002**, *17* (3), 239–249.
- (7) Widge, A. S.; Jeffries-El, M.; Cui, X.; Lagenaur, C. F.; Matsuoka, Y. Self-Assembled Monolayers of Polythiophene Conductive Polymers Improve Biocompatibility and Electrical Impedance of Neural Electrodes. *Biosens. Bioelectron.* **2007**, *22* (8), 1723–1732.
- (8) Wang, Y.; Papadimitrakopoulos, F.; Burgess, D. J. Polymeric “Smart” Coatings to Prevent Foreign Body Response to Implantable Biosensors. *J. Control. Release* **2013**, *169* (3), 341–347.
- (9) Andreescu, D.; Andreescu, S.; Sadik, O. A. B. T.-C. A. C. Chapter 7 New Materials for Biosensors, Biochips and Molecular Bioelectronics. In *Biosensors and Modern Biospecific Analytical Techniques*; Elsevier, 2005; Vol. 44, pp 285–327.
- (10) Lee, Y. H.; Mutharasan, R. Biosensors. In *Sensor Technology Handbook*; Elsevier, 2005; pp 161–180.
- (11) Chakraborty, M.; Hashmi, M. S. J. An Overview of Biosensors and Devices. *Ref. Modul. Mater. Sci. Mater. Eng.* **2017**, 1–24.
- (12) Sang, S.; Zhang, W.; Zhao, Y. Review on the Design Art of Biosensors. In *State of the Art in Biosensors - General Aspects*; 2013.
- (13) Monošík, R.; Stredánský, M.; Šturdík, E. Biosensors - Classification, Characterization and New Trends. *Acta Chim. Slovaca* **2012**, *5* (1), 109–120.
- (14) Wu, S.; Zhang, H.; Shi, Z.; Duan, N.; Fang, C.; Dai, S.; Wang, Z. Aptamer-Based Fluorescence Biosensor for Chloramphenicol Determination Using Upconversion Nanoparticles. *Food Control* **2015**, *50*, 597–604.
- (15) Meng, X.; Wei, J.; Ren, X.; Ren, J.; Tang, F. A Simple and Sensitive Fluorescence Biosensor for Detection of Organophosphorus Pesticides Using H<sub>2</sub>O<sub>2</sub>-Sensitive Quantum Dots/Bi-Enzyme. *Biosens. Bioelectron.* **2013**, *47*, 402–407.
- (16) Yu, J.; Ge, L.; Huang, J.; Wang, S.; Ge, S. Microfluidic Paper-Based Chemiluminescence Biosensor for Simultaneous Determination of Glucose and Uric Acid. *Lab Chip* **2011**, *11* (7), 1286–1291.
- (17) Roda, A.; Guardigli, M.; Calabria, D.; Calabretta, M. M.; Cevenini, L.; Michelini, E. A 3D-Printed Device for a Smartphone-Based Chemiluminescence Biosensor for Lactate in Oral Fluid and Sweat. *Analyst* **2014**, *139* (24), 6494–6501.
- (18) Gow, S. M.; Caldwell, G.; Toft, A. D.; Beckett, G. J. SimulTRAC Simultaneous Radioimmunoassay of Thyrotropin and Free Thyroxin Evaluated. *Clin. Chem.* **1986**, *32* (12), 2191 LP-2194.
- (19) Nedelkov, D.; Nelson, R. W. Practical Considerations in BIA/MS: Optimizing the Biosensor–mass Spectrometry Interface. *J. Mol. Recognit.* **2000**, *13* (3), 140–145.
- (20) Indyk, H. E.; Filonzi, E. L. Determination of Immunoglobulin G in Bovine Colostrum and Milk by Direct Biosensor SPR-Immunoassay. *J. AOAC Int.* **2003**, *86*, 386–393.

- (21) Dudak, F. C.; Boyacı, İ. H. Rapid and Label-Free Bacteria Detection by Surface Plasmon Resonance (SPR) Biosensors. *Biotechnol. J.* **2009**, *4* (7), 1003–1011.
- (22) Barrios, C. A.; Bañuls, M. J.; González-Pedro, V.; Gylfason, K. B.; Sánchez, B.; Griol, A.; Maquieira, A.; Sohlström, H.; Holgado, M.; Casquel, R. Label-Free Optical Biosensing with Slot-Waveguides. *Opt. Lett.* **2008**, *33* (7), 708–710.
- (23) Mun, K.-S.; Alvarez, S. D.; Choi, W.-Y.; Sailor, M. J. A Stable, Label-Free Optical Interferometric Biosensor Based on TiO<sub>2</sub> Nanotube Arrays. *ACS Nano* **2010**, *4* (4), 2070–2076.
- (24) Bazin, I.; Tria, S. A.; Hayat, A.; Marty, J.-L. New Biorecognition Molecules in Biosensors for the Detection of Toxins. *Biosens. Bioelectron.* **2017**, *87*, 285–298.
- (25) Saini, R. K.; Bagri, L. P.; Bajpai, A. K. *Smart Nanosensors for Pesticide Detection*; Elsevier Inc., 2017.
- (26) Justino, C. I. L.; Freitas, A. C.; Pereira, R.; Duarte, A. C.; Rocha Santos, T. A. P. Recent Developments in Recognition Elements for Chemical Sensors and Biosensors. *TrAC - Trends Anal. Chem.* **2015**, *68*, 2–17.
- (27) Odobašić, A.; Šestan, I.; Begić, S. Biosensors for Determination of Heavy Metals in Waters. In *Biosensors for environmental monitoring*; Rinken, T., Kivirand, K., Eds.; 2019.
- (28) Adrian, P. Key Opportunities and Trends in Biosensors <https://fhi.nl/app/uploads/sites/57/2018/12/Micro-Nano-Slides-December-8-2018-Final.pdf>.
- (29) Justino, C. I. L.; Duarte, A. C.; Rocha-Santos, T. A. P. Critical Overview on the Application of Sensors and Biosensors for Clinical Analysis. *TrAC - Trends Anal. Chem.* **2016**, *85*, 36–60.
- (30) Yusan, S.; Rahman, M. M.; Mohamad, N.; Arrif, T. M.; Latif, A. Z. A.; M. A., M. A.; Nik, W. S. B. W. Development of an Amperometric Glucose Biosensor Based on the Immobilization of Glucose Oxidase on the Se-MCM-41 Mesoporous Composite. *J. Anal. Methods Chem.* **2018**, *2018*, 8.
- (31) Bahadir, E. B.; Sezgintürk, M. K. Applications of Commercial Biosensors in Clinical, Food, Environmental, and Biothreat/Biowarfare Analyses. *Anal. Biochem.* **2015**, *478*, 107–120.
- (32) Ali, J.; Najeeb, J.; Asim Ali, M.; Farhan Aslam, M.; Raza, A. Biosensors: Their Fundamentals, Designs, Types and Most Recent Impactful Applications: A Review. *J. Biosens. Bioelectron.* **2017**, *08* (01), 1–9.
- (33) Fan, J.; Wang, M.; Wang, C.; Cao, Y. Advances in Human Chorionic Gonadotropin Detection Technologies: A Review. *Bioanalysis* **2017**, *9* (19), 1509–1529.
- (34) Infiniti Research Limited. *Global Cholesterol Testing Devices Market 2018-2022*; 2018.
- (35) Saylan, Y.; Erdem, Ö.; Ünal, S.; Denizli, A. An Alternative Medical Diagnosis Method: Biosensors for Virus Detection. *Biosensors* **2019**, *9* (2), 65.
- (36) GRAN VIEW RESEARCH. Helicobacter Pylori Diagnostics Market Size, Share & Trends Analysis Report By Technology (Immunoassays, POC, Molecular Diagnostics), By End User, By Region, And Segment Forecasts, 2019 - 2026 <https://www.grandviewresearch.com/industry-analysis/helicobacter-pylori-diagnostics-market>.
- (37) Gray, E. R.; Turbé, V.; Lawson, V. E.; Page, R. H.; Cook, Z. C.; Ferns, R. B.; Nastouli, E.; Pillay, D.; Yatsuda, H.; Athey, D.; et al. Ultra-Rapid, Sensitive and Specific Digital Diagnosis of HIV with a Dual-Channel SAW Biosensor in a Pilot Clinical Study. *npj Digit. Med.* **2018**, *1* (1), 35.
- (38) Kanayeva, D.; Bekniyazov, I.; Ashikbayeva, Z. Detection of Tuberculosis Using Biosensors: Recent Progress and Future Trends. *Sensors & Transducers* **2013**, *149* (2), 166.
- (39) Martín-Díaz, A.; Rubio, J. M.; Herrero-Martínez, J. M.; Lizasoain, M.; Ruiz-Giardin, J. M.; Jaqueti, J.; Cuadros, J.; Rojo-Marcos, G.; Martín-Rabadán, P.; Calderón, M.; et al. Study of the Diagnostic Accuracy of Microbiological Techniques in the Diagnosis of Malaria in the Immigrant Population in Madrid. *Malar. J.* **2018**, *17* (1), 1–8.

- (40) Terry, L. A.; White, S. F.; Tigwell, L. J. The Application of Biosensors to Fresh Produce and the Wider Food Industry. *J. Agric. Food Chem.* **2005**, *53* (5), 1309–1316.
- (41) Mustafa, F.; Andreescu, S. Chemical and Biological Sensors for Food-Quality Monitoring and Smart Packaging. *Foods* **2018**, *7* (10).
- (42) Singh, R.; Mukherjee, M. Das; Sumana, G.; Gupta, R. K.; Sood, S.; Malhotra, B. D. Biosensors for Pathogen Detection: A Smart Approach towards Clinical Diagnosis. *Sensors Actuators B Chem.* **2014**, *197*, 385–404.
- (43) Thakur, M. S.; Ragavan, K. V. Biosensors in Food Processing. *J. Food Sci. Technol.* **2013**, *50* (4), 625–641.
- (44) Majdinasab, M.; Yaqub, M.; Rahim, A.; Catanante, G.; Hayat, A.; Marty, J. An Overview on Recent Progress in Electrochemical Biosensors for Antimicrobial Drug Residues in Animal-Derived Food. *Sensors* **2017**, *17*.
- (45) Oluwaseun, A. C.; Phazang, P.; Sarin, N. B. Biosensors: A Fast-Growing Technology for Pathogen Detection in Agriculture and Food Sector. In *Biosensing Technologies for the Detection of Pathogens - A Prospective Way for Rapid Analysis*; Rinken, T., Kivirand, K., Eds.; IntechOpen, 2017.
- (46) Edelstein, R. L.; Tamanaha, C. R.; Sheehan, P. E.; Miller, M. M.; Baselt, D. R.; Whitman, L. J.; Colton, R. J. The BARC Biosensor Applied to the Detection of Biological Warfare Agents. *Biosens. Bioelectron.* **2000**, *14* (10), 805–813.
- (47) Pohanka, M. Current Trends in the Biosensors for Biological Warfare Agents Assay. *Materials (Basel)*. **2019**, *12* (14).
- (48) Kumar, H.; Rani, R. Development of Biosensors for the Detection of Biological Warfare Agents: Its Issues and Challenges. *Sci. Prog.* **2013**, *96* (3), 294–308.
- (49) Scognamiglio, V.; Pezzotti, G.; Pezzotti, I.; Cano, J.; Buonasera, K.; Giannini, D.; Giardi, M. T. Biosensors for Effective Environmental and Agrifood Protection and Commercialization: From Research to Market. *Microchim. Acta* **2010**, *170* (3), 215–225.
- (50) Liu, J.; Mattiasson, B. Microbial BOD Sensors for Wastewater Analysis. *Water Res.* **2002**, *36* (15), 3786–3802.
- (51) Ríos, Á.; Zougagh, M.; Avila, M. Miniaturization through Lab-on-a-Chip: Utopia or Reality for Routine Laboratories? A Review. *Anal. Chim. Acta* **2012**, *740*, 1–11.
- (52) Menegatti, E.; Berardi, D.; Messina, M.; Ferrante, I.; Giachino, O.; Spagnolo, B.; Restagno, G.; Cognolato, L.; Roccatello, D. Lab-on-a-Chip: Emerging Analytical Platforms for Immune-Mediated Diseases. *Autoimmun. Rev.* **2013**, *12* (8), 814–820.
- (53) Whitesides, G. M. The Origins and the Future of Microfluidics. *Nature* **2006**, *442* (7101), 368–373.
- (54) Gad-el-Hak, M. *MEMS: Introduction and Fundamentals*; CRC press, 2005.
- (55) Terry, S. C.; Jerman, J. H.; Angell, J. B. A Gas Chromatographic Air Analyzer Fabricated on a Silicon Wafer. *IEEE Trans. Electron Devices* **1979**, *26* (12), 1880–1886.
- (56) Manz, A.; Graber, N.; Widmer, H. M. Miniaturized Total Chemical Analysis Systems: A Novel Concept for Chemical Sensing. *Sensors Actuators B Chem.* **1990**, *1* (1), 244–248.
- (57) Castillo-Leon, J.; Svendsen, W. E. *Lab-on-a-Chip Devices and Micro-Total Analysis Systems: A Practical Guide*; Springer, 2014.
- (58) Reyes, D. R.; Iossifidis, D.; Auroux, P.-A.; Manz, A. Micro Total Analysis Systems. 1. Introduction, Theory, and Technology. *Anal. Chem.* **2002**, *74* (12), 2623–2636.
- (59) Xia, Y.; Whitesides, G. M. SOFT LITHOGRAPHY. *Annu. Rev. Mater. Sci.* **1998**, *28* (1), 153–184.
- (60) Qin, D.; Xia, Y.; Black, A. J.; Whitesides, G. M. Photolithography with Transparent Reflective Photomasks. *J. Vac. Sci. Technol. B Microelectron. Nanom. Struct. Process. Meas. Phenom.* **1998**, *16* (1), 98–103.
- (61) Zhao, X.-M.; Xia, Y.; Whitesides, G. M. Soft Lithographic Methods for Nano-Fabrication. *J. Mater. Chem.* **1997**, *7* (7), 1069–1074.
- (62) Liu, C.-X.; Choi, J.-W. Patterning Conductive PDMS Nanocomposite in an Elastomer Using

- Microcontact Printing. *J. Micromechanics Microengineering* **2009**, *19* (8), 85019.
- (63) Martinez, A. W.; Phillips, S. T.; Butte, M. J.; Whitesides, G. M. Patterned Paper as a Platform for Inexpensive, Low-Volume, Portable Bioassays. *Angew. Chemie Int. Ed.* **2007**, *46* (8), 1318–1320.
- (64) Yazdi, A. A.; Popma, A.; Wong, W.; Nguyen, T.; Pan, Y.; Xu, J. 3D Printing: An Emerging Tool for Novel Microfluidics and Lab-on-a-Chip Applications. *Microfluid. Nanofluidics* **2016**, *20* (3), 50.
- (65) Vakilian, M.; Yeop Majlis, B.; Mousavi, M. A Bibliometric Analysis of Lab-on-a-Chip Research from 2001 to 2013. *Scientometrics* **2015**, *105* (2), 789–804.
- (66) Mendes, F. M. L.; Castor, K.; Monteiro, R.; Mota, F. B.; Rocha, L. F. M. Mapping the Lab-on-a-Chip Patent Landscape through Bibliometric Techniques. *World Pat. Inf.* **2019**, *58*, 101904.
- (67) Nikoleli, G.-P.; Siontorou, C. G.; Nikolelis, D. P.; Bratakou, S.; Karapetis, S.; Tzamtzis, N. Chapter 13 - Biosensors Based on Microfluidic Devices Lab-on-a-Chip and Microfluidic Technology. In *Advanced Nanomaterials*; Nikolelis, D. P., Nikoleli, G.-P. B. T.-N. and B., Eds.; Elsevier, 2018; pp 375–394.
- (68) Jung, W.; Han, J.; Choi, J. W.; Ahn, C. H. Point-of-Care Testing (POCT) Diagnostic Systems Using Microfluidic Lab-on-a-Chip Technologies. *Microelectron. Eng.* **2015**, *132*, 46–57.
- (69) Dittrich, P. S.; Manz, A. Lab-on-a-Chip: Microfluidics in Drug Discovery. *Nat. Rev. Drug Discov.* **2006**, *5* (3), 210–218.
- (70) Koczula, K. M.; Gallotta, A. Lateral Flow Assays. *Essays Biochem.* **2016**, *60* (1), 111–120.
- (71) An, D.; Kim, K.; Kim, J. Microfluidic System Based High Throughput Drug Screening System for Curcumin/TRAIL Combinational Chemotherapy in Human Prostate Cancer PC3 Cells. *Biomol. Ther. (Seoul)*. **2014**, *22* (4), 355–362.
- (72) Byrnes, S. A.; Weigl, B. H. Selecting Analytical Biomarkers for Diagnostic Applications: A First Principles Approach. *Expert Rev. Mol. Diagn.* **2018**, *18* (1), 19–26.
- (73) Warsinke, A. Point-of-Care Testing of Proteins. *Anal. Bioanal. Chem.* **2009**, *393*, 1393–1405.
- (74) Burcu Bahadir, E.; Kemal Sezgintürk, M. Applications of Electrochemical Immunosensors for Early Clinical Diagnostics. *Talanta* **2015**, *132*, 162–174.
- (75) Mahato, K.; Kumar, S.; Srivastava, A.; Maurya, P. K.; Singh, R.; Chandra, P. Chapter 14 - Electrochemical Immunosensors: Fundamentals and Applications in Clinical Diagnostics. In *Handbook of Immunoassay Technologies*; Vashist, S. K., Luong, J. H. T. B. T.-H. of I. T., Eds.; Academic Press, 2018; pp 359–414.
- (76) Felix, F. S.; Angnes, L. Electrochemical Immunosensors – A Powerful Tool for Analytical Applications. *Biosens. Bioelectron.* **2018**, *102* (November 2017), 470–478.
- (77) Bartlett, P. N. *Bioelectrochemistry: Fundamentals, Experimental Techniques and Applications*; Wiley, 2008.
- (78) Heineman, W. R.; Halsall, H. B. Strategies for Electrochemical Immunoassay. *Anal. Chem.* **1985**, *57* (12), 1321A–1331A.
- (79) Killard, A. J.; Deasy, B.; O’Kennedy, R.; Smyth, M. R. Antibodies: Production, Functions and Applications in Biosensors. *TrAC Trends Anal. Chem.* **1995**, *14* (6), 257–266.
- (80) Fowler, J. M.; Wong, D. K. Y.; Halsall, H. B.; Heineman, W. R. CHAPTER 5 - Recent Developments in Electrochemical Immunoassays and Immunosensors; Zhang, X., Ju, H., Wang Biosensors and their Biomedical Applications, J. B. T.-E. S., Eds.; Academic Press: San Diego, 2008; pp 115–143.
- (81) Makaraviciute, A.; Ramanaviciene, A. Site-Directed Antibody Immobilization Techniques for Immunosensors. *Biosens. Bioelectron.* **2013**, *50*, 460–471.
- (82) Lim, S. A.; Yoshikawa, H.; Tamiya, E.; Yasin, H. M.; Ahmed, M. U. A Highly Sensitive Gold Nanoparticle Bioprobe Based Electrochemical Immunosensor Using Screen Printed Graphene Biochip. *RSC Adv.* **2014**, *4* (102), 58460–58466.
- (83) Rezaei, B.; Majidi, N.; Rahmani, H.; Khayamian, T. Electrochemical Impedimetric

- Immunosensor for Insulin like Growth Factor-1 Using Specific Monoclonal Antibody-Nanogold Modified Electrode. *Biosens. Bioelectron.* **2011**, *26* (5), 2130–2134.
- (84) Wilson, M. S.; Rauh, R. D. Novel Amperometric Immunosensors Based on Iridium Oxide Matrices. *Biosens. Bioelectron.* **2004**, *19* (7), 693–699.
- (85) Sánchez, S.; Roldán, M.; Pérez, S.; Fàbregas, E. Toward a Fast, Easy, and Versatile Immobilization of Biomolecules into Carbon Nanotube/Polysulfone-Based Biosensors for the Detection of HCG Hormone. *Anal. Chem.* **2008**, *80* (17), 6508–6514.
- (86) Eissa, S.; Tlili, C.; L'Hocine, L.; Zourob, M. Electrochemical Immunosensor for the Milk Allergen  $\beta$ -Lactoglobulin Based on Electrografting of Organic Film on Graphene Modified Screen-Printed Carbon Electrodes. *Biosens. Bioelectron.* **2012**, *38* (1), 308–313.
- (87) Hayat, A.; Barthelmebs, L.; Sassolas, A.; Marty, J.-L. An Electrochemical Immunosensor Based on Covalent Immobilization of Okadaic Acid onto Screen Printed Carbon Electrode via Diazotization-Coupling Reaction. *Talanta* **2011**, *85* (1), 513–518.
- (88) Reverté, L.; Campbell, K.; Rambla-Alegre, M.; Elliott, C. T.; Diogène, J.; Campàs, M. Immunosensor Array Platforms Based on Self-Assembled Dithiols for the Electrochemical Detection of Tetrodotoxins in Puffer Fish. *Anal. Chim. Acta* **2017**, *989*, 95–103.
- (89) Pampalakis, G.; Kelley, S. O. An Electrochemical Immunosensor Based on Antibody–nanowire Conjugates. *Analyst* **2009**, *134* (3), 447–449.
- (90) Zhang, X.; Shen, G.; Sun, S.; Shen, Y.; Zhang, C.; Xiao, A. Direct Immobilization of Antibodies on Dialdehyde Cellulose Film for Convenient Construction of an Electrochemical Immunosensor. *Sensors Actuators B Chem.* **2014**, *200*, 304–309.
- (91) Liu, X.; Wang, X.; Zhang, J.; Feng, H.; Liu, X.; Wong, D. K. Y. Detection of Estradiol at an Electrochemical Immunosensor with a Cu UPD|DTBP–Protein G Scaffold. *Biosens. Bioelectron.* **2012**, *35* (1), 56–62.
- (92) Gao, D.; McBean, N.; Schultz, J. S.; Yan, Y.; Mulchandani, A.; Chen, W. Fabrication of Antibody Arrays Using Thermally Responsive Elastin Fusion Proteins. *J. Am. Chem. Soc.* **2006**, *128* (3), 676–677.
- (93) Ho, J. A.; Hsu, W.-L.; Liao, W.-C.; Chiu, J.-K.; Chen, M.-L.; Chang, H.-C.; Li, C.-C. Ultrasensitive Electrochemical Detection of Biotin Using Electrically Addressable Site-Oriented Antibody Immobilization Approach via Aminophenyl Boronic Acid. *Biosens. Bioelectron.* **2010**, *26* (3), 1021–1027.
- (94) Wang, J.; Liu, G.; Jan, M. R. Ultrasensitive Electrical Biosensing of Proteins and DNA: Carbon-Nanotube Derived Amplification of the Recognition and Transduction Events. *J. Am. Chem. Soc.* **2004**, *126* (10), 3010–3011.
- (95) Jung, Y.; Lee, J. M.; Jung, H.; Chung, B. H. Self-Directed and Self-Oriented Immobilization of Antibody by Protein G–DNA Conjugate. *Anal. Chem.* **2007**, *79* (17), 6534–6541.
- (96) Vallina-García, R.; del Mar García-Suárez, M.; Fernández-Abedul, M. T.; Méndez, F. J.; Costa-García, A. Oriented Immobilisation of Anti-Pneumolysin Fab through a Histidine Tag for Electrochemical Immunosensors. *Biosens. Bioelectron.* **2007**, *23* (2), 210–217.
- (97) Ricci, F.; Adornetto, G.; Palleschi, G. A Review of Experimental Aspects of Electrochemical Immunosensors. *Electrochim. Acta* **2012**, *84*, 74–83.
- (98) Kissinger, P.; Heineman, W. R. *Laboratory Techniques in Electroanalytical Chemistry, Revised and Expanded*; CRC Press, Ed.; 1996.
- (99) Gogotsi, Y. *Nanomaterials Handbook*; CRC Press, 2017.
- (100) Reverté, L.; Prieto-Simón, B.; Campàs, M. New Advances in Electrochemical Biosensors for the Detection of Toxins: Nanomaterials, Magnetic Beads and Microfluidics Systems. A Review. *Anal. Chim. Acta* **2016**, *908*, 8–21.
- (101) Wang, G.; Huang, H.; Zhang, G.; Zhang, X.; Fang, B.; Wang, L. Gold Nanoparticles/l-Cysteine/Graphene Composite Based Immobilization Strategy for an Electrochemical Immunosensor. *Anal. Methods* **2010**, *2* (11), 1692–1697.
- (102) Ahirwal, G. K.; Mitra, C. K. Gold Nanoparticles Based Sandwich Electrochemical

- Immunosensor. *Biosens. Bioelectron.* **2010**, *25* (9), 2016–2020.
- (103) Kong, F.-Y.; Xu, M.-T.; Xu, J.-J.; Chen, H.-Y. A Novel Label-Free Electrochemical Immunosensor for Carcinoembryonic Antigen Based on Gold Nanoparticles–thionine–reduced Graphene Oxide Nanocomposite Film Modified Glassy Carbon Electrode. *Talanta* **2011**, *85* (5), 2620–2625.
- (104) Lu, D.; Wang, J.; Wang, L.; Du, D.; Timchalk, C.; Barry, R.; Lin, Y. A Novel Nanoparticle-Based Disposable Electrochemical Immunosensor for Diagnosis of Exposure to Toxic Organophosphorus Agents. *Adv. Funct. Mater.* **2011**, *21* (22), 4371–4378.
- (105) Huang, J.; Yang, G.; Meng, W.; Wu, L.; Zhu, A.; Jiao, X. An Electrochemical Impedimetric Immunosensor for Label-Free Detection of *Campylobacter Jejuni* in Diarrhea Patients' Stool Based on O-Carboxymethylchitosan Surface Modified Fe<sub>3</sub>O<sub>4</sub> Nanoparticles. *Biosens. Bioelectron.* **2010**, *25* (5), 1204–1211.
- (106) Lin, J.; He, C.; Zhang, L.; Zhang, S. Sensitive Amperometric Immunosensor for  $\alpha$ -Fetoprotein Based on Carbon Nanotube/Gold Nanoparticle Doped Chitosan Film. *Anal. Biochem.* **2009**, *384* (1), 130–135.
- (107) Wang, G.; He, X.; Chen, L.; Zhu, Y.; Zhang, X. Ultrasensitive IL-6 Electrochemical Immunosensor Based on Au Nanoparticles-Graphene-Silica Biointerface. *Colloids Surfaces B Biointerfaces* **2014**, *116*, 714–719.
- (108) Kavosi, B.; Hallaj, R.; Teymourian, H.; Salimi, A. Au Nanoparticles/PAMAM Dendrimer Functionalized Wired Ethyleneamine–viologen as Highly Efficient Interface for Ultra-Sensitive  $\alpha$ -Fetoprotein Electrochemical Immunosensor. *Biosens. Bioelectron.* **2014**, *59*, 389–396.
- (109) Li, H.; He, J.; Li, S.; Turner, A. P. F. Electrochemical Immunosensor with N-Doped Graphene-Modified Electrode for Label-Free Detection of the Breast Cancer Biomarker CA 15-3. *Biosens. Bioelectron.* **2013**, *43*, 25–29.
- (110) Sánchez-Tirado, E.; González-Cortés, A.; Yáñez-Sedeño, P.; Pingarrón, J. M. Carbon Nanotubes Functionalized by Click Chemistry as Scaffolds for the Preparation of Electrochemical Immunosensors. Application to the Determination of TGF-Beta 1 Cytokine. *Analyst* **2016**, *141* (20), 5730–5737.
- (111) Serafín, V.; Martínez-García, G.; Agúí, L.; Yáñez-Sedeño, P.; Pingarrón, J. M. Multiplexed Determination of Human Growth Hormone and Prolactin at a Label Free Electrochemical Immunosensor Using Dual Carbon Nanotube–screen Printed Electrodes Modified with Gold and PEDOT Nanoparticles. *Analyst* **2014**, *139* (18), 4556–4563.
- (112) Lu, J.; Liu, S.; Ge, S.; Yan, M.; Yu, J.; Hu, X. Ultrasensitive Electrochemical Immunosensor Based on Au Nanoparticles Dotted Carbon Nanotube–graphene Composite and Functionalized Mesoporous Materials. *Biosens. Bioelectron.* **2012**, *33* (1), 29–35.
- (113) Xue, X.; Wei, D.; Feng, R.; Wang, H.; Wei, Q.; Du, B. Label-Free Electrochemical Immunosensors for the Detection of Zeranol Using Graphene Sheets and Nickel Hexacyanoferrate Nanocomposites. *Anal. Methods* **2013**, *5* (16), 4159–4164.
- (114) Tang, J.; Su, B.; Tang, D.; Chen, G. Conductive Carbon Nanoparticles-Based Electrochemical Immunosensor with Enhanced Sensitivity for  $\alpha$ -Fetoprotein Using Irregular-Shaped Gold Nanoparticles-Labeled Enzyme-Linked Antibodies as Signal Improvement. *Biosens. Bioelectron.* **2010**, *25* (12), 2657–2662.
- (115) Samanman, S.; Numnuam, A.; Limbut, W.; Kanatharana, P.; Thavarungkul, P. Highly-Sensitive Label-Free Electrochemical Carcinoembryonic Antigen Immunosensor Based on a Novel Au Nanoparticles–graphene–chitosan Nanocomposite Cryogel Electrode. *Anal. Chim. Acta* **2015**, *853*, 521–532.
- (116) Ma, L.; Ning, D.; Zhang, H.; Zheng, J. Au@Ag Nanorods Based Electrochemical Immunoassay for Immunoglobulin G with Signal Enhancement Using Carbon Nanofibers-Polyamidoamine Dendrimer Nanocomposite. *Biosens. Bioelectron.* **2015**, *68*, 175–180.
- (117) Viswanathan, S.; Wu, L.; Huang, M.-R.; Ho, J. A. Electrochemical Immunosensor for Cholera Toxin Using Liposomes and Poly(3,4-Ethylenedioxythiophene)-Coated Carbon

- Nanotubes. *Anal. Chem.* **2006**, *78* (4), 1115–1121.
- (118) Ojeda, I.; Moreno-Guzmán, M.; González-Cortés, A.; Yáñez-Sedeño, P.; Pingarrón, J. M. A Disposable Electrochemical Immunosensor for the Determination of Leptin in Serum and Breast Milk. *Analyst* **2013**, *138* (15), 4284–4291.
- (119) Zhang, L.; Song, P.; Long, H.; Meng, M.; Yin, Y.; Xi, R. Magnetism Based Electrochemical Immunosensor for Chiral Separation of Amlodipine. *Sensors Actuators B Chem.* **2017**, *248*, 682–689.
- (120) Rong, Q.; Han, H.; Feng, F.; Ma, Z. Network Nanostructured Polypyrrole Hydrogel/Au Composites as Enhanced Electrochemical Biosensing Platform. *Sci. Rep.* **2015**, *5* (1), 11440.
- (121) Liu, Z.; Ma, Z. Fabrication of an Ultrasensitive Electrochemical Immunosensor for CEA Based on Conducting Long-Chain Polythiols. *Biosens. Bioelectron.* **2013**, *46*, 1–7.
- (122) Wang, L.; Shan, J.; Feng, F.; Ma, Z. Novel Redox Species Polyaniline Derivative-Au/Pt as Sensing Platform for Label-Free Electrochemical Immunoassay of Carbohydrate Antigen 199. *Anal. Chim. Acta* **2016**, *911*, 108–113.
- (123) Guo, Y.; Wang, Y.; Liu, S.; Yu, J.; Wang, H.; Cui, M.; Huang, J. Electrochemical Immunosensor Assay (EIA) for Sensitive Detection of E. Coli O157:H7 with Signal Amplification on a SG–PEDOT–AuNPs Electrode Interface. *Analyst* **2015**, *140* (2), 551–559.
- (124) Yang, H. Enzyme-Based Ultrasensitive Electrochemical Biosensors. *Curr. Opin. Chem. Biol.* **2012**, *16* (3), 422–428.
- (125) Jiaul Haque, A.-M.; Kim, J.; Dutta, G.; Kim, S.; Yang, H. Redox Cycling-Amplified Enzymatic Ag Deposition and Its Application in the Highly Sensitive Detection of Creatine Kinase-MB. *Chem. Commun.* **2015**, *51* (77), 14493–14496.
- (126) Singh, A.; Park, S.; Yang, H. Glucose-Oxidase Label-Based Redox Cycling for an Incubation Period-Free Electrochemical Immunosensor. *Anal. Chem.* **2013**, *85* (10), 4863–4868.
- (127) Volpe, G.; Draisci, R.; Palleschi, G.; Compagnone, D. 3,3',5,5'-Tetramethylbenzidine as Electrochemical Substrate for Horseradish Peroxidase Based Enzyme Immunoassays. A Comparative Study. *Analyst* **1998**, *123* (6), 1303–1307.
- (128) Preechaworapun, A.; Dai, Z.; Xiang, Y.; Chailapakul, O.; Wang, J. Investigation of the Enzyme Hydrolysis Products of the Substrates of Alkaline Phosphatase in Electrochemical Immunosensing. *Talanta* **2008**, *76* (2), 424–431.
- (129) Pemberton, R. M.; Mottram, T. T.; Hart, J. P. Development of a Screen-Printed Carbon Electrochemical Immunosensor for Picomolar Concentrations of Estradiol in Human Serum Extracts. *J. Biochem. Biophys. Methods* **2005**, *63* (3), 201–212.
- (130) Lim, S. A.; Ahmed, M. U. Electrochemical Immunosensors and Their Recent Nanomaterial-Based Signal Amplification Strategies: A Review. *RSC Adv.* **2016**, *6* (30), 24995–25014.
- (131) Idegami, K.; Chikae, M.; Kerman, K.; Nagatani, N.; Yuhi, T.; Endo, T.; Tamiya, E. Gold Nanoparticle-Based Redox Signal Enhancement for Sensitive Detection of Human Chorionic Gonadotropin Hormone. *Electroanalysis* **2008**, *20* (1), 14–21.
- (132) Martín-Yerga, D.; González-García, M. B.; Costa-García, A. Electrochemical Immunosensor for Anti-Tissue Transglutaminase Antibodies Based on the in Situ Detection of Quantum Dots. *Talanta* **2014**, *130*, 598–602.
- (133) Wang, Y.; Fan, D.; Wu, D.; Zhang, Y.; Ma, H.; Du, B.; Wei, Q. Simple Synthesis of Silver Nanoparticles Functionalized Cuprous Oxide Nanowires Nanocomposites and Its Application in Electrochemical Immunosensor. *Sensors Actuators B Chem.* **2016**, *236*, 241–248.
- (134) Sánchez-Tirado, E.; Arellano, L. M.; González-Cortés, A.; Yáñez-Sedeño, P.; Langa, F.; Pingarrón, J. M. Viologen-Functionalized Single-Walled Carbon Nanotubes as Carrier Nanotags for Electrochemical Immunosensing. Application to TGF-B1 Cytokine. *Biosens. Bioelectron.* **2017**, *98*, 240–247.

- (135) Zhong, Z.; Li, M.; Qing, Y.; Dai, N.; Guan, W.; Liang, W.; Wang, D. Signal-on Electrochemical Immunoassay for APE1 Using Ionic Liquid Doped Au Nanoparticle/Graphene as a Nanocarrier and Alkaline Phosphatase as Enhancer. *Analyst* **2014**, *139* (24), 6563–6568.
- (136) Liang, J.; Wang, J.; Zhang, L.; Wang, S.; Yao, C.; Zhang, Z. Glucose Oxidase-Loaded Liposomes for in Situ Amplified Signal of Electrochemical Immunoassay on a Handheld PH Meter. *New J. Chem.* **2019**, *43* (3), 1372–1379.
- (137) Dong, S.; Wang, S.; Gyimah, E.; Zhu, N.; Wang, K.; Wu, X.; Zhang, Z. A Novel Electrochemical Immunosensor Based on Catalase Functionalized AuNPs-Loaded Self-Assembled Polymer Nanospheres for Ultrasensitive Detection of Tetrabromobisphenol A Bis(2-Hydroxyethyl) Ether. *Anal. Chim. Acta* **2019**, *1048*, 50–57.
- (138) Chang, H.; Zhang, H.; Lv, J.; Zhang, B.; Wei, W.; Guo, J. Pt NPs and DNAzyme Functionalized Polymer Nanospheres as Triple Signal Amplification Strategy for Highly Sensitive Electrochemical Immunosensor of Tumour Marker. *Biosens. Bioelectron.* **2016**, *86*, 156–163.
- (139) Zhang, D.; Li, W.; Ma, Z. Improved Sandwich-Format Electrochemical Immunosensor Based on “Smart” SiO<sub>2</sub>@polydopamine Nanocarrier. *Biosens. Bioelectron.* **2018**, *109*, 171–176.
- (140) Díez-Buitrago, B.; Briz, N.; Liz-Marzán, L. M.; Pavlov, V. Biosensing Strategies Based on Enzymatic Reactions and Nanoparticles. *Analyst* **2018**, *143* (8), 1727–1734.
- (141) Barroso, J.; Saa, L.; Grinyte, R.; Pavlov, V. Photoelectrochemical Detection of Enzymatically Generated CdS Nanoparticles: Application to Development of Immunoassay. *Biosens. Bioelectron.* **2016**, *77*, 323–329.
- (142) Chen, Z.-P.; Peng, Z.-F.; Luo, Y.; Qu, B.; Jiang, J.-H.; Zhang, X.-B.; Shen, G.-L.; Yu, R.-Q. Successively Amplified Electrochemical Immunoassay Based on Biocatalytic Deposition of Silver Nanoparticles and Silver Enhancement. *Biosens. Bioelectron.* **2007**, *23* (4), 485–491.
- (143) Lin, Y.; Zhou, Q.; Tang, D.; Niessner, R.; Knopp, D. Signal-On Photoelectrochemical Immunoassay for Aflatoxin B1 Based on Enzymatic Product-Etching MnO<sub>2</sub> Nanosheets for Dissociation of Carbon Dots. *Anal. Chem.* **2017**, *89* (10), 5637–5645.
- (144) Lai, G.; Cheng, H.; Xin, D.; Zhang, H.; Yu, A. Amplified Inhibition of the Electrochemical Signal of Ferrocene by Enzyme-Functionalized Graphene Oxide Nanoprobe for Ultrasensitive Immunoassay. *Anal. Chim. Acta* **2016**, *902*, 189–195.
- (145) Wang, J.; Zhao, W. W.; Tian, C. Y.; Xu, J. J.; Chen, H. Y. Highly Efficient Quenching of Electrochemiluminescence from CdS Nanocrystal Film Based on Biocatalytic Deposition. *Talanta* **2012**, *89*, 422–426.
- (146) Lin, Y.; Zhou, Q.; Tang, D.; Niessner, R.; Knopp, D. Signal-On Photoelectrochemical Immunoassay for Aflatoxin B1 Based on Enzymatic Product-Etching MnO<sub>2</sub> Nanosheets for Dissociation of Carbon Dots. *Anal. Chem.* **2017**, *89* (10), 5637–5645.
- (147) Chen, Z.-P.; Peng, Z.-F.; Luo, Y.; Qu, B.; Jiang, J.-H.; Zhang, X.-B.; Shen, G.-L.; Yu, R.-Q. Successively Amplified Electrochemical Immunoassay Based on Biocatalytic Deposition of Silver Nanoparticles and Silver Enhancement. *Biosens. Bioelectron.* **2007**, *23* (4), 485–491.
- (148) Lai, G.; Cheng, H.; Xin, D.; Zhang, H.; Yu, A. Amplified Inhibition of the Electrochemical Signal of Ferrocene by Enzyme-Functionalized Graphene Oxide Nanoprobe for Ultrasensitive Immunoassay. *Anal. Chim. Acta* **2016**, *902*, 189–195.







## **CHAPTER 2: MOTIVATION AND OBJECTIVES**

---



## Motivation and objectives

Biosensors are sophisticated devices with a growing presence in our daily life because of their application in almost every field focused on the detection and monitoring of relevant analytes. In the medical/healthcare sector they present a great advancement for clinical applications with an important impact in point-of-care testing. Nowadays, analytical methodology based on immunoassays is considered as one of the most powerful tools for the detection of the majority of biomarkers with clinical interest. Therefore, there is a great interest in research and development of miniaturized, portable and sensitive immunosensors suitable for rapid and reliable measurements. Nevertheless, there is often a need to improve the sensitivity and stability of the sensors, as well as to adapt them for application in miniaturized systems suitable for on-site applications. So far, there is still no evidence of a successful device on the market with electrochemical immunosensing applications.

Motivated by this stimulating challenge, we decided to start this project based on a principal hypothesis: **the use of the enzymatic activity to modulate properties of some nanomaterials leads to an improvement of the detection and signal amplification and can be integrated in a lab-on-a-chip platform for the development of a photoelectrochemical immunosensor.** This proposal was made based on the strong scientific background from the laboratories of Biosensing Lab (CIC biomaGUNE) and Biomaterials (Tecnalia R&D). One research line of Biosensing Lab group (CIC biomaGUNE) is the design and application of enzymatic modulation of properties of nanoparticles and quantum dots for bioanalysis. Previously, the Biosensing Lab Group applied growth and etching of metal and semiconductor nanoparticles to the various assays based on optical, electrochemical and photoelectrochemical detection. On the other hand, Biomaterials group (Tecnalia R&D) has expertise in polystyrene surface modification for bioanalytical applications and has recently started a line of research focused on the design and development of miniaturized chips for immunosensing.

Since I was motivated and keen on biosensor development, I decided to start this PhD thesis under the supervision of Dr. Nerea Briz (Tecnalia R&D) and Dr. Valery Pavlov (CIC biomaGUNE). The main goal of this work was to adapt enzymatic systems, which are used for detection and signal amplification, to fabrication of a miniaturized portable chip used as a photoelectrochemical immunosensor.

In order to achieve this, some specific objectives were proposed to be addressed:

- 1. Evaluation of different enzymatic systems suitable for the detection and signal amplification in terms of sensitivity and detection limits.**
- 2. Selection of the best detection system for the design of the portable immunosensor.**
- 3. Study of the improvement of antibody immobilization on polystyrene substrates.**
- 4. Integration of both methodologies into a lab-on-a-chip platform.**

The first task of the work was to investigate possible enzymatic systems to enhance the detection and signal amplification processes. Here, we evaluated three different protocols ([chapter 3](#)): enzymatic modulation of CdS quantum dots growth for methanol detection in alcoholic beverages through fluorogenic and photoelectrochemical methods; enzymatic growth of Ag/Ag<sub>2</sub>S nanoparticles for glucose detection in human serum by colorimetry; and enzymatic blocking or enhancement of the electrochemiluminescence signal from CdS nanoparticles for the detection of methanol in alcoholic beverages and acetylthiocholine in human serum, respectively. From the different detection methods used, we selected the photoelectrochemical one as the most suitable for lab-on-a-chip applications because of the easiness of miniaturization, low cost of manufacturing and high sensitivity.

At the same time, we went through the adaptation to our system of the polystyrene modification protocol developed by Biomaterials group. Herein, we studied the procedure for the modification of polystyrene substrates with a variety of functional groups for the immobilization of antibodies ([chapter 4](#), first part). We explored different strategies to link the antibodies to the surface in order to achieve their ordered orientation ensuring an improved biorecognition and thus, increasing the sensitivity of the immunoassay. Additionally, this procedure allows for the integration of the active layer to a lab-on-a-chip platform.

Finally, the last objective was to integrate the enzymatic reaction with the antibody immobilization into a portable platform for the photoelectrochemical detection. For this, several parameters had to be optimised such as incubation time, temperature, order of reaction steps, volumes and operational method ([chapter 4](#), second part). Furthermore, it was also essential to improve the design, fabrication and printing of the electrodes to guarantee the electrochemical process and its validation against the commercial ceramic ones.





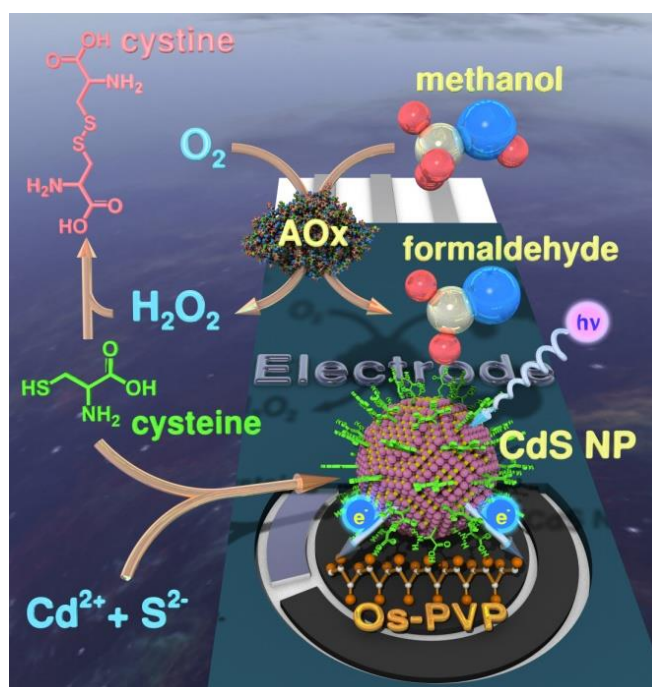


## CHAPTER 3: ENZYMATIC GROWTH OF NANOPARTICLES AND APPLICATIONS

---

- Specific bioanalytical optical and photoelectrochemical assays for detection of methanol in alcoholic beverages
- Facile synthesis and characterization of Ag/Ag<sub>2</sub>S nanoparticles enzymatically grown in situ and their application to the colorimetric detection of glucose oxidase
- Development of portable CdS screen printed carbon electrode platform for electrochemiluminescence measurements and bioanalytical applications





## SPECIFIC BIOANALYTICAL OPTICAL AND PHOTOELECTROCHEMICAL ASSAYS FOR DETECTION OF METHANOL IN ALCOHOLIC BEVERAGES

Methanol is a poison which is frequently discovered in alcoholic beverages. Innovative methods to detect methanol in alcoholic beverages are being constantly developed. We report for the first time a new strategy for the detection of methanol using fluorescence spectroscopy and photoelectrochemical (PEC) analysis. The analytical system is based on the oxidation of cysteine (CSH) with hydrogen peroxide ( $\text{H}_2\text{O}_2$ ) enzymatically generated by alcohol oxidase (AOx).  $\text{H}_2\text{O}_2$  oxidizes capping agent CSH, modulating the growth of CSH-stabilized cadmium sulfide quantum dots (CdS QDs). Disposable screen-printed carbon electrodes (SPCE) modified with a conductive osmium polymer (Os-PVP) complex were employed to quantify resulting CdS QDs. This polymer facilitates the “wiring” of in situ enzymatically generated CdS QDs, which photocatalyze oxidation of 1-thioglycerol (TG), generating photocurrent as the readout signal. Likewise, we proved that our systems did not suffer from interference by ethanol. The PEC assays showed better sensitivity than conventional methods, covering a wide range of potential applications for methanol quantification.

---

The work presented was previously published: Barroso, J.; Díez-Buitrago, B.; Saa, L.; Möller, M.; Briz, N.; Pavlov, V. *Biosensors and Bioelectronics* 2018, 101, 116–122.

## 1. Introduction

The uncontrollable use of hazardous materials in food and beverages instigates the development of sensitive, affordable and simple assays and sensors for industrial laboratories, distributors and end users. One of the most toxic compounds is methanol. It can be found mainly in alcoholic beverages generated by natural fermentation or distillation. Humans do not tolerate methanol because of its conversion to formate which inhibits mitochondrial cytochrome C oxidase, causing hypoxia at the cellular level, and acidosis.<sup>1</sup> It is well-known that the ingestion of methanol provokes disturbances in the central nervous system, affecting to the optical system and even death. The lethal dose of methanol lies between 30 and 120 mL (i.e. 1–2 mL kg<sup>-1</sup> body weight of pure methanol). Usually, humans are exposed to methanol by oral ingestion of alcoholic beverages containing this simplest alcohol. Nowadays, strict regulations contribute to avoiding the deceptive practices of adulteration of alcoholic beverages. Fermentation of alcoholic beverages under standard conditions usually yields aqueous ethanol solutions with negligible concentration of methanol. Nevertheless, incidence of methanol contamination of traditionally fermented beverages is increasing globally due to activities of contaminating pectinase producing yeasts, fungi and bacteria.<sup>2</sup> In addition, the alcoholic strength is altered using “extra” methanol as illicit alcohol.<sup>3</sup>

Since the beginning of the last century, the development of methods for methanol detection in alcoholic beverages gained in importance.<sup>4</sup> The standard detection methods are based on gas chromatography as the standard method.<sup>5</sup> Among other physical techniques for methanol detection are Raman spectroscopy,<sup>6,7</sup> Fourier transform infrared spectrometry,<sup>8–10</sup> flow tube mass spectrometry,<sup>11</sup> surface plasmon resonance,<sup>12</sup> measurement of refractive index and evaporation rate,<sup>13</sup> hybrid capillary electrophoresis,<sup>14</sup> evanescent wave optical sensor,<sup>15</sup> quartz tuning forks.<sup>16</sup> Those published physical techniques require expensive devices to read out the signal and cannot be readily miniaturized. Electrochemical biosensors and analytical assays employing enzymes as recognition elements for selective determination of methanol in ethanol are not very common, and usually need at least two enzymes. For instance, a bi-enzymatic analytical system was published, which consists of two biosensors, one based on alcohol dehydrogenase (ADH) that responds only to the ethanol and the second one based on alcohol oxidase (AOX) that responds to both methanol and ethanol. Bi-enzymatic biosensor responsive to both ethanol and methanol employing alcohol oxidase and horseradish peroxidase was reported.<sup>17</sup>

The development of new nanomaterials opens up new opportunities for detection of analytes using enzymes as biorecognition elements. Several enzymes can catalyze biocatalytic generation in situ of metallic nanoparticles (NPs).<sup>18–20</sup> However, the reported use of metallic NPs for detection of enzymatic activities is restricted due to their low photocatalytic activities and fluorescent properties. As opposed, semiconductor nanoparticles (SNPs) exhibit quantum effects during a photoexcitation process, hence those particles are referred to as quantum dots (QDs) and are exploited extensively in bioanalytical applications. Combining electrochemistry with the light, photoelectrochemical (PEC) assays are an emergent technique for innovative detection.<sup>21–23</sup> The PEC process transforms luminous energy directly into electrochemical energy. The presence of capping agent as stabilizer favours the quantum confinement effect. One of the efficient stabilizers is cysteine (CSH) that owing to its thiol functional group easily binds to SNPs.<sup>24,25</sup> However, CSH is easily oxidized to cystine (CSSC) in the presence of redox mediator such as hydrogen peroxide ( $H_2O_2$ ) produced during oxidation of methanol by alcohol oxidase from *Hansenula sp.* specific to only to methanol. The modulation of in situ growth of CSH-stabilized SNPs could be followed by fluorescence spectroscopy and PEC assays. The fluorescence readout signal is related to the rate of in situ formation of CSH-stabilized CdS QDs inhibited by  $H_2O_2$ . Likewise, we carried out PEC studies to evaluate the quantification of CdS QDs grown in situ. The amount of formed CdS QDs is related with the photocurrent generated in the system. Other factors defining the electrochemical response are applied potential, energy of photons, intensity of excitation light and rate of electron transfer between the electrode surface and QDs. Previous works based on PEC technology employed electrocatalysts deposited onto expensive electrodes.<sup>26</sup> Nonetheless, PEC is a powerful tool that allows manufactured low-cost devices. In the present work, we employ disposable screen-printed carbon electrodes (SPCE) as simple and inexpensive disposable devices. To facilitate the electron transfer, a conductive polymer was employed to “wire” CdS QDs to the electrode surface. Previously, poly(vinylpyridine) osmium bipyridine (Os-PVP) conductive polymer was used for “wiring” redox enzymes.<sup>27–29</sup> Here, we modified disposable SPCE with Os-PVP complex to validate our fluorogenic and PEC approaches to the methanol quantification in real alcoholic beverages such as vodka and cider opening up a new opportunity for the manufacture of inexpensive and easy-handle mobile analytical systems.

## 2. Experimental section

### 2.1. Materials

Methanol specific alcohol oxidase from *Hansenula sp.*, sodium sulfide ( $\text{Na}_2\text{S}$ ), cadmium nitrate  $\text{Cd}(\text{NO}_3)_2$ , 1-thioglycerol, methanol, ethanol and another chemicals were purchased from Sigma Aldrich. Different alcoholic beverages such as ciders and vodka were purchased in local market in San Sebastián (Spain).

### 2.2. Apparatus

Transmission electron microscopy images were collected with a JEOL JEM 2100F operating at 120 kV. Axio Observer Microscope (Zeiss) controlled with Axiovision software was employed to take fluorescence images of CdS QDs on SPCE modified with Os-PVP complex. Fluorescence measurements were performed on a Varioskan Flash microplate reader (Thermo Scientific) using black microwell plates at room temperature. The system was controlled by SkanIt Software 2.4.3. RE for Varioskan Flash.

Every electrochemical test was led in a Autolab Electrochemical Workstation (Model: PGSTAT302N, Metrohm Autolab, The Netherlands) furnished with NOVA 1.10 software. Disposable screen-printed carbon electrodes (SCPEs) were purchased from DropSens (model DRP-110). Electrical contact to workstation was finished with a special boxed connector provided by DropSens. The light source was a compact UV illuminator (UVP, Analytik Jena AG). All PEC measurements were performed at room temperature. All the potentials reported in our work were measured against Ag/AgCl. Unless otherwise specified, all experimental outcomes described here are averaged from three autonomous estimations ( $n = 3$ ).

### 2.3. Methods

#### 2.3.1. AOx assay

Varying amounts of methanol or ethanol were incubated with different amounts of AOx in citrate-phosphate buffer (pH 7.5) for 40 min at room temperature, in the presence of CSH (7.5  $\mu\text{L}$ , 1 mM). After that,  $\text{Na}_2\text{S}$  (10  $\mu\text{L}$ , 1 mM) and  $\text{Cd}(\text{NO}_3)_2$  (2.5  $\mu\text{L}$ , 50 mM ) were added to the samples (87.5  $\mu\text{L}$ ). The emission spectra of the resulting CdS QDs were recorded after 5 min at  $\lambda_{\text{exc}} = 300 \text{ nm}$ .

### 2.3.2. CdS QD-mediated determination of alcohol mixtures

Different mixtures of methanol and ethanol were incubated with CSH (7.5  $\mu\text{L}$ , 1 mM) in citrate-phosphate buffer (pH 7.5) for 40 min at room temperature (taking into account that two alcoholic solutions with ethanol content of 40% and 6% were prepared). After that,  $\text{Na}_2\text{S}$  (10  $\mu\text{L}$ , 1 mM) and  $\text{Cd}(\text{NO}_3)_2$  (2.5  $\mu\text{L}$ , 50 mM) were added to the samples (87.5  $\mu\text{L}$ ). The emission spectra of the resulting suspensions were recorded after 5 min at  $\lambda_{\text{exc}} = 300 \text{ nm}$ .

### 2.3.3. Quantification of methanol in real samples

Quantification of methanol in cider and vodka was performed by the standard addition method. Samples of alcoholic beverages were spiked with known different concentrations of methanol. Thus, the corresponding final concentration of methanol in mixtures was determined. The dilution factor of samples in the assay was 1:10000.

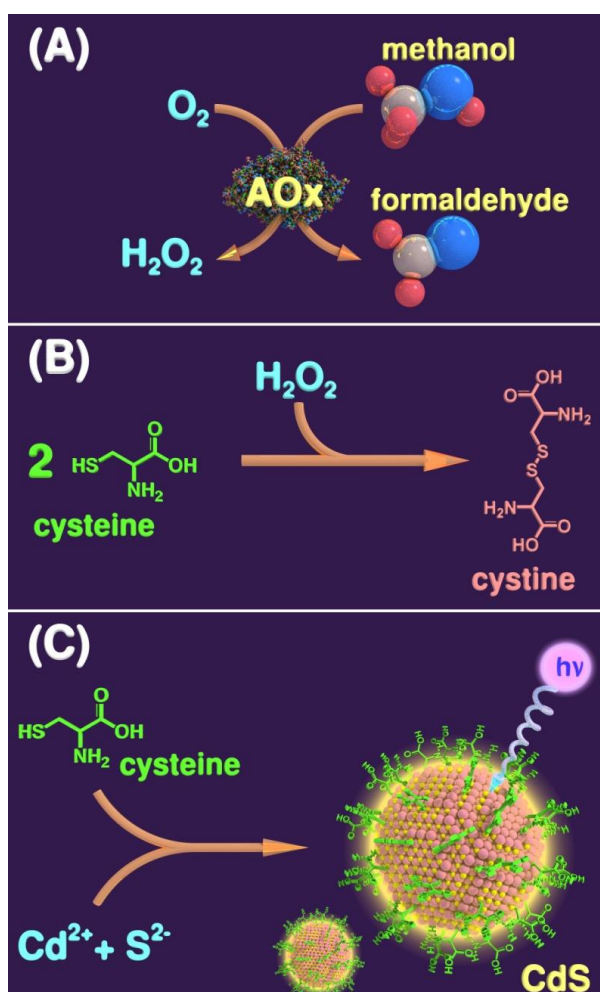
### 2.3.4. Photoelectrochemical detection

Before beginning the PEC assays, the SPCE were at first pretreated electrochemically by cyclic voltammetry (CV) at a potential range of 0 – 0.6 V in citrate-phosphate buffer (pH 7.5). Subsequently, a 40  $\mu\text{L}$  drop of Os-PVP complex (1.375  $\text{mg mL}^{-1}$ ) was dropcasted on the SPCE and electrodeposited by CV scanning (2 cycles at scan rate of 50  $\text{mV s}^{-1}$ ). Afterwards, SPCE were flushed out with ultrapure water and dried under argon atmosphere. At last, 40  $\mu\text{L}$  of sample were dropped on the SPCE and PEC measurements were carried out with an UV-illuminator at 302 nm and a controlled potential of 0.3 V vs. Ag/AgCl. The reliance of photocurrent on time was measured at 5 minutes during 10 seconds. It is important to point out that it is necessary to add the reducing agent 1-thioglycerol (20 mM) to amplify the photocurrent response.

### 3. Results and discussion

#### 3.1. Fluorogenic assays

We developed the fluorogenic assay for methanol using evaluation assessment of the enzymatic activity of AOX as represented in Scheme 1. First, the enzyme AOX catalyzes the oxidation of methanol with oxygen to yield hydrogen peroxide ( $\text{H}_2\text{O}_2$ ). Second, hydrogen peroxide, resulting from the enzymatic oxidation of the target analyte, converts two molecules of cysteine to one molecule of cystine. This process leads to conversion of two active thiol groups (-SH) into one inactive disulfide bridge (-SS-) which does not stabilize the growth of CdS QDs. Third, cysteine carrying one thiol group is a very efficient stabilizer for CdS QDs formed in situ from  $\text{Cd}^{2+}$  and  $\text{S}^{2-}$  ions. Thus, the bio-catalytic process ending up in formation  $\text{H}_2\text{O}_2$  decreases concentration of the stabilizing agent cysteine, and consequently, the amount of CdS QDs formed in situ.



**Scheme 1.** Fluorometric assay of methanol using alcohol oxidase. (A) Biocatalytic oxidation of methanol. (B) Oxidation of cysteine with hydrogen peroxide. (C) Formation of fluorescent CdS QDs stabilized with cysteine.



In previous works, it was demonstrated that CSH is able to stabilize CdS QDs under harsh experimental conditions that include high reaction temperatures (over 80 °C)<sup>30</sup> or irradiation with  $\gamma$ -rays.<sup>24</sup> Under our experimental conditions the growth of CdS QDs occurs under mild physiological conditions in aqueous buffer solutions. CdS QDs growth is time dependent as it can be seen in Figure 1. The fluorescence intensity increases up to 30 min and then it levels off. This increase could be due to the high amount of reagents in the media that provides a constant source of reagents up to their complete consumption. After 5 min of incubation more than 60% of maximum fluorescence intensity was observed. After 60 min the signal achieved 100% of intensity, but this long incubation time will not be suitable for a point of care device or its use in clinical diagnosis that requires short procedure times. That is why we chose 5 min as the best time in relation with the signal obtained and the total time consumed.

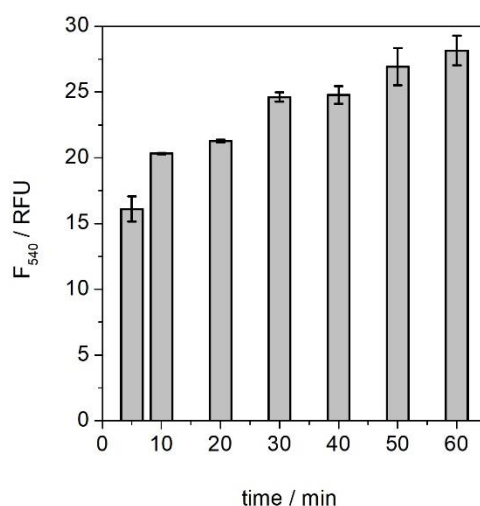


**Figure 1.** The effect of incubation time on the fluorescence intensity for CdS QDs obtained from CSH (0.075 mM),  $\text{Na}_2\text{S}$  (0.1 mM),  $\text{Cd}(\text{NO}_3)_2$  (1.25 mM).

In order to verify the operating mechanism of described system, various control experiments were carried out as shown in Figure 2. The influence of oxygen on non-specific oxidation of cysteine was evaluated with the control experiment in which ions of  $\text{Cd}^{2+}$  and  $\text{S}^{2-}$  were mixed in the presence of cysteine in citrate-phosphate buffer (pH 7.5). Fluorescent QDs were formed as one can see in curve 1. The reaction mixture containing CSH, AOx,  $\text{Cd}^{2+}$ ,  $\text{S}^{2-}$  ions demonstrated emission peak characteristic of CdS QDs (curve 2). The mixture composed of CSH, methanol,  $\text{Cd}^{2+}$ ,  $\text{S}^{2-}$  ions exhibited high emission peak too (curve 3). Curves 1, 2 and 3 are identical. According to Figure 1 the fluorescence of CdS QDs kept in open air doesn't decrease with time. Thus, under our experimental conditions, oxygen is not able to oxidase cysteine non-specifically. The presence of oxygen in the media is mandatory since it allows AOx to transform

methanol into formaldehyde. In the absence of oxygen the enzyme would not be able to catalyse the oxidation of methanol.

The emission peaks of similar mixtures prepared without CSH, containing methanol,  $\text{Cd}^{2+}$ ,  $\text{S}^{2-}$  ions (curve 5) or AOx,  $\text{Cd}^{2+}$ ,  $\text{S}^{2-}$  ions (curve 6) were much lower. Fluorescence decreases only in the absence of the capping agent (cysteine) in open air (curve 5 and 6). The reaction mixture containing all components (AOx, methanol, CSH,  $\text{Cd}^{2+}$ ,  $\text{S}^{2-}$  ions) exhibited low emission peak (curve 4). This can be explained by the decrease in CSH concentration caused by its oxidation with  $\text{H}_2\text{O}_2$ , produced in the course of enzymatic redox process according to Scheme 1. An extra control was also conducted to rule out the influence of AOx on the fluorescence signal in absence of alcohol, CSH,  $\text{Cd}(\text{NO}_3)_2$  and  $\text{Na}_2\text{S}$ . Under these conditions no fluorescence was observed (curve 7).

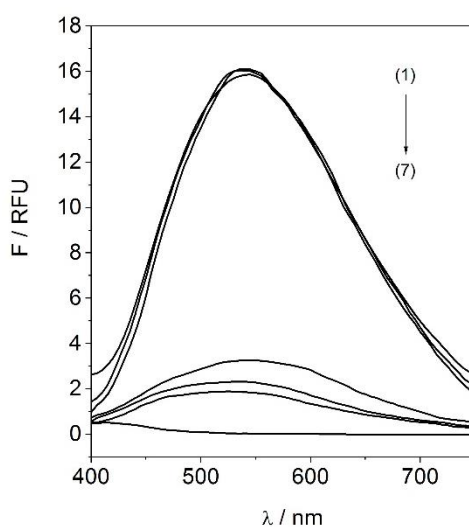


**Figure 2.** Fluorescence emission spectra of assay mixtures containing (1) Cysteine (CSH, 0.075 mM),  $\text{Na}_2\text{S}$  (0.1 mM),  $\text{Cd}(\text{NO}_3)_2$  (1.25 mM); (2) Cysteine (CSH, 0.075 mM), alcohol oxidase (AOx,  $5 \mu\text{g L}^{-1}$ ),  $\text{Na}_2\text{S}$  (0.1 mM),  $\text{Cd}(\text{NO}_3)_2$  (1.25 mM); (3) Cysteine (CSH, 0.075 mM), methanol ( $0.03 \text{ g L}^{-1}$ ),  $\text{Na}_2\text{S}$  (0.1 mM),  $\text{Cd}(\text{NO}_3)_2$  (1.25 mM); (4) Methanol ( $0.003 \text{ g L}^{-1}$ ), AOx,  $5 \mu\text{g L}^{-1}$ , CSH (0.075 mM),  $\text{Na}_2\text{S}$  (0.1 mM),  $\text{Cd}(\text{NO}_3)_2$  (1.25 mM); (5) Methanol ( $0.03 \text{ g L}^{-1}$ ),  $\text{Na}_2\text{S}$  (0.1 mM),  $\text{Cd}(\text{NO}_3)_2$  (1.25 mM); (6) Oxidase (AOx,  $5 \mu\text{g L}^{-1}$ ),  $\text{Na}_2\text{S}$  (0.1 mM),  $\text{Cd}(\text{NO}_3)_2$  (1.25 mM); (7) AOx ( $5 \mu\text{g L}^{-1}$ ). Incubation time 5 min,  $\lambda_{\text{exc}} = 300 \text{ nm}$ .

Time of incubation and CSH concentration were optimized. Different incubation times were tried in the presence and absence of methanol. The greatest difference between fluorescence signals registered in reaction mixtures with and without methanol was achieved when the incubation time was 40 minutes (Figure 3A). Hence, incubation time of AOx with cysteine and methanol was employed in the following experiments. Published protocols for the synthesis of CSH-stabilized NPs require much longer incubation time and harsh experimental conditions.<sup>24,25,30</sup> Incubation was performed at varying concentrations of CSH. It was found that the optimum CSH concentration was 0.075 mM (Figure 3B). At this concentration, the

fluorescence readout signal showed the highest intensity, indicating the presence of higher amount of CSH-stabilized CdS QDs.

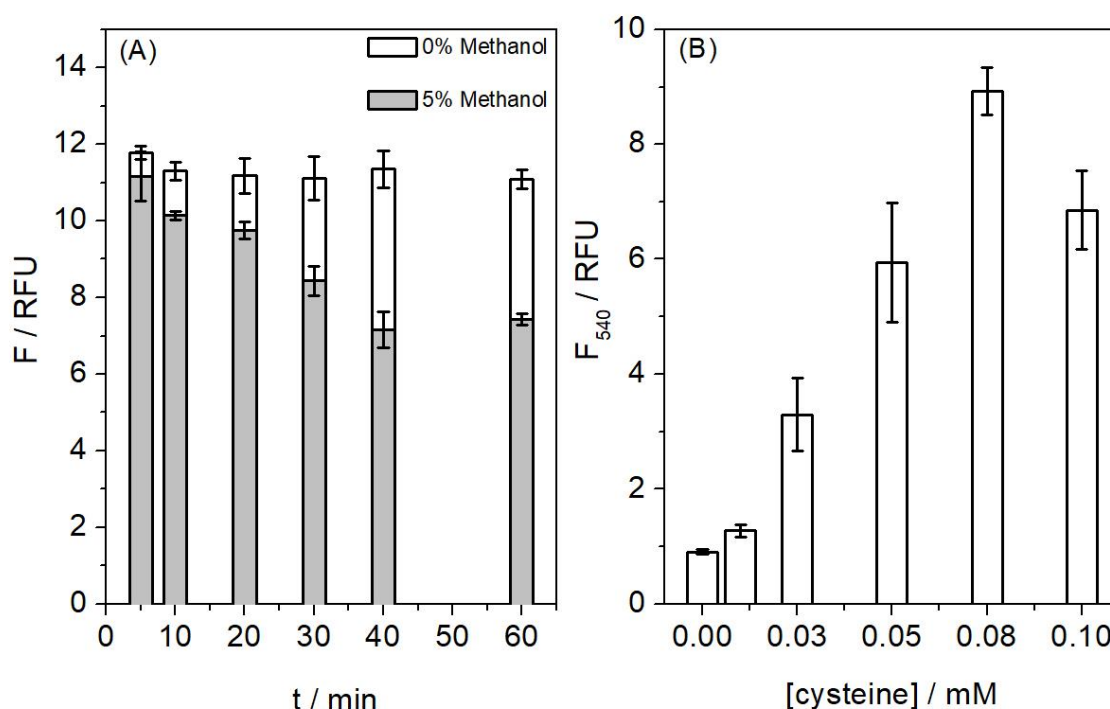


**Figure 3.** (A) The effect of incubation time on fluorescence intensity for the system containing methanol ( $0.008 \text{ g L}^{-1}$ ) and no methanol ( $0 \text{ g L}^{-1}$ ). (B) Effect of cysteine concentration on fluorescence intensity of the reaction mixture composed of  $\text{Na}_2\text{S}$  ( $0.1 \text{ mM}$ ) and  $\text{Cd}(\text{NO}_3)_2$  ( $1.25 \text{ mM}$ ). Incubation time 5 min,  $\lambda_{\text{exc}} = 300 \text{ nm}$ .

The amount of AOX was also optimized using different concentrations of the enzyme in the presence of a fixed alcohol (methanol or ethanol) concentration ( $0.03 \text{ g L}^{-1}$ ) as shown in Figure 4A and 4B. In the presence of methanol fluorescence intensity was inversely related to the amount of AOX in the assay mixture Figure 4B (solid line) reaching saturation at  $5 \mu\text{g L}^{-1}$  of this enzyme. According to the calibration plot this assay for enzymatic activity of AOX has a limit of detection (LOD) equal to  $0.14 \mu\text{g L}^{-1}$  at a signal-to-noise ratio of 3 ( $S/N=3$ ). The average relative standard deviation (RSD) calculated from the calibration plot was 8% (unless otherwise specified, RSD was always acquired utilizing no less than three independent measurements). When ethanol was used instead of methanol no response to increasing concentrations of AOX was observed (Figure 4B dashed line). Transmission electron microscopy was used to determine the morphological characteristics of obtained CdS QDs (Figure 5). TEM images confirmed the presence of spheroidal QDs with an average diameter of  $2.03 \pm 0.86 \text{ nm}$ . CdS QDs could not be detected by TEM at saturating methanol concentration of  $0.03 \text{ g L}^{-1}$  (Figure 5C).

The emission spectra of CdS QDs recorded at varying concentrations of a methanol or ethanol in the presence of a fixed AOx concentration of  $5 \mu\text{g L}^{-1}$  are depicted in Figure 4C. In the case of methanol, decrease in the fluorescence signal is inversely proportional to methanol concentration as one can observe in Figure 4D (solid line). The response to increasing concentrations of methanol is typical for an enzymatic system governed by the Michaelis-Menten kinetic model considering affinity of the enzyme to its substrate. Lower Michaelis-Menten constant ( $K_M$ ) value means higher affinity of an enzyme to its substrate. The assay demonstrated a linear response up to  $1.5 \text{ mg L}^{-1}$  and asymptotically approaches its maximum starting from  $5 \text{ mg L}^{-1}$ . The apparent Michaelis-Menten constant ( $K_M$ ) was calculated by fitting the experimental results to the equation  $I = I_{\text{max}}[\text{Methanol}]/(K_M + [\text{Methanol}])$ . The value of  $1.66 \text{ mg L}^{-1}$  correlates well with the literature data.<sup>31–33</sup> Furthermore, the LOD was found equal to  $0.21 \text{ mg L}^{-1}$  ( $6.8 \mu\text{M}$ ) at  $S/N=3$ . The RSD calculated from the alcohol calibration plot was 10%. The fluorogenic assay showed a better sensitivity than classical chromatography tests<sup>5,34,35</sup> and other fluorometric assays<sup>36</sup> as can be seen in Table 1. The influence of ethanol on the performance of this fluorogenic assay was studied. In the presence of increasing amounts of ethanol (Figure 4D dashed line) the fluorescence signal did not decrease, remaining constant within the experimental error.

Additional calibration was performed using aqueous 40% (v/v%) alcohol mixtures with different methanol/ethanol molar ratios ranging between 0.0 and 1.0. According to the experimental calibration plot (Figure 6A) LOD was equal to 0.047 (molar fraction) with RSD of 8.15% ( $S/N=3$ ). Thus, this simple fluorogenic assay based on enzymatic modulation of the growth of CdS QDs is able to determine methanol in the presence of high amounts of ethanol. Other previously published enzymatic optical assays based on AOx either are not able to detect methanol in the presence of ethanol<sup>37,38</sup> or employ rare reagents which are not commercially available<sup>39</sup> (Table 1).

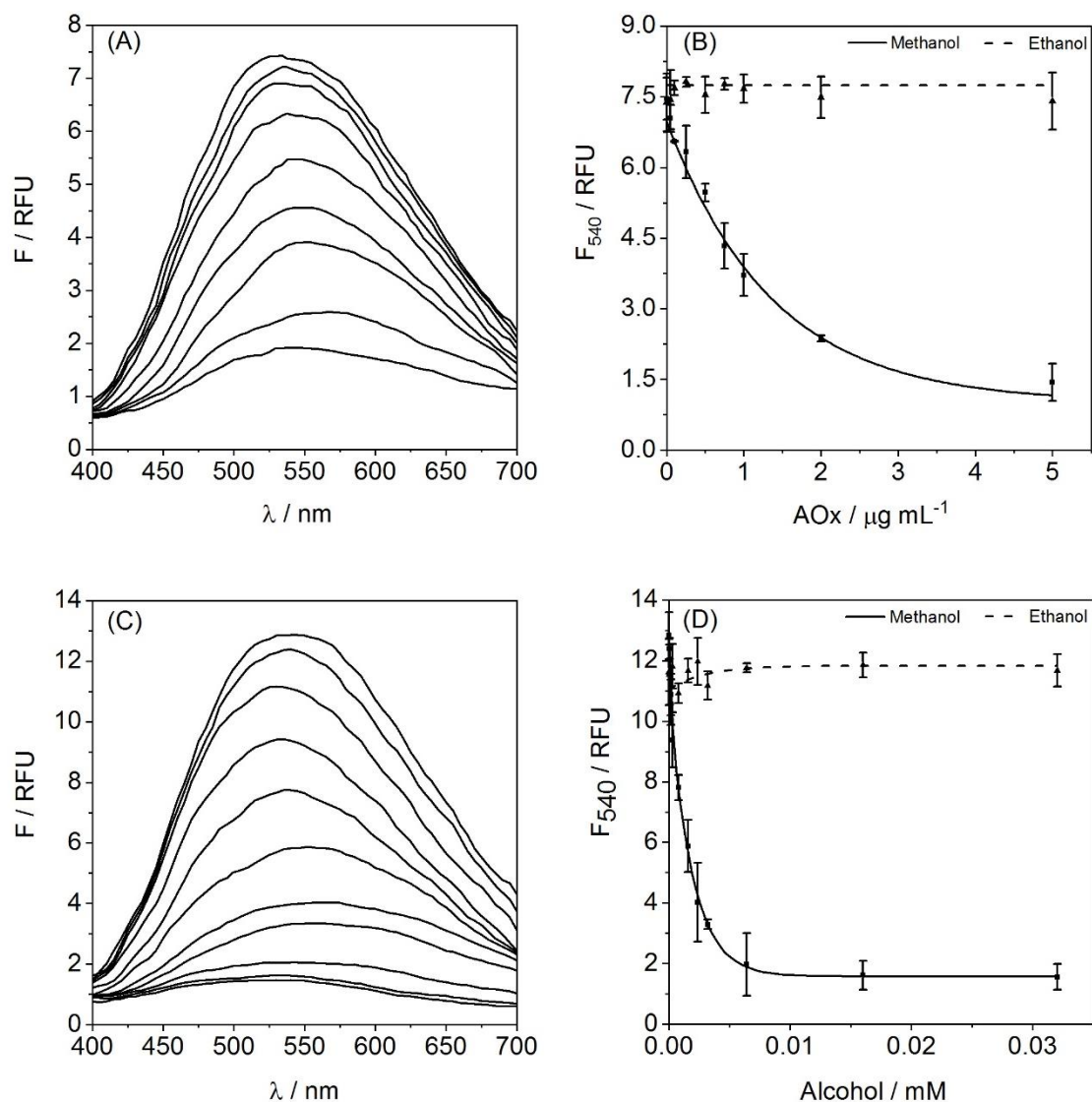


**Figure 4.** (A) Fluorescence emission spectra of the system containing methanol (0.03 g L<sup>-1</sup>), cysteine (CSH, 0.075 mM), Na<sub>2</sub>S (0.1 mM), Cd(NO<sub>3</sub>)<sub>2</sub> (1.25 mM) and different concentrations of AOx (0 to 5 μg mL<sup>-1</sup>). (B) Calibration curves of AOx for methanol (dark line) and ethanol (dashed line) obtained using F<sub>540</sub>. (C) Fluorescence emission spectra of the system containing alcohol oxidase (AOx, 5 μg mL<sup>-1</sup>), CSH (0.075 mM), Na<sub>2</sub>S (0.1 mM), Cd(NO<sub>3</sub>)<sub>2</sub> (1.25 mM) and different concentrations of methanol (0 to 0.03 g L<sup>-1</sup>). (D) Calibration curves of methanol (dark line) and ethanol (dashed line) obtained using F<sub>540</sub>.

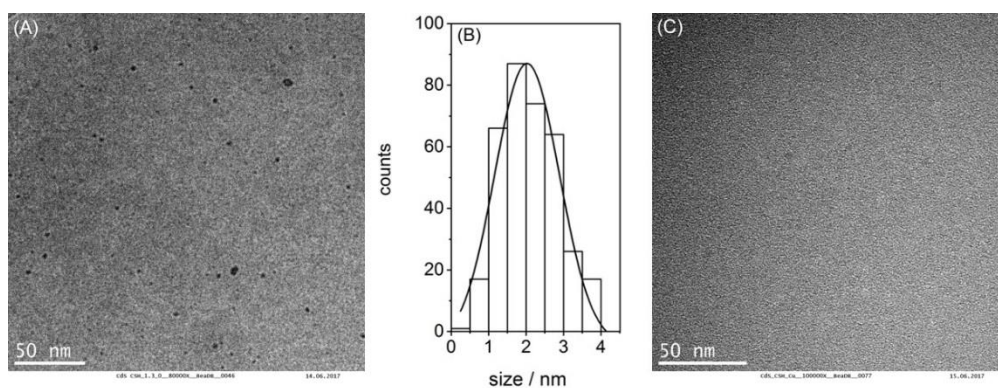


**Figure 5.** TEM image of cysteine (CSH)-stabilized CdS QDs in the presence of (A) Alcohol oxidase (AOx,  $5 \mu\text{g L}^{-1}$ ), CSH ( $0.075 \text{ mM}$ ),  $\text{Na}_2\text{S}$  ( $0.1 \text{ mM}$ ),  $\text{Cd}(\text{NO}_3)_2$  ( $1.25 \text{ mM}$ ); (B) Size distribution of previously described system. (C) TEM image of the system containing methanol ( $0.03 \text{ g L}^{-1}$ ), CSH ( $0.075 \text{ mM}$ ), AOx ( $5 \mu\text{g L}^{-1}$ ),  $\text{Na}_2\text{S}$  ( $0.1 \text{ mM}$ ) and  $\text{Cd}(\text{NO}_3)_2$  ( $1.25 \text{ mM}$ ).

**Table 1.** Comparison of sensibilities, selectivities and more characteristics of different methodologies for alcohol detection in alcoholic beverages.

Methodology	Comments	Sensitivity
Gas chromatography	Need of standards, differentiate between	LOQ $62.42 \mu\text{M}^5$
	methanol and ethanol	LOQ $156.05 \mu\text{M}^{40}$
	Time consuming, laborious pre-treatment	LOQ $0.41 \text{ mM}^{34}$
Fluorogenic assays	Indirect detection, selective to methanol	LOD $1.3 \mu\text{M}^{36}$
Review	Only ethanol detection	- 37
Colorimetric assays	No differentiation between ethanol and methanol	LOD $156.05 \mu\text{M}^{38}$
	Expensive reagents, differentiation between methanol and ethanol	- 39
Amperometry	Not selective to methanol but general alcohols, indirect detection	LOD <sub>EtOH</sub> $2.3 \mu\text{M}^{41}$ LOD <sub>EtOH</sub> $7 \mu\text{M}^{42}$
	Not selective for methanol	EtOH linear range $3.12 \mu\text{M} - 31.21 \text{ mM}^{43}$
	Selective to methanol, indirect detection	LOD $47 \mu\text{M}^{44}$
	Selective to methanol, laborious setup	LOD $10 \mu\text{M}^{17}$
	Indirect detection, not selective to methanol	LOD $1 \text{ mM}^{45}$

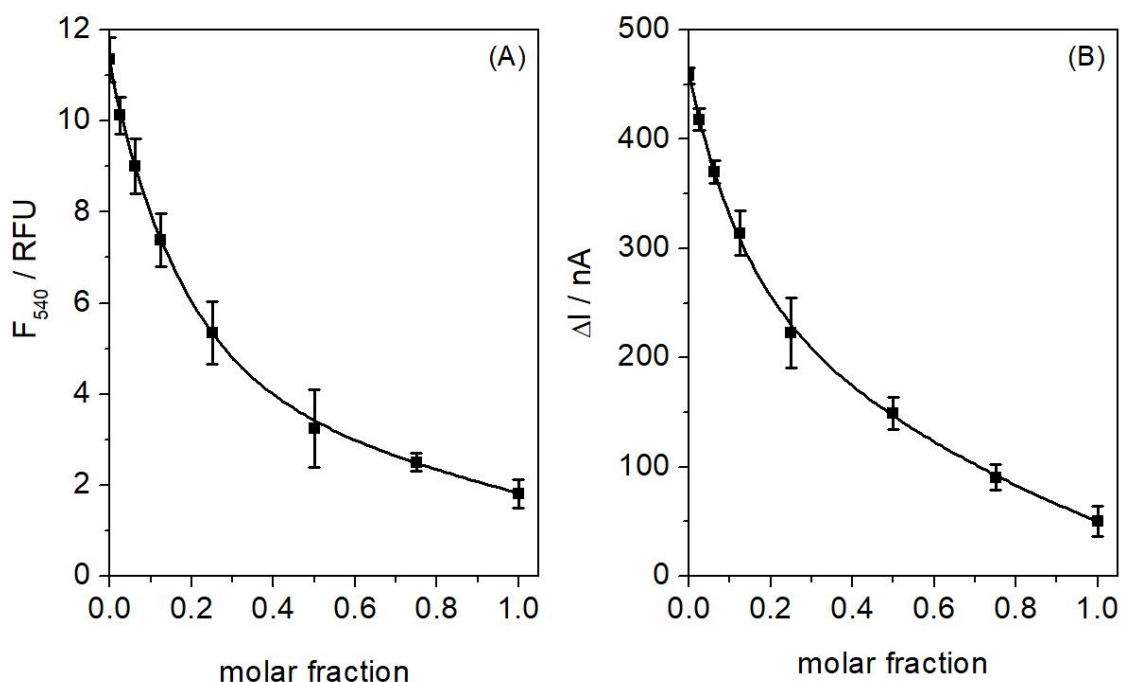


**Figure 6.** Calibration plots of 40% (v/v%) of aqueous solutions of alcohols with different methanol/ethanol molar fractions obtained with (A) fluorogenic and (B) photoelectrochemical assays. The system contains AOX ( $5 \mu\text{g mL}^{-1}$ ), cysteine (0.075 mM),  $\text{Na}_2\text{S}$  (0.1 mM) and  $\text{Cd}(\text{NO}_3)_2$  (1.25 mM).

### 3.2. PEC assays

#### 3.2.1. Optimization of photoelectrochemical response

Several parameters were optimized to obtain maximum performance of PEC measurements. We used Os-PVP conductive polymer complex immobilized on the surface of SPCE to “wire” CSH-stabilized CdS QDs generated during the assay. The efficient anchoring of osmium polymer on the electrode surface was achieved through electrostatic adsorption during CV. We optimized the protocol for the deposition of Os-PVP complex controlling the number of scans of CV. This methodology consists of ramping the potential linearly versus time in cyclical phases in the range between 0 and 0.6 V vs. Ag/AgCl. Final CV revealed redox reversible waves related to the central osmium atom.<sup>46</sup> Another aspect of PEC assays is the employment of a reducing agent to neutralize holes generated in CdS QDs upon excitation of electrons by photons. We selected TG because it has high affinity to CdS QDs due to thiol functional group. Therefore, the electronic transfer rate between the surface of CdS QDs and TG is very high.<sup>47</sup> On the other hand, TG can be used as a capping agent.<sup>48–50</sup>

Figure 7 shows the effect of TG concentration on photocurrent observed at SPCE modified with Os-PVP complex in the presence of fixed amounts of CdS QDs. According to this plot,

registered photocurrent achieved a plateau in the presence of 20 mM TG. This concentration of TG was selected for subsequent PEC measurements.

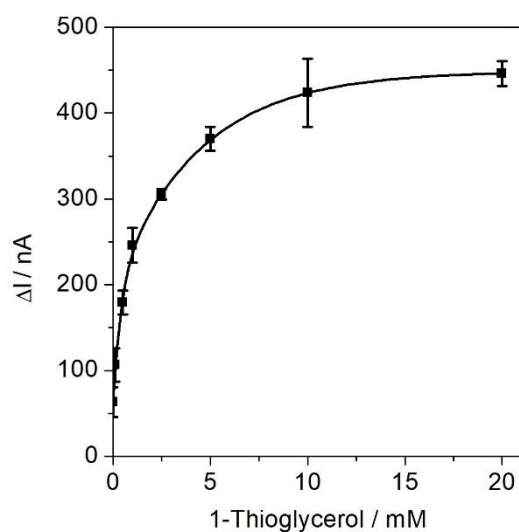


**Figure 7.** Effect of the increasing 1-thioglycerol (TG) concentrations on photocurrent observed in the presence of CdS QDs at 0.3 V (vs. Ag/AgCl) and 300 nm excitation light. Concentrations of TG: a) 0 mM; b) 0.25 mM; c) 0.5 mM; d) 1 mM; e) 2 mM; f) 5 mM; g) 20 mM. The system contains  $\text{Cd}(\text{NO}_3)_2$  (1.25 mM),  $\text{Na}_2\text{S}$  (0.1 mM) and cysteine (0.075 mM). The average relative standard deviation (RSD) calculated from the plot (obtained using at least three independent SPCE modified by Os-PVP) was 7%.

Finally, the effect of applied potential on the anodic photocurrents was studied. The applied potential was optimized in order to minimize the small background photocurrent originated from nonspecific photoelectrochemical oxidation of TG on the electrode surface modified with Os-PVP complex in the absence of CdS QDs. Photocurrents were registered in the presence ( $\Delta I_{\text{Os-PVP/TG}}$ ) and absence ( $\Delta I_{\text{Os-PVP}}$ ) of TG using SPCE modified with the redox polymer. The lowest ratio between both responses ( $\Delta I_{\text{Os-PVP/TG}}/\Delta I_{\text{Os-PVP}}$ ) was achieved at 0.3 V vs. Ag/AgCl as it can be noticed in Figure 8. At this applied potential the ratio  $\Delta I_{\text{Os-PVP/TG}}/\Delta I_{\text{Os-PVP}}$  was close to 1.0 indicating that nonspecific photooxidation of TG does not influence the response of the PEC assay. Hence the potential of 0.3 V vs. Ag/AgCl was used in the following experiments.



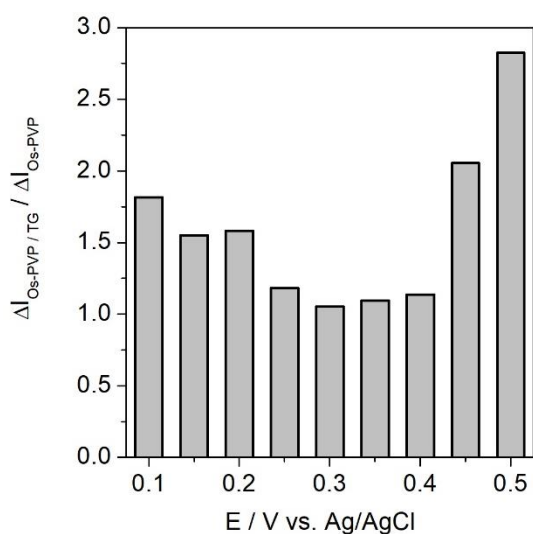


**Figure 8.** Selection of the applied potential based on the study of photocurrents registered in the absence ( $\Delta I_{Os-PVP}$ ) and the presence ( $\Delta I_{Os-PVP/TG}$ ) of 1-thioglycerol (TG). Plot demonstrates the ( $\Delta I_{Os-PVP/TG} / \Delta I_{Os-PVP}$ ) ratio versus applied potential (E).

### 3.2.2. Photocurrent response

The operation of the developed PEC assay for methanol is based on the interaction between SPCE, osmium polymer and CSH-stabilized CdS QDs whose quantity depends on the enzymatic oxidation of methanol as illustrated in Scheme 2. Biocatalytic oxidation of MeOH catalyzed by AOX ends up in formation of hydrogen peroxide which oxidizes CSH. Concentration of the latter influences the rate of formation of CSH-stabilized CdS QDs in situ. A droplet of the assay mixture is placed on the surface of a SPCE (without drying) modified with Os-PVP complex and irradiated with a UV lamp. CSH-stabilized QDs absorb photons with energies upper than that of their band gaps, producing the excitation of electrons from occupied valance band (VB) to the empty conduction band (CB). Electron holes-pairs with enough long life are generated due to the charge separation. Holes on VB are neutralized by electrons originating from TG. Free electrons are transferred from CB to Os-PVP complex, and finally to the electrode surface. This flow of electrons is driven by the UV light with an emission peak at 300 nm and an applied potential of 0.3 V vs. Ag/AgCl. The influence on photocurrent of varying concentrations of AOX in the presence of a fixed alcohol (methanol or ethanol) concentration ( $0.03 \text{ g L}^{-1}$ ) is shown in Figure 9A and 9B. The determination of AOX in using methanol as a substrate demonstrated a LOD of  $0.01 \mu\text{g L}^{-1}$  ( $S/N=3$ ) based on the calibration plot showed in Figure 9B. The RSD calculated from calibration plot was 6.3%. As before, the photocurrent was not affected by ethanol (Figure 9B dashed line).



**Scheme 2.** Photoelectrochemical assay for methanol through detection of CdS QDs “wired” by an Os-PVP complex to the surface of a screen-printed carbon electrode.

The presence of CSH-stabilized CdS QDs in droplets of assay mixture placed on SPCE was corroborated by fluorescence spectroscopy as depicted in Figure 10. In the absence of methanol, the fluorescence is maintained (Figure 10A). When methanol was present in the assay mixture, the registered fluorescence was significantly lower (Figure 10B). It should be noted that the osmium polymer is not fluorescent.

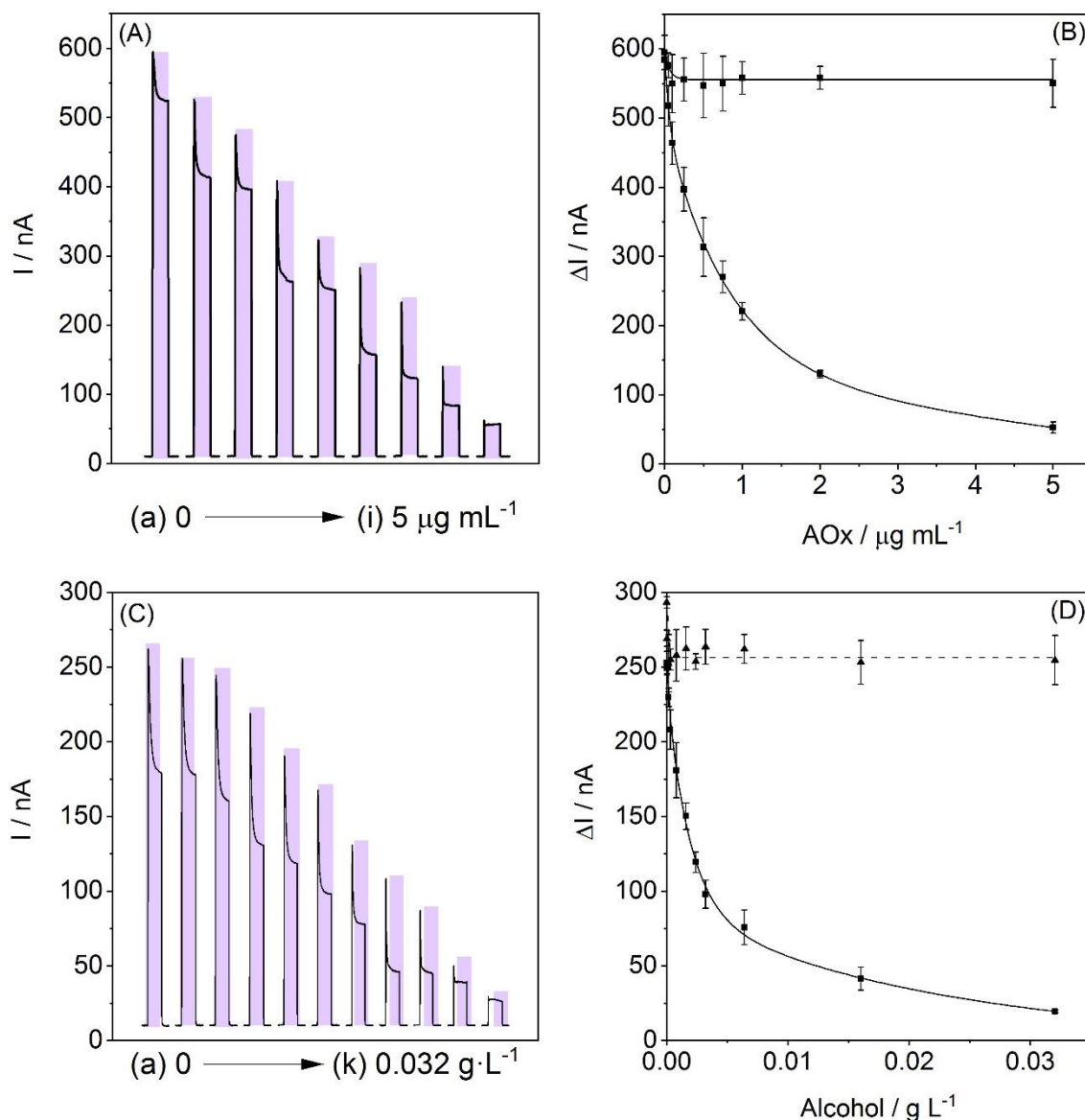


**Figure 9.** (A) Photocurrent response of the system containing methanol (0.03 g L<sup>-1</sup>), cysteine (CSH, 0.075 mM), 1-thioglycerol (TG, 20 mM), Na<sub>2</sub>S (0.1 mM), Cd(NO<sub>3</sub>)<sub>2</sub> (1.25 mM) and different concentrations of AOx (0 to 5 μg mL<sup>-1</sup>). (B) Calibration curves of AOx for methanol (dark line) and ethanol (dashed line) obtained at 0.3 V (vs. Ag/AgCl) and 300 nm excitation light. (C) Photocurrent response of the system containing alcohol oxidase (AOx, 5 μg mL<sup>-1</sup>), CSH (0.075 mM), TG (20 mM), Na<sub>2</sub>S (0.1 mM), Cd(NO<sub>3</sub>)<sub>2</sub> (1.25 mM) and different concentrations of methanol (0 to 0.03 g L<sup>-1</sup>). (D) Calibration curves of methanol (dark line) and ethanol (dashed line) obtained at 0.3 V (vs. Ag/AgCl) and 300 nm excitation light.

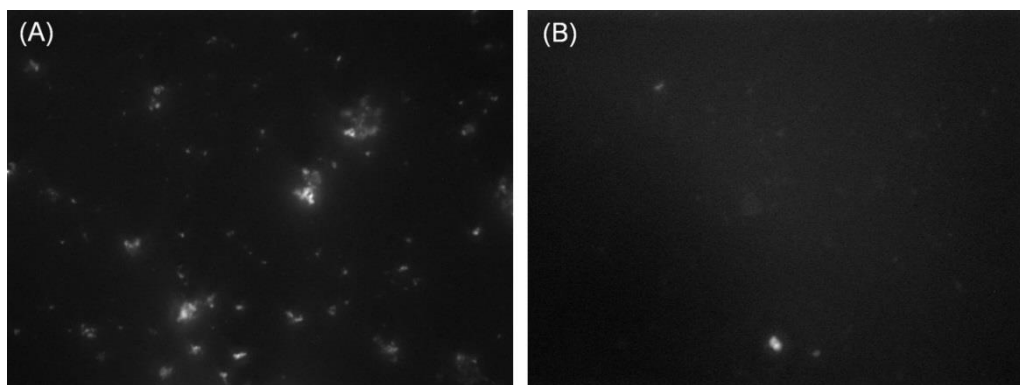


**Figure 10.** Fluorescence microscope images of assay mixtures placed on top of screen-printed carbon electrodes (SPCE) modified with osmium polymer (Ps-PVP complex) for the system containing (A) Alcohol oxidase (AOx,  $5 \mu\text{g L}^{-1}$ ), cysteine (CSH, 0.075 mM),  $\text{Na}_2\text{S}$  (0.1 mM),  $\text{Cd}(\text{NO}_3)_2$  (1.25 mM) and (B) the same system in presence of methanol ( $0.03 \text{ g L}^{-1}$ ).

The photocurrent response to varying concentrations of alcohol (methanol or ethanol) using a fixed amount of AOx ( $5 \mu\text{g L}^{-1}$ ) are depicted in Figure 9A. The observed behaviour of PEC assay is similar to that of the fluorogenic assay. The photocurrent intensities decreased in the presence of increasing methanol amounts, remaining stable in the presence of ethanol (Figure 9B solid and dashed line respectively). The PEC assay demonstrated a consistent  $K_M$  value of  $1.88 \text{ mg L}^{-1}$  similar to one obtained in fluorogenic assay. The LOD of PEC assay was  $0.16 \text{ mg L}^{-1}$  ( $5 \mu\text{M}$ ) at  $S/N=3$ . The average relative standard (RSD) deviation was 5.8%. The PEC methodology proved to be more sensitive by two times in comparison with previously published amperometric biosensor for methanol which is not able to detect methanol in the presence of ethanol.<sup>17,41-44</sup> The previously published bi-enzymatic biosensor for determination of methanol in the presence of ethanol has worse detection limit (5 mM) 1000 time higher than the LOD of the present PEC assay<sup>45</sup> (Table 1). It should be noted that the fluorometric assay is ten times less sensitive than the novel PEC method. It provides a simple and reliable method to determine methanol content in real samples. To best our knowledge this is the first PEC assay for methanol suitable for its determination in the presence of ethanol.

PEC assay was also applied to detection of methanol in aqueous 40% (v/v%) alcohol mixtures with different methanol/ethanol molar ratios ranging between 0.0 and 1.0. According to the calibration plot (Figure 6B) LOD was equal to 0.017 (molar fraction) with RSD of 5.80%. This detection limit is less than that of the fluorogenic assay for methanol.

In Table 2 there are some examples of the main reported techniques utilized to detect methanol. These procedures present some disadvantages like the need of standards or internal/external references, sophisticated or expensive apparatus or reagents, expert operators, long measuring times and sample pre-treatment. On the other hand, in our case both the optical and photoelectrochemical procedure are simpler and easier handling, they do

not need expensive reagents or apparatus and can be easily miniaturized. Moreover, no pre-treatment nor standards or references are required. All these advantages make our procedures more suitable for methanol detection and its application in analytical laboratories.

**Table 2.** Comparison of different techniques for methanol detection.

Methodology	Comments	Sensitivity
Specific gravities and refractive index	Not sensible, laborious procedure	LOD 1.23 M <sup>51</sup>
Colorimetric assays	Unreliable or too much time consuming and manipulation	- 52
Gas chromatography	Time consuming, expensive apparatus, expert operators	LOQ 156 μM <sup>53</sup>
Raman spectroscopy	Need of a standard and internal/external reference	LOD >6.17 M <sup>6</sup> LOD 3.4 mM <sup>7</sup>
Fourier transform infrared spectroscopy	Need of references, time-consuming, sample pre-treatment, harsh conditions	LOD 12.64 mM <sup>8</sup> LOD 0.99 M <sup>9</sup> Lineal range 2.46-246.88 M <sup>10</sup>
Flow tube mass spectrometry	Previous sample manipulation, sophisticated instruments, expensive reagents, expert operators	LOD 312.11 mM <sup>11</sup>
Surface Plasmon resonance	Previous sample manipulation, complicated structures, laborious procedure	LOD 0.37 M <sup>12</sup>
Optical fiber with a photodetector	Expensive equipment	LOD 98.75 mM <sup>13</sup>
Hybrid capillary electrophoresis	Derivatization needed, complicated mechanism	LOD 50 μM <sup>14</sup>
Evanescence wave optical sensor	Laborious setup	- 15
Quartz tuning forks	Laborious setup and procedure, time consuming	LOD 1.23 M <sup>16</sup>

### 3.3. Validation with alcoholic beverages

#### 3.3.1. Simulation of alcoholic strength

It is well known that methanol is not suitable for humans. Thus, its content must be controlled. Alcoholic beverages are classified by the regulation 110/2008 of the European Parliament and of the Council (15 January 2008). It describes the definition, description, presentation, labelling and the protection of geographical indications of spirit drinks. We simulated two types of alcoholic beverages: cider and vodka. Our aim was to validate our fluorogenic and PEC assays using two aqueous solutions of different alcoholic strengths (6% and 40%, v/v%). In order to simulate cider, mixtures containing 6% of total alcohol were spiked with different concentrations ( $\mu\text{g L}^{-1}$ ) of methanol (Figure 11A and 11C). The protocol was slightly modified for alcoholic beverages with the higher alcoholic strength of 40% such as vodka. Fig. 4A and 4C represents the effect of varying concentrations of methanol spiked into 40% ethanol solution. As one can see the increase in the methanol concentration is linearly related with the decrease in the readout signal.

The methanol content for different alcoholic beverages is described by regulation (EC) No 110/2008. In case of vodka, the value should not exceed  $100 \text{ mg L}^{-1}$  (3.12 mM). For ciders, we take as the reference the royal decree 72/2017 by Spanish Government stating that the maximum content of methanol should be not higher than  $200 \text{ mg L}^{-1}$  (6.24 mM). We applied the standard addition method in order to validate the fluorogenic and PEC methods.

#### 3.3.2 Cider

Three local ciders (Etxeberria, Gurutzeta and Izeta) were selected for this study. Different known methanol concentrations close to maximum allowed were added to ciders (added concentrations of methanol were 0, 1, 2, 3, 4 and  $5 \mu\text{g L}^{-1}$ ). Thereafter, the fluorescence signal and PEC response were evaluated, plotting the concentrations of added standards on the x-axis against their corresponding readout signal on the y-axis. The linear regression for each dilution was performed to calculate the intercept of the calibration lines with the x-axis, which represents the content of methanol in the dilute real samples (Figure 11B and 11D). Taking into consideration dilution factors of the ciders samples, we found out that the methanol concentration was under the limit established by law as depicted in Table 3. Both methods corroborated well the content of methanol. PEC method demonstrated better sensitivity.

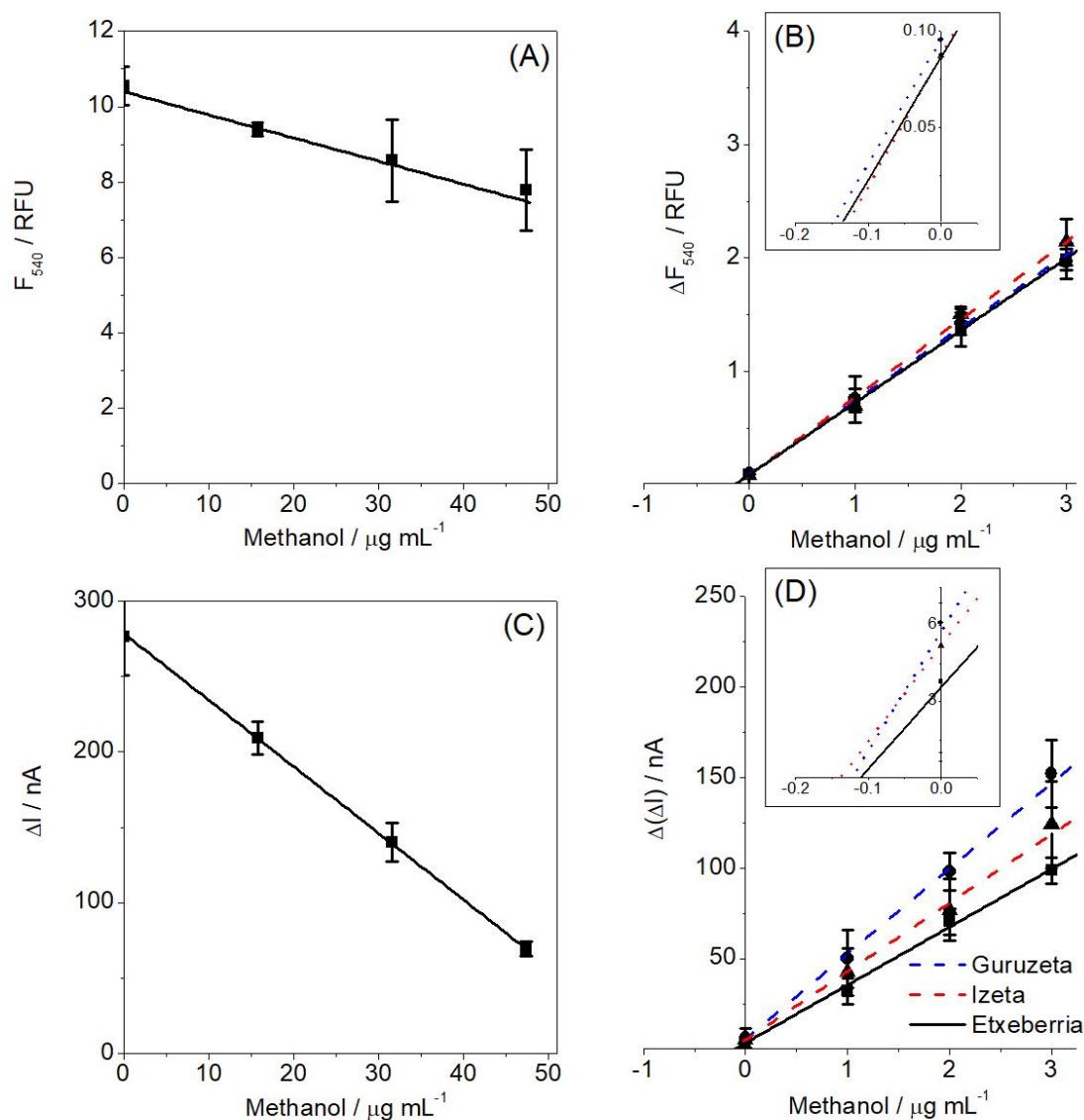


**Figure 11.** Calibration curve of methanol obtained by (A) fluorescence and (C) photoelectrochemical (PEC) assays. Quantification of methanol in three different ciders with the method of standard addition for (B) fluorescence and (D) PEC methods. The system contained different known amounts of added methanol standards. Insets are amplified areas of added standard curves.

### 3.3.3 Vodka

Vodka was chosen because it is the most popular alcoholic beverage in the Eastern European countries and Russia.<sup>54</sup> So, a large number of potential consumers could be intoxicated by the adulterated vodka. The same procedure of added standards described in the above section was applied. Known quantities of methanol were added to vodka samples (Fig. 4B and 4D). By linear regression the amount of methanol was computed (Table 1) which was within the methanol levels specified by the corresponding legislation.

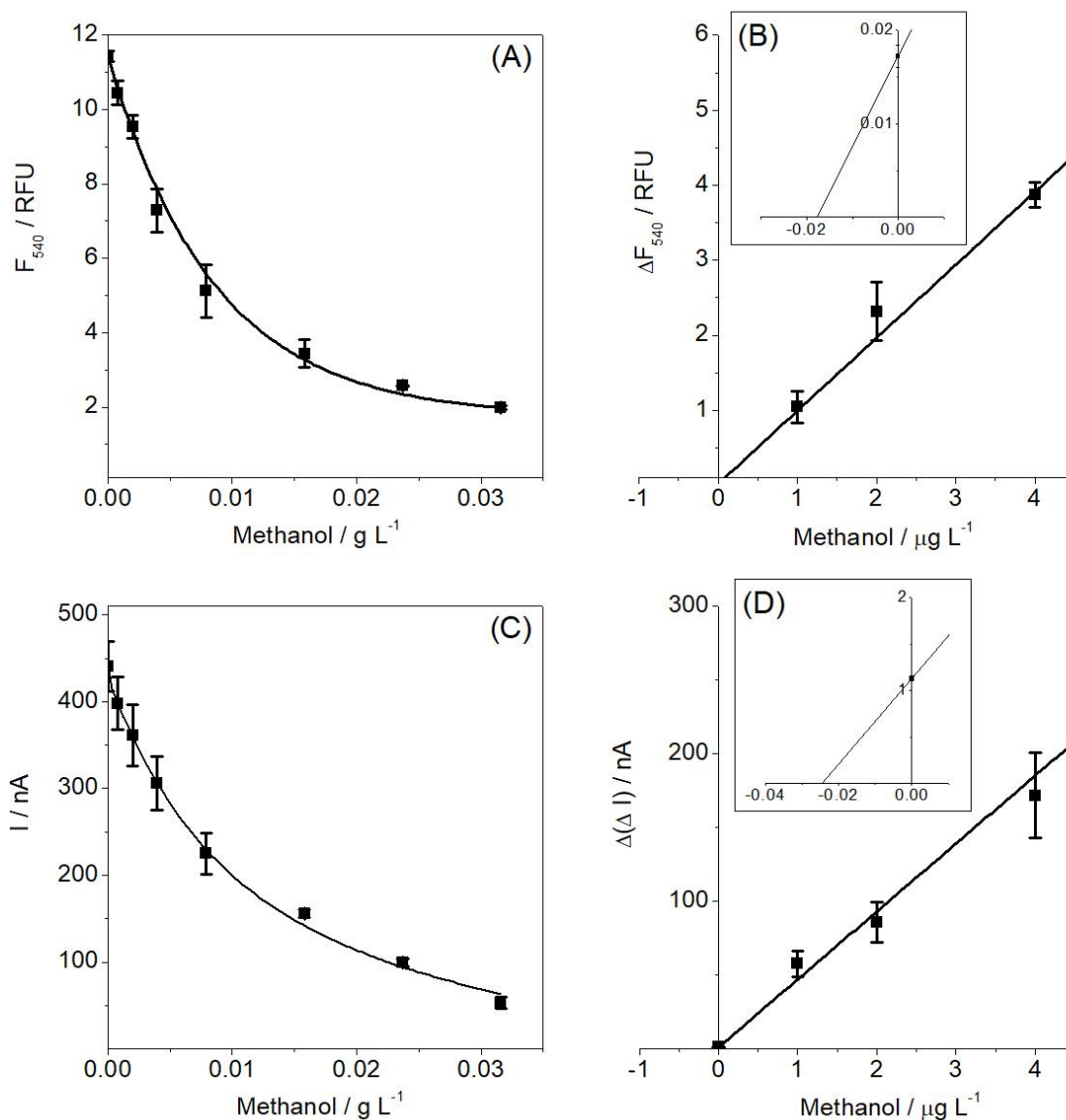


**Figure 12.** Calibration curve of methanol obtained by (A) fluorescence and (C) photoelectrochemical (PEC) assays. Quantification of methanol in vodka with the method of standard addition for (B) fluorescence and (D) PEC methods. The system contained different known amounts of added methanol standards. Insets are amplified areas of added standard curves.

**Table 3.** Content of methanol in different alcoholic beverages quantified by fluorogenic and PEC methods.

Methanol / mg L <sup>-1</sup>	Fluorescence / au	PEC / nA
Etxeberria	134 ± 21	111 ± 25
Izeta	124 ± 33	121 ± 30
Guruzeta	145 ± 25	137 ± 20
Vodka	18 ± 3	24 ± 5



## 4. Conclusions

Adulterated alcoholic beverages with extra methanol drive the searching of new detection methods. This work opens a new concept based on the specificity of AOx to methanol producing H<sub>2</sub>O<sub>2</sub>, which influences in the concentration of the capping agent CSH, ending up in the modulation of in situ generated CdS QDs. The quantification of methanol was followed by classical fluorescence spectroscopy and emerging PEC process. The latter facilities the “wiring” of CdS QDs with disposable SPCE sensitized with Os-PVP complex. This strategy allows the reproducible fabrication of a very simple device. Both methods are more sensitive and more selective than the previously reported bioassays and biosensors. The present approach proved to be efficient for the fast monitoring of methanol in any alcoholic beverages.

## References

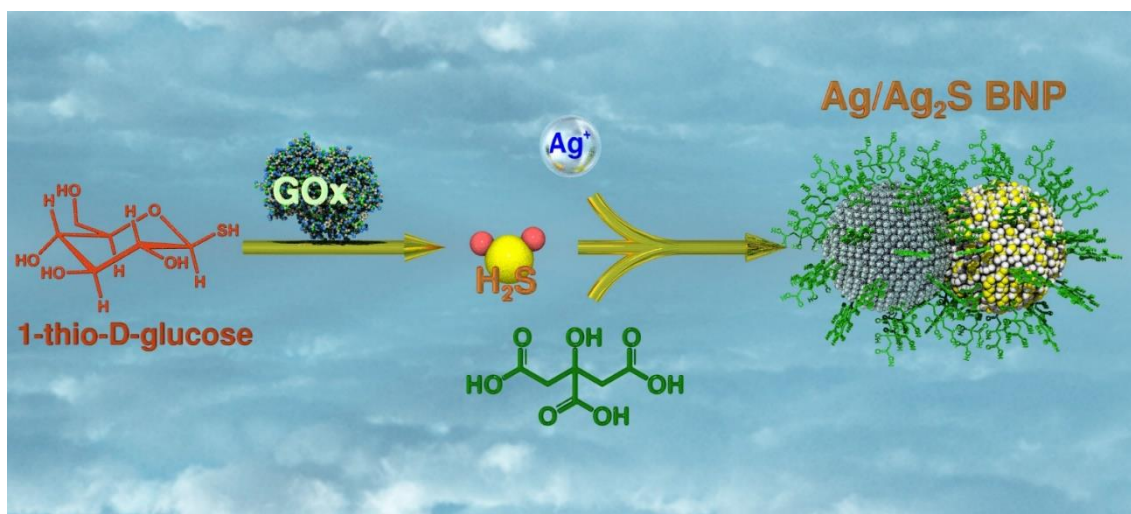
- (1) Skrzydlewska, E. Toxicological and Metabolic Consequences of Methanol Poisoning. *Toxicol. Mech. Methods* **2003**, *13*, 277–293.
- (2) Ohimain, E. I. Methanol Contamination in Traditionally Fermented Alcoholic Beverages: The Microbial Dimension. *Springerplus* **2016**, *5*.
- (3) Paine, A. J.; Dayan, A. D. Defining a Tolerable Concentration of Methanol in Alcoholic Drinks. *Hum. Exp. Toxicol.* **2001**, *20*, 563–568.
- (4) Georgia, F. R.; Morales, R. Detection of Methanol in Alcoholic Beverages. *Ind. Eng. Chem.* **1926**, *18*, 304–306.
- (5) Wang, M. L.; Wang, J. T.; Choong, Y. M. Simultaneous Quantification of Methanol and Ethanol in Alcoholic Beverage Using a Rapid Gas Chromatographic Method Coupling with Dual Internal Standards. *Food Chem.* **2004**, *86*, 609–615.
- (6) de Góes, R. E.; Fabris, L. V. M.; Muller, M.; Fabris, J. L. Light-Assisted Detection of Methanol in Contaminated Spirits. *J. Light. Technol.* **2016**, *34*, 4499–4505.
- (7) Boyaci, I. H.; Genis, H. E.; Guven, B.; Tamer, U.; Alper, N. A Novel Method for Quantification of Ethanol and Methanol in Distilled Alcoholic Beverages Using Raman Spectroscopy. *J. Raman Spectrosc.* **2012**, *43*, 1171–1176.
- (8) Bangalore, A. S.; Small, G. W.; Combs, R. J.; Knapp, R. B.; Kroutil, R. T. Automated Detection of Methanol Vapour by Open Path Fourier Transform Infrared Spectrometry. *Anal. Chim. Acta* **1994**, *297*, 387–403.
- (9) Garrigues, J. M.; Pérez-Ponce, A.; Garrigues, S.; de la Guardia, M. Direct Determination of Ethanol and Methanol in Liquid Samples by Means of Vapor Phase-Fourier Transform Infrared Spectroscopy. *Vib. Spectrosc.* **1997**, *15*, 219–228.
- (10) Yang, Y. R.; Ren, Y. F.; Dong, G. M.; Yang, R. J.; Liu, H. X.; Du, Y. H.; Zhang, W. Y. Determination of Methanol in Alcoholic Beverages by Two-Dimensional Near-Infrared Correlation Spectroscopy. *Anal. Lett.* **2016**, *49*, 2279–2289.
- (11) Chambers-Bédard, C.; Ross, B. M. Quantification of Methanol in the Presence of Ethanol by Selected Ion Flow Tube Mass Spectrometry. *Eur. J. Mass Spectrom.* **2016**, *22*, 159–164.
- (12) Manera, M. G.; Leo, G.; Curri, M. L.; Cozzoli, P. D.; Rella, R.; Siciliano, P.; Agostiano, A.; Vasanelli, L. Investigation on Alcohol Vapours/TiO<sub>2</sub> Nanocrystal Thin Films Interaction by

- SPR Technique for Sensing Application. *Sensors Actuators B Chem.* **2004**, *100*, 75–80.
- (13) Tai, Y.; Pan, M.; Lin, E.; Huang, D.; Wei, P. Quality Detection of Alcoholic Beverages Using Optical Fiber Tips. *IEEE Sens. J.* **2016**, *16*, 5626–5631.
- (14) Santos, M. S. F.; da Costa, E. T.; Gutz, I. G. R.; Garcia, C. D. Analysis of Methanol in the Presence of Ethanol, Using a Hybrid Capillary Electrophoresis Device with Electrochemical Derivatization and Conductivity Detection. *Anal. Chem.* **2017**, *89*, 1362–1368.
- (15) OKUDA, H.; WANG, T. A. O.; LEE, S.-W. Selective Methanol Gas Detection Using a U-Bent Optical Fiber Modified with a Silica Nanoparticle Multilayer. *Electron. Commun. Japan* **2017**, *100*, 43–49.
- (16) Sampson, S. A.; Panchal, S. V.; Mishra, A.; Banerjee, S.; Datar, S. S. Quartz Tuning Fork Based Portable Sensor for Vapor Phase Detection of Methanol Adulteration of Ethanol by Using Aniline-Doped Polystyrene Microwires. *Microchim. Acta* **2017**, *184*, 1659–1667.
- (17) Hasunuma, T.; Kuwabata, S.; Fukusaki, E.; Kobayashi, A. Real-Time Quantification of Methanol in Plants Using a Hybrid Alcohol Oxidase–Peroxidase Biosensor. *Anal. Chem.* **2004**, *76*, 1500–1506.
- (18) Xiao, Y.; Pavlov, V.; Shlyahovsky, B.; Willner, I. An OsII–Bisbipyridine–4-Picolinic Acid Complex Mediates the Biocatalytic Growth of Au Nanoparticles: Optical Detection of Glucose and Acetylcholine Esterase Inhibition. *Chem. – A Eur. J.* **2005**, *11*, 2698–2704.
- (19) Fanjul-Bolado, P.; Hernández-Santos, D.; González-García, M. B.; Costa-García, A. Alkaline Phosphatase-Catalyzed Silver Deposition for Electrochemical Detection. *Anal. Chem.* **2007**, *79*, 5272–5277.
- (20) Shlyahovsky, B.; Katz, E.; Xiao, Y.; Pavlov, V.; Willner, I. Optical and Electrochemical Detection of NADH and of NAD<sup>+</sup>-Dependent Biocatalyzed Processes by the Catalytic Deposition of Copper on Gold Nanoparticles. *Small* **2005**, *1*, 213–216.
- (21) Zhao, W.-W.; Yu, X.-D.; Xu, J.-J.; Chen, H.-Y. Recent Advances in the Use of Quantum Dots for Photoelectrochemical Bioanalysis. *Nanoscale* **2016**, *8*, 17407–17414.
- (22) Zhou, H.; Liu, J.; Zhang, S. Quantum Dot-Based Photoelectric Conversion for Biosensing Applications. *TrAC Trends Anal. Chem.* **2015**, *67*, 56–73.
- (23) Huang, H.; Zhu, J.-J. The Electrochemical Applications of Quantum Dots. *Analyst* **2013**, *138*, 5855–5865.
- (24) Chatterjee, A.; Priyam, A.; Das, S. K.; Saha, A. Size Tunable Synthesis of Cysteine-Capped CdS Nanoparticles by  $\gamma$ -Irradiation. *J. Colloid Interface Sci.* **2006**, *294*, 334–342.
- (25) Huang, F.; Lan, Y. Aqueous Synthesis of Water-Soluble L-Cysteine-Modified Cadmium Sulfide Doped with Silver Ion/Zinc Sulfide Nanocrystals. *Spectrosc. Lett.* **2015**, *48*, 159–162.
- (26) Devadoss, A.; Sudhagar, P.; Terashima, C.; Nakata, K.; Fujishima, A. Photoelectrochemical Biosensors: New Insights into Promising Photoelectrodes and Signal Amplification Strategies. *J. Photochem. Photobiol. C Photochem. Rev.* **2015**, *24*, 43–63.
- (27) Katakis, I.; Ye, L.; Heller, A. Electrostatic Control of the Electron-Transfer Enabling Binding of Recombinant Glucose Oxidase and Redox Polyelectrolytes. *J. Am. Chem. Soc.* **1994**, *116*, 3617–3618.
- (28) Vreeke, M.; Maidan, R.; Heller, A. Hydrogen Peroxide and .Beta.-Nicotinamide Adenine Dinucleotide Sensing Amperometric Electrodes Based on Electrical Connection of Horseradish Peroxidase Redox Centers to Electrodes through a Three-Dimensional Electron Relaying Polymer Network. *Anal. Chem.* **1992**, *64*, 3084–3090.
- (29) Yang, L.; Janle, E.; Huang, T.; Gitzen, J.; Kissinger, P. T.; Vreeke, M.; Heller, A. Applications of “Wired” Peroxidase Electrodes for Peroxide Determination in Liquid Chromatography Coupled to Oxidase Immobilized Enzyme Reactors. *Anal. Chem.* **1995**, *67*, 1326–1331.
- (30) Kumar, P.; Kumar, P.; Bharadwaj, L. M.; Paul, A. K.; Sharma, S. C.; Kush, P.; Deep, A. Aqueous Synthesis of L-Cysteine Stabilized Water-Dispersible CdS:Mn Quantum Dots for

- Biosensing Applications. *Bionanoscience* **2013**, *3*, 95–101.
- (31) Gülce, H.; Gülce, A.; Kavanoz, M.; Coşkun, H.; Yıldız, A. A New Amperometric Enzyme Electrode for Alcohol Determination. *Biosens. Bioelectron.* **2002**, *17*, 517–521.
  - (32) Yildiz, H. B.; Toppare, L. Biosensing Approach for Alcohol Determination Using Immobilized Alcohol Oxidase. *Biosens. Bioelectron.* **2006**, *21*, 2306–2310.
  - (33) Barsan, M. M.; Brett, C. M. A. An Alcohol Oxidase Biosensor Using PNR Redox Mediator at Carbon Film Electrodes. *Talanta* **2008**, *74*, 1505–1510.
  - (34) Zhang, C.-Y.; Lin, N.-B.; Chai, X.-S.; Zhong-Li; Barnes, D. G. A Rapid Method for Simultaneously Determining Ethanol and Methanol Content in Wines by Full Evaporation Headspace Gas Chromatography. *Food Chem.* **2015**, *183*, 169–172.
  - (35) Płotka-Wasyłka, J.; Simeonov, V.; Namieśnik, J. An in Situ Derivatization – Dispersive Liquid–Liquid Microextraction Combined with Gas-Chromatography – Mass Spectrometry for Determining Biogenic Amines in Home-Made Fermented Alcoholic Drinks. *J. Chromatogr. A* **2016**, *1453*, 10–18.
  - (36) Kučera, I.; Sedláček, V. An Enzymatic Method for Methanol Quantification in Methanol/Ethanol Mixtures with a Microtiter Plate Fluorometer. *Food Anal. Methods* **2017**, *10*, 1301–1307.
  - (37) Azevedo, A. M.; Prazeres, D. M. F.; Cabral, J. M. S.; Fonseca, L. P. Ethanol Biosensors Based on Alcohol Oxidase. *Biosens. Bioelectron.* **2005**, *21*, 235–247.
  - (38) Verduyn, C.; van Dijken, J. P.; Scheffers, W. A. Colorimetric Alcohol Assays with Alcohol Oxidase. *J. Microbiol. Methods* **1984**, *2*, 15–25.
  - (39) Anthon, G. E.; Barrett, D. M. Comparison of Three Colorimetric Reagents in the Determination of Methanol with Alcohol Oxidase. Application to the Assay of Pectin Methyltransferase. *J. Agric. Food Chem.* **2004**, *52*, 3749–3753.
  - (40) Wang, M.-L. L.; Wang, J.-T. T.; Choong, Y.-M. M. A Rapid and Accurate Method for Determination of Methanol in Alcoholic Beverage by Direct Injection Capillary Gas Chromatography. *J. Food Compos. Anal.* **2004**, *17*, 187–196.
  - (41) Chinnadayala, S. R.; Kakoti, A.; Santhosh, M.; Goswami, P. A Novel Amperometric Alcohol Biosensor Developed in a 3rd Generation Bioelectrode Platform Using Peroxidase Coupled Ferrocene Activated Alcohol Oxidase as Biorecognition System. *Biosens. Bioelectron.* **2014**, *55*, 120–126.
  - (42) Chinnadayala, S. R.; Santhosh, M.; Singh, N. K.; Goswami, P. Alcohol Oxidase Protein Mediated In-Situ Synthesized and Stabilized Gold Nanoparticles for Developing Amperometric Alcohol Biosensor. *Biosens. Bioelectron.* **2015**, *69*, 155–161.
  - (43) Du, X.; Anzai, J.; Osa, T.; Motohashi, R. Amperometric Alcohol Sensors Based on Protein Multilayers Composed of Avidin and Biotin-Labeled Alcohol Oxidase. *Electroanalysis* **1996**, *8*, 813–816.
  - (44) Wen, G.; Wen, X.; Shuang, S.; Choi, M. M. F. Whole-Cell Biosensor for Determination of Methanol. *Sensors Actuators B Chem.* **2014**, *201*, 586–591.
  - (45) Bucur, B.; Radu, G. L.; Toader, C. N.; Lucian, A. E. G. Analysis of Methanol–Ethanol Mixtures from Falsified Beverages Using a Dual Biosensors Amperometric System Based on Alcohol Dehydrogenase and Alcohol Oxidase. *Eur. Food Res. Technol.* **2008**, *226*, 1335–1342.
  - (46) Barroso, J.; Saa, L.; Grinyte, R.; Pavlov, V. Photoelectrochemical Detection of Enzymatically Generated CdS Nanoparticles: Application to Development of Immunoassay. *Biosens. Bioelectron.* **2016**, *77*, 323–329.
  - (47) Yang, Y. J. The Thioglycerol Catalyzed Reaction of Metal Salts and Elemental Sulfur: A New Approach for the Preparation of Nanocrystalline Metal Sulfides. *Colloids Surfaces A Physicochem. Eng. Asp.* **2006**, *276*, 192–196.
  - (48) Brahim, N. Ben; Mohamed, N. B. H.; Echabaane, M.; Haouari, M.; Chaâbane, R. Ben; Negrierie, M.; Ouada, H. Ben. Thioglycerol-Functionalized CdSe Quantum Dots Detecting Cadmium Ions. *Sensors Actuators B Chem.* **2015**, *220*, 1346–1353.

### Chapter 3

- (49) DEEPIKA; DHAR, R.; SINGH, S.; KUMAR, A. Effect of Capping Agents on Optical and Antibacterial Properties of Cadmium Selenide Quantum Dots. *Bull. Mater. Sci.* **2015**, *38*, 1247–1252.
- (50) Silva, A. C. A.; da Silva, S. W.; Morais, P. C.; Dantas, N. O. Shell Thickness Modulation in Ultrasmall CdSe/CdS<sub>x</sub>Se<sub>1-x</sub>/CdS Core/Shell Quantum Dots via 1-Thioglycerol. *ACS Nano* **2014**, *8*, 1913–1922.
- (51) Leach, A. E.; Lythgoe, H. C. THE DETECTION AND DETERMINATION OF ETHYL AND METHYL ALCOHOLS IN MIXTURES BY THE IMMERSION REFRACTOMETER. *J. Am. Chem. Soc.* **1905**, *27*, 964–972.
- (52) Gettler, A. CRITICAL STUDY OF METHODS FOR THE DETECTION OF METHYL ALCOHOL. *J. Biol. Med.* **1920**, *42*, 311.
- (53) Wang, M. L.; Wang, J. T.; Choong, Y. M. A Rapid and Accurate Method for Determination of Methanol in Alcoholic Beverage by Direct Injection Capillary Gas Chromatography. *J. Food Compos. Anal.* **2004**, *17*, 187–196.
- (54) Wiśniewska, P.; Śliwińska, M.; Dymerski, T.; Wardencki, W.; Namieśnik, J. The Analysis of Vodka: A Review Paper. *Food Anal. Methods* **2015**, *8*, 2000–2010.



## FACILE SYNTHESIS AND CHARACTERIZATION OF Ag/Ag<sub>2</sub>S NANOPARTICLES ENZYMATICALLY GROWN IN SITU AND THEIR APPLICATION TO THE COLORIMETRIC DETECTION OF GLUCOSE OXIDASE

This work describes a simple, fast and reproducible biochemical reaction to modulate the growth of silver/silver sulfide nanoparticles (Ag/Ag<sub>2</sub>S NPs) through the enzymatic activity of the glucose oxidase (GOx). This process occurs in aqueous buffered solutions at room temperature under physiological conditions with participation of inexpensive precursors. Oxidation of 1-thio-β-D-glucose is catalyzed by GOx yielding hydrogen sulfide. Direct interaction between silver nitrate and enzymatically produced H<sub>2</sub>S in the presence of citric acid as capping agent leads to the generation of Ag/Ag<sub>2</sub>S NPs with a spherical shape. UV-vis spectroscopy is employed to characterize absorbance spectra of resulting Ag/Ag<sub>2</sub>S NPs with the highest signal-to-noise ratio at 385 nm. Enzymatically produced Ag/Ag<sub>2</sub>S NPs are characterized by TEM, XPS, DLS and XRD. This new colorimetric method based on the enzymatic growth in situ of NPs was applied to the detection of enzymatic activity of GOx (LOD 0.557 μg mL<sup>-1</sup> and linear range up to 1.5 μg mL<sup>-1</sup>). The effect of D-glucose on the read-out signal has been studied to confirm the enzymatic mechanism of this process (LOD 176.21 μM and linear range up to 1.25 mM) and was applied to the detection of glucose in human plasma.

---

The work presented was previously published: Díez-Buitrago, B.; Barroso, J.; Saa, L.; Briz, N.; Pavlov, V. *ChemistrySelect* **2019**, *4* (28), 8212-8219

## 1. Introduction

Nanomaterials exhibit very interesting electrical, optical, magnetic and chemical properties, which are not shown by their bulk equivalents. Nanoparticles have high surface area to volume ratios and their shape can be tailored by varying concentrations of their precursors and capping agents. In recent years nanomaterial based analytical assays have attracted much attention due to their versatility, high sensitivity and inexpensive fabrication of new devices for the detection of a wide range of analytes. Among the nanomaterials, both metallic and semiconductor nanoparticles (NPs) are considered to be the most broadly utilized structures in bioanalytical assays and biosensors. Their exceptional physicochemical properties, easy structure and shape determination and their nanoscale sizes similar to those of some biomolecules make them promising structures for their use as labels, transducers and amplifiers in biosensing.<sup>1</sup>

Silver sulfide nanostructures such as NPs, quantum dots and nanostructured films possess unique optical and electrical properties. They have been intensively investigated in the recent years and their several applications such as infrared detectors,<sup>2</sup> photoconductors, semiconductors in solar cells<sup>3</sup> or fluorescent labels in biology and medicine<sup>4</sup> were reported. Moreover, aqueous colloidal solutions of silver sulfide nanoparticles ( $\text{Ag}_2\text{S}$  NPs) are considered to be much less toxic in comparison to other commonly used nanomaterials such as PbSe, PbS, CdS, and CdSe QDs, holding particular promise for biological applications.<sup>5</sup>

$\text{Ag}_2\text{S}$  NPs have been prepared by numerous methods that include hydrothermal and sol-gel routes,<sup>6,7</sup> solvo-thermal methods,<sup>8</sup> hydrochemical bath deposition,<sup>9-11</sup> micro-emulsion methods<sup>12</sup> and electrochemical methods.<sup>13</sup> A number of procedures are based on the strong interaction between silver and sulfide ions in aqueous/organic solutions that tend to form solid and stable structures in an easy and fast way. While a simple silver salt is typically used as silver source (i.e.:  $\text{AgNO}_3$ ), various organic and inorganic sulfides are used to provide sulfide ions, including  $\text{H}_2\text{S}$ , alkyl thiols<sup>14</sup> or  $(\text{NH}_4)_2\text{S}$ .<sup>15,16</sup> Capping agents, on the other hand, are used to control particle size, shape and stability. Moreover, capping agents are an important factor also in controlling toxicity of  $\text{Ag}_2\text{S}$  NPs. Different capping agents such as mercapto-derivates,<sup>15,17,18</sup> triton X-100,<sup>14</sup> PVP and citrate<sup>9-11</sup> have been used to stabilize NPs. Although, the above mentioned procedures present some advantages and produce particles with particular properties, they often require harsh preparation conditions, toxic solvents, they are time consuming, suffer from energy consumption and large size distribution. Hence, finding

routes for production of Ag<sub>2</sub>S NPs under physiological conditions compatible with biological proteins is a challenging task.

The use of biological agents like enzymes in bioanalytical assays is receiving a lot of attention nowadays. Enzymes are proteins with catalytic properties and high specific activity. The products of enzymatic reactions can interact with nanomaterials, resulting in modification of their measurable properties.<sup>19</sup> Normally two main approaches are followed: modulation of nanoparticles or growth in situ. On one hand, enzymatic reactions generate specific products that can enhance or decrease the NPs read-out signal as the result of their growth,<sup>20</sup> quenching<sup>21</sup> or etching.<sup>22</sup> This procedure presents some advantages such as high sensitivity and versatility, but it requires the previous synthesis of the NPs. To overcome this issue, the in situ formation of nanomaterials as a result of an enzymatic reaction is presented as the best alternative. Increasing number of publications in bioanalysis is dedicated to the use of enzymes for the in situ formation of nanoparticles as the read-out signal mainly due to their optical<sup>23</sup> and electrochemical<sup>24</sup> properties. This approach maintains the advantages of the previous strategy and also avoids the need of pre-synthesized nanoparticles simplifying the bioassay.

Enzymatic in situ production of silver containing NPs can find broad application in bioanalysis because enzymes are extensively employed for detection of analytes and amplification of the read-out signal. Given the fact that the silver containing NPs strongly absorb UV and visible light, the in situ formation, triggered by an enzyme, can be conveniently followed by UV-vis spectroscopy.

In this work we propose a simple enzymatic method for the synthesis of Ag/Ag<sub>2</sub>S spherical nanoparticles in an aqueous solution in the presence of citrate ions as capping agent. This present system based on formation of Ag/Ag<sub>2</sub>S NPs was applied to the detection of enzymatic activity of glucose oxidase (GOx) and the detection of glucose in real samples. This system was selected considering glucose importance in clinical for diabetes management. During the last decades, glucose biosensor technology including point-of-care devices, continuous glucose monitoring systems and non-invasive glucose monitoring systems have been significantly improved<sup>25,26</sup> and great efforts have been made to achieve better accuracy, precision and sensitivity by using different techniques (colorimetry,<sup>27,28</sup> photoelectrochemistry,<sup>29</sup> electrochemistry<sup>30</sup>). Here we present an easy colorimetric method that could be integrated in a smartphone application for a rapid, easy and cost-effective determination of the desired analyte. Some recent studies have been developed in this direction for a wide range of bioanalytical substances.<sup>31-34</sup> To the best of our knowledge, enzymatic assays based on biocatalytic generation of silver sulfide NPs have never been reported before.

## 2. Experimental section

### 2.1. Materials

Glucose oxidase type VII from *Aspergillus Niger* (GOx), 1-thio- $\beta$ -D-glucose (analytical reagent), silver nitrate ( $\geq 99\%$  AgNO<sub>3</sub>), sodium sulfide (analytical grade Na<sub>2</sub>S), citric acid anhydrous (analytical reagent) and sodium citrate tribasic dihydrate ( $\geq 99\%$ ) were obtained from Sigma-Aldrich. Anhydrous D (+)-glucose (HPLC grade,  $\geq 99\%$ ) was purchased from PanReac AppliChem.

### 2.2. Apparatus

Absorbance measurements were performed on a Varioskan Flash microplate reader (Thermo Scientific) using transparent microwell plates at room temperature. The system was controlled by the SkanIt Software 2.4.3. RE for Varioskan Flash. The pH was measured using a Seven Easy pH meter (Mettler Toledo, Schwerzenbach, Switzerland) equipped with an InLab micro electrode (Mettler Toledo, Schwerzenbach, Switzerland). Transmission electron microscopy (TEM) images were recorded with a JEOL JEM 2100F microscope equipped with a high-angle annular dark field (HAADF) detector and an energy-dispersive X-ray spectroscopy system (EDX), operating at 120 kV. X-ray diffraction measurements were carried out using a D8 Advance, Bruker AXS diffractometer. Measurements were carried out in the  $\vartheta$ - $2\vartheta$  step scan mode using CuK $\alpha$  radiation and a step size of 0.05. X-ray photoelectron spectroscopy (XPS) experiments were performed in a SPCE Sage HR 100 spectrometer with a non-monochromatic X-ray source (Aluminum K $\alpha$  line of 1486.6 eV energy and 253 W). Dynamic light scattering (DLS) measurements were carried out using a Malvern Instruments particle sizer (Zetasizer Nano ZS, Malvern Instruments, UK) equipped with a He-Ne laser ( $\lambda$ /nm 632.8) working in backscattering mode at a scattering angle of  $2\theta = 173^\circ$ . The solutions were placed into 10x10 mm plastic cuvettes.

### 2.3. Methods

#### 2.3.1. Chemical synthesis of Ag/Ag<sub>2</sub>S NPs

In a transparent 96-well plate, varying amounts of AgNO<sub>3</sub> (from 0 to 8 mM) and Na<sub>2</sub>S (from 0 to 1 mM) were incubated in citrate buffer (10 mM, pH 4) in a final volume of 200  $\mu$ L for 3 min at room temperature. After that, the absorbance spectra were recorded.



### 2.3.2. Glucose oxidase assay

In a transparent 96-well plate, varying amounts of 1-thio- $\beta$ -D-glucose (from 0 to 1.2 mM) and GOx (from 0 to 7  $\mu\text{g mL}^{-1}$ ) mixtures were incubated in citrate buffer (10 mM, pH 4) for 45 min at room temperature. Next,  $\text{AgNO}_3$  (3  $\mu\text{L}$ , 66.67 mM) was added to the respective samples (197  $\mu\text{L}$ ). After 3 min the absorbance spectra were recorded.

### 2.3.3. Glucose assay

In a transparent 96-well plate, varying amounts of glucose (from 0 to 5 mM) were incubated in the presence of 1-thio- $\beta$ -D-glucose (0.5 mM) and GOx (19  $\mu\text{g mL}^{-1}$ ) in citrate buffer (10 mM, pH 4) for 45 min at room temperature. Next,  $\text{AgNO}_3$  (3  $\mu\text{L}$ , 66.67 mM) was added to the respective samples (197  $\mu\text{L}$ ). After 3 min the absorbance spectra were recorded.

### 2.3.4. Quantification of glucose in human serum

The quantification of glucose in human serum (Sigma-Aldrich) was performed by the standard addition method. Samples of pooled human serum was centrifuged using an Amicon Ultra filter with a 3000 molecular weight cut-off. After filtering, the serum was spiked with varying known concentrations of glucose, and the respective glucose concentration in these mixtures was then determined as described above. The dilution factor of plasma in the assay was 1:100.

## 3. Results and discussion

### 3.1. Chemical synthesis of Ag/Ag<sub>2</sub>S NPs

First, the optimal experimental conditions for the growth of Ag/Ag<sub>2</sub>S NPs from Ag<sup>+</sup> and S<sup>2-</sup> ions in aqueous citrate buffer, suitable for operation of GOx, were determined. As it is known, citrate acts as a capping agent and stabilizer for inorganic NPs.<sup>9-11</sup> The formation of Ag<sub>2</sub>S nanospherical moieties is almost instant in the presence of low concentrations of Ag<sup>+</sup> and S<sup>2-</sup> ions in aqueous solutions as one can conclude from very low solubility product constant of Ag<sub>2</sub>S ( $K_{\text{sp}} = 6.3 \times 10^{-50}$ ).<sup>35</sup> Aqueous solutions of Ag/Ag<sub>2</sub>S NPs are coloured dark yellow. The intensity of colour depends on the amount of Ag/Ag<sub>2</sub>S NPs in the media and colour turns brownish at high concentrations of NPs (Figure 1A). The absorbance spectrum of the synthesized NPs agrees well with literature data showing a broad band between 350 and 400 nm (Figure 1B).<sup>16,36</sup> No absorbance of UV-vis light was observed in the spectra of aqueous solutions containing only AgNO<sub>3</sub>, Na<sub>2</sub>S or citric acid, respectively. This indicates that the absorbance spectrum of Ag/Ag<sub>2</sub>S NPs is not influenced by the optical properties of individual reagents. Next, the selection of optimal wavelength for optical measurement was performed

in order to obtain the best signal-to-background ratio of readings observed in the absence ( $Abs_0$ ) and the presence ( $Abs$ ) of Ag/Ag<sub>2</sub>S NPs. According to the plot in Figure 1C, representing the ratio  $Abs/Abs_0$  vs. wavelength, the highest ratio of  $Abs/Abs_0$  was observed at the wavelength of 385 nm.

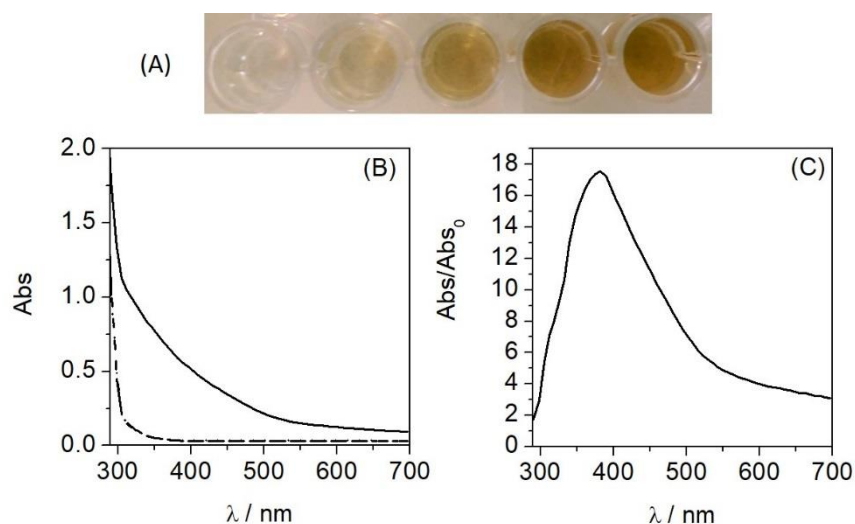


**Figure 1.** (A) Change in colour of reaction mixtures with increasing sulfide concentration, (B) Absorbance spectrum of citrate buffer 10 mM pH 4 (dashed line) and synthesized Ag/Ag<sub>2</sub>S NPs (solid line), (C) Signal-to-background ratio between absorbance spectra of Ag/Ag<sub>2</sub>S and citrate buffer 10 mM pH 4.

To optimize concentrations of reagents, varying amounts of S<sup>2-</sup> and Ag<sup>+</sup> were mixed up in the citrate buffer (10 mM, pH 4). The registered optical signals are directly related to the increase in the concentration of one of the precursors when the concentration of the other precursor was fixed, as depicted in Figure 2. In case of Na<sub>2</sub>S, the increase in its concentration causes the increase in the intensity of the absorbance peak, which asymptotically approaches maximum value starting from 0.5 mM (Figure 2C). For AgNO<sub>3</sub> the saturation starts from 2 mM (Figure 2F). The absorbance intensity reaches a maximum at stoichiometric concentrations of reagents (AgNO<sub>3</sub>:Na<sub>2</sub>S, 2:1) in all cases. The initial solution was completely transparent and upon addition of the second reagent the mixture turned dark yellow. This change in colour is caused by the formation of colloidal Ag/Ag<sub>2</sub>S nano-spheres up to the stoichiometric relation, where one of the reagents is completely consumed. Beyond this point, there was no change in colour, reaching a plateau. In order to test the response of the system, a number of control experiments were carried out (Figure 2C and Figure 2F, red line). No absorbance was observed in the absence of one of the precursors hence it was confirmed that the appearance of colour is caused by the formation of colloidal Ag/Ag<sub>2</sub>S NPs in citrate buffer at room temperature.

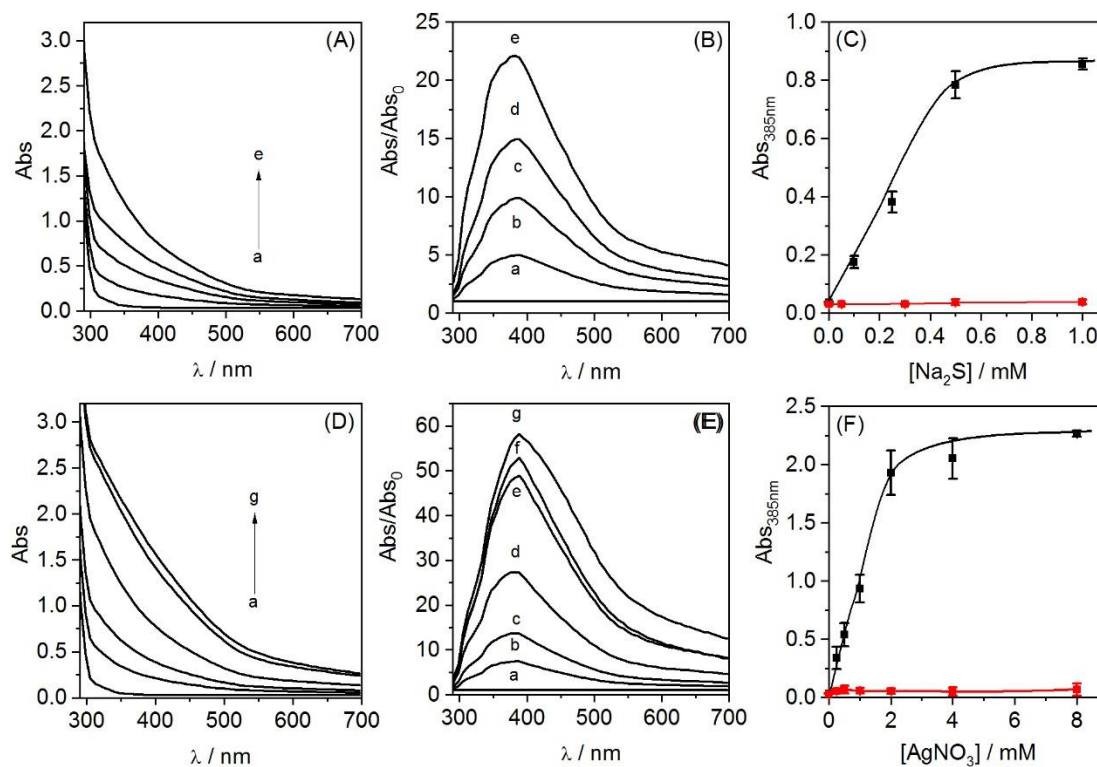


**Figure 2.** (A) UV-vis absorption spectra and (B) Abs/Abs<sub>300</sub> ratio of the system containing AgNO<sub>3</sub> (1 mM) and different concentrations of Na<sub>2</sub>S: a) 0 mM, b) 0.1 mM, c) 0.25 mM, d) 0.5 mM, e) 1 mM, (C) Calibration curve of Na<sub>2</sub>S in absence (red) and presence (black) of AgNO<sub>3</sub> (1 mM). (D) UV-vis absorption spectra and (E) Abs/Abs<sub>300</sub> ratio of the system containing Na<sub>2</sub>S (1 mM) and different concentrations of AgNO<sub>3</sub>: a) 0 mM, b) 0.25 mM, c) 0.5 mM, d) 1 mM, e) 2 mM, f) 4 mM, g) 8 mM, (F) Calibration curve of AgNO<sub>3</sub> in the absence (red) and presence (black) of Na<sub>2</sub>S (1 mM).

The other parameter optimized was the concentration of citrate ions acting as capping agent and reductant of silver ions.<sup>37,38</sup> The three carboxylate groups of citrate have a strong affinity to silver ions, favouring the stabilization of small Ag<sub>2</sub>S NPs and thus avoiding their agglomeration into large structures.<sup>9,10</sup> On the other hand, the reducing capacity of citric acid is well known and used in a wide number of syntheses. For that reason it is crucial to determine the proper conditions for the growth of Ag/Ag<sub>2</sub>S nanospherical moieties and its possible reductant behaviour to form spherical Ag NPs. The influence of varying concentrations of citrate (from 0.25 to 10 mM) on the absorbance at 385 nm demonstrated by mixtures containing AgNO<sub>3</sub> (1 mM) and Na<sub>2</sub>S (from 0 to 1 mM) is shown in Figure 3. The maximum absorbance signal, registered immediately after injection of all three components, was apparently reduced when citrate concentrations were increased reaching 25% drop in the signal intensity at 10 mM citrate concentration. Nevertheless, the solutions of Ag/Ag<sub>2</sub>S NPs prepared in the presence of 10 mM citrate demonstrated higher stability (data not shown). Taking into account the increased stability of Ag/Ag<sub>2</sub>S NPs in the presence of higher concentrations of citrate ions and the increased buffer capacity required for prospective

biological applications, 10 mM citrate was selected as an acceptable concentration of the capping agent and buffer for subsequent measurements.

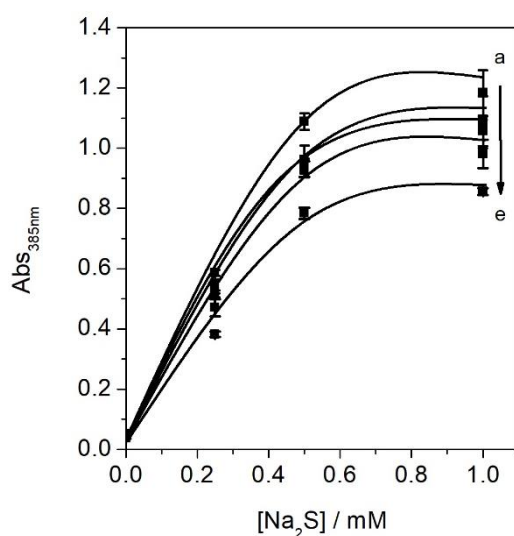


**Figure 3.** Ag/Ag<sub>2</sub>S NPs absorbance variation in the presence of AgNO<sub>3</sub> (1 mM), Na<sub>2</sub>S (from 0 to 1 mM) and different concentrations of citrate buffer pH 4: a) 0 mM, b) 0.25 mM, c) 0.5 mM, d) 5 mM, e) 10 mM.

The effect of pH on the amount of Ag/Ag<sub>2</sub>S NPs formed in situ was studied too. As depicted in Figure 4, the increase in the absorbance is related with the decrease in pH from 5 to 3, enhancing the signal almost in 60%. Even though acidic media apparently favours formation of more Ag/Ag<sub>2</sub>S NPs in the assay mixture, low pH compromises stability of proteins and other biopolymers. Thus, citrate buffer at pH of 4 was used in the following experimental work. This value was also selected considering that the optimum pH range for the glucose oxidase is between 3 and 5.

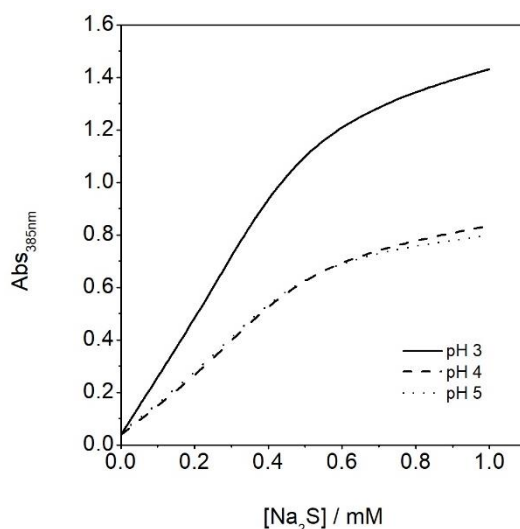


**Figure 4.** Ag/Ag<sub>2</sub>S NPs absorbance variation in the presence of AgNO<sub>3</sub> (1 mM), Na<sub>2</sub>S (from 0 to 1 mM) and different citrate buffer pH.

Another aspect to point out is the stability on Ag/Ag<sub>2</sub>S NPs produced under physiological conditions. The effect of different incubation times on absorbance measured at varying concentration of S<sup>2-</sup> and fixed concentration of Ag<sup>+</sup> was studied. As it can be seen in Figure 5, the absorbance remains almost constant even for incubation times up to 12 hours indicating that Ag/Ag<sub>2</sub>S NPs are stable in the 10 mM buffered citrate solution (10 mM, pH 4). It was decided to establish 3 min as incubating time for the all the following experiments.

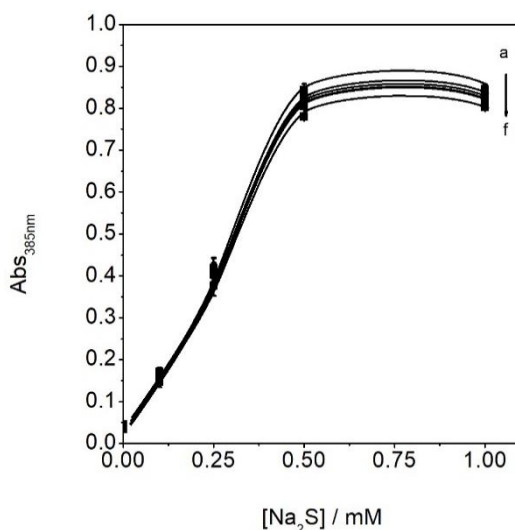


**Figure 5.** Ag/Ag<sub>2</sub>S NPs absorbance in the presence of AgNO<sub>3</sub> (1 mM), Na<sub>2</sub>S (from 0 to 1 mM), citrate buffer 10 mM pH 4 and different measuring times: a) 3 min, b) 17 min, c) 30 min, d) 60 min, e) 120 min, f) 12 hours.

Finally, optimization of Ag<sup>+</sup> concentration needed for quantification of sulfide ions was carried out. As shown in Figure 6, the best signal/background ratio was achieved at AgNO<sub>3</sub> 1 mM.

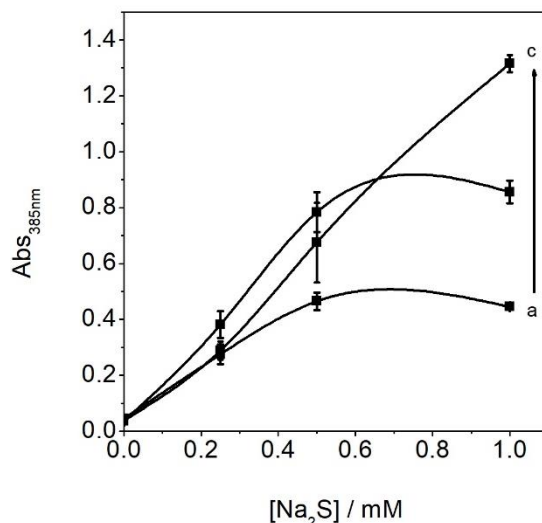


**Figure 6.** Ag/Ag<sub>2</sub>S NPs absorbance variation in the presence of Na<sub>2</sub>S (from 0 to 1 mM), citrate buffer 10 mM pH 4 and different AgNO<sub>3</sub> concentrations: a) 0.5 mM, b) 1 mM, c) 2 mM.

Considering the above-mentioned experimental data, the following optimal parameters for enzymatic generation of Ag/Ag<sub>2</sub>S NPs were used in subsequent experiments: AgNO<sub>3</sub> 1 mM, citrate 10 mM, pH 4, incubation time 3 min, measuring wavelength 385 nm.

### 3.2. Ag/Ag<sub>2</sub>S NPs characterization

TEM images displayed in Figure 7 confirmed the presence of spherical Ag NPs formed after 3 min under physiological conditions at different concentrations of S<sup>2-</sup>. Even when the sulfide ions were not present in the reaction mixture, spherical Ag NPs were observed with a medium diameter of 9 nm (Figure 3A). When sulfide concentration was increased to 0.25 mM, NPs of a different geometry were observed. They are composed of two different materials since they present different contrast in TEM imaging. Once again spherical Ag NPs with higher contrast were detected with the medium diameter of 9 nm but they are connected to Ag<sub>2</sub>S moieties of the same diameter, and lower contrast (Figure 3B).

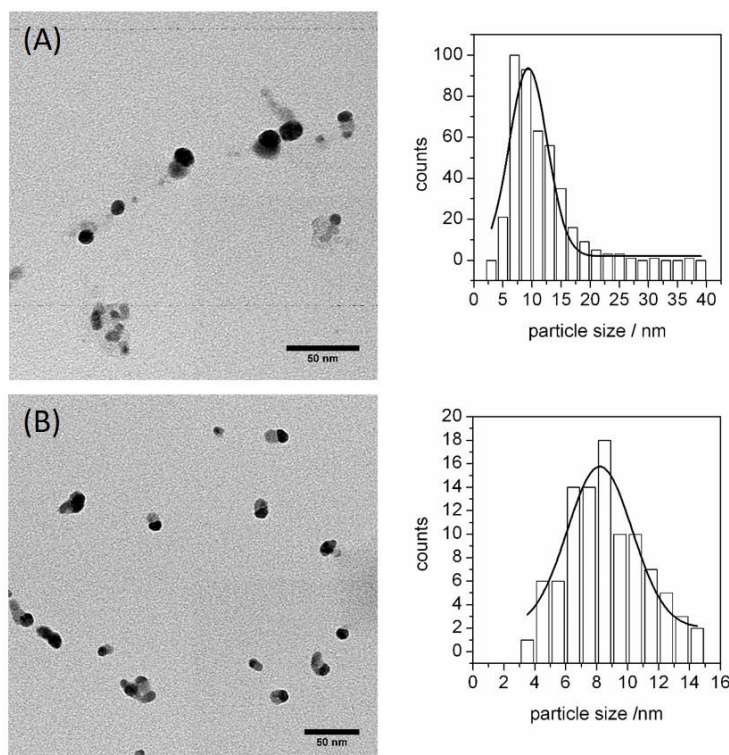


**Figure 7.** TEM images and size distribution of Ag cores obtained at different  $\text{Na}_2\text{S}$  concentrations: (A) 0 mM, (B) 0.25 mM.

According to the histograms, diameter of the Ag NPs does not significantly change when sulfide concentration is increasing in the media. Under our experimental conditions, Ag NPs serve as crystallization centers for growth of  $\text{Ag}_2\text{S}$  NPs attached to the surface of Ag NPs yielding Ag/ $\text{Ag}_2\text{S}$  NPs. TEM images reveal the mechanism of Ag/ $\text{Ag}_2\text{S}$  NPs formation. This is, some silver ions are immediately reduced by citrate ions forming seeding spherical Ag NPs, then sulfide anions and silver cations form  $\text{Ag}_2\text{S}$  NPs on the surface of seeding Ag NPs. The resulting NPs have lengths up to 18-19 nm and an average diameter of 9 nm. This structure of silver cores interconnected through silver sulfide moieties has also been presented in recent works.<sup>39-41</sup>

The NPs size in solution was determined by DLS measurements as it is included in Figure 8. The aggregation of Ag NPs in solution is appreciable when no sulfide is present in the media reaching diameter sizes of 115 nm or bigger. On the other hand, when adding sulfide smaller NPs are stabilized as the concentration is increased up to 30 nm as the concentration is increased. The slight change in diameter between TEM images and DLS measurements might be due to the different behaviour of the NPs in solution and in solid state regarding the hydrodynamic diameter. The presence of the capping agent leads to a stabilization of the NPs in solution, therefore, avoiding their agglomeration, as it has been previously demonstrated in literature.<sup>9-11</sup>

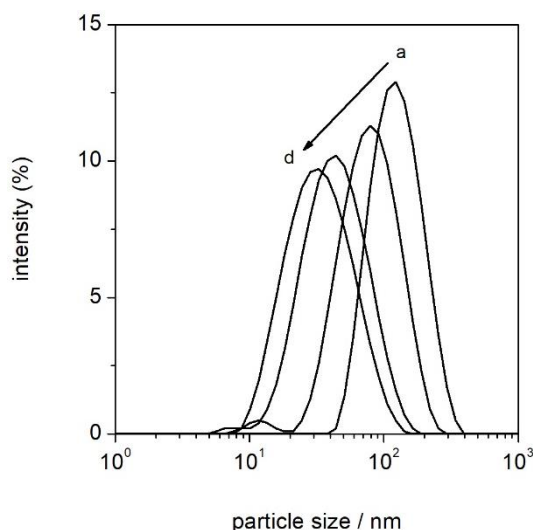


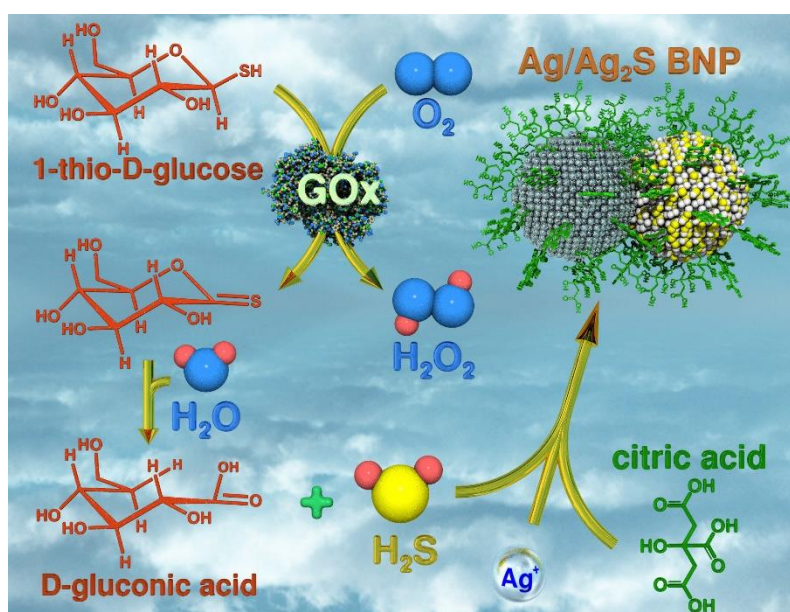
**Figure 8.** DLS measurements of Ag/Ag<sub>2</sub>S NPs in citrate buffer 10 mM pH 4 in the presence of AgNO<sub>3</sub> (1 mM), and different Na<sub>2</sub>S concentrations: a) 0 mM, b) 0.25 mM, c) 0.5 mM, d) 1 mM.

### 3.3. Glucose oxidase assay

Having optimized our colorimetric system for detection of sulfide ions based on rapid formation of Ag/Ag<sub>2</sub>S NPs we coupled it with an enzymatic system producing hydrogen sulfide. We used the oxidation of the artificial substrate 1-thio- $\beta$ -D-glucose with oxygen catalyzed by GOx to produce D-gluconic acid and hydrogen peroxide. This enzyme has been widely used and studied since the early 1950's<sup>42</sup> due to its relatively low cost and good stability. GOx has seen large-scale technological applications in chemical, pharmaceutical, food, beverage, clinical chemistry, biotechnology and other industries.<sup>43</sup> In addition, this enzyme is the mostly used biorecognition element in bioanalysis mainly for specific and sensitive determination of glucose. It operates in concert with other enzymes or nanoparticles<sup>44</sup> and can be immobilized on different substrates in bioreactors and biosensors.<sup>45</sup> In order to fabricate reproducible biosensors for glucose the initial enzymatic activity of GOx aqueous solutions should be quantified. According to the standard enzymatic assay for GOx from Sigma-Aldrich its activity is determined with an assay mixture containing an additional horseradish peroxidase (HRP) enzyme that is used for the detection of H<sub>2</sub>O<sub>2</sub> produced by GOx in the course of oxidation of D-glucose with oxygen. Our approach allows avoiding the use of HRP as described in Scheme 1. GOx catalyzes the oxidation of the artificial substrate 1-thio- $\beta$ -D-glucose in presence of oxygen to gluconic acid and hydrogen sulfide. The latter readily interacts with silver ions in the presence of citric acid, acting as a capping agent, to yield Ag/Ag<sub>2</sub>S NPs in situ. UV-vis spectroscopy is applied to follow the growth of Ag/Ag<sub>2</sub>S NPs which strongly adsorb UV-vis light. The amount of generated Ag/Ag<sub>2</sub>S NPs and consequently the observed optical signal are



directly correlated with the enzymatic activity of GOx and concentration of 1-thio- $\beta$ -D-glucose in the assay mixture.



**Scheme 1.** Colorimetric GOx assay based on detection of Ag/Ag<sub>2</sub>S NPs formed enzymatically in situ.

The effect of increasing concentrations of 1-thio- $\beta$ -D-glucose on the observed absorbance spectrum was studied. Figure 9A demonstrates the ratios ( $Abs/Abs_0$ ) of the registered absorbance in the presence of varying concentrations 1-thio- $\beta$ -D-glucose ( $Abs$ ) to absorbance registered in the absence of 1-thio- $\beta$ -D-glucose in the assay mixture ( $Abs_0$ ). The plots of  $Abs/Abs_0$  vs. wavelength reveal that the maximal ratio of the readout signal to the background signal was reached at 385 nm. Figure 9B depicts the influence of increasing 1-thio- $\beta$ -D-glucose concentrations on the absorbance signal registered at 385 nm ( $Abs_{385nm}$ ). As one can notice in Figure 9B the increase in 1-thio- $\beta$ -D-glucose concentration is directly related to the increase in the intensity of absorption peaks at 385 nm. This calibration curve shows linearity from 0 to 0.5 mM and saturation starting from 0.55 mM of substrate concentration. It means that the number of Ag/Ag<sub>2</sub>S NPs generated is directly related with the quantity of 1-thio- $\beta$ -D-glucose in the reaction mixture. According to the shape of the curve this biocatalytic reaction is consistent with typical Michaelis-Menten kinetic model.

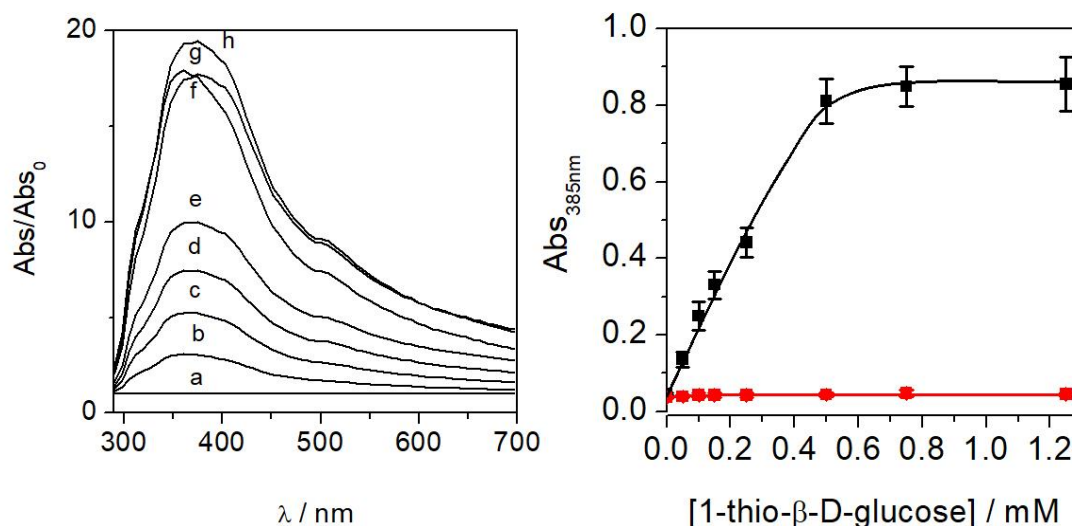


**Figure 9.** (A) Abs/Abs<sub>0</sub> ratio of the system containing AgNO<sub>3</sub> (1 mM), GOx (95 μg mL<sup>-1</sup>) and different concentrations of 1-thio-β-D-glucose: a) 0 mM, b) 0.05 mM, c) 0.1 mM, d) 0.15 mM, e) 1.25 mM, f) 0.5 mM, g) 0.75 mM, h) 1.25 mM in citrate buffer 10 mM pH 4. (B) Calibration curve of 1-thio-β-D-glucose in absence (red) and presence (black) of AgNO<sub>3</sub> (1 mM).

The experimental data were fitted by nonlinear regression method according to the Michaelis-Menten equation  $Abs_{385} = Abs_{max385} [S] / (K_M + [S])$ , where  $[S]$  is the concentration of 1-thio-β-D-glucose and  $K_M$  is the apparent Michaelis-Menten constant equal to  $256.1 \pm 1.02$  mM. The IUPAC definition was used to determine the limit of detection (LOD).<sup>45</sup> This enzymatic colorimetric assay for 1-thio-β-D-glucose detection showed a LOD equal to 4.82 μM. The average relative standard deviation (RSD) calculated from the 1-thio-β-D-glucose calibration plot was 8.46% (unless otherwise specified, RSD was always acquired utilizing not less than three independent measurements). The shape of the calibration plot in Figure 9B implies that the saturating concentration of 1-thio-β-D-glucose is 1 mM. This concentration of the artificial substrate was used to evaluate enzymatic activity of GOx by optical detection of resulting Ag/Ag<sub>2</sub>S NPs.

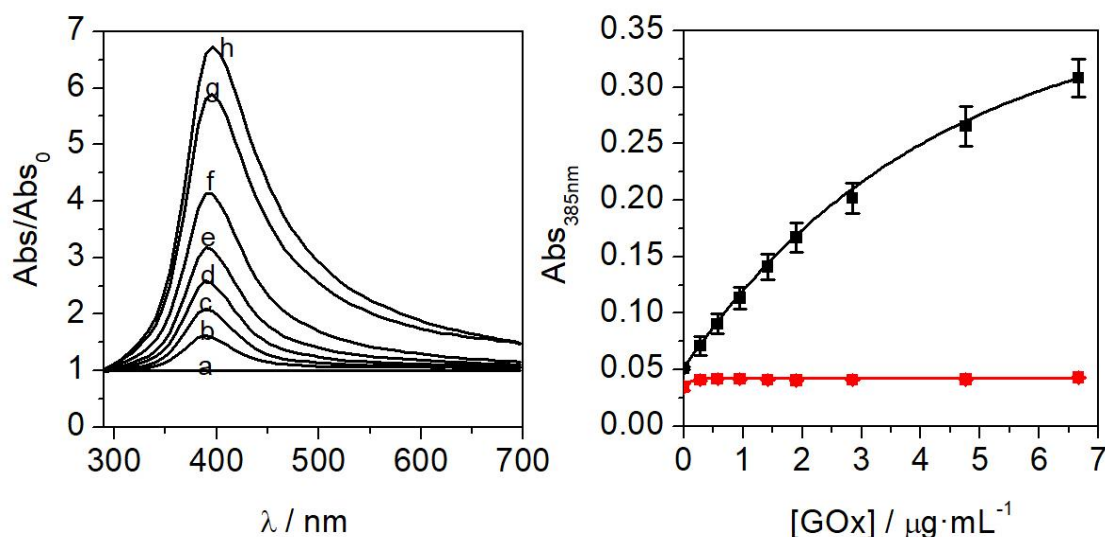
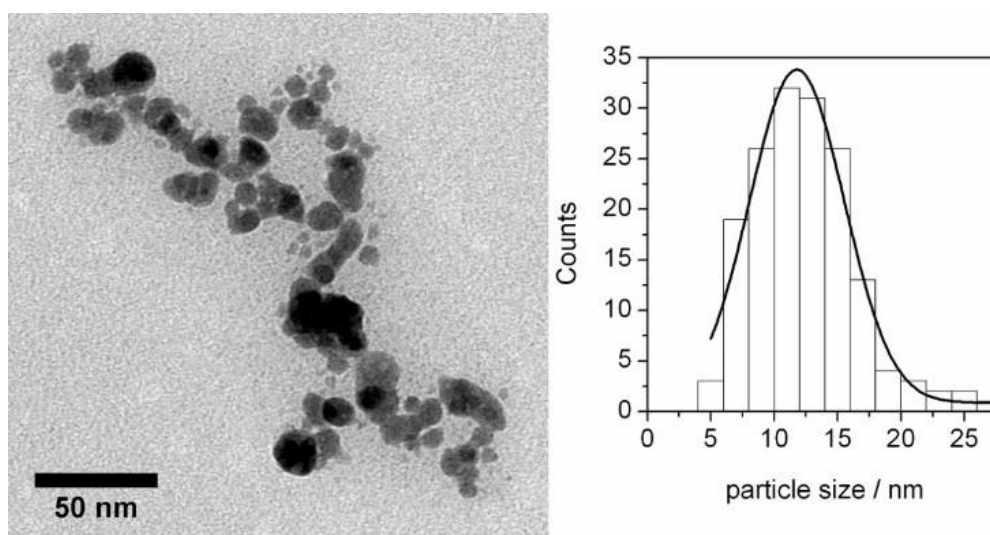


**Figure 10.** (A) Abs/Abs<sub>0</sub> ratio of the system containing AgNO<sub>3</sub> (1 mM), 1-thio-β-D-glucose (1 mM) and different concentrations of GOx: a) 0 μg mL<sup>-1</sup>, b) 0.28 μg mL<sup>-1</sup>, c) 0.57 μg mL<sup>-1</sup>, d) 0.95 μg mL<sup>-1</sup>, e) 1.42 μg mL<sup>-1</sup>, f) 1.9 μg mL<sup>-1</sup>, g) 2.85 μg mL<sup>-1</sup>, h) 6.66 μg mL<sup>-1</sup> in citrate buffer 10 mM pH 4. (B) Calibration curve of GOx in the absence (red) and presence (black) of AgNO<sub>3</sub> (1 mM).

The effect of varying GOx concentrations on the absorbance response observed at saturating 1 mM concentration of 1-thio-β-D-glucose is depicted in Figure 10. Figure 10A represents the ratios (Abs/Abs<sub>0</sub>) of the registered absorbance in the presence of varying concentrations GOx (Abs) to the absorbance recorded in the absence of GOx (Abs<sub>0</sub>) in the assay mixture vs. wavelength. Once again, the highest ratio was reached at 385 nm. Figure 10B demonstrates de calibration curve obtained by plotting the intensities of absorbance at 385 nm (Abs<sub>385nm</sub>) against GOx concentration. The LOD for GOx in the linear range (from 0 to 1.5 μg mL<sup>-1</sup>) was 0.557 μg mL<sup>-1</sup>. The average relative standard deviation (RSD) calculated from the GOx calibration plot (obtained using at least three independent measurements) was 7.09%. The standard assay for GOx requires the second enzyme HRP for detection of the resulting hydrogen peroxide. Our method does not use the second enzyme allowing simplification and decreasing the cost of GOx assays. Moreover, no enzymatic in situ growth of Ag<sub>2</sub>S structures has ever been reported.

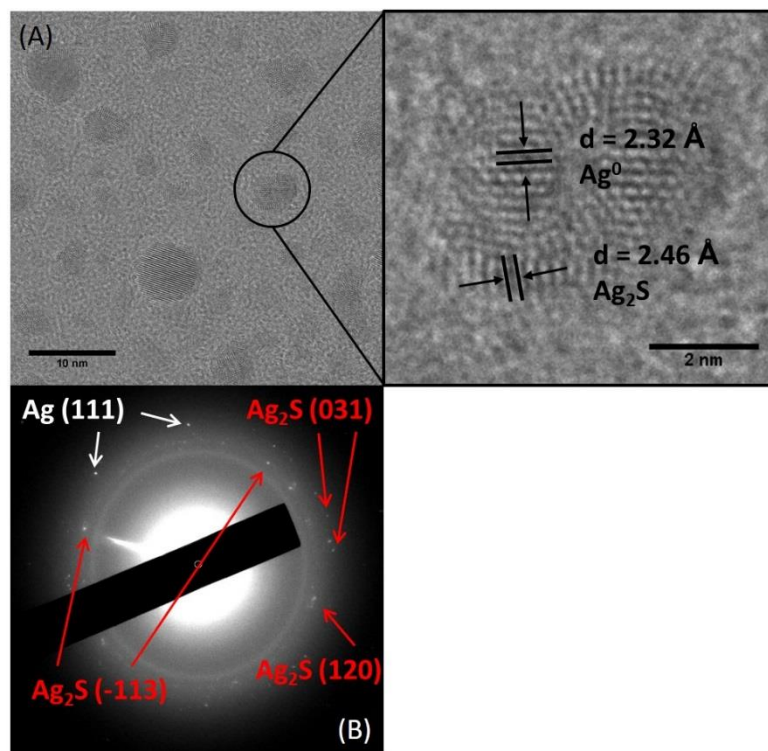
In order to provide more experimental evidence that silver cations constitute NPs in the enzymatic system control experiments were carried out in the absence Ag<sup>+</sup> cations. No absorbance was detected when the concentration of GOx was fixed and the concentration of 1-thio-β-D-glucose was varied (Figure 9B, red curve), neither when the concentration of 1-thio-β-D-glucose was fixed and the concentration of GOx was varied (Figure 10B, red curve).

TEM images displayed in Figure 11 shows the Ag/Ag<sub>2</sub>S NPs enzymatically synthesized. Ag cores appear with more contrast surrounded by an amorphous unshaped product with a final average particle size of 11.78 nm due to the formation of Ag<sub>2</sub>S moieties around the Ag cores. These results agree with the chemically synthesized Ag/Ag<sub>2</sub>S NPs structures previously described.



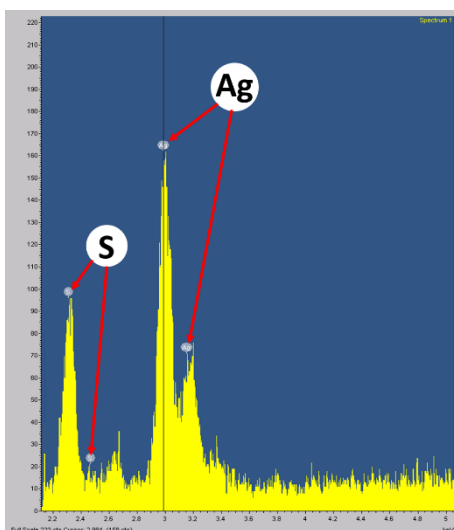
**Figure 11.** TEM images and size distribution of enzymatically synthesized Ag/Ag<sub>2</sub>S NPs.

Furthermore, we carried out HR-TEM and electron diffraction analysis to identify the phase forming the cores and the unshaped material. Figure 12 shows a HR-TEM image from enzymatically synthesized Ag/Ag<sub>2</sub>S NPs with the magnification of a selected nanoparticle and the interplanar distances from each moiety (A) and the electron diffraction pattern (B). From the HR-TEM images we can slightly distinguish two heteronanostructures containing two phases: monoclinic silver sulfide with  $\alpha$ -Ag<sub>2</sub>S acanthite structure and metallic cubic Ag. The lattice fringe spacing of 2.33 Å is consistent with the (111) lattice planes of the cubic metallic Ag and the one of 2.46 Å is associated with the (111) planes of the acanthite, the natural structure of Ag<sub>2</sub>S at low temperatures.<sup>10,40,46,47</sup> Electron diffraction analysis also showed the presence of crystalline Ag structures (reflection from (111) plane) and an amorphous shell associated to the Ag<sub>2</sub>S moiety containing the reflection from the (-113), (031) and (120) planes. Comparing spacing values of their respective crystal structures it is found that the lattice interplanar distances of the monoclinic Ag<sub>2</sub>S NPs are larger than those of the corresponding crystal planes of the fcc Ag NPs. Therefore, the increase in particle size from Ag NPs to Ag/Ag<sub>2</sub>S NPs can be explained by the enlargement of lattice d-spacings as the structure changed.



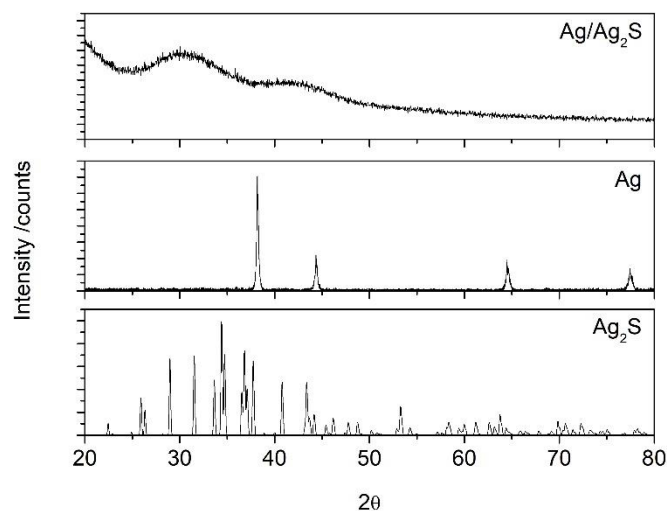
**Figure 12.** HR-TEM image of enzymatically synthesized Ag/Ag<sub>2</sub>S (a) and electron diffraction images (b).

Moreover, the chemical composition of enzymatically synthesized Ag/Ag<sub>2</sub>S NPs was corroborated by EDX, XRD and XPS measurements. EDX spectra from enzymatically synthesized Ag/Ag<sub>2</sub>S have been acquired in a transmission electron microscope and the data analysis is shown in Figure 13. These results confirmed the presence of elements Ag and S in the sample once filtrated and concentrated, indicating that the elements found can only be localized in the Ag/Ag<sub>2</sub>S structures.



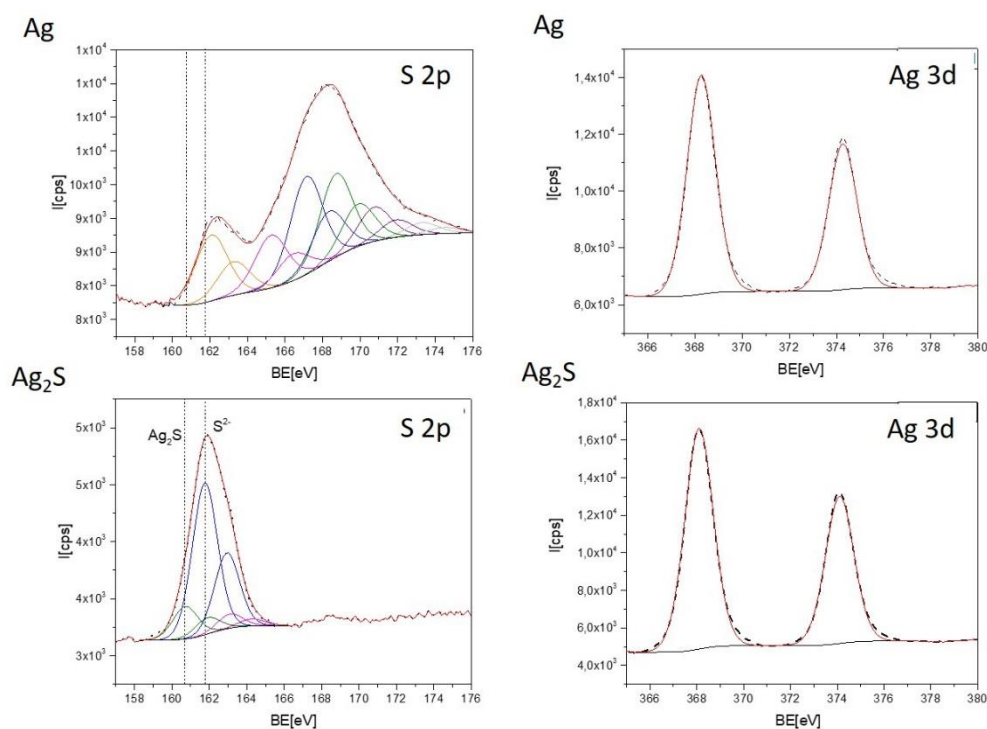
**Figure 13.** EDX analysis of enzymatically synthesized Ag/Ag<sub>2</sub>S.

Figure 14 shows the results from the XRD analysis of concentrated and dried samples. It can be seen two broad peaks in the range of Ag and Ag<sub>2</sub>S signals attributed to the amorphous structure of the final material. These results agree with the HR-TEM and electron diffraction measurements confirming the presence of both crystalline and amorphous phases.



**Figure 14.** XRD measurements of enzymatically synthesized Ag/Ag<sub>2</sub>S NPs compared to Ag and Ag<sub>2</sub>S reference signals.

Figure 15 presents the XPS results of two samples in presence and absence of the enzyme showing intense peaks at around 160.7 and 161.8 eV associated to the 2p 3/2 peak of Ag-S and S<sup>2-</sup>, respectively.<sup>48</sup> The peak area associated to Ag-S and S<sup>2-</sup> increase in the presence of the enzyme. On the other hand, the Ag peak 3d 5/2 shifts slightly at lower binding energies when Ag-S is formed. This shift corroborates the formation of Ag-S bonds only in presence of the enzyme.



**Figure 15.** XPS measurements of Ag/Ag<sub>2</sub>S NPs in citrate buffer 10 mM pH 4 in the presence and absence of GOx (Ag and Ag/Ag<sub>2</sub>S, respectively).

### 3.4. Glucose assay

To validate the proposed enzymatic mechanism of Ag/Ag<sub>2</sub>S NPs formation, the effect of the natural substrate D-glucose on the optical readout was studied. The natural substrate and the artificial one 1-thio- $\beta$ -D-glucose compete for binding with FAD that is the active center of GOx. The influence of different amounts of D-glucose at fixed amount of 1-thio- $\beta$ -D-glucose (1 mM) on absorbance is shown in Figure 16. The decrease in the readout signal is directly related to the concentration of glucose added to the system. The response shows linearity from 0 to 1.25 mM and the LOD was found to be 176.21  $\mu$ M. The average relative standard deviation (RSD) calculated from the glucose calibration plot (obtained using at least three independent measurements) was 2.08%.

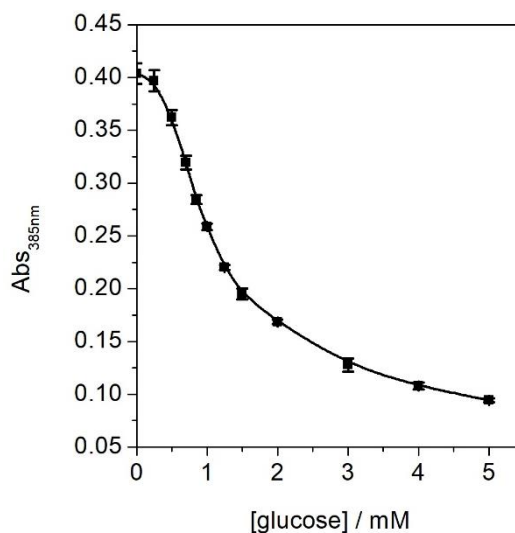


**Figure 16.** Effect of glucose on the response of the assay mixtures containing of  $\text{AgNO}_3$  (1 mM), 1-thio- $\beta$ -D-glucose (0.5 mM) and GOx ( $19 \mu\text{g mL}^{-1}$ ) in citrate buffer 10 mM pH 4.

Given the fact that the normal levels in human plasma vary from 2.8 mM (hypoglycemia)<sup>49</sup> to 7 mM (hyperglycemia),<sup>50</sup> our method could be used in routine laboratories. Therefore, we applied our assay to the detection of glucose in human serum by employing the standard addition method. In this method, several serum samples of the same volume were distributed in separate eppendorfs and standard solution containing known glucose concentrations was injected. Thereafter, the same enzymatic reaction as before was followed and the absorbance was measured. The concentrations of respective standards ( $x$ -axis) were plotted against their corresponding absorbance signal ( $y$ -axis). A linear regression analysis was performed to calculate the intercept of the calibration curve with the  $x$ -axis, representing the concentration of glucose in the serum (Figure 17). Taking into consideration all sample dilutions, the concentration of glucose was established at 6.02 mM, which lies within the limits of normal glucose level in human serum.



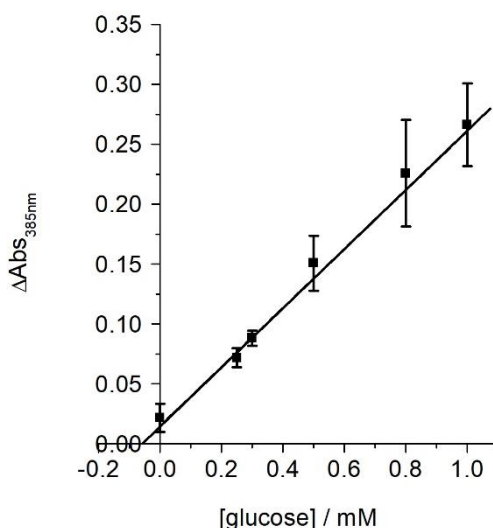


**Figure 17.** Quantification of glucose in human plasma with the method of standard addition. The system contained  $\text{AgNO}_3$  (1 mM), 1-thio- $\beta$ -D-glucose (0.5 mM) and GOx ( $19 \mu\text{g mL}^{-1}$ ) in citrate buffer 10 mM pH 4.

Although recent works have reported better limits of detection for glucose like some electrochemical<sup>29,30</sup> or colorimetric methods,<sup>27,28</sup> they usually require sophisticated devices or protocols, long procedure times, expensive reagents or the previous synthesis of the materials to use. Moreover, as it can be seen in Table 1, the majority of the colorimetric methods are based on the change of colour from a chemical substrate<sup>51,52</sup> or due to a morphological change of nanoparticles.<sup>53,54</sup> These procedures need the use of pre-synthesized structures and/or a second reactive as a read-out signal to be able to follow the reaction. In our case, our protocol does not require the previous synthesis of the nanoparticles because we synthesized them in situ, what makes it easier and enables to gain time. Moreover, the Ag/Ag<sub>2</sub>S nanoparticles serve as read-out signal themselves because of their intrinsic colour, so no additional colour-sensitizer is required. Finally, the procedure proposed has demonstrated to be sensible enough for glucose detection in real samples with no pre-treatment needed.

**Table 1.** Comparison table of glucose detection methodologies and limit of detection.

Detecting method	Sensing method	LOD [ $\mu\text{M}$ ]
Electrochemistry	Graphene functionalized with metal oxide nanostructures. Non-enzymatic.	0.001-12 <sup>30</sup>
	Photoelectrochemistry, in situ enzymatic CdS generation. Applied to real samples.	20 <sup>29</sup>
	Dendritic Cu-Cu <sub>2</sub> S nanocomposite electrodeposited on GCE. Non-enzymatic reaction. Applied to real samples.	0.33 <sup>55</sup>
Fluorescence	Poly(vinyl alcohol)-pyrene-glucose oxidase polymer with fluorescence and oxidant properties.	190 <sup>56</sup>
	Non-enzymatic redox reaction between glucose and aminopropyltriethoxysilane and in situ formation of blue-green emitting silicon nanodots. Applied to real samples.	7 <sup>57</sup>
	Glucose oxidase in situ CdS generation. Applied to real samples.	100 <sup>29</sup>
	Glucose oxidase-conjugated graphene oxide/MnO <sub>2</sub> nanozymes. TMB colour change read-out signal. Applied to real samples.	172 <sup>51</sup>
Colorimetry	Glucose oxidase immobilized on magnetite gold folate nanoparticles. ABTS colour change read-out signal. Applied to real samples.	4 <sup>52</sup>
	Enzymatic oxidation of silver nanoparticles and graphene quantum dots. Change in nanoparticle colour as read-out signal. Applied to real samples.	30 <sup>53</sup>
	SPR change as read-out signal from Au@Ag etching with H <sub>2</sub> O <sub>2</sub> enzymatic generation. Applied to real samples.	10 <sup>54</sup>
	Enzymatic in situ generation of Ag/Ag <sub>2</sub> S as read-out signal. Applied to real samples.	176 (this work)

## 4. Conclusions

In summary, a rapid and easy procedure for preparation of stable Ag/Ag<sub>2</sub>S spherical nanoparticles in an aqueous buffered solution under physiological conditions is reported. The mild conditions of this process allowed us to couple it to the biocatalytic oxidation of 1-thio-β-D-glucose catalyzed by glucose oxidase. The resulting optical assay for enzymatic activity of GOx is much simpler and faster than the standard activity test relying on the second enzyme HRP and the dangerous carcinogenic substrate o-Dianisidine. GOx activity, limits of detection and dynamic range were determined showing similar or better results than fluorogenic and photoelectrochemical procedures previously developed. Moreover, we have demonstrated the applicability of this system for glucose detection in real samples.

This colorimetric method is cost-effective, allows for real-time measurements and does not require sophisticated instruments. To the best of our knowledge this is the first enzymatic synthesis in situ of silver containing NPs with analytical applications.

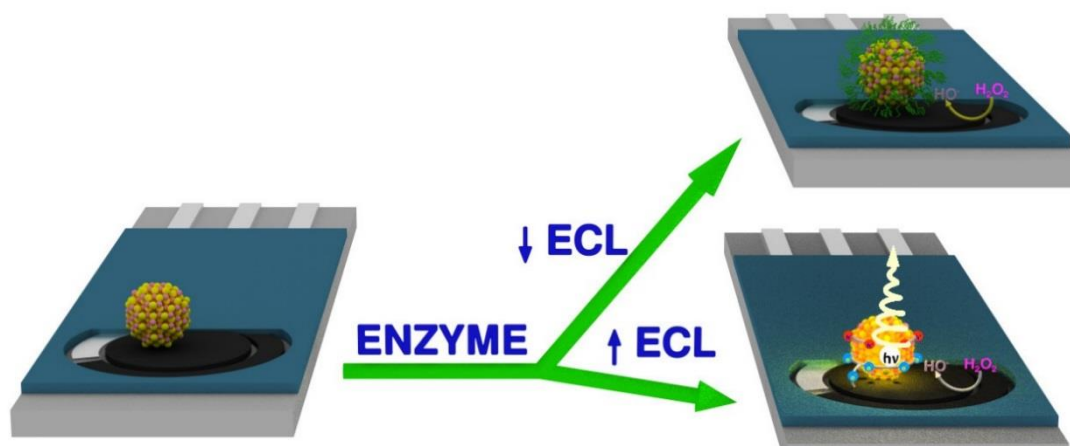
## References

- (1) Doria, G.; Conde, J.; Veigas, B.; Giestas, L.; Almeida, C.; Assunção, M.; Rosa, J.; Baptista, P. V. Noble Metal Nanoparticles for Biosensing Applications. *Sensors* **2012**, *12*, 1657–1687.
- (2) Liu, L.; Hu, S.; Dou, Y.; Liu, T.; Lin, J.; Wang, Y. Nonlinear Optical Properties of Near-Infrared Region Ag<sub>2</sub>S Quantum Dots Pumped by Nanosecond Laser Pulses. *Beilstein J. Nanotechnol.* **2015**, *6*, 1781–1787.
- (3) Hu, X.; Li, Y.; Tian, J.; Yang, H.; Cui, H. Highly Efficient Full Solar Spectrum (UV-Vis-NIR) Photocatalytic Performance of Ag<sub>2</sub>S Quantum Dot/TiO<sub>2</sub>nanobelt Heterostructures. *J. Ind. Eng. Chem.* **2017**, *45*, 189–196.
- (4) Li, C.; Zhang, Y.; Wang, M.; Zhang, Y.; Chen, G.; Li, L.; Wu, D.; Wang, Q. In Vivo Real-Time Visualization of Tissue Blood Flow and Angiogenesis Using Ag<sub>2</sub>S Quantum Dots in the NIR-II Window. *Biomaterials* **2014**, *35*, 393–400.
- (5) Zhang, Y.; Hong, G.; Zhang, Y.; Chen, G.; Li, F.; Dai, H.; Wang, Q. Ag<sub>2</sub>S Quantum Dot: A Bright and Biocompatible Fluorescent Nanoprobe in the Second near-Infrared Window. *ACS Nano* **2012**, *6*, 3695–3702.
- (6) Xiang, J.; Cao, H.; Wu, Q.; Zhang, S.; Zhang, X.; Watt, A. A. R. L-Cysteine-Assisted Synthesis and Optical Properties of Ag<sub>2</sub>S Nanospheres. *J. Phys. Chem. C* **2008**, *112*, 3580–3584.
- (7) Xiao, J.; Xie, Y.; Tang, R.; Luo, W. Template-Based Synthesis of Nanoscale Ag<sub>2</sub>E (E = S, Se) Dendrites. *J. Mater. Chem.* **2002**, *12*, 1148–1151.
- (8) Fan, X.; Qin, X.; Jing, L.; Luan, Y.; Xie, M. Controllable Synthesis of Floatable Nanocrystalline Ag<sub>2</sub>S and Ag by a Silane Coupling Agent-Modified Solvothermal Method. *Mater. Res. Bull.* **2012**, *47*, 3732–3737.
- (9) Sadovnikov, S. I.; Gusev, A. I.; Gerasimov, E. Y.; Rempel, A. A. Facile Synthesis of Ag<sub>2</sub>S Nanoparticles Functionalized by Carbon-Containing Citrate Shell. *Chem. Phys. Lett.* **2015**,

- 642, 17–21.
- (10) Sadovnikov, S. I.; Kuznetsova, Y. V.; Rempel, A. A. Ag<sub>2</sub>S Silver Sulfide Nanoparticles and Colloidal Solutions: Synthesis and Properties. *Nano-Structures and Nano-Objects* **2016**, *7*, 81–91.
  - (11) Sadovnikov, S. I.; Gusev, A. I.; Rempel, A. A. Nanocrystalline Silver Sulfide Ag<sub>2</sub>S. *Rev. Adv. Mater. Sci.* **2015**, *51*, 7–19.
  - (12) Liu, J.; Raveendran, P.; Ikushima, Y. Synthesis of Ag<sub>2</sub>S Quantum Dots in Water-in-CO<sub>2</sub> Microemulsions. *Chem. Commun.* **2004**, *22*, 2582–2583.
  - (13) Kumar, R.; Kumar, V.; Chakarvarti, S. K. Electrochemical Synthesis of Conical Ag<sub>2</sub>S Nanostructures and Their Optical Properties. *J. Mater. Sci.* **2005**, *40*, 3523–3525.
  - (14) Schaaff, T. G.; Rodinone, A. J. Preparation and Characterization of Silver Sulfide Nanocrystals Generated from Silver(I)-Thiolate Polymers. *J. Phys. Chem. B* **2003**, *107*, 10416–10422.
  - (15) Martínez-Castañón, G. A.; Sánchez-Loredo, M. G.; Dorantes, H. J.; Martínez-Mendoza, J. R.; Ortega-Zarzosa, G.; Ruiz, F. Characterization of Silver Sulfide Nanoparticles Synthesized by a Simple Precipitation Method. *Mater. Lett.* **2005**, *59*, 529–534.
  - (16) León-Velázquez, M. S.; Irizarry, R.; Castro-Rosario, M. E. Nucleation and Growth of Silver Sulfide Nanoparticles. *J. Phys. Chem. C* **2010**, *114*, 5839–5849.
  - (17) Kuznetsova, Y. V.; Rempel, S. V.; Popov, I. D.; Gerasimov, E. Y.; Rempel, A. A. Stabilization of Ag<sub>2</sub>S Nanoparticles in Aqueous Solution by MPS. *Colloids Surfaces A Physicochem. Eng. Asp.* **2017**, *520*, 369–377.
  - (18) Hocaoglu, I.; Çizmeciyen, M. N.; Erdem, R.; Ozen, C.; Kurt, A.; Sennaroglu, A.; Acar, H. Y. Development of Highly Luminescent and Cytocompatible Near-IR-Emitting Aqueous Ag<sub>2</sub>S Quantum Dots. *J. Mater. Chem.* **2012**, *22*, 14674–14681.
  - (19) Díez-Buitrago, B.; Briz, N.; Liz-Marzán, L. M.; Pavlov, V. Biosensing Strategies Based on Enzymatic Reactions and Nanoparticles. *Analyst* **2018**, *143*, 1727–1734.
  - (20) Yan, J.; Wang, L.; Tang, L.; Lin, L.; Liu, Y.; Li, J. Enzyme-Guided Plasmonic Biosensor Based on Dual-Functional Nanohybrid for Sensitive Detection of Thrombin. *Biosens. Bioelectron.* **2015**, *70*, 404–410.
  - (21) Zong, C.; Wang, M.; Li, B.; Liu, X.; Zhao, W.; Zhang, Q.; Liang, A.; Yu, Y. Sensing of Hydrogen Peroxide and Glucose in Human Serum: Via Quenching Fluorescence of Biomolecule-Stabilized Au Nanoclusters Assisted by the Fenton Reaction. *RSC Adv.* **2017**, *7*, 26559–26565.
  - (22) Saa, L.; Coronado-Puchau, M.; Pavlov, V.; Liz-Marzán, L. M. Enzymatic Etching of Gold Nanorods by Horseradish Peroxidase and Application to Blood Glucose Detection. *Nanoscale* **2014**, *6*, 7405–7409.
  - (23) Saa, L.; Virel, A.; Sanchez-Lopez, J.; Pavlov, V. Analytical Applications of Enzymatic Growth of Quantum Dots. *Chem. - A Eur. J.* **2010**, *16*, 6187–6192.
  - (24) Barroso, J.; Díez-Buitrago, B.; Saa, L.; Möller, M.; Briz, N.; Pavlov, V. Specific Bioanalytical Optical and Photoelectrochemical Assays for Detection of Methanol in Alcoholic Beverages. *Biosens. Bioelectron.* **2018**, *101*, 116–122.
  - (25) Yoo, E. H.; Lee, S. Y. Glucose Biosensors: An Overview of Use in Clinical Practice. *Sensors* **2010**, *10*, 4558–4576.
  - (26) Moodley, N.; Ngxamngxa, U.; Turzyniecka, M. J.; Pillay, T. S. Historical Perspectives in Clinical Pathology: A History of Glucose Measurement. *J. Clin. Pathol.* **2015**, *68*, 258–264.
  - (27) Zhang, X.; Wei, M.; Lv, B.; Liu, Y.; Liu, X.; Wei, W. Sensitive Colorimetric Detection of Glucose and Cholesterol by Using Au@Ag Core-Shell Nanoparticles. *RSC Adv.* **2016**, *6*, 35001–35007.
  - (28) Zhang, L.; Hai, X.; Xia, C.; Chen, X.-W.; Wang, J.-H. Growth of CuO Nanoneedles on Graphene Quantum Dots as Peroxidase Mimics for Sensitive Colorimetric Detection of Hydrogen Peroxide and Glucose. *Sensors Actuators B Chem.* **2017**, *248*, 374–384.
  - (29) Grinyte, R.; Barroso, J.; Saa, L.; Pavlov, V. Modulating the Growth of Cysteine-Capped

- Cadmium Sulfide Quantum Dots with Enzymatically Produced Hydrogen Peroxide. *Nano Res.* **2017**, *10*, 1932–1941.
- (30) Kumar, S.; Bukkitgar, S. D.; Singh, S.; Pratibha; Singh, V.; Reddy, K. R.; Shetti, N. P.; Venkata Reddy, C.; Sadhu, V.; Naveen, S. Electrochemical Sensors and Biosensors Based on Graphene Functionalized with Metal Oxide Nanostructures for Healthcare Applications. *ChemistrySelect* **2019**, *4*, 5322–5337.
  - (31) Upadhyay, Y.; Bothra, S.; Kumar, R.; Sahoo, S. K. Smartphone-Assisted Colorimetric Detection of Cr<sup>3+</sup> Using Vitamin B6 Cofactor Functionalized Gold Nanoparticles and Its Applications in Real Sample Analyses. *ChemistrySelect* **2018**, *3*, 6892–6896.
  - (32) Venkatesan, V.; Kumar, S. K. A.; Sahoo, S. K. Spectrophotometric and RGB Performances of a New Tetraphenylcyclopenta-Derived Schiff Base for the Quantification of Cyanide Ions. *Anal. Methods* **2019**, *11*, 1137–1143.
  - (33) Zhang, W.; Niu, X.; Li, X.; He, Y.; Song, H.; Peng, Y.; Pan, J.; Qiu, F.; Zhao, H.; Lan, M. A Smartphone-Integrated Ready-to-Use Paper-Based Sensor with Mesoporous Carbon-Dispersed Pd Nanoparticles as a Highly Active Peroxidase Mimic for H<sub>2</sub>O<sub>2</sub> Detection. *Sensors Actuators, B Chem.* **2018**.
  - (34) Hong, J. Il; Chang, B. Y. Development of the Smartphone-Based Colorimetry for Multi-Analyte Sensing Arrays. *Lab Chip* **2014**, *14*, 1725–1732.
  - (35) Pradyot Patnaik. *Dean's Analytical Chemistry Handbook*; McGraw-Hill, 2004.
  - (36) Jarosz, A. P.; Yep, T.; Mutus, B. Microplate-Based Colorimetric Detection of Free Hydrogen Sulfide. *Anal Chem* **2013**, *85*, 3638–3643.
  - (37) Zhang, Q.; Li, N.; Goebel, J.; Lu, Z.; Yin, Y. A Systematic Study of the Synthesis of Silver Nanoplates: Is Citrate a “Magic” Reagent? *J. Am. Chem. Soc.* **2011**, *133*, 18931–18939.
  - (38) Sadovnikov, S. I.; Gusev, A. I.; Rempel, A. A. Artificial Silver Sulfide Ag<sub>2</sub>S: Crystal Structure and Particle Size in Deposited Powders. *Superlattices Microstruct.* **2015**, *83*, 35–47.
  - (39) Liu, L.; Wang, Y.; Fu, W. Highly Selective Detection of Sulfide through Poisoning Silver Nanoparticle Catalysts. *Sensors Actuators, B Chem.* **2017**, *247*, 414–420.
  - (40) Levard, C.; Reinsch, B. C.; Michel, F. M.; Oumahi, C.; Lowry, G. V.; Brown, G. E. Sulfidation Processes of PVP-Coated Silver Nanoparticles in Aqueous Solution: Impact on Dissolution Rate. *Environ. Sci. Technol.* **2011**, *45*, 5260–5266.
  - (41) Zeng, J.; Tao, J.; Su, D.; Zhu, Y.; Qin, D.; Xia, Y. Selective Sulfuration at the Corner Sites of a Silver Nanocrystal. *Nano Lett.* **2011**, 3010–3015.
  - (42) Gromada, A.; Fiedurek, J. Selective Isolation of *Aspergillus Niger* Mutants with Enhanced Glucose Oxidase Production. *J. Appl. Microbiol.* **1997**, *82*, 648–652.
  - (43) Bankar, S. B.; Bule, M. V.; Singhal, R. S.; Ananthanarayan, L. Glucose Oxidase - An Overview. *Biotechnol. Adv.* **2009**, *27*, 489–501.
  - (44) Zhang, X.; Liu, M.; Liu, H.; Zhang, S. Low-Toxic Ag<sub>2</sub>S Quantum Dots for Photoelectrochemical Detection Glucose and Cancer Cells. *Biosens. Bioelectron.* **2014**, *56*, 307–312.
  - (45) Wilkinson, A. D. M.; A. *IUPAC Compendium of Chemical Terminology*; Blackwell Scientific Publications: Oxford, UK, 1997.
  - (46) Sadovnikov, S. I.; Gusev, A. I.; Rempel, A. A. Nonstoichiometry of Nanocrystalline Monoclinic Silver Sulfide. *Phys. Chem. Chem. Phys.* **2015**, *17*, 12466–12471.
  - (47) Sadovnikov, S. I.; Gusev, A. I. Universal Approach to the Synthesis of Silver Sulfide in the Forms of Nanopowders, Quantum Dots, Core-Shell Nanoparticles, and Heteronanostructures. *Eur. J. Inorg. Chem.* **2016**, No. 31, 4944–4957.
  - (48) John F Moulder, William F Stickle, Peter E Sobol, K. D. B. *Handbook of X-Ray Photoelectron Spectroscopy*; Physical Electronics, Ed.; Perkin-Elmer, 1995.
  - (49) Patrick, A. W.; Quinn, J. D.; Fisher, B. M. Symptoms of Acute Insulin-Induced Hypoglycemia in Humans With and Without IDDM. *Diabetes Care* **1991**, *14*, 949–957.
  - (50) Sommerfield, A. J.; Deary, I. J.; Frier, B. M. And Impairs Cognitive Performance in People

- With Type 2 Diabetes. *Diabetes Care* **2004**, *27*, 2335–2340.
- (51) Lee, P. C.; Li, N. S.; Hsu, Y. P.; Peng, C.; Yang, H. W. Direct Glucose Detection in Whole Blood by Colorimetric Assay Based on Glucose Oxidase-Conjugated Graphene Oxide/MnO<sub>2</sub> Nanozymes. *Analyst* **2019**, *144*, 3038–3044.
- (52) Ponlakheth, K.; Amatatongchai, M.; Sroysee, W.; Jarujamrus, P.; Chairam, S. Development of Sensitive and Selective Glucose Colorimetric Assay Using Glucose Oxidase Immobilized on Magnetite-Gold-Folate Nanoparticles. *Anal. Methods* **2016**, *8*, 8288–8298.
- (53) Nguyen, N. D.; Nguyen, T. Van; Chu, A. D.; Tran, H. V.; Tran, L. T.; Huynh, C. D. A Label-Free Colorimetric Sensor Based on Silver Nanoparticles Directed to Hydrogen Peroxide and Glucose. *Arab. J. Chem.* **2018**, *11*, 1134–1143.
- (54) Kang, F.; Hou, X.; Xu, K. Highly Sensitive Colorimetric Detection of Glucose in a Serum Based on DNA-Embedded Au@Ag Core-Shell Nanoparticles. *Nanotechnology* **2015**, *26*, 405–407.
- (55) Xu, G.-R.; Ge, C.; Liu, D.; Jin, L.; Li, Y.-C.; Zhang, T.-H.; Rahman, M. M.; Li, X.-B.; Kim, W. In-Situ Electrochemical Deposition of Dendritic Cu-Cu<sub>2</sub>S Nanocomposites onto Glassy Carbon Electrode for Sensitive and Non-Enzymatic Detection of Glucose. *J. Electroanal. Chem.* **2019**, *847*, 113–177.
- (56) Odaci, D.; Gacal, B. N.; Gacal, B.; Timur, S.; Yagci, Y. Fluorescence Sensing of Glucose Using Glucose Oxidase Modified by PVA-Pyrene Prepared via “Click” Chemistry. *Biomacromolecules* **2009**, *10*, 2928–2934.
- (57) Cai, Q.; Meng, H.; Liu, Y.; Li, Z. Fluorometric Determination of Glucose Based on a Redox Reaction between Glucose and Aminopropyltriethoxysilane and In-Situ Formation of Blue-Green Emitting Silicon Nanodots. *Microchim. Acta* **2019**, *186*, 1–6.



## DEVELOPMENT OF PORTABLE CdS SCREEN-PRINTED CARBON ELECTRODE PLATFORM FOR ELECTROCHEMILUMINESCENCE MEASUREMENTS AND BIOANALYTICAL APPLICATIONS

In this chapter, a portable and disposable screen-printed electrode-based platform for CdS electrochemiluminescence (ECL) detection is presented. CdS nanoparticles were synthesized in aqueous media and placed on top of carbon electrodes by drop casting. The CdS spherical assemblies consisted of nanoparticles about 4 nm diameters and served as ECL sensitizers to enzymatic assays. The nanoparticles were characterized by optical techniques, TEM and XPS. Besides, the electrode modification process was optimized and further studied by SEM and confocal microscopy. The ECL emission from CdS was triggered with  $\text{H}_2\text{O}_2$  as cofactor and enzymatic assays were employed to modulate the CdS ECL signal by blocking the surface or generating  $\text{H}_2\text{O}_2$  in situ. Thiol-bearing compounds such as thiocholine generated through the hydrolysis of acetylthiocholine by acetylcholinesterase interacted with the surface of CdS thus blocking the ECL. Moreover, the inhibition mechanism of the enzyme was studied by using 1,5-bis-(4-allyldimethylammonium-phenyl)pentan-3-one dibromide. On the other hand, the natural production of  $\text{H}_2\text{O}_2$  from the oxidation of methanol by the action of alcohol oxidase was utilized to carry out the ECL process. The reported methodology shows potential applications for the development of sensitive and easy to hand biosensors and was applied to the determination of acetylcholinesterase and methanol in real samples.

## 1. Introduction

Electrochemiluminescence (ECL) is a robust analytical tool that combines the unsophistication of electrochemistry with its inherent sensitivity and the wide linearity of chemiluminescence method.<sup>1</sup> ECL is the process whereby reactive species generated at electrodes undergo high-energy electron-transfer reactions to form excited states that emit light.<sup>2-6</sup> ECL is broadly applied in analytical chemistry, as well as in mechanism studies, as it provides not only the electrochemical information but also the spectrum data simultaneously, which gives very useful insight into the complex mechanisms.<sup>3</sup> This technique presents unique advantages such as high sensitivity, excellent temporal and spatial controllability, simplified optical setup, low background signal and no need of an external light source.<sup>4,5</sup>

In the past few decades, many novel ECL emitters were synthesized and used in ECL reactions, for example luminol and ruthenium complex, etc.<sup>4</sup> Nanomaterials with different sizes, shapes, chemical components and unique properties have been extensively adopted as an alternative for biosensing applications.<sup>7</sup> They offer several advantages such as the ability to enhance the efficiency of both biological element part and transducer part in many different ways within the biosensor platform.<sup>8,9</sup> Compared with conventional molecular emitters, nanomaterials have some distinctive merits such as size/surface-trap controlled luminescence and good stability against photobleaching. Most noteworthy, semiconductor nanocrystals also known as quantum dots (QDs) with unique optical and electrical properties have opened promising fields for new ECL emitters.<sup>10</sup> Since the first report on the ECL study of silicon nanoparticles,<sup>11</sup> many elemental and compound semiconductor QDs have been developed to apply in ECL analytical techniques. Recent works indicated that water-soluble QDs were excellent luminescent reagents for ECL systems, avoiding using toxic organic solutions and complicated modifying electrode procedures.<sup>12,13</sup> Previous works have demonstrated that ECL emission of QDs occurs *via* surface electron-hole recombination and is highly dependent on their surface state which can be tuned with desired element ratios and dopants to enhance the efficiency of the process.<sup>7,14,15</sup> The need of new formulations and easy and friendly procedures to get more efficient nanomaterials for ECL applications aimed to develop outstanding nanomaterials and platforms suitable for biosensors set up.

In electrochemiluminescence biosensors the light is only detected upon ECL reaction at the application of a specific potential for each system.<sup>4,6</sup> Highly sensitive photon detection is required and this is achieved by high performance detectors and further development to more sensitive and smaller sensor systems. This detection system presents great advantages over



other optical techniques such as fluorescence. The mechanism doesn't require an external light source so light scattering and the background signal are reduced, reaching higher signal-to-noise ratios and lower limits of detection. Besides, ECL is highly localized and time-triggered detection method, since the reaction only takes places at the potential application.<sup>16</sup>

ECL devices display great potential for miniaturization because of its few hardware requirements. The power source can be supplied with a battery,<sup>17</sup> the electrodes can be design at a microscale size<sup>18</sup> and the light sensors could be integrated via small photodiodes.<sup>19</sup> This, combined with the advances in miniaturization systems could fulfil the current need of portable instruments for fast analytical determination in situ. Usually, ECL devices are controlled by an external potentiostat or an amperometric unit that establishes potential differences or electric current to the electrodes. The photon detector utilized will depend on the practical requirements of the final system. When no size restriction is applied, a good solution is the use of a photomultiplier tube (PMT) which presents a high sensitivity towards low amounts of photons, but they need very high voltage supply (up to thousands of volts) for a proper performance.<sup>20,21</sup> Moreover, the large dimension of these detectors makes them inadequate for portable instruments. Another technique for light detection is the use of a CCD camera.<sup>22</sup> Despite their good sensitivity, the main disadvantage of these devices is its complexity in their use and the need of low temperature working conditions to reach a good detection limit. On the other hand, photodiodes present features that make them appropriate for the design of a portable, miniaturized and hand-held devices. Photodiodes have a small size, lower power consumption, they present less complex opto-electronic systems and they are cost-effective.<sup>19,23</sup>

In order to meet the needs for portability, sensitivity and friendly fabrication process of an ECL biosensor, we proposed a CdS screen-printed carbon electrode sensing platform combined with a Si-photodiode integrated in an ECL cell for bioanalytical applications. The ECL portable device integrates a potentiostat/galvanostat and a Si-photodiode ( $\mu$ STAT ECL, DropSens). Screen-printed carbon electrodes (SPCE) enabled the use of reduced volumes making the system cost-effective and simpler than conventional three electrode cells. Moreover, the surface modification with CdS synthesized in aqueous solutions was carried out by simple but reproducible and stable adsorption. The applicability of our new CdS-SPCE ECL portable device was validated for the detection of acetylcholinesterase and methanol in real samples. For the best of our knowledge, it is the first time that this ECL commercial device is applied to a different system than expensive luminol/[Ru(pby)<sub>3</sub>]<sup>2+</sup> ECL classical reactions. These luminophores are commonly used because of their high luminescent efficiency that makes

possible the use of less sensitive and portable detectors.<sup>24,25</sup> In this work, facile synthesis of inexpensive CdS nanoparticles was carried out to fabricate CdS-SPCE that served as ECL efficient platform with high sensitivity towards enzymatic activity of some analytes of interest.

## 2. Experimental section

### 2.1. Materials

Cadmium nitrate ( $\text{Cd}(\text{NO}_3)_2$ ), sodium sulfide ( $\text{Na}_2\text{S}$ ), hydrogen peroxide, methanol (MeOH), ethanol (EtOH), alcohol oxidase (AOx) from *Hansenula sp.*, acetylcholinesterase (AChE) from *Electrophorus electricus sp.*, glucose oxidase type VII from *Aspergillus Niger* (GOx), acetylthiocholine chloride (ATCh), 1,5-bis-(4-allyldimethylammonium-phenyl)pentan-3-one dibromide (BW284c51), human serum (HS) and other chemicals were purchased from Sigma-Aldrich. Anhydrous D (+)-glucose was purchased from PanReac AppliChem. The alcoholic beverage (vodka) was purchased in local supermarkets in San Sebastián (Spain).

### 2.2. Apparatus

Fluorescence measurements were performed on a Varioskan Flash microplate reader (Thermo Scientific) using black microwell plates at room temperature. The system was controlled by the SkanIt Software 2.4.3. RE for Varioskan Flash. Electrochemical and electrochemiluminescence measurements were recorded with a potentiostat/galvanostat ( $\pm 4$  V DC potential range,  $\pm 40$  mA maximum measurable current) and Si-photodiode integrated in the ECL cell, combined in one portable instrument (DropSens S.L., Spain). The ECL equipment was controlled by the specific software DropView 8400. Disposable screen-printed carbon electrodes (SPCE; DRP-110; DropSens) were employed as the electrode surface throughout this work. Transmission electron microscopy (TEM) images were recorded with a JEOL JEM 2100F microscope equipped with a high-angle annular dark field (HAADF) detector operating at 120 kV. Scanning electron microscopy (SEM) images were recorded with a JEOL JSM-6490LV at 15 kV, running in a point by point scanning mode with a dual beam FIB-FEI Helios 450S microscope. Confocal microscopy was carried out with a Zeiss Axio Observer epifluorescence microscope. Images were acquired with a 20x (air, NA 0.8) objective, in reflection mode, using excitation 365nm LED at 48% power and an emission filter for DAPI (ex 335/383 and em 420/470nm). AxiocamMR R3 detector was used for acquisition, exposure adjust to 2 s. Microscope controlled with Zen blue software v2.3 also used for image processing. X-ray photoelectron spectroscopy (XPS) experiments were performed in a SPCE Sage HR 100 spectrometer with a

non-monochromatic X-ray source (Aluminum K $\alpha$  line of 1486.6 eV energy and 253 W) placed perpendicular to the analyser axis and calibrated using the 3d $_{5/2}$  line of Ag with a full width at half maximum (FWHM) of 1.1 eV.

## 2.3. Methods

### 2.3.1. CdS synthesis and CdS-SPCE fabrication

Varying amounts of Cd(NO $_3$ ) $_2$  and Na $_2$ S were mixed up in tris-HCl 5 mM pH 8 for 5 min at room temperature. After that, the fluorescence spectra of the resulting CdS were recorded at  $\lambda_{\text{exc}}=280$  nm. For the fabrication of the biosensor the SPCE were pretreated electrochemically by cyclic voltammetry (CV) at a potential range from 0 to 0.6 V in tris-HCl 5 mM pH 8 buffer at 50 mV s $^{-1}$ . Subsequently, a 7  $\mu$ L drop of CdS was drop casted on the SPCE and let dry at 37  $^{\circ}$ C during 1 h. Afterwards, CdS-SPCE were leave at room temperature overnight in dark. At last, SPCE were washed with distilled water, dried under argon atmosphere and stored in the fridge.

### 2.3.2. Acetylcholinesterase enzymatic assay

Different amounts of AChE and ATCh were incubated in citrate-phosphate buffer pH 7.5 at 37  $^{\circ}$ C for 30 min. Next, a 40  $\mu$ L drop was drop casted on the CdS-SPCE surface and let react at room temperature for 30 min. After that, CdS-SPCE were washed with buffer and dried under argon atmosphere. Finally, ECL measurements were recorded in a 60  $\mu$ L drop of H $_2$ O $_2$  10 mM in PBS with voltage scanned between 0 and -1.6 V at 50 mV s $^{-1}$ .

### 2.3.3. Inhibition of acetylcholinesterase

Acetylcholinesterase (5 mU mL $^{-1}$ ) was incubated with different concentration of the inhibitor BW284c51 in citrate-phosphate buffer pH 7.5 at room temperature for 30 min. Next, a solution of acetylthiocholine chloride (5  $\mu$ L, 5 mM) was added to the mixture (45  $\mu$ L) and incubated for 15 min at 37  $^{\circ}$ C. After that, 40  $\mu$ L drop was drop casted on the CdS-SPCE surface and let react at room temperature for 30 min. Then, CdS-SPCE were washed with buffer and dried under argon atmosphere. Finally, ECL measurements were recorded in a 60  $\mu$ L drop of H $_2$ O $_2$  10 mM in PBS with voltage scanned between 0 and -1.6 V at 50 mV s $^{-1}$ .

### 2.3.4. Alcohol oxidase enzymatic assay

Varying amounts of AOx and MeOH were incubated in citrate-phosphate buffer pH 7.5 at room temperature for 30 min. After that, ECL measurements were recorded in a 60  $\mu$ L drop of the mixture with voltage scanned between 0 and -1.6 V at 50 mV s $^{-1}$ .

### 2.3.5. Quantification of AChE and MeOH in real samples

Quantification of AChE in human serum and MeOH in vodka were performed by standard addition method. Samples of pooled human serum were centrifuged using Amicon Ultra filter with a 3000 molecular weight cut-off. After filtering, the serum was spiked with varying known concentrations of AChE. The respective AChE concentration in these mixtures was then determined. The dilution factor of plasma in the assay was 1:600. Samples of vodka were spiked with known different concentrations of methanol. Thus, the corresponding final concentration of methanol in mixtures was determined as described above. The dilution factor of samples in the assay was 1:10000.

## 3. Results and discussion

### 3.1. Properties and characterization of synthesized CdS

In this work, CdS nanoparticles were synthesized by direct reaction of  $\text{Cd}(\text{NO}_3)_2$  2 mM and  $\text{Na}_2\text{S}$  0.5 mM in tris-HCl buffer at room temperature with no capping agent. The resulting nanoparticles presented a light-yellow colour with a maximum absorbance peak at 460 nm and a broad fluorescence peak with a maximum at around 700 nm (Figure 1). From the spectral absorption edge, the diameter of CdS nanoparticles could be calculated using Henglein's empirical curve that relates the wavelength of the absorption threshold ( $\lambda_{em}$ ) to the diameter of the CdS structures ( $2R$ ) ( $2R_{\text{CdS}} = 0.1 / (0.1338 - 0.0002345\lambda_{em})$  nm).<sup>26-29</sup> The mean diameters of the synthesized nanoparticles were calculated to be 3.86 nm. TEM and XPS data were further investigated to confirm the CdS structures.

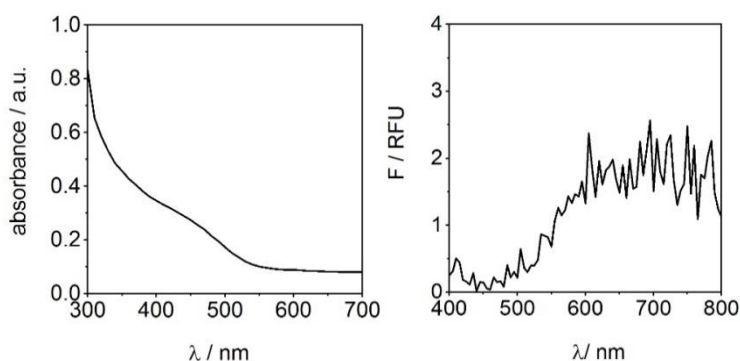


**Figure 1.** Absorbance and fluorescence spectra from CdS formed in presence of  $\text{Na}_2\text{S}$  0.5 mM and  $\text{Cd}(\text{NO}_3)_2$  2 mM in tris-HCl 5 mM pH 8 at room temperature.

TEM images from Figure 2 shows the CdS nanoparticles with an average diameter of 3.89 nm, thus in agreement with the previous theoretical value. Even though there was no capping agent, sulfide and cadmium formed spherical nanoparticles aggregated in a big homogenous net as it has been demonstrated in the literature.<sup>15,29–32</sup> Moreover, XPS analysis was performed to study the surface composition and the oxidation state of elements for solid state materials. As can be seen in Figure 3, almost all the cadmium and sulfide in the sample are forming Cd-S bonds. We also found some signals related to cadmium oxide and sulfide oxide on the surface as result of the easy metal oxidation in the air.<sup>30,33</sup>

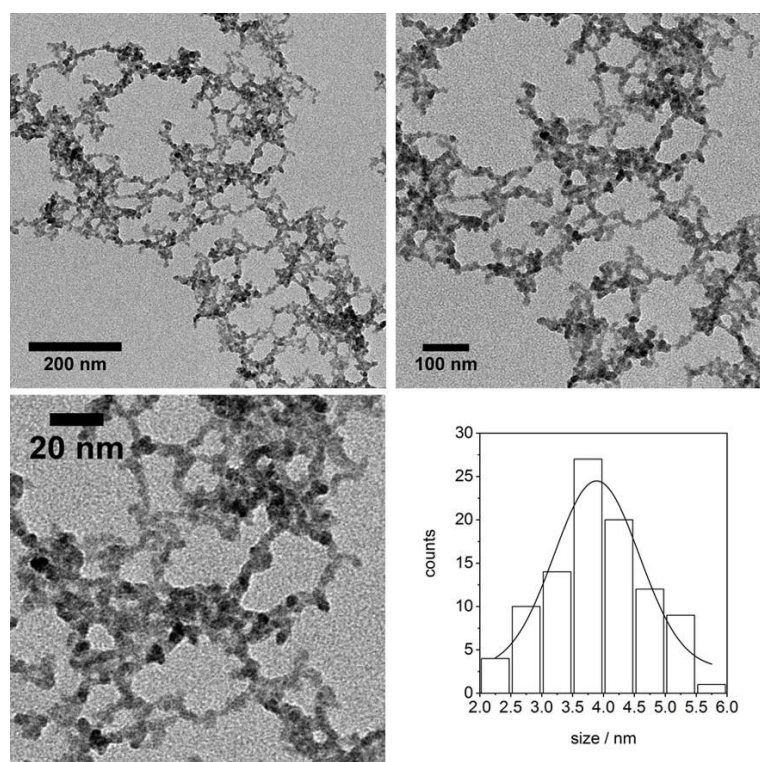


**Figure 2.** TEM images from CdS and size histogram.

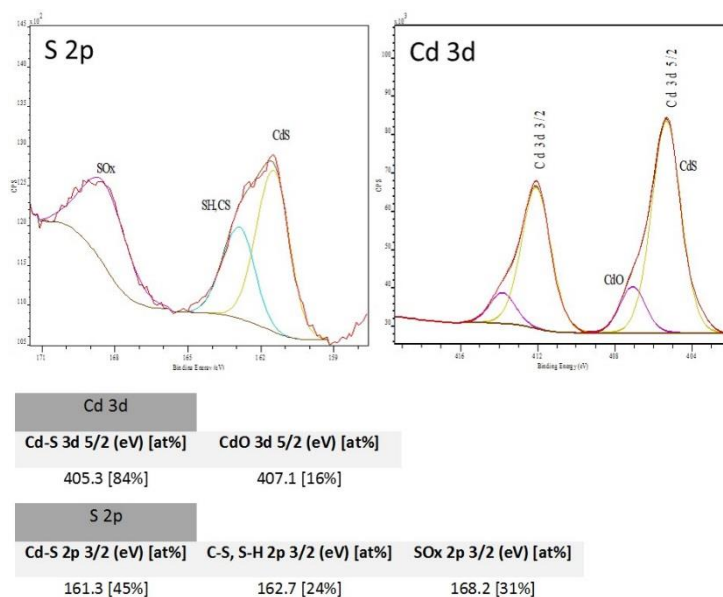


**Figure 3.** XPS analysis of CdS synthesized.

### 3.2. Properties and characterization of electrodes

For the biosensor platform, the CdS nanoparticles synthesized were immobilized by simple adsorption on the surface of a screen-printed carbon electrode. The electrodes were first washed in buffer by cyclic voltammetry and dried under argon before their modification. Afterwards, a 7  $\mu\text{L}$  drop of freshly prepared CdS was placed on top of the working electrode and let dry at 37  $^{\circ}\text{C}$  for 1 h. Finally, they were kept overnight in dark at room temperature. The following day, the CdS-SPCE were washed in buffer and dried under argon to ensure homogeneity and stored in the fridge for further utilization. SEM and confocal microscopy were carried out to characterize the resulting modified electrodes. SEM images evidenced the modification on the surface of the working electrode (Figure 4). In the images, the nanoparticles were homogeneously distributed all over the working electrode with no alteration of the rest electrodes even after the washing step. Carbon ink from the screen-printed electrodes is porous and presents a rough surface, enabling the adsorption of the nanoparticles with high stability. This approach is the simplest and most straight forward for the modification of the electrode surface and has been widely used in electrochemical biosensors.<sup>20,34–36</sup>

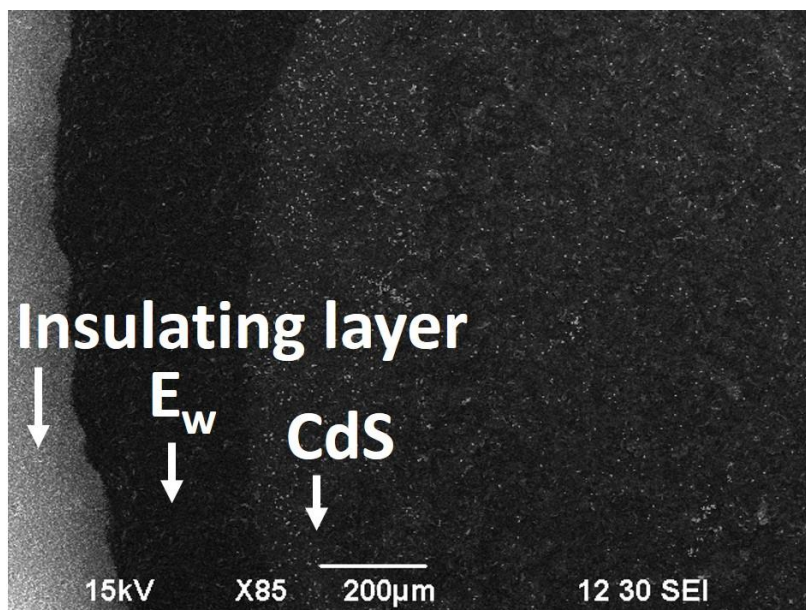


**Figure 4.** SEM images of the modified electrodes: insulating area in white, working electrode ( $E_w$ ) not modified in black and the modified CdS area in grey.

In addition, confocal microscopy was performed to confirm the modification and stability of the modified electrodes. In Figure 5 the fluorescence spectroscopy images from the three different electrodes are displayed: one bare electrode, one electrode with CdS after 1 h of incubation at 37 °C, and the same electrode after washing step and stored for one day. The bare electrode didn't show any fluorescence because carbon ink is not fluorescence (Figure 5A). After the CdS deposition, the fluorescence signal appeared from all the modified surface of the electrode (Figure 5B). Subsequently, the fluorescence slightly diminished due to the washing step and the removal of the CdS excess on the surface (Figure 5C). The final electrode presented a homogeneous fluorescence signal coming from the CdS adsorbed on the carbon surface even after their washing and storage in the fridge, thus confirming their stability.

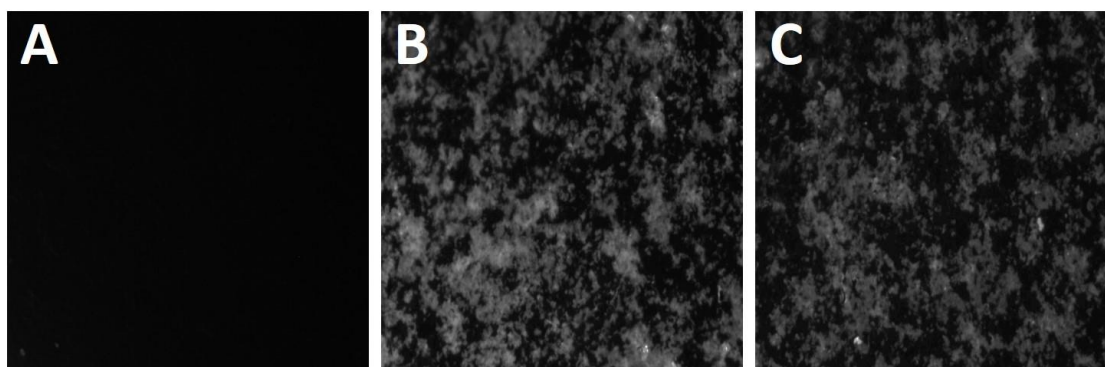


**Figure 5.** Fluorescence microscope images of A) bare SPCE, B) CdS-SPCE before washing and C) CdS-SPCE after washing and storage.

### 3.3. Electrochemical and electrochemiluminescence behaviours of CdS-SPCE

The ECL system presented is based on the light emission of the CdS nanoparticles, as they are one of the most popular ECL emitters of semiconductor NCs.<sup>28,37-40</sup> This process was carried out in presence of the oxidant H<sub>2</sub>O<sub>2</sub>, an important coreactant in cathodic ECL emission.<sup>14,15,31,37,41</sup> The proposed mechanism is described as follows. As the electrode potential was scanned to negative values, the CdS were reduced to (CdS)<sup>•-</sup> (eq 1) and the coreactant H<sub>2</sub>O<sub>2</sub> was reduced to OH<sup>•</sup> (eq 2). Then, OH<sup>•</sup> could react with (CdS)<sup>•-</sup> producing excited state (CdS)<sup>\*</sup> (eq 3). Finally, when (CdS)<sup>\*</sup> decayed back to the ground-state CdS, an intense emission was obtained (eq 4).

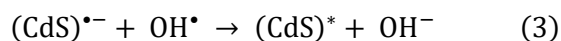
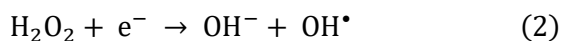
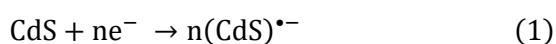
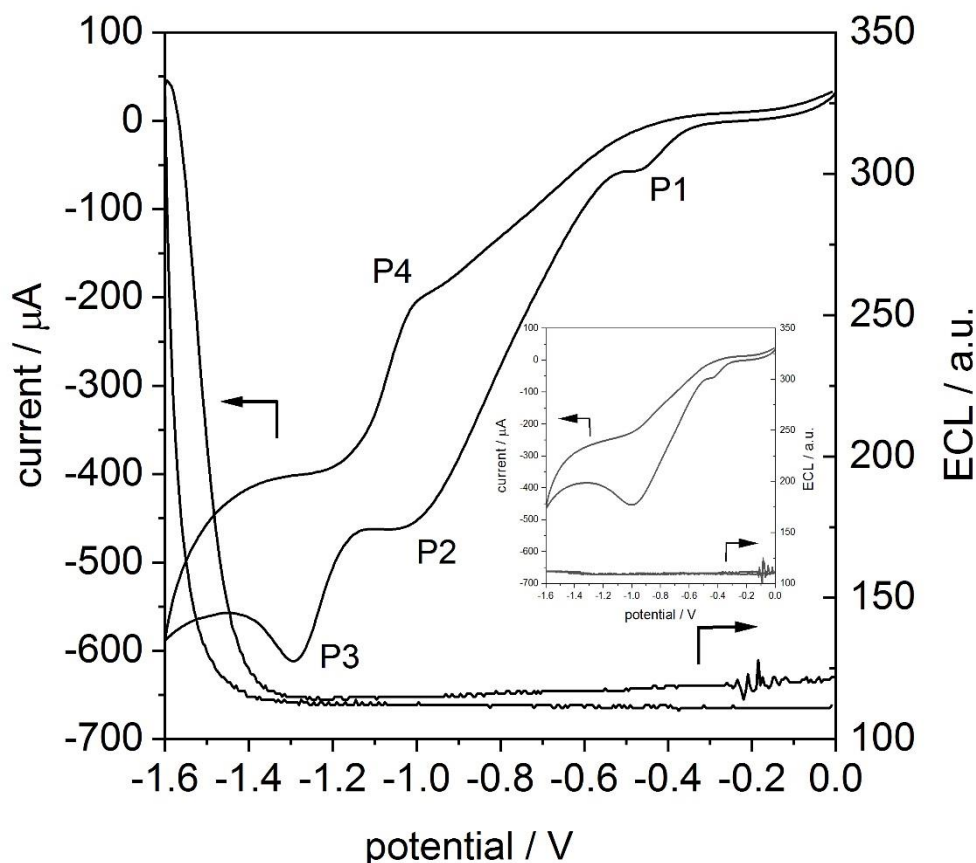


Figure 6 shows the EC and ECL behaviours of our CdS-SPCE and the bare SPCE (inset) in PBS containing 10 mM H<sub>2</sub>O<sub>2</sub>. Three cathodic peaks (P1, P2, P3) and one anodic peak (P4) were found at -0.46, -0.99, -1.29 and -1 V, respectively. Among them, P1 corresponded to the reduction of dissolved oxygen and P2 is assigned to the reduction of H<sub>2</sub>O<sub>2</sub> as it can be seen in the inset of Figure 6 for bare SPCE in presence of H<sub>2</sub>O<sub>2</sub>.<sup>14,42</sup> P3 and P4 were attributed to the reduction and oxidation of CdS<sup>14,15,38,40</sup> that only appeared in the CdS-SPCE curve (Figure 6) and not for the control SPCE (Figure 6, inset). Regarding the ECL curve, one peak was detected when scanning to negative potentials corresponding to CdS<sup>\*</sup> emission (Figure 6), but not when analysing the bare SPCE (Figure 6, inset) in presence of H<sub>2</sub>O<sub>2</sub> 10 mM.





**Figure 6.** Cyclic voltammetry and electrochemiluminescence signals from CdS-SPCE in presence of  $\text{H}_2\text{O}_2$  50 mM in PBS. Inset: CV and ECL curves from bare SPCE in presence of  $\text{H}_2\text{O}_2$  50 mM in PBS.

### 3.4. Optimization of ECL working conditions

In order to achieve the optimal ECL response, the amount of cadmium for CdS formation, the deposition volume and incubation temperature, the concentration of  $\text{H}_2\text{O}_2$  and the reagent controls were carefully studied (Figure 7). In Figure 7A the ECL signals for cadmium calibration curve are presented. ECL signal increased with the concentration of cadmium added to a well-known sulfide solution (0.5 mM) reaching a plateau at 2 mM. The optimum volume for CdS deposition was set at 7  $\mu\text{L}$ , considering the working electrode size (4 mm) and the viscosity and surface tension of the CdS solution. The incubation temperature for CdS adsorption on the working electrode was compared in Figure 7B. When incubating at 37  $^\circ\text{C}$ , the ECL signal obtained was more than three times higher than the one obtained when incubating at room temperature. Moreover, the concentration of the coreactant is one of the most important parameters for an optimum ECL signal. The ECL intensities from the calibration curve are shown in Figure 7C. The ECL signal increased when increasing  $\text{H}_2\text{O}_2$  up to 10 mM. After that concentration, the ECL signal decrease because of the alteration on the surface due to the oxidant nature of the coreactant. Finally, we tested the ECL response of the SPCE modified

with CdS, Cd(NO<sub>3</sub>)<sub>2</sub>, Na<sub>2</sub>S and with no modification in presence of H<sub>2</sub>O<sub>2</sub> 10 mM in PBS (Figure 7C). Only CdS-SPCE gave a high ECL signal and no significant peak was found for any of the controls. This result confirms the need of both reagents and a proper coreactant to yield an ECL signal.

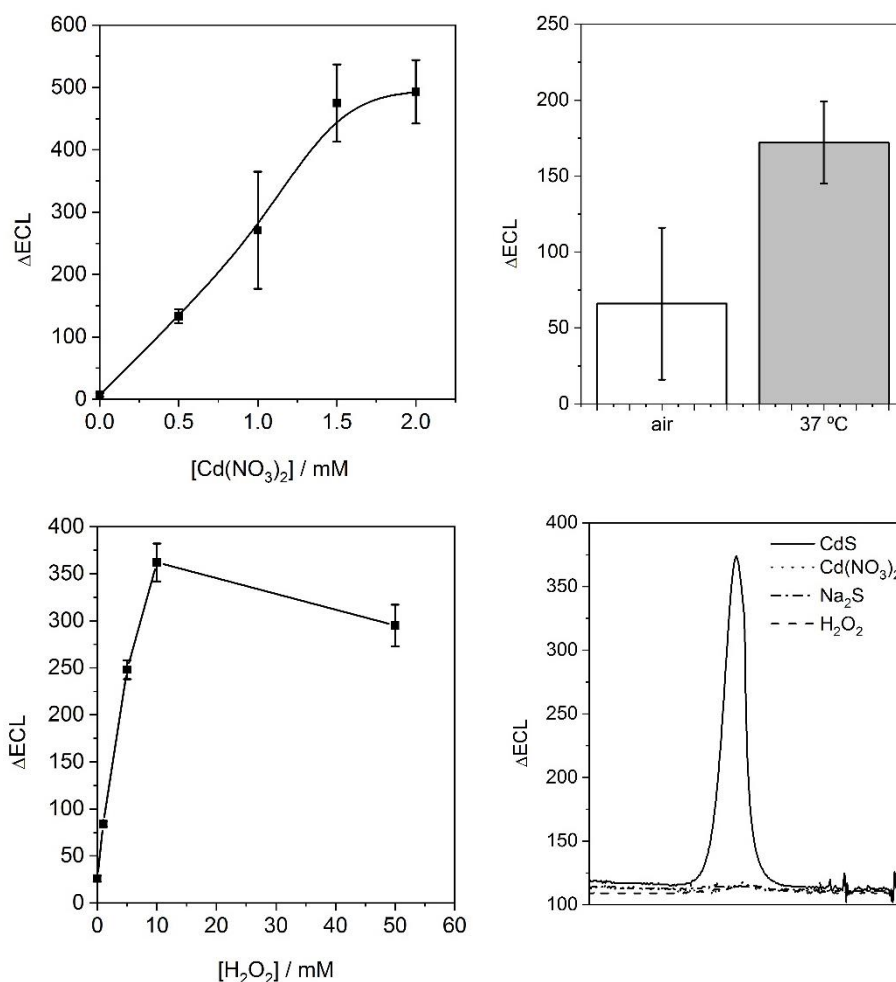


**Figure 7.** ECL signal from (A) Cadmium calibration plot, (B) CdS-SPCE modified at room temperature and at 37 °C, (C) H<sub>2</sub>O<sub>2</sub> calibration plot and (D) control signals from individual reagents.

The final values for the parameters studied were Cd(NO<sub>3</sub>)<sub>2</sub> 2mM, H<sub>2</sub>O<sub>2</sub> 10 mM in PBS, 37 °C for CdS adsorption and 7 μL CdS volume. If nothing specified, this were the parameters used throughout the work.

### 3.5. ECL sensing application of CdS-SPCE

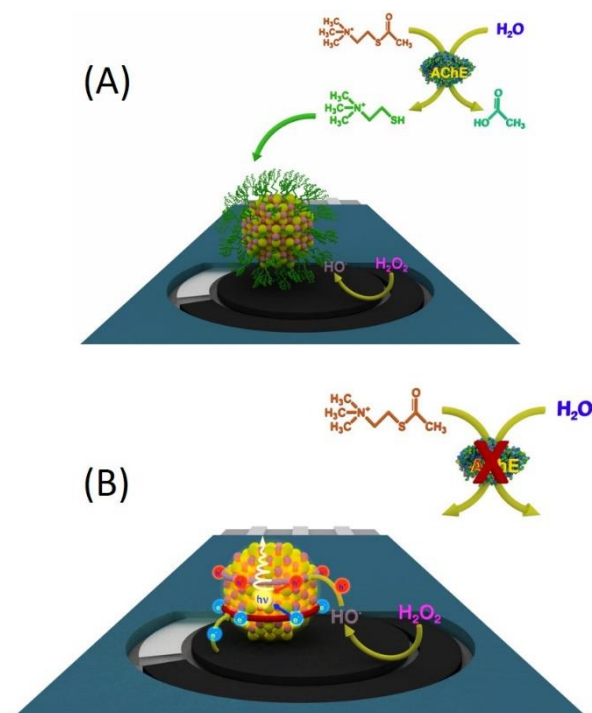
The new CdS-SPCE fabricated were employed as ECL sensing platform for biosensing. ECL biosensor can be fabricated based on several approaches, such as generation or depletion of coreactant catalyst,<sup>43,44</sup> modulation of the communication between the electrode and coreactants by impedance effect,<sup>45</sup> and promotion of electron transfer by compositing

nanomaterials with ECL emitters.<sup>46</sup> With the previous studies, CdS-SPCE were validated as sensitive ECL emitters by using H<sub>2</sub>O<sub>2</sub> as cofactor regarding its good performance and suitability for ECL biosensors.<sup>47-50</sup> Taking this into account, we followed two different strategies for their application: affinity and direct assays.

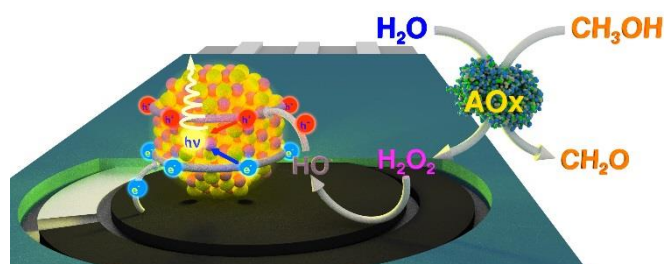
Affinity assays were based on the interaction of the CdS nanoparticles with the analyte of interest and the subsequent variation on the ECL intensities. Thiols were selected as model analyte regarding their strong interaction with CdS surface.<sup>21,28,37,40,51-55</sup> In the proposed procedure, enzymatic assays were defined for the production of thiol-compounds capable of interact with the surface of our CdS-SPCE. These thiols could link to the CdS conferring hydrophobic properties to the surface and blocking the interaction with the H<sub>2</sub>O<sub>2</sub>. Considering this mechanism, we could associate the decrease in the ECL intensity with the enzymatic activity.

For the direct assays we took advantage of the natural enzymatic production of H<sub>2</sub>O<sub>2</sub> of some bioassays to conduct the ECL process. This approach enables the direct use of enzymatic H<sub>2</sub>O<sub>2</sub> as it can act as a ready-made coreactant for ECL emissions without the introduction of exogenous coreactants which makes the system neat, green and facile.<sup>15,41,56,57</sup>

Schemes 1 and 2 show the two applications of our modified electrodes. For the affinity assays, we used the enzymatic production of thiocholine from acetylthiocholine oxidation of acetylthiocholine taking advantage of our expertise on previous works from the group.<sup>54,58,59</sup> The incubation of the enzyme with its substrate leads to the production of thiocholine in solution. Afterwards, CdS-SPCE is kept in contact with the thiol solution and let react. After washing the electrodes, ECL measurements were carried out and the variation on the ECL intensity was related to the enzymatic activity (Scheme 1). For the direct assay, we selected the alcohol oxidase as model enzyme for H<sub>2</sub>O<sub>2</sub> production.<sup>60-62</sup> Thus, in presence of methanol, this enzyme is able to produce enough amounts of the coreactant to yield the ECL process. In this case, the increase on the ECL intensities were correlated to the enzymatic activity (Scheme 2).



**Scheme 1.** (A) Enzymatic generation of thiocholine and interaction with the CdS modified electrode. Blocking of the surface and diminution of the ECL signal. (B) Inhibition of AChE through BW inhibitor and increase of the ECL signal.



**Scheme 2.** Enzymatic generation of  $H_2O_2$  and ECL performance.

### 3.5.1. Affinity assays: acetylcholinesterase enzymatic assay

The effect of varying concentrations of ATCh on the ECL response was studied in presence of a fixed amount of AChE ( $50 \text{ mU mL}^{-1}$ ). According to Figure 8A the response to increasing concentrations of ATCh is typical for an enzymatic system governed by the Michaelis-Menten kinetic model. One can notice the linear part of the calibration plot up to  $0.05 \text{ mM}$  of the substrate followed by the plot section approaching asymptotically the maximum response from  $0.5 \text{ mM}$ . The apparent Michaelis-Menten constant was calculated by fitting the experimental results to the equation  $\Delta ECL = \Delta ECL_{\text{max}}[ATCh] / (K_M + [ATCh])$ . The value of  $0.15 \pm 0.034 \text{ mM}$  correlated well with the literature data.<sup>54,63,64</sup> We calculated the LOD for ATCh ( $S/N=3$ ) of  $26.03 \mu\text{M}$ . This value was equal or even better than some amperometric procedures.<sup>65,66</sup> For subsequent experiments we selected a concentration of ATCh equal to  $0.5$

mM. Figure 8B shows the response of the analytical system to increasing amounts of AChE at a fixed concentration of ATCh. The system demonstrated a linear decrease of the ECL signal from 0 to 5 mU mL<sup>-1</sup> and reached a saturation point at around 50 mU mL<sup>-1</sup>. The LOD for AChE was found at 0.73 mU mL<sup>-1</sup> and it is lower than some amperometric<sup>67</sup>, fiber-optic<sup>68</sup> and ECL<sup>69</sup> biosensors.

In order to provide more evidence that the biosensor platform is sensitive to AChE detection, we employed the cholinesterase inhibitor 1,5-bis-(4-allyldimethylammonium-phenyl)pentan-3-one dibromide (BW284c51), which has a mechanism of toxicity similar to organophosphorus nerve agents and is frequently utilized as an analogue of nerve gases.<sup>70-72</sup> This inhibitor has a high selectivity for AChE and competes with the enzyme substrate for binding to the active site in an irreversible manner.<sup>72</sup> Figure 8C represents the ECL signal when pre-incubating the AChE with different amounts of BW. We observed that increasing amounts of BW were associated to an increase in the ECL signal related to the inhibition of the enzyme and the subsequent diminution in the amount of thiols produced. According to  $S/N = 3$ , we calculated a detection limit for BW of 79.22 nM similar to other fiber optic<sup>73</sup> and fluorogenic<sup>58</sup> methods.

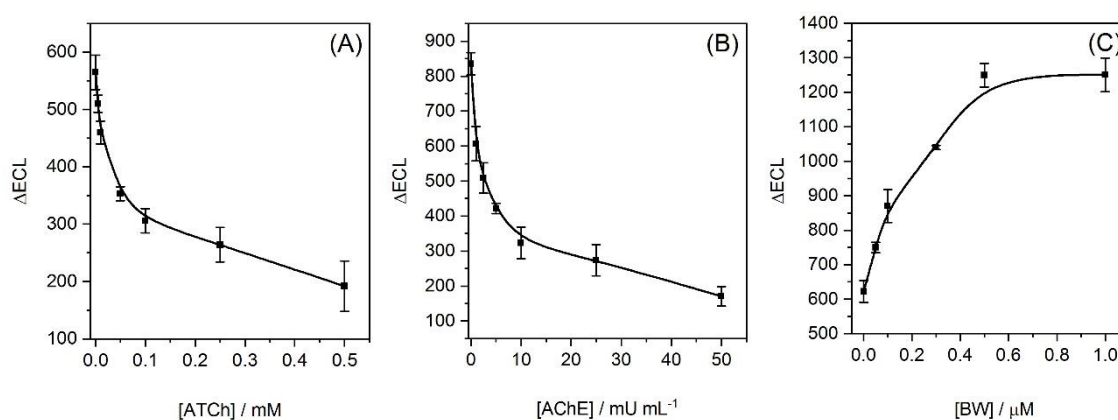


**Figure 8.** Calibration curves of (A) ATCh from 0 to 0.5 mM in presence of AChE 50 mU mL<sup>-1</sup>, (B) AChE from 0 to 50 mU mL<sup>-1</sup> in presence of ATCh 0.5 mM and (C) BW from 0 to 1 μM in presence of AChE 5 mU mL<sup>-1</sup> and ATCh 0.5 mM, measured in PBS with H<sub>2</sub>O<sub>2</sub> 10 mM.

Moreover, to validate the proposed system we used this method to determine AChE in commercially available HS. Different concentrations of the enzyme were added to diluted HS and the enzymatic activity was measured as previously described. We plotted the experimental data with the concentration of the standard (x-axis) against the ECL signal acquired (y-axis) (Figure 11A). A linear regression analysis was performed to calculate the intercept of the calibration curve with the x-axis, representing the concentration of AChE in the HS. Taking into consideration the dilution of the samples, the concentration of AChE was established at 5176

mU mL<sup>-1</sup>. This value is similar to that reported in the literature for human plasma (5675±195 mU mL<sup>-1</sup>).<sup>54,74</sup>

In addition, we also performed control experiments with different thiols to probe the mechanism of the presented system. We tested two pair of oxidized and reduced thiol compounds of interest in biosensing: cystine/cysteine (CSSC/CSH) and glutathione/oxidized glutathione (GSH/GSSG). The interaction with the CdS-SPCE surface was conducted by drop casting a 7 µL of the thiol solution on the working electrode for 20 min. After the washing step we measured their ECL behaviours in PBS with H<sub>2</sub>O<sub>2</sub> 10 mM. Only the reduced forms of the thiols (CSH and GSH) were able to interact with the CdS on the outer layer and block the surface against the coreactant, thus decreasing the ECL signal (Figure 9). On the other hand, the oxidized forms (CSSC and GSSG) didn't affect the ECL intensity of the CdS-SPCE. These experiments confirmed our previous hypothesis regarding the selective interaction of our CdS-SPCE surface towards thiol groups and its blocking for the interaction with the coreactant, decreasing the ECL signal.

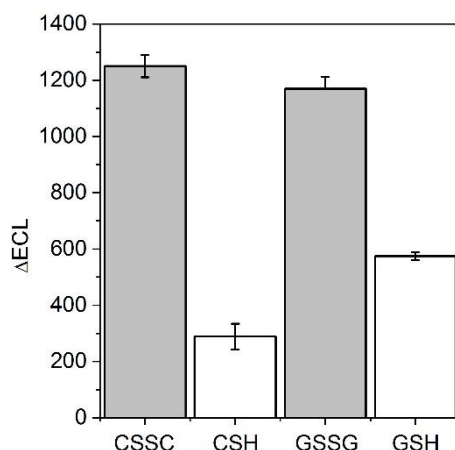


**Figure 9.** ECL signals of CSSG 0.15 mM, CSH 0.15 mM, GSSG 10 µM and GSH 10 µM.

### 3.5.2. Direct assays: alcohol oxidase enzymatic assay

The influence on the ECL intensity of varying amounts of AOx in the presence of a fixed MeOH concentration (0.03 g L<sup>-1</sup>) is shown in Figure 10A. The ECL intensity increased with increasing amounts of enzyme in the range studied. The determination of AOx using methanol as substrate demonstrated a LOD of 6.59 ng mL<sup>-1</sup> (S/N=3). In Figure 10B is presented the calibration plot of varying amount of MeOH and a fixed concentration of AOx (0.05 µg mL<sup>-1</sup>). The increased amounts of MeOH led to an increase in the ECL signal, as more H<sub>2</sub>O<sub>2</sub> is produced in situ. The LOD for MeOH was calculated for 61.46 µg L<sup>-1</sup> (1.92 µM). This ECL assay showed a better sensitivity than classical Raman spectroscopy<sup>75</sup> and amperometric biosensors.<sup>76,77</sup>

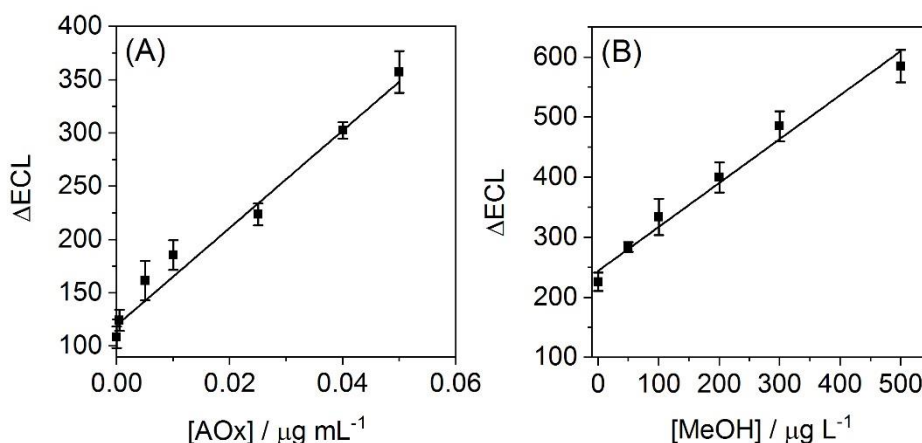


**Figure 10.** Calibration curves of (A) AOx from 0 to 0.05  $\mu g mL^{-1}$  in presence of MeOH 0.03  $g L^{-1}$ , (B) MeOH from 0 to 500  $\mu g mL^{-1}$  in presence of AOx 0.05  $\mu g mL^{-1}$ , measured in PBS with  $H_2O_2$  10 mM.

Additionally, we applied this method to the detection of methanol in vodka. It is well known that methanol is toxic for humans and its content in alcoholic beverages must be controlled. Vodka was chosen as a model alcoholic beverage because of its high consumption, mostly in the Eastern European countries.<sup>78</sup> The same procedure of standard additions was performed. Known quantities of methanol were added to vodka samples. By linear regression the amount of methanol was calculated as 13  $mg L^{-1}$  (Figure 11B). This value was within the methanol levels permitted for alcohol beverages specified by the regulation (EC) No 110/2008, this value should not exceed 100  $mg L^{-1}$ .

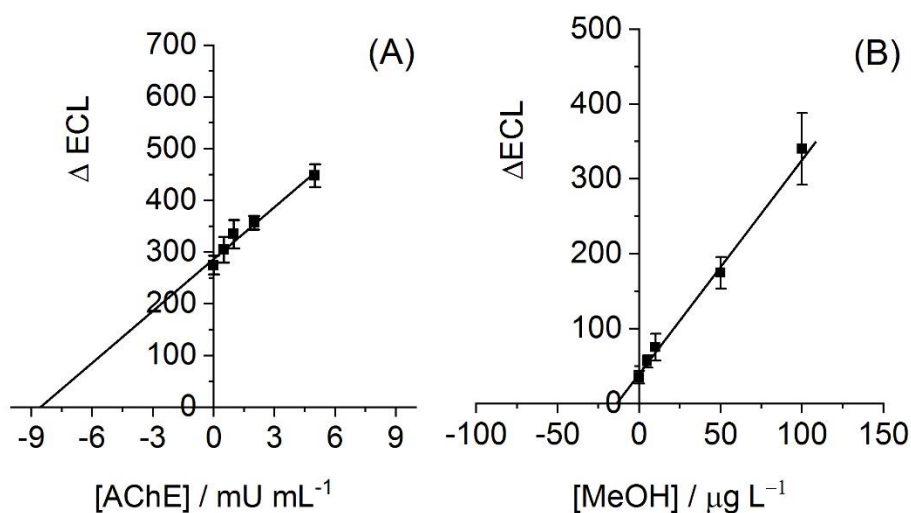


**Figure 11.** Quantification of (A) AChE in solutions containing different concentrations of added standard solution of AChE (from 0 to 5  $mU mL^{-1}$ ), ATCh (0.5 mM) and diluted HS; (B) MeOH in solutions containing different concentrations of added standard (from 0 to 100  $\mu g L^{-1}$ , AOx (0.05  $\mu g mL^{-1}$ ) and diluted vodka.

More evidence of the mechanism proposed was studied with a different enzymatic system. Glucose oxidase was selected because of its ability to produce  $\text{H}_2\text{O}_2$ .<sup>79</sup> GOx is able to oxidize glucose in presence of oxygen yielding  $\text{H}_2\text{O}_2$  that was used to carry out the ECL process. In Figure 12 is shown the ECL intensity results of GOx concentrations  $3.5 \text{ mg mL}^{-1}$  in presence of glucose (2 mM) and the controls of individual reagents. ECL was only generated when the enzyme and substrate were present in solution and interacted to produce  $\text{H}_2\text{O}_2$  that was used as ECL cofactor. Increasing amounts of enzyme produced a higher  $\text{H}_2\text{O}_2$  concentration that led to an increase on the ECL intensity. No significant signal was detected when the reagents were analysed separately. With this additional prove of concept we could confirm our second hypothesis: the enzymatic production in situ of  $\text{H}_2\text{O}_2$  can be used as ECL coreactant for our CdS-SPCE, avoiding the use of an external reagent.

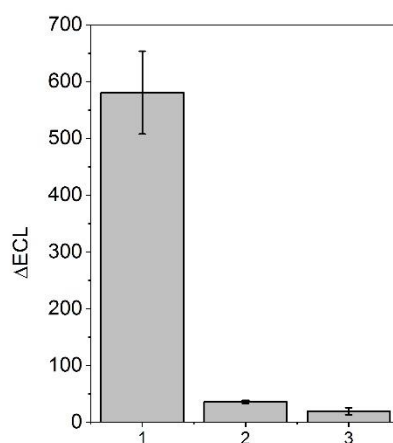


**Figure 12.** ECL peaks of 1) GOx  $3.5 \text{ mg mL}^{-1}$  and glucose 2 mM, 2) GOx  $3.5 \text{ mg mL}^{-1}$ , 3) glucose 2 mM.



## 4. Conclusions

The need of portable, cheap and easy to hand devices for bioanalytical applications promotes the development of new strategies for its accomplishment. The present study shows a novel ECL platform based on CdS nanoparticles with real bioanalytical applications on the detection of analytes of interest. The easy screen-printed electrode modification and the direct, facile and aqueous friendly synthesis of the nanoparticles simplifies the fabrication process of the final CdS-SPE ECL platform. Two approaches were carried out to modulate the ECL emission: enzymatic generation of thiols to block the CdS surface and the in situ production of the H<sub>2</sub>O<sub>2</sub> cofactor needed to produce the ECL signal. First, acetylcholinesterase was employed to release thiocholine that interacted with the CdS thus decreasing the ECL signal. The inhibition mechanism of the enzyme was demonstrated by using the inhibitor BW284c51. On the other hand, alcohol oxidase produced H<sub>2</sub>O<sub>2</sub> and promoted the ECL signal when increasing the amounts of enzyme and substrate. Both strategies were applied to the detection of AChE and MeOH in real samples with successfully results. The proposed procedures are uncomplexed, cost effective and highly sensitive. To the best of our knowledge, this is the first time that this commercial portable  $\mu$ -STAT ECL device is employed for the direct detection of the CdS ECL emission.

## References

- (1) Qiu, B.; Miao, M.; She, L.; Jiang, X.; Lin, Z. Y.; Chen, G. N. An Ultrasensitive Biosensor for Glucose Based on Solid-State Electrochemiluminescence on GOx/CdS/GCE Electrode. *Anal. Methods* **2013**, *5*, 1941–1945.
- (2) Wilkinson, A. D. M.; A. *IUPAC Compendium of Chemical Terminology*; Blackwell Scientific Publications: Oxford, UK, 1997.
- (3) Bard, A. J. *Electrogenerated Chemiluminescence*; CRC Press, Ed.; Monographs in electroanalytical chemistry and electrochemistry; CRC Press, 2004.
- (4) Richter, M. M. Electrochemiluminescence ( ECL ). *Chem. Rev.* **2004**, *104*, 3003–3036.
- (5) Miao, W. ChemInform Abstract: Electrogenerated Chemiluminescence and Its Biorelated Applications. *ChemInform* **2008**, *39*, 2506–2553.
- (6) Miao, W. Electrogenerated Chemiluminescence. *Handb. Electrochem.* **2007**, 541–590.
- (7) Chen, Y.; Zhou, S.; Li, L.; jie Zhu, J. Nanomaterials-Based Sensitive Electrochemiluminescence Biosensing. *Nano Today* **2017**, *12*, 98–115.
- (8) Liu, Z.; Qi, W.; Xu, G. Recent Advances in Electrochemiluminescence. *Chem. Soc. Rev.* **2015**, *44*, 3117–3142.
- (9) Yao, J.; Li, L.; Li, P.; Yang, M. Quantum Dots: From Fluorescence to Chemiluminescence, Bioluminescence, Electrochemiluminescence, and Electrochemistry. *Nanoscale* **2017**, *9*, 13364–13383.
- (10) Lei, J.; Ju, H. Fundamentals and Bioanalytical Applications of Functional Quantum Dots as Electrogenerated Emitters of Chemiluminescence. *TrAC - Trends Anal. Chem.* **2011**, *30*,

- 1351–1359.
- (11) Ding, Z.; Quinn, B. M.; Haram, S. K.; Pell, L. E.; Korgel, B. A.; Bard, A. J. Electrochemistry and Electrogenated Chemiluminescence from Silicon Nanocrystal Quantum Dots. *Science (80-. )*. **2002**, *296*, 1293–1297.
  - (12) Zhu, Q.; Liu, H.; Zhang, J.; Wu, K.; Deng, A.; Li, J. Ultrasensitive QDs Based Electrochemiluminescent Immunosensor for Detecting Ractopamine Using AuNPs and Au Nanoparticles@PDDA-Graphene as Amplifier. *Sensors Actuators, B Chem.* **2017**, *243*, 121–129.
  - (13) Ding, S. N.; Jin, Y.; Chen, X.; Bao, N. Tunable Electrochemiluminescence of CdSe@ZnSe Quantum Dots by Adjusting ZnSe Shell Thickness. *Electrochem. commun.* **2015**, *55*, 30–33.
  - (14) Fang, Y. M.; Song, J.; Zheng, R. J.; Zeng, Y. M.; Sun, J. J. Electrogenated Chemiluminescence Emissions from Cds Nanoparticles for Probing of Surface Oxidation. *J. Phys. Chem. C* **2011**, *115*, 9117–9121.
  - (15) Zhang, Y. Y.; Zhou, H.; Wu, P.; Zhang, H. R.; Xu, J. J.; Chen, H. Y. In Situ Activation of CdS Electrochemiluminescence Film and Its Application in H<sub>2</sub>S Detection. *Anal. Chem.* **2014**, *86*, 8657–8664.
  - (16) Kirschbaum, S. E. K.; Baeumner, A. J. A Review of Electrochemiluminescence (ECL) in and for Microfluidic Analytical Devices. *Anal. Bioanal. Chem.* **2015**, *407*, 3911–3926.
  - (17) Li, W.; Li, M.; Ge, S.; Yan, M.; Huang, J.; Yu, J. Battery-Triggered Ultrasensitive Electrochemiluminescence Detection on Microfluidic Paper-Based Immunodevice Based on Dual-Signal Amplification Strategy. *Anal. Chim. Acta* **2013**, *767*, 66–74.
  - (18) Sardesai, N. P.; Kadimisetty, K.; Faria, R.; Rusling, J. F. A Microfluidic Electrochemiluminescent Device for Detecting Cancer Biomarker Proteins. *Anal. Bioanal. Chem.* **2013**, *405*, 3831–3838.
  - (19) Carvajal, M. A.; Ballesta-Claver, J.; Morales, D. P.; Palma, A. J.; Valencia-Mirón, M. C.; Capitán-Vallvey, L. F. Portable Reconfigurable Instrument for Analytical Determinations Using Disposable Electrochemiluminescent Screen-Printed Electrodes. *Sensors Actuators, B Chem.* **2012**, *169*, 46–53.
  - (20) Ballesta Claver, J.; Valencia Mirón, M. C.; Capitán-Vallvey, L. F. Disposable Electrochemiluminescent Biosensor for Lactate Determination in Saliva. *Analyst* **2009**, *134*, 1423–1432.
  - (21) Lu, L.; Wu, J.; Li, M.; Kang, T.; Cheng, S. Detection of DNA Damage by Exploiting the Distance Dependence of the Electrochemiluminescence Energy Transfer between Quantum Dots and Gold Nanoparticles. *Microchim. Acta* **2015**, *182*, 233–239.
  - (22) Kadimisetty, K.; Malla, S.; Sardesai, N. P.; Joshi, A. A.; Faria, R. C.; Lee, N. H.; Rusling, J. F. Automated Multiplexed Ecl Immunoarrays for Cancer Biomarker Proteins. *Anal. Chem.* **2015**, *87*, 4472–4478.
  - (23) Carvajal, M. A.; Ballesta-Claver, J.; Martínez-Olmos, A.; Capitán-Vallvey, L. F.; Palma, A. J. Portable System for Photodiode-Based Electrochemiluminescence Measurement with Improved Limit of Detection. *Sensors Actuators, B Chem.* **2015**, *221*, 956–961.
  - (24) Habekost, A. Rapid and Sensitive Spectroelectrochemical and Electrochemical Detection of Glyphosate and AMPA with Screen-Printed Electrodes. *Talanta* **2017**, *162*, 583–588.
  - (25) Neves, M. M. P. S.; Bobes-Limenes, P.; Pérez-Junquera, A.; González-García, M. B.; Hernández-Santos, D.; Fanjul-Bolado, P. Miniaturized Analytical Instrumentation for Electrochemiluminescence Assays: A Spectrometer and a Photodiode-Based Device. *Anal. Bioanal. Chem.* **2016**, *408*, 7121–7127.
  - (26) Spanhel, L.; Haase, M.; Weller, H.; Henglein, A. Photochemistry of Colloidal Semiconductors. 20. Surface Modification and Stability of Strong Luminescing CdS Particles. *J. Am. Chem. Soc.* **1987**, *109*, 5649–5655.
  - (27) Narayanan, S. S.; Pal, S. K. Aggregated CdS Quantum Dots: Host of Biomolecular Ligands. *J. Phys. Chem. B* **2006**, *110*, 24403–24409.

- (28) Liu, J. X.; Ding, S. N. Multicolor Electrochemiluminescence of Cadmium Sulfide Quantum Dots to Detect Dopamine. *J. Electroanal. Chem.* **2016**, *781*, 395–400.
- (29) Zhang, Y. Y.; Feng, Q. M.; Xu, J. J.; Chen, H. Y. Silver Nanoclusters for High-Efficiency Quenching of CdS Nanocrystal Electrochemiluminescence and Sensitive Detection of MicroRNA. *ACS Appl. Mater. Interfaces* **2015**, *7*, 26307–26314.
- (30) Huang, H.; Li, J.; Zhu, J. J. Electrochemiluminescence Based on Quantum Dots and Their Analytical Application. *Anal. Methods* **2011**, *3*, 33–42.
- (31) Zhou, H.; Han, T.; Wei, Q.; Zhang, S. Efficient Enhancement of Electrochemiluminescence from Cadmium Sulfide Quantum Dots by Glucose Oxidase Mimicking Gold Nanoparticles for Highly Sensitive Assay of Methyltransferase Activity. *Anal. Chem.* **2016**, *88*, 2976–2983.
- (32) Based, S. P. Highly Sensitive Electrochemiluminescence Detection of Single-Nucleotide Polymorphisms Based on Isothermal Cycle-Assisted Triple-Stem Probe with Dual-Nanoparticle Label. *Anal. Chem.* **2011**, *83*, 8320–8328.
- (33) Griffis, D. P.; Linton, R. W. Quantitative Comparison of Direct and Derivative AES with XPS of Metal Sulfides. *Surf. Interface Anal.* **1982**, *4*, 197–203.
- (34) Rico, M. Á. G.; Olivares-Marín, M.; Gil, E. P. Modification of Carbon Screen-Printed Electrodes by Adsorption of Chemically Synthesized Bi Nanoparticles for the Voltammetric Stripping Detection of Zn(II), Cd(II) and Pb(II). *Talanta* **2009**, *80*, 631–635.
- (35) Lu, B. W.; Chen, W. C. A Disposable Glucose Biosensor Based on Drop-Coating of Screen-Printed Carbon Electrodes with Magnetic Nanoparticles. *J. Magn. Magn. Mater.* **2006**, *304*, 400–402.
- (36) Wang, J.; Zhao, W. W.; Tian, C. Y.; Xu, J. J.; Chen, H. Y. Highly Efficient Quenching of Electrochemiluminescence from CdS Nanocrystal Film Based on Biocatalytic Deposition. *Talanta* **2012**, *89*, 422–426.
- (37) Ding, S. N.; Xu, J. J.; Chen, H. Y. Enhanced Solid-State Electrochemiluminescence of CdS Nanocrystals Compositing with Carbon Nanotubes in H<sub>2</sub>O<sub>2</sub> Solution. *Chem. Commun.* **2006**, No. 34, 3631–3633.
- (38) Ren, T.; Xu, J. Z.; Tu, Y. F.; Xu, S.; Zhu, J. J. Electrogenated Chemiluminescence of CdS Spherical Assemblies. *Electrochem. Commun.* **2005**, *7*, 5–9.
- (39) Zhao, W. W.; Wang, J.; Zhu, Y. C.; Xu, J. J.; Chen, H. Y. Quantum Dots: Electrochemiluminescent and Photoelectrochemical Bioanalysis. *Anal. Chem.* **2015**, *87*, 9520–9531.
- (40) Shan, Y.; Xu, J. J.; Chen, H. Y. Distance-Dependent Quenching and Enhancing of Electrochemiluminescence from a CdS:Mn Nanocrystal Film by Au Nanoparticles for Highly Sensitive Detection of DNA. *Chem. Commun.* **2009**, No. 8, 905–907.
- (41) Deng, S.; Ju, H. Electrogenated Chemiluminescence of Nanomaterials for Bioanalysis. *Analyst* **2013**, *138*, 43–61.
- (42) Wang, X. F.; Zhou, Y.; Xu, J. J.; Chen, H. Y. Signal-on Electrochemiluminescence Biosensors Based on CdS-Carbon Nanotube Nanocomposite for the Sensitive Detection of Choline and Acetylcholine. *Adv. Funct. Mater.* **2009**, *19*, 1444–1450.
- (43) Zhou, H.; Zhang, Y. Y.; Liu, J.; Xu, J. J.; Chen, H. Y. Efficient Quenching of Electrochemiluminescence from K-Doped Graphene-CdS:Eu NCs by G-Quadruplex-Hemin and Target Recycling-Assisted Amplification for Ultrasensitive DNA Biosensing. *Chem. Commun.* **2013**, *49*, 2246–2248.
- (44) Niu, H.; Yuan, R.; Chai, Y.; Mao, L.; Liu, H.; Cao, Y. Highly Amplified Electrochemiluminescence of Peroxydisulfate Using Bionzyme Functionalized Palladium Nanoparticles as Labels for Ultrasensitive Immunoassay. *Biosens. Bioelectron.* **2013**, *39*, 296–299.
- (45) Dai, B.; Wang, L.; Shao, J.; Huang, X.; Yu, G. CdS-Modified Porous Foam Nickel for Label-Free Highly Efficient Detection of Cancer Cells. *RSC Adv.* **2016**, *6*, 32874–32880.
- (46) Valenti, G.; Rampazzo, E.; Bonacchi, S.; Khajvand, T.; Juris, R.; Montalti, M.; Marcaccio,

- M.; Paolucci, F.; Prodi, L. A Versatile Strategy for Tuning the Color of Electrochemiluminescence Using Silica Nanoparticles. *Chem. Commun.* **2012**, *48*, 4187–4189.
- (47) Marquette, C. A.; Ravaud, S.; Blum, L. J. Luminol Electrochemiluminescence-Based Biosensor for Total Cholesterol Determination in Natural Samples. *Anal. Lett.* **2000**, *33*, 1779–1796.
- (48) Kitte, S. A.; Gao, W.; Zholudov, Y. T.; Qi, L.; Nsabimana, A.; Liu, Z.; Xu, G. Stainless Steel Electrode for Sensitive Luminol Electrochemiluminescent Detection of H<sub>2</sub>O<sub>2</sub>, Glucose, and Glucose Oxidase Activity. *Anal. Chem.* **2017**, *89*, 9864–9869.
- (49) Dai, H.; Chi, Y.; Wu, X.; Wang, Y.; Wei, M.; Chen, G. Biocompatible Electrochemiluminescent Biosensor for Choline Based on Enzyme/Titanate Nanotubes/Chitosan Composite Modified Electrode. *Biosens. Bioelectron.* **2010**, *25*, 1414–1419.
- (50) Liu, X.; Cheng, L.; Lei, J.; Liu, H.; Ju, H. Formation of Surface Traps on Quantum Dots by Bidentate Chelation and Their Application in Low-Potential Electrochemiluminescent Biosensing. *Chem. - A Eur. J.* **2010**, *16*, 10764–10770.
- (51) Haye, D.; Meisel, D.; Mididb, O. I. Size Control and Properties of Thiol Capped CdS Particles \* T+. *colloids and Surfaces* **1991**, *55*, 121–136.
- (52) Li, H.; Shih, W. Y.; Shih, W. H. Synthesis and Characterization of Aqueous Carboxyl-Capped CdS Quantum Dots for Bioapplications. *Ind. Eng. Chem. Res.* **2007**, *46*, 2013–2019.
- (53) Liji Sobhana, S. S.; Vimala Devi, M.; Sastry, T. P.; Mandal, A. B. CdS Quantum Dots for Measurement of the Size-Dependent Optical Properties of Thiol Capping. *J. Nanoparticle Res.* **2011**, *13*, 1747–1757.
- (54) Garai-Ibabe, G.; Saa, L.; Pavlov, V. Thiocholine Mediated Stabilization of in Situ Produced CdS Quantum Dots: Application for the Detection of Acetylcholinesterase Activity and Inhibitors. *Analyst* **2014**, *139*, 280–284.
- (55) Jie, G.; Liu, B.; Pan, H.; Zhu, J. J.; Chen, H. Y. CdS Nanocrystal-Based Electrochemiluminescence Biosensor for the Detection of Low-Density Lipoprotein by Increasing Sensitivity with Gold Nanoparticle Amplification. *Anal. Chem.* **2007**, *79*, 5574–5581.
- (56) Jiang, H.; Ju, H. Enzyme-Quantum Dots Architecture for Highly Sensitive Electrochemiluminescence Biosensing of Oxidase Substrates. *Chem. Commun.* **2007**, No. 4, 404–406.
- (57) Poulpique, A. De; Buitrago, B. D.; Milutinovic, M. D.; Arbault, S.; Bouffier, L.; Kuhn, A.; Sojic, N. Dual Enzymatic Detection by Bulk Electrogenerated Chemiluminescence. **2016**.
- (58) Saa, L.; Virel, A.; Sanchez-Lopez, J.; Pavlov, V. Analytical Applications of Enzymatic Growth of Quantum Dots. *Chem. - A Eur. J.* **2010**, *16*, 6187–6192.
- (59) Virel, A.; Saa, L.; Pavlov, V. Modulated Growth of Nanoparticles. Application for Sensing Nerve Gases. *Anal. Chem.* **2009**, *81*, 268–272.
- (60) Kaszycki, P.; Koloczek, H. Formaldehyde and Methanol Biodegradation with the Methylophilic Yeast *Hansenula Polymorpha* in a Model Wastewater System. **2000**, *154*, 289–296.
- (61) Bucur, B.; Lucian, A. E. G. Analysis of Methanol – Ethanol Mixtures from Falsified Beverages Using a Dual Biosensors Amperometric System Based on Alcohol Dehydrogenase and Alcohol Oxidase. **2008**, 1335–1342.
- (62) Barroso, J.; Díez-Buitrago, B.; Saa, L.; Möller, M.; Briz, N.; Pavlov, V. Specific Bioanalytical Optical and Photoelectrochemical Assays for Detection of Methanol in Alcoholic Beverages. *Biosens. Bioelectron.* **2018**, *101*, 116–122.
- (63) Pohanka, M.; Hrabínova, M.; Kuca, K.; Simonato, J. P. Assessment of Acetylcholinesterase Activity Using Indoxylacetate and Comparison with the Standard Ellman's Method. *Int. J. Mol. Sci.* **2011**, *12*, 2631–2640.

- (64) Barteri, M.; Pala, A.; Rotella, S. Structural and Kinetic Effects of Mobile Phone Microwaves on Acetylcholinesterase Activity. *Biophys. Chem.* **2005**, *113*, 245–253.
- (65) Kesik, M.; Ekiz Kanik, F.; Turan, J.; Kolb, M.; Timur, S.; Bahadir, M.; Toppare, L. An Acetylcholinesterase Biosensor Based on a Conducting Polymer Using Multiwalled Carbon Nanotubes for Amperometric Detection of Organophosphorous Pesticides. *Sensors Actuators B Chem.* **2014**, *205*, 39–49.
- (66) Turdean, G. L.; Popescu, I. C.; Oniciu, L.; Thevenot, D. R. Sensitive Detection of Organophosphorus Pesticides Using a Needle Type Amperometric Acetylcholinesterase-Based Bioelectrode. Thiocholine Electrochemistry and Immobilised Enzyme Inhibition. *J. Enzyme Inhib. Med. Chem.* **2002**, *17*, 107–115.
- (67) Bucur, B.; Fournier, D.; Danet, A.; Marty, J. L. Biosensors Based on Highly Sensitive Acetylcholinesterases for Enhanced Carbamate Insecticides Detection. *Anal. Chim. Acta* **2006**, *562*, 115–121.
- (68) Doong, R. A.; Tsai, H. C. Immobilization and Characterization of Sol-Gel-Encapsulated Acetylcholinesterase Fiber-Optic Biosensor. *Anal. Chim. Acta* **2001**, *434*, 239–246.
- (69) Deng, S.; Lei, J.; Cheng, L.; Zhang, Y.; Ju, H. Biosensors and Bioelectronics Amplified Electrochemiluminescence of Quantum Dots by Electrochemically Reduced Graphene Oxide for Nanobiosensing of Acetylcholine. *Biosens. Bioelectron.* **2011**, *26*, 4552–4558.
- (70) Vale, A.; Bradberry, S.; Rice, P.; Marrs, T. C. Chemical Warfare and Terrorism. *Medicine (Baltimore)*. **2004**, *31*, 26–29.
- (71) Mileson, B. E.; Chambers, J. E.; Chen, W. L.; Dettbarn, W.; Ehrich, M.; Eldefrawi, A. T.; Gaylor, D. W.; Hamernik, K.; Hodgson, E.; Karczmar, A. G.; et al. Common Mechanism of Toxicity: A Case Study of Organophosphorus Pesticides. *Toxicol. Sci.* **1998**, *41*, 8–20.
- (72) Austin, L.; Berry, W. K. Two Selective Inhibitors of Cholinesterase. *Biochem. J.* **1953**, *54*, 695–700.
- (73) Trettnak, W.; Reiningger, F.; Zinterl, E.; Wolfbeis, O. S. Fiber-Optic Remote Detection of Pesticides and Related Inhibitors of the Enzyme Acetylcholine Esterase. *Sensors Actuators B Chem.* **1993**, *11*, 87–93.
- (74) Worek, F.; Mast, U.; Kiderlen, D.; Diepold, C.; Eyer, P. Improved Determination of Acetylcholinesterase Activity in Human Whole Blood. *Clin. Chim. Acta* **1999**, *288*, 73–90.
- (75) Boyacı, I. H.; Genis, H. E.; Guven, B.; Tamer, U.; Alper, N. A Novel Method for Quantification of Ethanol and Methanol in Distilled Alcoholic Beverages Using Raman Spectroscopy. *J. Raman Spectrosc.* **2012**, *43*, 1171–1176.
- (76) Kučera, I.; Sedláček, V. An Enzymatic Method for Methanol Quantification in Methanol/Ethanol Mixtures with a Microtiter Plate Fluorometer. *Food Anal. Methods* **2017**, *10*, 1301–1307.
- (77) Park, D.-S.; Won, M.-S.; Goyal, R. N.; Shim, Y.-B. The Electrochemical Sensor for Methanol Detection Using Silicon Epoxy Coated Platinum Nanoparticles. *Sensors Actuators B Chem.* **2012**, *174*, 45–50.
- (78) Wiśniewska, P.; Śliwińska, M.; Dymerski, T.; Wardencki, W.; Namieśnik, J. The Analysis of Vodka: A Review Paper. *Food Anal. Methods* **2015**, *8*, 2000–2010.
- (79) Wilson, R.; Turner, A. P. D. Glucose Oxidase: An Ideal Enzyme. *Biosens. Bioelectron.* **1992**, *13*, 165–185.



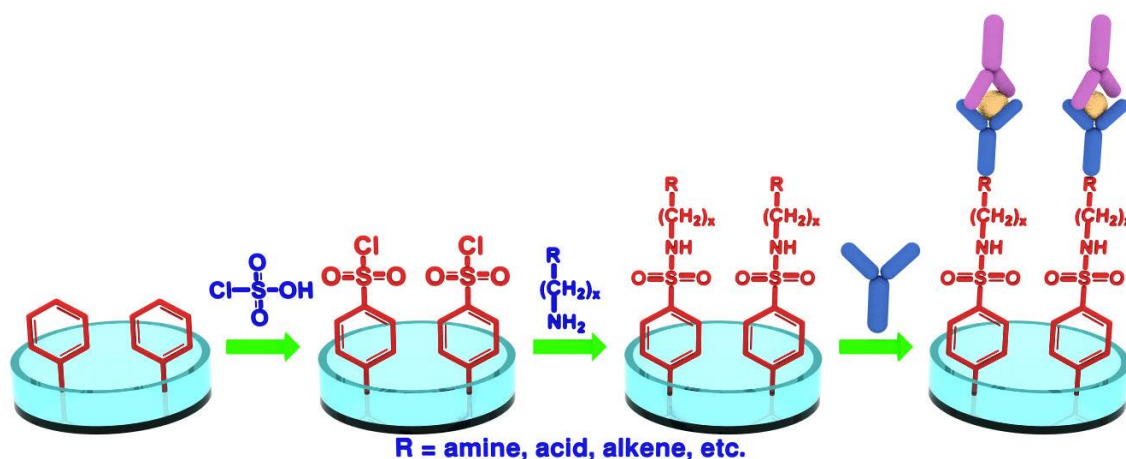
## **CHAPTER 4: DESIGN AND DEVELOPMENT OF A LAB-ON-A-CHIP**

---

- Modification of chlorosulfonated polystyrene substrates for bioanalytical applications
- Design of a photoelectrochemical lab-on-a-chip immunosensor based on enzymatic production of quantum dots in situ







## MODIFICATION OF CHLOROSULFONATED POLYSTYRENE SUBSTRATES FOR BIOANALYTICAL APPLICATIONS

This chapter describes the modification of polystyrene micro-well plates and their use as bioanalytical platform is described. A wet-chemical procedure was applied for the chlorosulfonation of these polystyrene substrates (PS) resulting in well-controlled and reactive surfaces. This method enabled the production of transparent and stable substrates under ambient conditions. The chlorosulfonyl moieties at the substrate surface were converted under mild conditions into different functional groups. The modification of PS served to increase the hydrophilic properties of the surface and thus, the improvement of interaction with biocompounds. The resulting substrates were characterized by contact angle measurements, X-Ray Photoelectron Spectroscopy and colorimetry. PS substrates modified with different functional groups and attachment approaches (covalent link and direct adsorption of the antibodies) were used as the platform for immunoassays and the results compared to a commercial Human Serum Albumin ELISA kit. Aminated surfaces gave better results than those with carboxyl, alkene or epoxy groups and even the commercial kit.

---

The work presented is under review: Díez-Buitrago, B.; Fernández-SanArgimiro, F. J.; Lorenzo, L.; Briz, N.; Pavlov, V. Materials Science and Engineering: C

## 1. Introduction

Biomaterials can be defined as materials that come into contact with biological environments produced by natural or synthetic materials.<sup>1-3</sup> Biomaterials can be metals, ceramics, composite materials or polymers; and the way they interact with a biological environment is complex and depends on the physico-chemical properties of their surface. Therefore, great efforts are being made in the study and development of surface and interface science regarding the seeking of the appropriate properties for a specific application.<sup>3-6</sup> Due to the extensive variety of biomaterials they present diversified structural, physical, chemical and mechanical properties and hence offer various alternative applications. Among these materials, polymer substrates are one of the most widely utilized materials in the bioanalytical sector.<sup>1,7-9</sup> They may proceed from synthetic or natural sources and they offer a wide spectrum of physico-chemical properties due to the large variety in their structure and chemical composition which can be further altered by different surface treatment methods to achieve appropriate properties for each application.<sup>10</sup> Polymers present some advantages over other classes of biomaterials such as ease to manufacture, availability, low cost and ease to modulate for final applications. Moreover, since they present high biocompatibility with many biological molecules and living cells, they are a good alternative for glass or silicon in most biotechnological applications. Hence, polymeric materials have increasingly gained importance as attractive support materials for biomedical applications,<sup>9,11-13</sup> tissue engineering,<sup>14,15</sup> textile,<sup>16,17</sup> food industry,<sup>18,19</sup> biosensors<sup>20-24</sup> and bioanalytical assays.<sup>25-27</sup>

Polystyrene (PS) is among the most extended commercialized polymer materials in the bioanalytical sector that presents several advantages over classic materials such as silicon, metal or glass as the substrate material in bioanalysis like its excellent optical clarity, ease to mold, low cost and biocompatibility because of its excellent optical clarity, ease to mold and low cost.<sup>28-30</sup> Moreover, it is often utilized in microscopic techniques, normally employed as detection method in immunoassays, due to its transparency. Furthermore, the machining, fabrication and shaping of this polymer is cheaper, scalable to mass production, less time-consuming and allows the production of a wide variety products (films, multiwell plates, beads, etc.). This, combined with the relatively easy automatization of pipetting, washing and signal detection, has led to their multiple-well plates, nanostructures, films and slides having gained widespread acceptance as bioanalytical platform. Nonetheless, PS presents one important drawback: it is relatively hydrophobic and non-wettable, what hinders the attachment of cells, enzymes and other biocompounds. Surface modification with hydrophilic functional groups

prior to attachment of a bioactive compound is a way to circumvent this inconvenience. Physical or chemical treatments change the properties of the modified polymer but should be limited to the surface of the polymeric material, while the bulk should remain unaltered.<sup>10</sup>

Direct attachment to the polymer surface through a covalent link is the shortest path to straight immobilization of the bioactive compounds. This method offers the advantage of a more stable and strong bond, and can be applied to most of the polymers, varying the final application in the nature of the substrate (poly(styrene), poly(dimethyl siloxane), poly(pyrrole), poly(ethylene terephthalate), etc.).<sup>31-33</sup> Depending on the applications only minute percent of modification is required, or it might be necessary to increase the number of groups introduced per unit area. This can be accomplished by grafting a polyfunctional agent onto the surface or tethering the compound via spacer molecules in order to improve the bioactivity by reducing the steric interactions. Despite the covalent attachment, another frequently used method of immobilization is the adsorption via electrostatic interactions or ligand-receptor strategy. Non-covalent adsorption is simple and convenient for certain applications such as drug delivery, antimicrobial textiles and bioanalysis. One of the most representative systems of this group is the biotin-avidin interaction, the strongest reported non-covalent bond,<sup>34</sup> very attractive in surface bioconjugation due to the large number of biotinylated compounds normally used in biotechnology. Despite the final interaction between the surface and the biocompound, the intrinsic hydrophobic and inert nature of the polymer makes it necessary to functionalize the surface in order to introduce the desired type and quantity of reactive functional groups which will interact with the compound through a covalent bond or non-covalent interactions.

Typical surface treatments of PS use plasma or corona discharge to introduce selected functional groups varying the plasma gas and operating parameters. This procedure modifies the top nanometer of the surface without using solvents or producing any waste and can be coupled to other techniques such as UV irradiation. Oxygen plasma is often used to create oxygen containing groups,<sup>35,36</sup> carbon dioxide for carbonyl groups,<sup>37</sup> air plasma to oxidize the surface<sup>38</sup> and ammonia or nitrogen plasma have been used to aminate PS.<sup>39,40</sup> In spite of the good results and variability of the process, this type of physical modification shows a disadvantage regarding the lack of selectivity and control, resulting in a large number of different groups created on the surface. An alternative to circumvent this problem is the use of wet-chemical surface treatments that consist of treating the polymer with reactive organic solutions to generate functional groups on the surface. This classical approach is capable of penetrating porous three-dimensional substrates and allows for in situ surface functionalization of microfluidic devices. It has recently been shown that PS substrates can be

activated by a simple and economic wet-chemical treatment with chlorosulfonic acid at low temperatures providing surface selectivity with a tunable number of chlorosulfonic groups.<sup>41-43</sup> The chlorosulfonated species at the surface can be converted in a second step into a different functional group leading to the formation of specifically modified substrates under mild conditions. This protocol provides high control of the final amount of functional groups on the surface and stable samples in ambient conditions without losing their activity. Moreover, it enables the production of a wide range of chemistries while maintaining the transparency of the samples and can be applied to multiple substrates (films, micro-well plates, slides). Thus, the main objective of this work is to develop homogenous, well-defined and stable PS platforms with a specific reactivity for their use in bioanalysis. In our case the suitability of the substrate modification will be coupled with an immunoassay in order to test the best chemistry for the attachment of the antibodies and the improvement of a commercial kit.

## **2. Experimental section**

### **2.1. Materials**

Chlorosulfonic acid and sulfuric acid were acquired from Panreac. If nothing else specified, the rest of reagents were purchased from Sigma. Polystyrene 96-well plates were purchased from Falcon. Transparent polystyrene sheets of 1.2 mm thickness were purchased from GoodFellow (England). The Human Serum Albumin detection ELISA set was purchased from R&D Systems.

### **2.2. Apparatus**

Absorbance measurements were performed on a Synergy H1 microplate reader (BioTek) using transparent microwell plates at room temperature. Contact angle measurements were carried out using a DigiDrop GBX instrument at room temperature on polystyrene sheets. X-ray Photoelectron Spectroscopy (XPS) experiments were performed in a SPECS Sage HR 100 spectrometer with a non-monochromatic X-ray source (Magnesium K $\alpha$  line of 1253.6 eV energy and 251 W).

### **2.3. Methods**

#### **2.3.1. Chlorosulfonation of PS substrates**

In a thermostatable reactor polystyrene substrates (96-well plates or films) were immersed in chlorosulfonic acid at -10 °C. After 20 min the samples were taken out and washed with cold (-

10 °C) concentrated sulfuric acid. Finally, they were washed in an ice/water mixture and dried at room temperature.

### 2.3.2. Functionalization of PS substrates

*Amination.* Chlorosulfonated substrates were brought into contact with 250  $\mu\text{L}$  of different aqueous diamine solutions (0.33, 1.7 and 5 M) and reacted for 20 min at room temperature. After that, they were rinsed with water and dried at room temperature. *Carboxylation.* Chlorosulfonated substrates were brought into contact with 250  $\mu\text{L}$  of different aqueous aminoacid solutions (0.05, 0.075 and 0.1 M) and reacted overnight at 70 °C. The following day, they were rinsed with water and dried at room temperature. *Alkene addition.* Chlorosulfonated substrates were brought into contact with 250  $\mu\text{L}$  of a 10% aqueous solution (v/v) of allylamine and reacted for 15 min at room temperature. Next, the plates were rinsed with water and dried. *Epoxidation.* Alkene substrates were brought into contact with 250  $\mu\text{L}$  of meta-chloroperoxybenzoic acid (mCPBA) and reacted overnight at 0 °C. The following day, they were washed with a 10% aqueous solution (v/v) of NaOH and kept at 0 °C.

## 2.4. Characterization of modified substrates

### 2.4.1. Colorimetry

For the determination of the concentration of  $\text{SO}_2\text{Cl}$  and carboxyl groups on the surfaces, a variation of the method previously described<sup>44</sup> was used. Modified micro-plates were brought into contact with 250  $\mu\text{L}$  of a 0.5 mM Toluidine Blue O (TBO) solution in water at pH 10 where it reacted overnight at room temperature. The following day, the samples were rinsed with water at pH 10 to remove uncomplexed dye. To desorb the complexed dye, the samples were brought into contact with 250  $\mu\text{L}$  of 37 wt% hydrochloric acid for 15 min. The TBO concentration (which corresponds to the acid concentration of the surfaces) of the solution was colorimetrically determined at 697 nm.

Amine groups were determined by a method described by Hamerli.<sup>45</sup> Modified micro-plates were brought into contact with 250  $\mu\text{L}$  of an 0.175 mg  $\text{mL}^{-1}$  Orange II solution in water at pH 3 and reacted overnight at room temperature. The following day, the samples were rinsed with water at pH 3. To dissolve the adsorbed dye, the samples were brought into contact with 250  $\mu\text{L}$  of water at pH 12 and reacted for 15 min. The dye concentration (which corresponds to the amine concentration of the surfaces) was colorimetrically determined at 485 nm.

#### 2.4.2. Contact angle

Transparent polystyrene sheets were chlorosulfonated and modified with the different functionalities. Water contact angles (WCA) were determined by dropping distilled water (3 $\mu$ L) on the surface and calculating the angle between the surface and the edge of the drop. An average value of contact angle was calculated by measuring five replicates per sheet.

#### 2.4.3. XPS

Transparent PS sheets were chlorosulfonated and modified with different functionalities. XPS analysis was performed with a non-monochromatic X-ray source placed perpendicular to the analyser axis and calibrated using the 3d<sub>5/2</sub> line of Ag with a full width at half maximum (FWHM) of 1.1 eV. The selected resolution for the spectra was 15 eV of Pass Energy and 0.15 eV/step. All Measurements were made in an ultra-high vacuum (UHV) chamber at a pressure around 2·10<sup>-8</sup> mbar. An electron flood gun was used to neutralize for charging.

### 2.5. Bioanalytical applications: ELISA assay

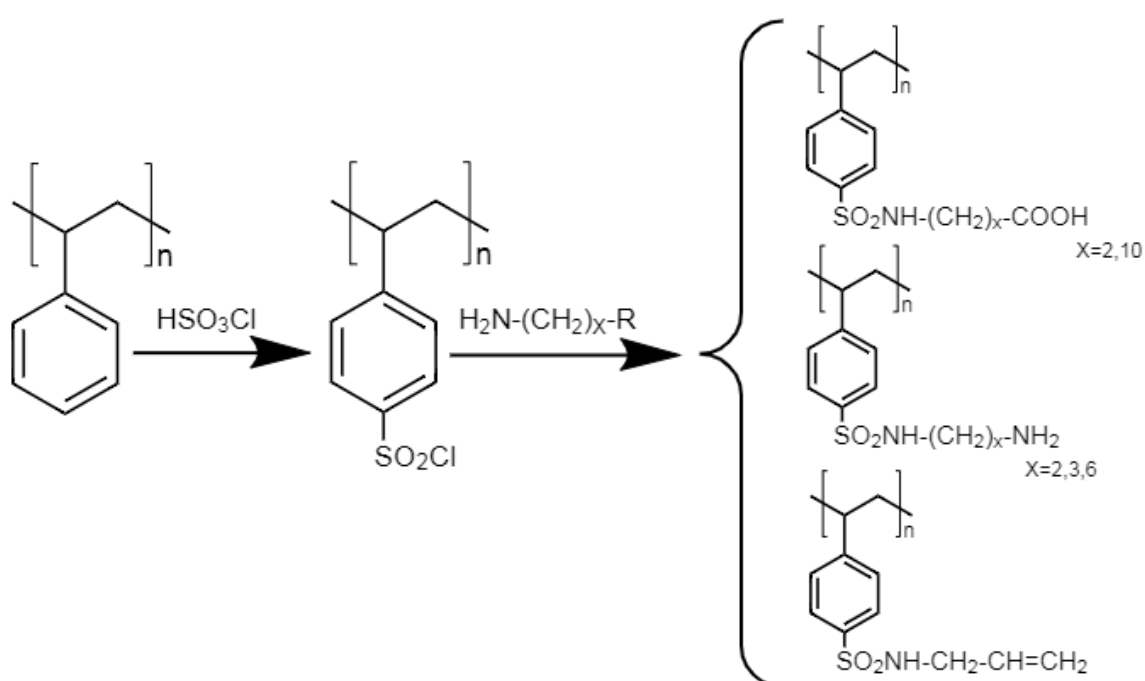
A Human Serum Albumin (HSA) set was used to evaluate the bioanalytical application of the modified surfaces. Polystyrene 96-well plates were modified according to previous methodologies prior to the assay. All the surfaces were compared with a control surface provided in the kit. The bioassay was carried out following the protocol of the kit.

## 3. Results and discussion

### 3.1. Polystyrene chlorosulfonation and functionalization

PS substrates can be easily chlorosulfonated by immersion of the polymeric material in a cold solution of pure chlorosulfonic acid.<sup>42</sup> The PS substrate is first immersed in a solution of chlorosulfonic acid at -10 °C where the polymer suffers an electrophilic aromatic substitution (Scheme 1). The substrates are washed afterwards in cold sulfuric acid and then in water. The final substrates are stable and can be stored in ambient conditions for months without losing their reactivity.<sup>41-43</sup> Moreover, PS modified samples show excellent transparency properties, essential for optical applications. Furthermore, this surface modification of PS substrates leads to the improvement of their hydrophilicity. PS is hydrophobic and shows low wettability, but by the addition of chlorosulfonic groups the surface becomes more hydrophilic (Figure 1) and makes it more suitable for the anchoring of biomolecules.

Chlorosulfonated PS substrates present high reactivity towards primary aliphatic amines. Therefore,  $\alpha,\omega$ -substituted amine-derivates are used to introduce different functionalities to the surface. The primary amine group is used to react with the chlorosulfonyl group forming a sulfonamide link leaving the other side of the chain unreacted with a specific functionality (Scheme 1). Experimentally, the PS substrates are immersed in the specific solutions where they react. This procedure generates specific homogenous products under mild conditions and short reaction times.



**Scheme 1.** Polystyrene modification.

### 3.2. Surface characterization

Colorimetric measurements, contact angle studies and XPS analysis were carried out in order to characterize the surface of the modified PS substrates. The number of available functional groups on the surface has been determined by colorimetry using Orange II for amine and Toluidine O for acid groups. The method consists in the reversible formation of a salt complex between the functional group and the dye. When the complex is formed on the surface, excess dye can be washed off. Then the adhered dye is extracted by immersing the substrate in a fixed volume of basic water for amine groups and acidic solution for acid groups. Finally, the dye concentration can be determined photometrically. The colorimetric results are shown in Table 1. The absolute density of  $SO_2Cl$  groups detected in the chlorosulfonated PS plates was

246 nmol cm<sup>-2</sup>, which is consistent with previous studies<sup>41-43</sup> and corresponds to the number of reactive sites on the surface that can be modified. In the case of aminated surfaces, we compared three diamines with different chain length: ethylenediamine (C2), 1,3-diaminopropane (C3) and hexamethylenediamine (C6). The highest degree of modification found was around 10 nmol cm<sup>-2</sup> using the C2 amine while the C3 and the C6 amine lead to 1 and 2 nmol cm<sup>-2</sup>, respectively. Apart from the concentration influence, this tendency can be explained considering the increased flexibility of the diamine with increasing number of carbons between the amines. Longer carbon chains favour the double interaction between one molecule and the surface. This double interaction from one single molecule with the surface results in a diminution in the final amount of available amines on the surface. Regarding the acids, we tested two acids with different chain length:  $\beta$ -alanine (C3) and undecanoic acid (C11). In this case, when increasing the chain length, the absolute density decreases from 192 to 186 nmol cm<sup>-2</sup> approximately. This behaviour is related to the increase in reactivity and mobility when decreasing the size of the reagent. Hence, the higher carboxylic modification compared to the amines was justified considering the double interaction of the amines with the surface, that leads to a minor amount of free amines on the surface, and the high temperature and time of reaction in the case of acids, that can favour the modification.

**Table 1.** Group density of modified polystyrene substrates.

	Conc. / M	mean	SD
PS-SO <sub>2</sub> Cl	-	246	42.0
PS-(CH <sub>2</sub> ) <sub>2</sub> -COOH	0.075	205	14.2
	0.1	212	17.3
PS-(CH <sub>2</sub> ) <sub>10</sub> -COOH	0.05	186	10.0
	0.1	192	23.8
PS-(CH <sub>2</sub> ) <sub>2</sub> -NH <sub>2</sub>	1.7	2.5	0.2
	5	9.8	1.4
PS-(CH <sub>2</sub> ) <sub>3</sub> -NH <sub>2</sub>	0.33	0.7	1.2
	1.7	1.1	0.6
PS-(CH <sub>2</sub> ) <sub>6</sub> -NH <sub>2</sub>	1.7	1.4	0.7
	5	2.1	1.2



Another important parameter is the wettability of the PS substrates. The surfaces were studied using WCA measurements because it is the easiest and quickest method to examine surface properties. Non-treated PS is very hydrophobic and not suitable for the interaction with biological agents. This issue is addressed with the modification of the surface and the introduction of hydrophilic groups. WCA measurements give information about the wettability of a surface by measuring the angle of a water drop deposited on the surface studied. The results can be correlated to a major or minor hydrophobicity of the surface as follows: the higher the value of the contact angle, the more hydrophobic is the surface, and vice versa. In Figure 1 it can be seen that the most hydrophobic surface is that of non-treated PS with a contact angle of 82° that decreases to 58° when introducing the chlorosulfonic group making it more hydrophilic. The most hydrophilic surface is that of the PS-epoxy system with a contact angle of 40°. Between these values, PS- carboxylic gives a contact angle of 49°, PS-amine shows a contact angle of 55°, and PS-alkene a value of 58°. From these results we can conclude that all the PS modifications increase its hydrophilic properties, thus improving its wettability and suitability for biochemical applications.

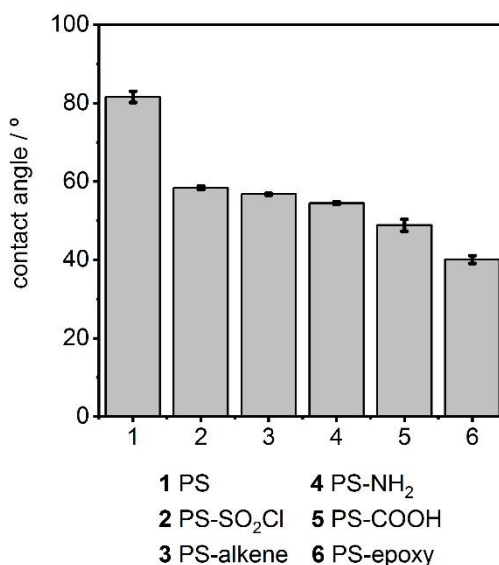


**Figure 1.** Contact angle of polystyrene modified substrates.

XPS measurements were used to analyse more precisely the chemical composition of the modified PS surfaces (PS, PS-SO<sub>2</sub>Cl, PS-COOH C3 0.1 M, PS-NH<sub>2</sub> C2 5M, PS-alkene, PS- epoxy). This spectroscopic technique can provide atomic composition information of the topmost surface layers of the modified PS. Table 2 shows the relative chemical composition of the samples and the ratios between the elements and Table 3 the results from the curve fitting of

the high-resolution peaks in each case to obtain further insight into the chemical bonds present on the surface.

**Table 2.** Relative chemical composition of the samples from XPS analysis.

Sample	Chemical composition (%)							
	C	O	S	N	Cl	S/N	O/N	O/S
PS	98.9	1.1	-	-	-	-	-	-
PS-SO <sub>2</sub> Cl	74.8	13.1	8.6	0.9	2.6	-	-	1.5
PS-COOH	78.3	11.7	6.7	3.2	0.1	2.1	3.7	1.8
PS-NH <sub>2</sub>	73.9	13.3	9.3	2.4	1.2	3.9	5.5	1.4
PS-alkene	73.1	13.2	7.5	6.1	0.1	1.2	2.2	1.8
PS-epoxy	75.2	16.4	7.0	1.2	0.2	5.8	13.7	2.3

**Table 3.** Peak position from the curve fitting of XPS results.

C 1s				
sample	Fitted position $\pi$ - $\pi^*$ (eV)[at%]	Fitted position C=O (eV)[at%]	Fitted position C-O/C-O-C/C-N/C-S (eV)[at%]	Fitted position C-C/C-H/C=C (eV)[at%]
PS	291.2 [5.3]	287 [1]	286 [1.5]	284.8 [92.2]
PS-SO <sub>2</sub> Cl	291.2 [1.4]	-	286.3 [8.1]	284.8 [90.5]
PS-COOH	291.1 [0.7]	288[2.4]	286.4 [14.9]	284.8 [82]
PS-NH <sub>2</sub>	291.3 [1.4]	287.0 [3.1]	286.2 [11.2]	284.8 [84.3]
PS-alkene	291.3 [0.7]	287.6 [2.9]	286.3 [13]	284.8 [80.6]
PS-epoxy	291.4 [0.8]	287.9 [1.2]	286.4 [14.2]	284.8 [82.9]
O 1s				
sample	Fitted position C-O-C/sulfonamide (eV) [at%]	Fitted position COOH/C-O/SO <sub>3</sub> <sup>2-</sup> (eV) [at%]	Fitted position C=O (eV) [at%]	
PS	533.8 [24]	532.6[76]	-	
PS-SO <sub>2</sub> Cl	533.5 [27]	531.9[73]	-	
PS-COOH	533.5 [7.3]	531.9 [40.9]	530.7 [51.8]	
PS-NH <sub>2</sub>	533.4 [15]	531.9 [80]	530.4[5]	
PS-alkene	533.5 [17]	532 [89]	530.3[4]	
PS-epoxy	533.7 [10]	532.2 [88]	530.3[2]	

<b>S 2p<sub>3/2</sub></b>			
<b>sample</b>	<b>Fitted position S=O, S-Cl (eV) [at%]</b>	<b>Fitted position SO<sub>3</sub><sup>2-</sup>/SO<sub>2</sub> (eV) [at%]</b>	<b>Fitted position S-N/ S-H (eV) [at%]</b>
PS	-	-	-
PS-SO <sub>2</sub> Cl	168.1 [93]	166.0 [3]	163.8 [4]
PS-COOH	168.2 [88]	166.3 [7]	164.0 [5]
PS-NH <sub>2</sub>	168.2 [87]	166.3 [10]	164.0 [3]
PS-alkene	168.2 [88]	166.3 [9]	164.1 [3]
PS-epoxy	168.5 [91]	166.4 [7]	164.2 [2]

<b>N 1s</b>		<b>Cl 2p<sub>3/2</sub></b>		
<b>Sample</b>	<b>Fitted position N-S (eV) [at%]</b>	<b>Fitted position N-H, C-N (eV) [at%]</b>	<b>Sample</b>	<b>Fitted position S-Cl 2p<sub>3/2</sub> (eV) [at%]</b>
PS	-	-	PS	-
PS-SO <sub>2</sub> Cl	402 [58]	400.1 [42]	PS-SO <sub>2</sub> Cl	200.6
PS-COOH	401.8 [10]	399.9 [90]	PS-COOH	200.4
PS-NH <sub>2</sub>	401.6 [9]	399.7 [91]	PS-NH <sub>2</sub>	200.2
PS-alkene	402 [12.7]	399.9 [87.3]	PS-alkene	200.3
PS-epoxy	402.1 [11.5]	400 [88.5]	PS-epoxy	200.5

Only carbon was detected on untreated PS and a small amount of oxygen probably due to some oxidation during the fabrication process. After chlorosulfonation we found a significant increase in oxygen, sulphur and chlorine that was consistent with the formation of SO<sub>2</sub>Cl groups. It was confirmed by the ratio O/S=1.5 and the high proportion of the S=O, S-Cl and SO<sub>3</sub><sup>2-</sup> bonds shown in Table 2 that agreed with previous work.<sup>42</sup> In the case of carboxylation, a notable amount of nitrogen was found as result of the sulphonamide group formation as well as the increase in S and O. The ratios S/N=2, O/N=4 and O/S=2 were higher than the theoretical ones and the presence of S and O was higher than that of N, which is related to the presence of SO<sub>3</sub><sup>2-</sup> groups that don't react with the amines. Moreover, the proportion of the bonds C-N, C=O, S=O and the low percentage of Cl confirmed the high degree of modification and is consistent with the results from the colorimetric studies. The aminated PS presented more Cl than the carboxylic ones due to the low reaction yield. This was also confirmed by the ratio S/N=4 and O/N=6 indicating the presence of unreacted SO<sub>2</sub>Cl. On the other hand, the peak positions and fitting of the N-H and S-N bonds demonstrated the presence of sulphonamide and amine groups in the sample. In the alkene PS we found a desirable ratio S/N=1, O/N=2 and O/S=2 that was consistent with a high yield in the formation of the

sulphonamide groups. These results confirmed the presence of C=C and C-N bonds. Finally, the epoxy PS presented a high amount of O and S compared to N and thus the ratio didn't match with the theoretical results. These data were explained by the presence of the oxidant meta-chloroperoxybenzoic acid (mCPBA). Complementary studies were carried out. 4-(Trifluoromethoxy)benzoic acid (TFMBA) interacts with epoxy groups but not with alkene groups therefore it was used to chemically derivatize epoxy groups and XPS analysis was performed to determine fluorine. In Table 4 the theoretical and experimental results for alkene and epoxy PS are compared. We can confirm from the ratio F/N=1.5 that the TFMBA only reacted with the epoxy groups from the epoxy PS and no significant amount of fluorine was detected in alkene PS.

**Table 4.** XPS results from the derivatization with TFMBA.

Sample	F (at%)	N (at%)	C (at%)	O (at%)	F/N theoretical	F/N experimental
PS-alkene	0.1	3.9	79.4	16.7	0	0.03
	0.2	5.6	76.5	17.7	0	0.04
	0.2	1.7	70.5	27.7	0	0.12
PS-epoxy	0.6	0.4	93.3	5.3	1.5	1.50
	0.7	0.4	93.7	5	1.5	1.75
	1.1	0.7	92.6	5.6	1.5	1.57

### 3.3. ELISA assays

In previous works it has been demonstrated that it is possible to chlorosulfonate and modify PS multiwell plates like those used for bioanalytical assays.<sup>41-43</sup> In the present work we have studied the effect of different PS chemistries on the attachment of antibodies for the improvement of commercial immunoassays. Considering the interaction between the antibodies and the surface one can distinguish between a direct covalent bond (chemisorption) or physical adsorption (physisorption). Even though covalent bonds are stronger and more stable than electrostatic interactions, the attachment of the antibodies to the surface will depend on its surface, which can vary among different antibodies.<sup>46,47</sup> In all cases the PS surface must undergo a first modification to introduce reactive groups for their further modification, which is achieved with the chlorosulfonation process. Subsequently, a double functional spacer is introduced to provide the final chemistry (amines, carboxylic acids, alkene, epoxy) as seen in Scheme 1. This spacer also allows to decrease the possible steric interactions between antibodies, maintaining their activity.

For the formation of a covalent bond between surface and antibody it is necessary to activate the functionalized PS surface prior to the reaction. In the case of amines we used the crosslinker disuccinimidyl suberate (DSS) in DMSO, for carboxylic acids, the well-known EDC/NHS protocol, and in the case of alkenes, we transformed the double bond into an epoxy group by using meta-chloroperoxybenzoic acid (mCPBA). The results of the immunoassays for the different substrates (PS, PS-SO<sub>2</sub>Cl, PS-COOH C3 0.1 M, PS-NH<sub>2</sub> C2 5M, PS-alkene, PS- epoxy) and the commercial kit are shown in Figure 2. The commercial kit has a detection limit of 2.5 ng mL<sup>-1</sup> and very good linearity in the range 0-100 ng mL<sup>-1</sup> ( $r^2=0.9994$ ). Even though aminated surfaces gave higher signals (red line), they also presented a higher detection limit (3.92 ng mL<sup>-1</sup>) and good linearity ( $r^2=0.9882$ ) in the same range. On the other hand, carboxylic (blue line) and epoxy (green line) surfaces showed higher limits of detection (8.20 and 44.50 ng mL<sup>-1</sup>, respectively) and non-linear behaviour in this range ( $r^2=0.9698$  and  $r^2=0.6148$ , respectively).

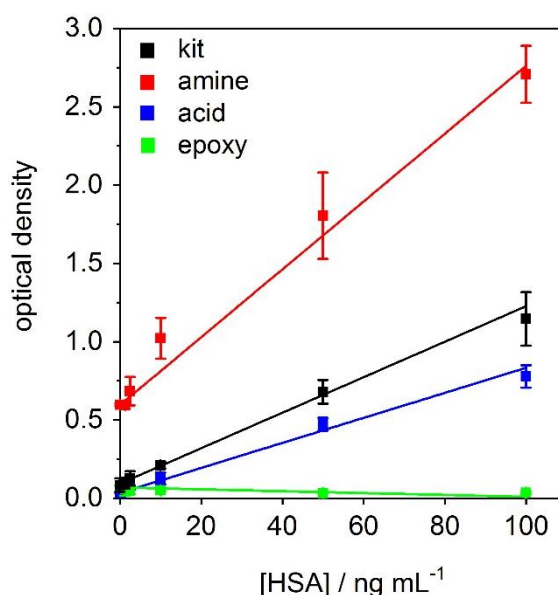


**Figure 2.** HSA ELISA results for covalent approach of PS-amine (red), PS-carboxylic (blue) and PS-epoxy (green) substrates compared to kit (black).

In order to study the direct interaction between the antibodies and the surface through a passive adsorption, no previous activation of the surface was needed. In this case we used amines, carboxylic acids and alkenes to modify the surface and put it in direct contact with the antibody. The results of the immunoassays for the different substrates and the commercial kit are shown in Figure 3. Aminated surfaces gave again higher signals (red line) and in this case with better detection limit (2.26 ng mL<sup>-1</sup>) than the commercial kit (black line) with similar linearity ( $r^2=0.9982$ ). Furthermore, alkene surfaces (green line) presented a higher detection limit (5.74 ng mL<sup>-1</sup>) and good linearity ( $r^2=0.9916$ ), and carboxylic surfaces (blue line) didn't

reach the kit signals giving a much higher detection limit ( $10.05 \text{ ng mL}^{-1}$ ) and lower linearity ( $r^2=0.9863$ ).

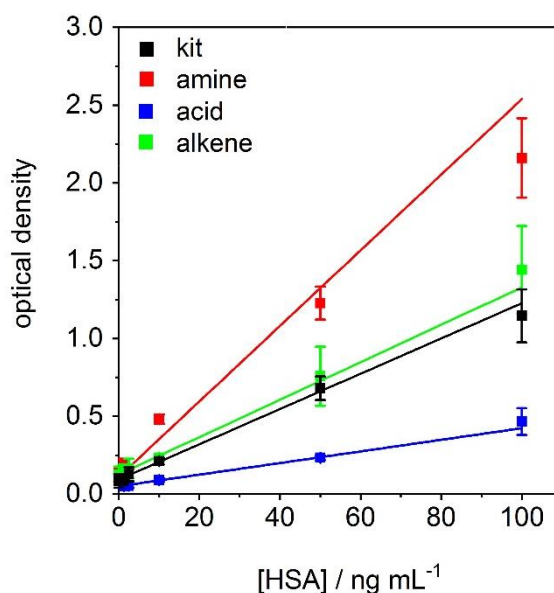


**Figure 3.** HSA ELISA results for passive adsorption approach of PS-amine (red), PS-carboxylic (blue) and PS-alkene (green) substrates compared to kit (black).

From these results we can conclude that the best results for this immunoassay are obtained with aminated surfaces. Moreover, the direct adsorption of the antibodies on the aminated surfaces presented a better detection limit and similar linearity than the commercial kit. We should also point out that the covalent approach gave worse results than the physical adsorption, what can be explained by the nature of the bond. Although covalent bonds are stronger, it implies the non-reversible link to the antibody, which can modify its structure and affect its functionality. In this case the covalent bond to the antibody alters its good performance and is not suitable for the immunoassay.

Considering the use of amines for the PS modification we studied the effect of the carbon chain length on the interaction between the surface and the antibody. First, we compared the two approaches previously mentioned: passive adsorption and covalent link between the antibodies and the surface aminated with ethylenediamine (C2) and hexamethylenediamine (C6). In Figure 4 we can see that the physical interaction of the antibodies with the non-activated surface gave better results than the covalent approach. With both amines we achieved lower detection limits,  $2.26$  and  $2.02 \text{ ng mL}^{-1}$  for C2 and C6, respectively, and good linearity ( $r^2=0.9922$  and  $r^2=0.9934$ , respectively). On the other hand, the activated surface didn't give good results neither for the detection limit ( $3.92$  and  $33.74 \text{ ng mL}^{-1}$  for C2 and C6, respectively) nor for the linearity ( $r^2=0.9882$  and  $r^2=0.6142$ , respectively). Finally, in Figure 5 we compared the effect of passive adsorption of the antibody on aminated surfaces with three

different amines: C2, C6 and 1,3-diaminopropane (C3). In all cases the aminated surfaces gave higher signals and lower detection limits (2.26, 1.27 and 2.02 ng mL<sup>-1</sup> for C2, C3 and C6, respectively) and good linearity for C2 and C6 ( $r^2=0.9982$  and  $r^2=0.9934$ , respectively) but not for C3 ( $r^2=0.9640$ ).

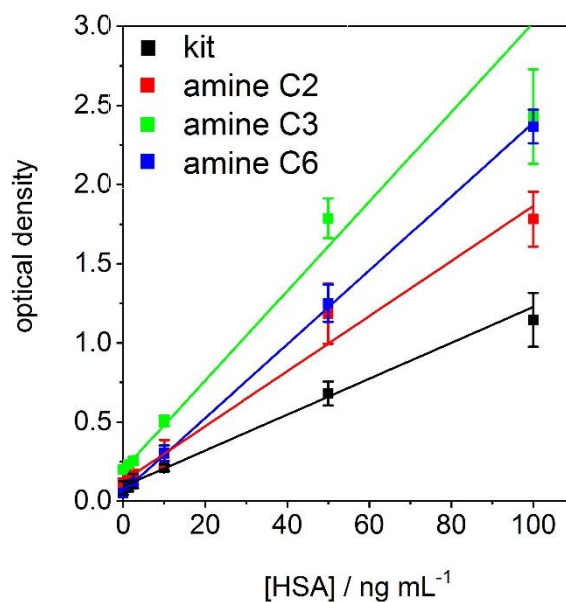


**Figure 4.** HSA ELISA results for covalent (dash) and passive adsorption (plain) approach of PS-aminated surfaces with amine C2 (red) and amine C6 (blue) compared to kit (black).

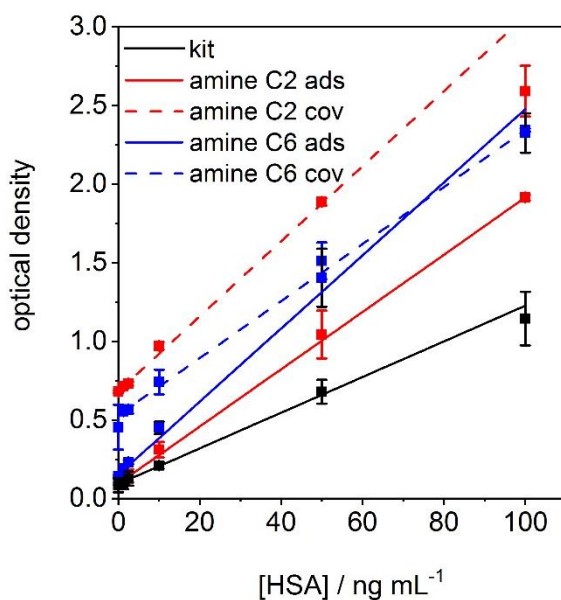


**Figure 5.** HSA ELISA results for passive adsorption approach of PS-aminated surfaces with amine C2 (red), amine C3 (green) and amine C6 (blue) compared to kit (black).

#### 4. Conclusion

The wet-chemical treatment proposed is a simple and economic procedure that provides transparent and stable substrates selectively modified with chlorosulfonic groups with a very high reactivity. Chlorosulfonated PS substrates can easily be converted into different functional groups leading to a wide library of chemistries. This procedure enables the fabrication of PS platforms for the rapid and easy screening of the best surface for bioanalytical applications. ELISA assays were carried out on different 96-well polystyrene plates modified with these chemistries, and two approaches were followed for the attachment of the antibodies. From the ELISA assays we can conclude that, for the commercial HSA kit, the antibodies interact preferably in a passive way with PS modified substrates. This means that the pre-treatment of the functional groups with crosslinkers for the covalent attachment doesn't improve the attachment of these antibodies to the surface. Nevertheless, the simple passive adsorption of the antibodies to the modified surfaces can improve the commercial kit for aminated PS. Varying the chain length of the amines doesn't change dramatically the detection limits of the immunoassays although the C3 aminated surface shows lower linearity than the rest of substrates.

Passive adsorption showed the best results when using aminated PS surfaces, giving better detection limits than the HSA commercial kit in the detection range 0-100 ng mL<sup>-1</sup>. These results show that the procedure can be applied to conventional materials used in bioanalysis giving the same or better characteristics.

#### References

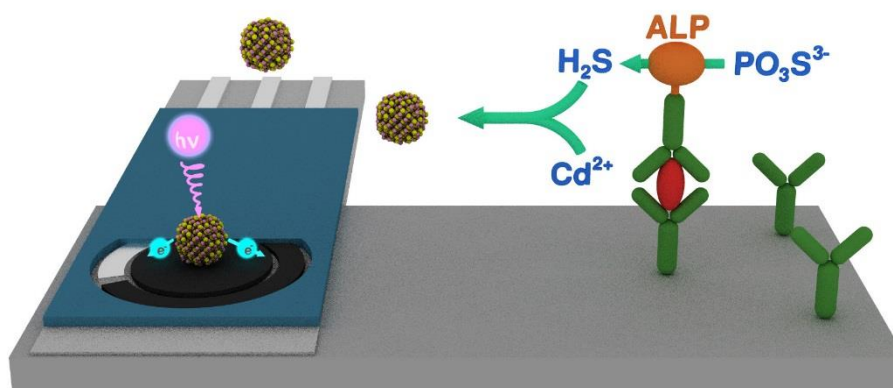
- (1) Nedela, O.; Slepicka, P.; Švorčík, V. Surface Modification of Polymer Substrates for Biomedical Applications. *Materials (Basel)*. **2017**, *10* (10), 1115.
- (2) *Functional Nanostructures: Processing, Characterization, and Applications*; Sudipta Seal, Ed.; Springer, 2008.
- (3) Raghavendra, G. M.; Varaprasad, K.; Jayaramudu, T. Biomaterials: Design, Development and Biomedical Applications. In *Nanotechnology Applications for Tissue Engineering*; Elsevier Inc., 2015; pp 21–44.
- (4) García, A. J. Surface Modification of Biomaterials. In *Principles of Regenerative Medicine*; Rachel Williams, Ed.; 2011; pp 663–673.
- (5) Bacakova, L.; Filova, E.; Parizek, M.; Ruml, T.; Svorcik, V. Modulation of Cell Adhesion, Proliferation and Differentiation on Materials Designed for Body Implants. *Biotechnol. Adv.* **2011**, *29* (6), 739–767.
- (6) Roach, P.; Eglin, D.; Rohde, K.; Perry, C. C. Modern Biomaterials: A Review - Bulk Properties and Implications of Surface Modifications. *J. Mater. Sci. Mater. Med.* **2007**, *18* (7), 1263–1277.



- (7) Griffith, L. G. Polymeric Biomaterials. *Acta Mater.* **2000**, *48* (1), 263–277.
- (8) He, W.; Benson, R. Polymeric Biomaterials. In *Applied Plastics Engineering Handbook*; Kutz, M., Ed.; Elsevier Inc., 2017; pp 145–164.
- (9) Maitz, M. F. Applications of Synthetic Polymers in Clinical Medicine. *Biosurface and Biotribology* **2015**, *1* (3), 161–176.
- (10) Hetemi, D.; Pinson, J. Surface Functionalisation of Polymers. *Chem. Soc. Rev.* **2017**, *46* (19), 5701–5713.
- (11) Zhao, W.; Liu, L.; Zhang, F.; Leng, J.; Liu, Y. Shape Memory Polymers and Their Composites in Biomedical Applications. *Mater. Sci. Eng. C* **2019**, *97* (December 2017), 864–883.
- (12) Shastri, V. P.; Lendlein, A. Materials in Regenerative Medicine. *Adv. Mater.* **2009**, *21* (32–33), 3231–3234.
- (13) Lendlein, A.; Behl, M.; Hiebl, B.; Wischke, C. Shape-Memory Polymers as a Technology Platform for Biomedical Applications. *Expert Rev. Med. Devices* **2010**, *7* (3), 357–379.
- (14) Rezwani, K.; Chen, Q. Z.; Blaker, J. J.; Boccaccini, A. R. Biodegradable and Bioactive Porous Polymer/Inorganic Composite Scaffolds for Bone Tissue Engineering. *Biomaterials* **2006**, *27* (18), 3413–3431.
- (15) Mikes, P.; Horakova, J.; Saman, A.; Vejsadova, L.; Topham, P.; Punyodom, W.; Dumklang, M.; Jencova, V. Comparison and Characterization of Different Polyester Nano/Micro Fibres for Use in Tissue Engineering Applications. *J. Ind. Text.* **2019**, 152808371984815.
- (16) Zhang, S.; Demir, B.; Ren, X.; Worley, S. D.; Broughton, R. M.; Huang, T. S. Synthesis of Antibacterial N-Halamine Acryl Acid Copolymers and Their Application onto Cotton. *J. Appl. Polym. Sci.* **2019**, *136* (16), 1–8.
- (17) Enescu, D. Use of Chitosan in Surface Modification of Textile Materials. *Roum. Biotechnol. Lett.* **2008**, *13* (6), 4037–4048.
- (18) Hanušová, K.; Vápenka, L.; Dobiáš, J.; Mišková, L. Development of Antimicrobial Packaging Materials with Immobilized Glucose Oxidase and Lysozyme. *Cent. Eur. J. Chem.* **2013**, *11* (7), 1066–1078.
- (19) Musetti, A.; Paderni, K.; Fabbri, P.; Pulvirenti, A.; Al-Moghazy, M.; Fava, P. Poly(Vinyl Alcohol)-Based Film Potentially Suitable for Antimicrobial Packaging Applications. *J. Food Sci.* **2014**, *79* (4).
- (20) Marasso, S. L.; Puliafito, A.; Mombello, D.; Benetto, S.; Primo, L.; Bussolino, F.; Pirri, C. F.; Cocuzza, M. Optimized Design and Fabrication of a Microfluidic Platform to Study Single Cells and Multicellular Aggregates in 3D. *Microfluid. Nanofluidics* **2017**, *21* (2), 1–14.
- (21) Manju.Gerard; Ashab.Choubey; B.D.Malhotra. Review: Application of Conducting Polymer to Biosensors. *Biosens. Bioelectron.* **2001**, *17*, 345–359.
- (22) Dhand, C.; Das, M.; Datta, M.; Malhotra, B. D. Recent Advances in Polyaniline Based Biosensors. *Biosens. Bioelectron.* **2011**, *26* (6), 2811–2821.
- (23) Kavetsky, T.; Smutok, O.; Demkiv, O.; Kasetaitė, S.; Ostrauskaite, J.; Švajdlenková, H.; Šauša, O.; Zubrytska, K.; Hoivanovych, N.; Gonchar, M. Dependence of Operational Parameters of Laccase-Based Biosensors on Structure of Photocross-Linked Polymers as Holding Matrixes. *Eur. Polym. J.* **2019**, *115* (March), 391–398.
- (24) Loo, J. F. C.; Ho, A. H. P.; Turner, A. P. F.; Mak, W. C. Integrated Printed Microfluidic Biosensors. *Trends Biotechnol.* **2019**.
- (25) Cho, S. J.; Noh, H. B.; Won, M. S.; Cho, C. H.; Kim, K. B.; Shim, Y. B. A Selective Glucose Sensor Based on Direct Oxidation on a Bimetal Catalyst with a Molecular Imprinted Polymer. *Biosens. Bioelectron.* **2018**, *99* (August 2017), 471–478.
- (26) Semerádtová, A.; Štofík, M.; Neděla, O.; Staněk, O.; Slepíčka, P.; Kolská, Z.; Malý, J. A Simple Approach for Fabrication of Optical Affinity-Based Bioanalytical Microsystem on Polymeric PEN Foils. *Colloids Surfaces B Biointerfaces* **2018**, *165*, 28–36.
- (27) Slepíčka, P.; Siegel, J.; Lyutakov, O.; Slepíčková Kasálková, N.; Kolská, Z.; Bačáková, L.; Švorčík, V. Polymer Nanostructures for Bioapplications Induced by Laser Treatment.

- Biotechnol. Adv.* **2018**, *36* (3), 839–855.
- (28) Palacios-Cuesta, M.; Cortajarena, A. L.; García, O.; Rodríguez-Hernández, J. Versatile Functional Microstructured Polystyrene-Based Platforms for Protein Patterning and Recognition. *Biomacromolecules* **2013**, *14* (9), 3147–3154.
- (29) An, S.; Lim, J.; Choi, D.; Hong, H.; Kim, H. W.; Park, S. M.; Rhie, J. W.; Kim, D. S. Fabrication of Polystyrene-Based Multi-Well Screening Platform for Micrometer-Scale Surface Topographies Promoting Stem Cell Functions. *Microelectron. Eng.* **2017**, *174*, 28–34.
- (30) Dou, M.; Sanjay, S. T.; Benhabib, M.; Xu, F.; Li, X. J. Low-Cost Bioanalysis on Paper-Based and Its Hybrid Microfluidic Platforms. *Talanta* **2015**, *145*, 43–54.
- (31) Sai, N.; Sun, W.; Wu, Y.; Sun, Z.; Yu, G.; Huang, G. A Highly Sensitive Immunoassay for Atrazine Based on Covalently Linking the Small Molecule Hapten to a Urea–glutaraldehyde Network on a Polystyrene Surface. *Int. Immunopharmacol.* **2016**, *40*, 480–486.
- (32) Bax, D. V.; Tipa, R. S.; Kondyurin, A.; Higgins, M. J.; Tsoutas, K.; Gelmi, A.; Wallace, G. G.; McKenzie, D. R.; Weiss, A. S.; Bilek, M. M. M. Cell Patterning via Linker-Free Protein Functionalization of an Organic Conducting Polymer (Polypyrrole) Electrode. *Acta Biomater.* **2012**, *8* (7), 2538–2548.
- (33) Zhang, Y.; Chai, C.; Jiang, X. S.; Teoh, S. H.; Leong, K. W. Fibronectin Immobilized by Covalent Conjugation or Physical Adsorption Shows Different Bioactivity on Aminated-PET. *Mater. Sci. Eng. C* **2007**, *27* (2), 213–219.
- (34) Hermanson, G. T. (Strept)Avidin–Biotin Systems. In *Bioconjugate Techniques*; 2013; pp 465–505.
- (35) Zhang, D.; Dougal, S. M.; Yeganeh, M. S. Effects of UV Irradiation and Plasma Treatment on a Polystyrene Surface Studied by IR–Visible Sum Frequency Generation Spectroscopy. *Langmuir* **2000**, No. 9, 4528–4532.
- (36) Ko, Y. G.; Kim, Y. H.; Park, K. D.; Lee, H. J.; Lee, W. K.; Park, H. D.; Kim, S. H.; Lee, G. S.; Ahn, D. J. Immobilization of Poly(Ethylene Glycol) or Its Sulfonate onto Polymer Surfaces by Ozone Oxidation. *Biomaterials* **2001**, *22* (15), 2115–2123.
- (37) Yang, R.; He, Q.; Wang, C.; Sun, S. Surface Modification of Polystyrene Microsphere Using Ozone Treatment. *Ferroelectrics* **2018**, *530* (1), 130–135.
- (38) Luo, H. L.; Sheng, J.; Wan, Y. Z. Plasma Polymerization of Styrene with Carbon Dioxide under Glow Discharge Conditions. *Appl. Surf. Sci.* **2007**, *253* (12), 5203–5207.
- (39) Sakti, S. P.; Khusnah, N. F.; Santjojo, D. J. D. H.; Masrurah; Sabarudin, A. Surface Modification of Polystyrene Coating on QCM Sensor Using Ambient Air Plasma at Low Pressure. *Mater. Today Proc.* **2018**, *5* (7), 15149–15154.
- (40) Morra, M.; Cassinelli, C.; Cascardo, G.; Nagel, M. D.; Della Volpe, C.; Siboni, S.; Maniglio, D.; Brugnara, M.; Ceccone, G.; Schols, H. A.; et al. Effects on Interfacial Properties and Cell Adhesion of Surface Modification by Pectic Hairy Regions. *Biomacromolecules* **2004**, *5* (6), 2094–2104.
- (41) Foerch, R.; McIntyre, N. S.; Sodhi, R. N. S.; Hunter, D. H. Nitrogen Plasma Treatment of Polyethylene and Polystyrene in a Remote Plasma Reactor. *J. Appl. Polym. Sci.* **1990**, *40* (11–12), 1903–1915.
- (42) Del Prado, A.; Briz, N.; Navarro, R.; Pérez, M.; Gallardo, A.; Reinecke, H. Transparent Polystyrene Substrates with Controllable Surface Chlorosulfonation: Stable, Versatile, and Water-Compatible Precursors for Functionalization. *Macromolecules* **2012**, *45* (6), 2648–2653.
- (43) Del Prado, A.; Briz, N.; Navarro, R.; Pérez, M.; Gallardo, A.; Reinecke, H. Chlorosulfonation of Polystyrene Substrates for Bioanalytical Assays: Distribution of Activated Groups at the Surface. *Analyst* **2012**, *137* (23), 5666–5671.
- (44) Del Prado, A.; Briz, N.; Navarro, R.; Pérez, M.; Gallardo, A.; Reinecke, H. Distribution of Chlorosulfonyl Groups in the Subsurface of Polystyrene Substrates. Analysis by Means of

- Vibrational Spectroscopy. *Vib. Spectrosc.* **2013**, *66*, 14–18.
- (45) Jeon, S. I.; Chung, I. J.; Ahn, C.-H. Surface Modification of Polystyrene Beads with Sulfonamide Derivatives and Application to Water Softening System. *Macromol. Res.* **2019**.
- (46) Kang, E. T.; Tan, K. L.; Kato, K.; Uyama, Y.; Ikada, Y. Surface Modification and Functionalization of Electroactive Polymer Films. *Macromolecules* **1996**, *29* (21), 6872–6879.
- (47) Hamerli, P.; Weigel, T.; Groth, T.; Paul, D. Surface Properties of and Cell Adhesion onto Allylamine-Plasma-Coated Polyethyleneterephthalat Membranes. *Biomaterials* **2003**, *24* (22), 3989–3999.
- (48) Shen, M.; Rusling, J. F.; Dixit, C. K. Site-Selective Orientated Immobilization of Antibodies and Conjugates for Immunodiagnosics Development. *Methods* **2017**, *116*, 95–111.
- (49) Kausaite-Minkstimiene, A.; Ramanaviciene, A.; Kirlyte, J.; Ramanavicius, A. Comparative Study of Random and Oriented Antibody Immobilization Techniques on the Binding Capacity of Immunosensor. *Anal. Chem.* **2010**, *82* (15), 6401–6408.
- (50) Hermanson, G. T. Chapter 24 - Bioconjugation in the Study of Protein Interactions. In *Bioconjugate Techniques*; Hermanson, G. T. B. T.-B. T. (Third E., Ed.; Academic Press: Boston, 2013; pp 989–1016.
- (51) Hermanson, G. T. Chapter 4 - Zero-Length Crosslinkers. In *Bioconjugate Techniques*; Hermanson, G. T. B. T.-B. T. (Third E., Ed.; Academic Press: Boston, 2013; pp 259–273.



## DESIGN OF A PHOTOELECTROCHEMICAL LAB-ON-A-CHIP IMMUNOSENSOR BASED ON ENZYMATIC PRODUCTION OF QUANTUM DOTS IN SITU

In this work we report the development and validation of a photoelectrochemical biosensor on the basis of alkaline phosphatase (ALP)-linked immunoassay for the detection of Human Serum Albumin as a model analyte. In this method, the antibodies are well orderly orientated on aminated polystyrene via physical adsorption. After the interaction with the analyte, ALP immobilised on surface through the sandwich immunoassay catalyses the hydrolysis of sodium thiophosphate (TP) to hydrogen sulphide ( $\text{H}_2\text{S}$ ) which in presence of cadmium ions yields CdS QDs. The current is generated in the photoelectrochemical process (PEC) during irradiation of the CdS QDs with UV LED (365 nm) on home-made screen-printed carbon electrodes modified with a conductive polymer. Reaction time, steps and volumes were optimized for the miniaturization of the process in order to develop a lab-on-a-chip platform. Microfluidics were design with optimised parameters for the immunoassay and PEC detection. The final system presents a sensitivity comparable to the commercial kit thanks to the signal amplification enabled by the enzymatic growth of CdS QDs in situ. This photoelectrochemical immunosensing strategy potentially opens a new avenue for detection of a wide range of analytes of interest due to the universal and effective enzymatic signal amplification method. Moreover, the developed protocol allows for a great reduction of time and reagents compared to current commercial assays, making it suitable for point-of-care applications.

---

The work presented is in preparation: Díez-Buitrago, B.; Fernández-SanArgimiro, F. J.; Lorenzo, L.; Bijelic, G.; Briz, N.; Pavlov, V.

## 1. Introduction

In the last decades the need of cheap, fast, and easy to use analytical tools have increased attention to the development of portable biosensors for the qualitative and quantitative determination of different analytes in environmental, clinical, agricultural, food, and security and defence applications.<sup>1-3</sup> Biosensors have gained much interest because of their features that provide high sensitivity, specificity, ease for integration with other devices and portability for utilization at point of use. Among the different biosensors on the market, immunosensors have demonstrated to be a valuable tool for rapid detection of a wide variety of target analytes with enhanced sensitivity and selectivity.<sup>1,4-6</sup> Despite the large amount of immunoassays developed in research laboratories, portable and miniaturized devices for rapid detection have not been successfully introduced in the market. The complexity of the process and the need of expensive detectors hinder their integration in portable devices and encourage the seek for new alternatives to address those drawbacks.

Immunosensors are based on the specific interaction between the antibody and the corresponded antigen leading to the formation of a stable complex. Transduction of biorecognition event results in a change of some physical property that can be transformed into a measurable electric signal. Depending on the transducer and the detector, the immunosensors can use optical, thermal, piezoelectric or electrochemical transduction. Electrochemical biosensors have been the most successfully and widely used in biomedical field and most areas of analytical chemistry due to their simplicity, short response time, easiness to miniaturize and relatively low cost.<sup>6,7</sup> Moreover, the biological recognition process provides high sensitivity and selectivity. Electrochemical biosensors offer some advantages over classical optical techniques such as the ability to directly perform electrical signal processing, higher signal-to-noise ratio, elimination of optical interferences and no need of expensive external equipment.<sup>8</sup> Consequently, electrochemical transducers are suitable for construction of on-site detection devices. Photoelectrochemistry (PEC) is a promising technique that has gradually become a widespread analytical technique for biological assays. PEC offers the inherent high sensitivity of electrochemical procedures and the possibility of signal amplification with the suppression of the background signal thanks to the independent optical input signal and electrochemical output signal.<sup>9,10</sup> So far, most of PEC immunoassays based on the amplified signal strategy are enzyme-labelled immunoassays.<sup>11,12</sup> In these procedures the detection antibody is labelled with a natural enzyme such as HRP<sup>13,14</sup> or ALP<sup>15</sup>

that are able to catalyze the formation of a particular product that is subsequently used to trigger the PEC response.

The combination of signal amplification strategies with electrochemical methods (e.g., PEC) has recently gained considerable interest because it allows to develop high-performance analytical tools for the ultrasensitive detection of trace amounts of a wide variety of analytes. Currently, point-of-use devices are compact systems with a performance comparable with that of the laboratory tests which can be utilized by users without technical background. Furthermore, some requirements such as portability and automatization are essential in the design of new systems. The combination of microfluidic systems with biosensing devices resulted in advent of laboratory-on-a-chip (LOC) technology has demonstrated to be a key strategy to meet most of analytical needs.<sup>2,16</sup> The integration of biosensors with microfluidic systems yields cost-effective miniaturized devices which are easy to handle. Miniaturization reduces volumes, dimensions and response time achieving better sensibilities and allowing the possible detection of different analytes with the same platform. The movement of fluidics can be precisely controlled electronically by pumps, valves or mixers<sup>17</sup> through a software, or manually by using syringes or blisters.<sup>18</sup> Miniaturization also makes the system more cost-effective because it utilizes batch fabrication manufacturing processes and requires only small volumes of potentially expensive reagents. Additionally, screen-printing methods provide a cost-effective and easy to scale technology to convert electrochemical biosensors into point-of-care devices.<sup>19-21</sup>

The aim of this work is to design, fabricate, characterize and validate an integrated platform for the development of a photoelectrochemical immunosensor. The proposed system is based on the enzymatic growth of CdS QDs in situ and their subsequent photoelectrochemical detection on a screen-printed carbon electrode. The immunoassay was optimised by ordered immobilization of antibodies on aminated polystyrene, reduction of the reaction steps, incubation time and injected volumes. The amplification of signal was achieved with the photoelectrochemical procedure coupled to the enzymatic reaction of the immunoassay. Moreover, we designed and fabricated the screen-printed carbon electrodes and integrated them into the microfluidic system. The presented device showed a good performance and a sensitivity comparable to that of a commercial kit for Human Serum Albumin ELISA assay. Finally, it is important to highlight the great advantage that this system presents due to the possibility to apply it to any kind of immunoassay employing enzymatic amplification based on ALP.

## 2. Materials and methods

### 2.1. Materials

Alkaline phosphatase (ALP) from bovine intestinal mucosa, magnesium chloride ( $\text{MgCl}_2$ ), sodium thiophosphate (TP), cadmium nitrate ( $\text{Cd}(\text{NO}_3)_2$ ), 1-thioglycerol (TG), Trizma<sup>®</sup> base and hydrochloridric acid (HCl) were obtained from Sigma. All water used was Mili-Q ultrapure grade. The electroconductive polymer was obtained by interaction of poly(vinylpyridine) with osmium ions (Os-PVP) according to the literature procedure.<sup>22</sup> Chlorosulfonic acid ( $\text{HClSO}_3$ ) and sulfuric acid ( $\text{H}_2\text{SO}_4$ ) were acquired from Panreac. Polystyrene 96-well plates were purchased from Falcon. Transparent polystyrene sheets of 190  $\mu\text{m}$  and 1.2 mm thickness were purchased from GoodFellow (England). Conductive inks and insulating paste were acquired from Henkel and the adhesive from KIWO, Inc. The Human Serum Albumin detection ELISA set was purchased from R&D Systems.

### 2.2. Apparatus

Absorbance measurements were performed on a Synergy H1 microplate reader (BioTek) using transparent microwell plates at room temperature. Fluorescence measurements were performed on a Varioskan Flash microplate reader (Thermo Scientific) using black microwell plates at room temperature. The system was controlled by the SkanIt Software 2.4.3. RE for Varioskan Flash. The electrochemical tests were performed on an Autolab Electrochemical Workstation (model PGSTAT204, Metrohm Autolab, The Netherlands) furnished with NOVA 2.1 software. Disposable screen-printed carbon electrodes (SPCEs) were purchased from DropSens (model DRP-110). Scanning Electron Microscopy (SEM) images were recorded in a FEG (Field Emission Gun) ESEM (Quanta 250, FEI), operated in the low vacuum mode. The beam voltage was set to 10 kV, the spot size was 5. Three different UV light source were employed: a compact UV illuminator Model UVLM-28 from EL Series UVB Lamp and two LED from Kingbright (ATS2012UV365 and ATDS3534UV365B).

### 2.3. Methods

#### 2.3.1. Enzymatic assay

Various amounts of ALP were incubated with TP 0.5 mM in tris-HCl buffer (50 mM, pH 9) containing  $\text{MgCl}_2$  (1 mM). After that,  $\text{Cd}(\text{NO}_3)_2$  (2.5 mM) and TG (20 mM) were added to the samples. Finally, fluorescence or photoelectrochemical response were recorded.

### 2.3.2. Chlorosulfonation and modification of polystyrene substrates

The chlorosulfonation procedure was carried out following a previously developed protocol.<sup>24–26</sup> In a thermostatable reactor polystyrene films of 1 mm were immersed in chlorosulfonic acid at -10 °C. After 20 min the samples were taken out and washed with cold (-10 °C) concentrated sulfuric acid. Finally, they were washed in an ice/water mixture and dried at room temperature. Afterwards, chlorosulfonated substrates were brought into contact with aqueous diamine solution 5 M and reacted for 20 min at room temperature. After that, they were rinsed with water and dried at room temperature.

### 2.3.3. Electrode printing

The electrodes were printed on the aminated polystyrene by a screen-printing technique. Silver/silver chloride ink (LOCTITE EDAG 965SS E&C) was used for vias, interconnections and the pseudo-reference electrode ( $E_{ref}$ ), carbon ink (LOCTITE EDAG 965SS E&C) was used for the working and counter electrodes ( $E_w$  and  $E_c$ , respectively). Initially, the silver paste was printed onto the substrate and dried at 80 °C for 40 min. Afterwards, the carbon ink was printed with the shape of the respective electrodes and dried at 80 °C for 40 min. This step was repeated for 3-5 times depending on the substrate. Finally, the connections were covered with an insulating layer leaving the active area of electrons accessible.

### 2.3.4. Immunoassay

A Human Serum Albumin (HSA) set was used to evaluate the bioanalytical performance of the system. Aminated polystyrene substrate was used as platform for the immunoassay and the bioassay was carried out following the protocol of the kit. The sandwich ELISA was coupled to enzymatic reaction catalysed by ALP resulting in formation of CdS QDs detected by PEC.

### 2.3.5. Photoelectrochemical detection

Before beginning the PEC assays, the SPCEs were cleaned by cyclic voltammetry (CV) in a potential range from 0 to 0.6 V at 50 mV s<sup>-1</sup> in citrate-phosphate buffer (pH 7.5). After that, Os-PVP polymer (40 µL drop of 2 mg mL<sup>-1</sup>) was electrodeposited by CV scanning (2 cycles at scan rate of 50 mV s<sup>-1</sup> and a potential range from 0 to 0.6 V).<sup>23,27</sup> Finally, the modified SPCEs were rinsed with water and dried under argon atmosphere. For PEC measurements, a 40 µL drop of sample was deposited on SPCEs surface and illuminated with a UV light emitting at 365 nm while applying a constant potential of 0.3 V vs. Ag/AgCl. For PEC measurements with the chip, UV light was irradiated to the channels with a powerful UV LED at 365 nm.



### 3. Results and discussion

#### 3.1. Characterization of screen-printed carbon electrodes

The investigation of electrode surface texture was carried out using scanning electron microscopy (SEM) to evaluate the electrode surface effects on electrochemical response. Commercial SPCEs presented a uniform carbon layer with numerous fractures that may be due to the application of high temperature and time during the curing of the ink (Figure 1A and 1D). Defects and cracks increase edge plane effect on the graphite surface with faster electrochemical reaction rate, which results in larger electron transfer.<sup>28</sup> Home-made SPCE (190  $\mu\text{m}$  and 1.2 mm thick) showed a rough structure with some gaps throughout the surface (Figure 1B, 1E and Figure 1C, 1F, respectively) typical from unpolished electrodes.<sup>29</sup> This supports the increase of electrode active surface area and thus the higher current peak recorded (Figure 2).

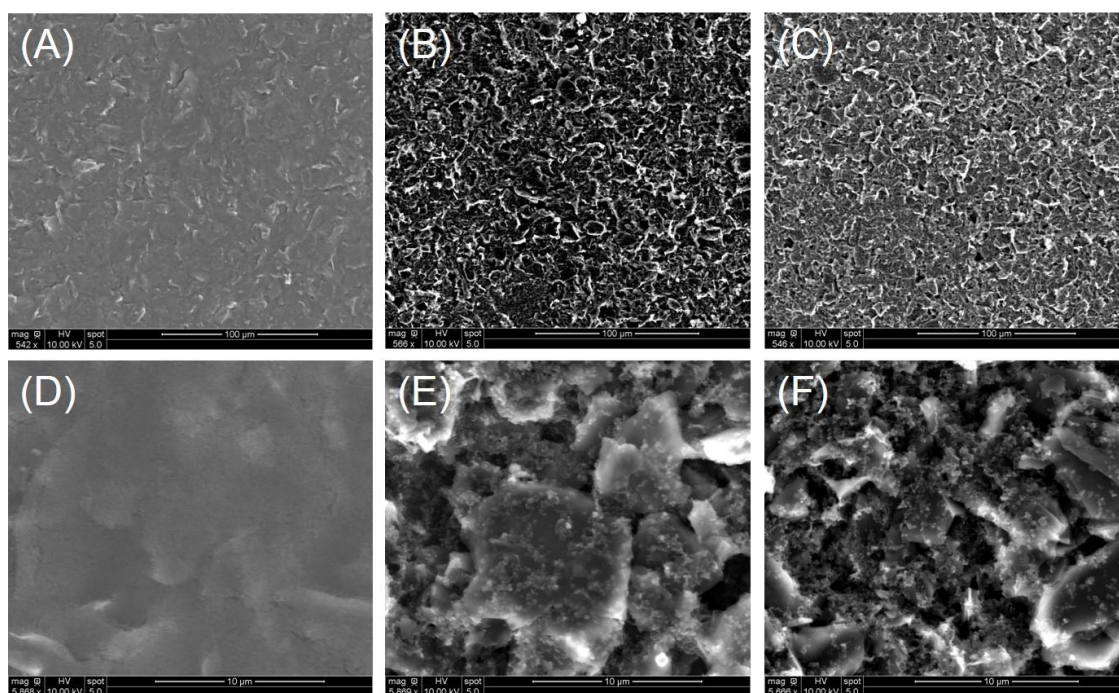


**Figure 1.** SEM images of commercial SPCE (A, D), home-made SPCE on PS 190  $\mu\text{m}$  (B, E) and PS 1.2 mm (C, F) with a magnification of 500x and 6000x, respectively.

The ferri/ferrocyanide redox couple was the redox system used for comparing the voltammetric behaviour of screen-printed electrodes. A comparison of cyclic voltammograms are presented in Figure 2. Resulting shapes of presented cyclic voltammograms obtained on SPCEs on polystyrene substrates are very similar to those recorded with a commercial SPCE.

Moreover, they exhibited a reversible behaviour towards the redox couple with an oxidation and reduction peaks well resolved and stable during at least 10 cycles (data not shown).

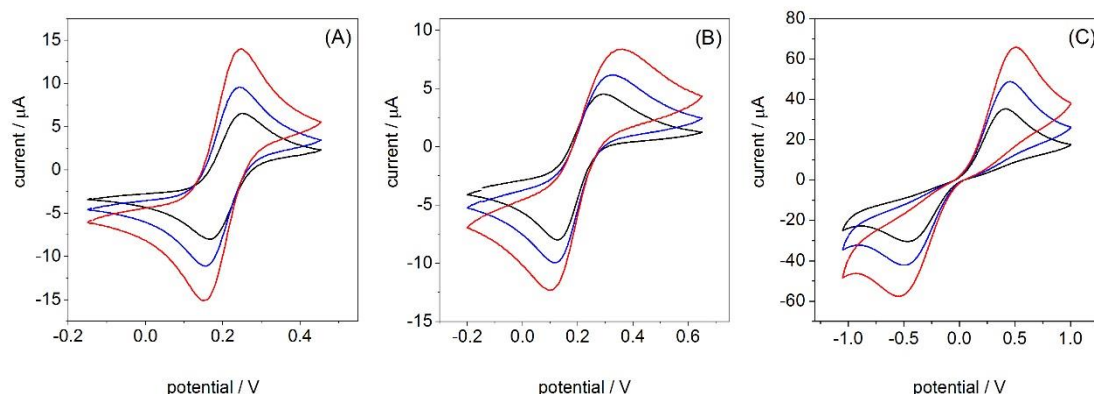


**Figure 2.** Cyclic voltammograms of (A) commercial SPCE, (B) home-made SPCE on PS 190  $\mu\text{m}$  and (C) home-made SPCE on PS 1.2 mm in presence of potassium ferro/ferrihexacyanide 5 mM in PB 10 mM pH 7.4, scan rate 50  $\text{mV s}^{-1}$  (black), 100  $\text{mV s}^{-1}$  (blue) and 200  $\text{mV s}^{-1}$  (red).

In Table 1, peak separations increased from 76 mV for commercial SPCE, 156 mV for carbon electrodes screen-printed on PS 190  $\mu\text{m}$  and 821 mV for those screen-printed on PS 1.2 mm, at scan rates ranging from 50 to 200  $\text{mV s}^{-1}$ . In all cases,  $\Delta E_p$  were higher than 59 mV, expected for the Nernstian one-electron transfer. These results are typical for the heterogeneous process at the electrode materials caused by slower kinetics of partial electrode reactions. Nevertheless, the ratio anodic/cathodic peak current ( $I_{\text{ox}}/I_{\text{red}}$ ) was always close to 1.

**Table 1.** Comparison of various carbon electrodes with potassium ferro/ferrihexacyanide redox couple.

Electrode	Scan rate / $\text{mV s}^{-1}$	$\Delta E_p$ / mV	$I_{\text{ox}}/I_{\text{red}}$
PS 190 $\mu\text{m}$	50	156	0.86
	100	181	0.85
	200	217	0.83
PS 1.2 mm	50	821	1.42
	100	871	1.41
	200	957	1.39
Commercial	50	76	0.92
	100	81	0.92
	200	81	0.91

A scan rate study of each electrode was done for further characterization (Table 2). Scan rate was varied from 50 to 200  $\text{mV s}^{-1}$  and cyclic voltammograms were recorded (Figure 2). For all the electrodes a straight line was obtained on the plot of the peak currents vs. the square root of the scan rate. This linear relationship between the peak current density (both anodic and cathodic) and the square root of the scan rate demonstrated that the process was diffusion

controlled. Parameters of the individual equations of the linear regressions ( $k$ : slope;  $q$ : intercept) with corresponding correlation coefficient ( $R^2$ ) are represented in Table 2.

**Table 2.** Parameters of equations obtained at various carbon electrodes under scan rate study.

Electrode	anodic			cathodic		
	$k$ $\text{mA cm}^{-2} / \text{mV}^{1/2} \text{ s}^{-1/2}$	$q$ $\text{mA cm}^{-2}$	$R^2$	$k$ $\text{mA cm}^{-2} / \text{mV}^{1/2} \text{ s}^{-1/2}$	$q$ $\text{mA cm}^{-2}$	$R^2$
PS 190 $\mu\text{m}$	0.376	3.050	0.992	0.484	3.215	0.993
PS 1 mm	2.441	11.743	0.998	1.676	9.210	0.990
Commercial	0.927	0.519	0.999	1.028	0.418	0.999

### 3.2. Optimization of experimental conditions

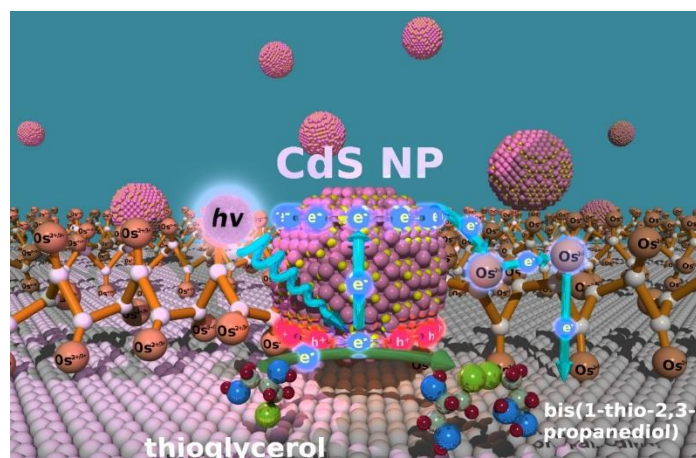
In order to adapt the studied system to the development of a miniaturized device some requirements must be fulfilled. Final volume, reagent concentration, incubation and reaction times should be optimized because they define the sensitivity and are the most important parameters to consider for miniaturization of the system. To produce fast and reliable device we optimised parameters regarding the photoelectrochemical detection (enzymatic reaction) and the immunoassay process with the aim of reducing time and volumes for further application in the miniaturized device.

#### 3.2.1. Enzymatic reaction

Bovine ALP is widely used in bioanalysis as an enzymatic label in ELISA processes. ALP activity is routinely estimated by optical methods by using colorimetric substrates such as pNPP and fluorogenic ones like 4-methylumbelliferyl phosphate (4-MUP) coupled to expensive UV-vis or fluorogenic readers.<sup>30,31</sup> In this work, a standard potentiostat was used to detect the enzymatic activity by measuring the photoelectrochemical signal.

The mechanism of our enzymatic assay is based on biocatalytic hydrolysis of TP by ALP to orthophosphate ( $\text{PO}_4^{3-}$ ) and  $\text{H}_2\text{S}$ . The latter reacts instantly with  $\text{Cd}^{2+}$  cations in Tris-HCl buffer generating CdS QDs stabilized by the buffer solution Trizma® base. The amount of resulting CdS QDs is quantified photoelectrochemically by using modified carbon electrodes and a UV-illuminator source (Scheme 1). Carbon electrodes are modified with a conducting osmium polymer that “wires” the CdS QDs to the surface of the electrode when applying a positive voltage. PEC signal is recorded after the application of 0.3 V (vs. pseudo reference electrode of Ag/AgCl) for 200 s and UV irradiation (365 nm) in presence of TG that acts as redox mediator

generating an electron flow through the CdS NPs to Os-PVP complexes and finally, the electrode.



**Scheme 1.** Detection of CdS QDs On screen-printed carbon electrode modified with an osmium polymer under UV irradiation.

The influence of the incubation temperature on the enzymatic activity is shown in Figure 3A. The growth in photocurrent is directly related to the increase in the concentration of the enzyme in the studied range. According to PEC measurements, the activity of the enzyme is almost the same at room temperature (RT) and at 37 °C. We decided to continue experiments at RT because portable and point of care devices should be able to work at ambient conditions to simplify the operation of the device. We also evaluated the effect of different reaction volumes on the system response. The volume of the reaction mixture is an important parameter for adaptation of the enzymatic process to a microfluidic system regarding the homogeneity of the reaction mixture in terms of diffusion of reagents. The enzymatic production of CdS NPs was carried out at two different reaction volumes of 100 and 50  $\mu\text{L}$  (Figure 3B). At these volumes the assay demonstrated a linear response up to 100  $\mu\text{g mL}^{-1}$  of ALP and detection limits of 28 and 14  $\mu\text{g mL}^{-1}$  for 100 and 50  $\mu\text{L}$ , respectively, at a signal-to-noise ratio of 3 ( $S/N=3$ ). The decrease in volume to 50  $\mu\text{L}$  improved the limit of detection by two times showing the same linearity as the process carried out in a volume of 100  $\mu\text{L}$ . These results confirmed the improvement of the analytical properties by reducing the reaction volume making it suitable for the integration into a microfluidic system. Then, the dependence of the photocurrent response on the varying enzyme concentrations was studied. In ELISA experiments the amount of the captured enzyme is usually very low, so a high signal/enzyme ratio is desired. In Figure 3C it can be seen that a diminution of the PEC signal is observed when the enzyme concentration is decreased. Nevertheless, the linear response was still maintained as well as the detection limit, so we concluded that this system could be used with small amounts of enzyme needed for the immunoassay. Finally, we evaluated the effect of the

reaction time on the response value. PEC response was determined after 30, 60 and 90 min of TP incubation as can be seen in Figure 3D. These results demonstrate that the longer the incubation time, the more sensitive to ALP is the system. We selected 60 min as the best reaction time in order to achieve an agreement between sensitivity and reduced analysis time.

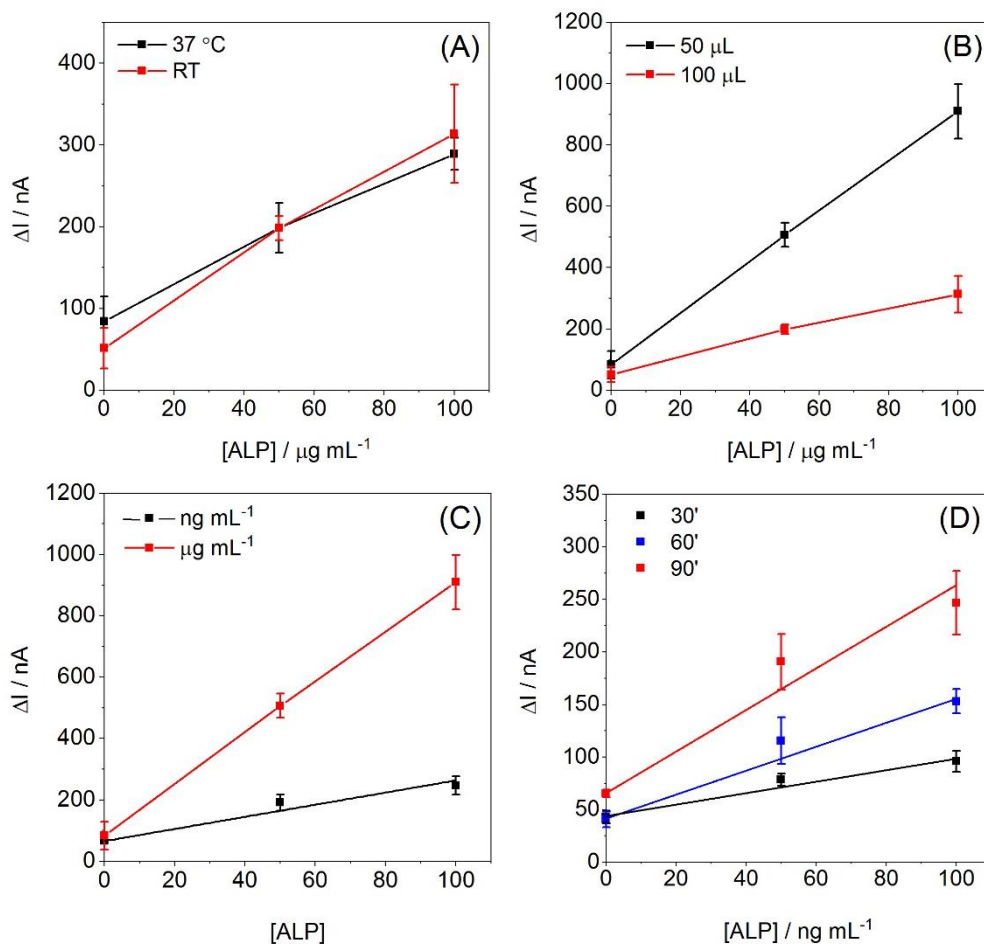


**Figure 3.** Calibration plots reflecting the photocurrent response of CdS QDs in the system containing TP (0.5 mM),  $Cd(NO_3)_2$  (2.5 mM), TG (20 mM) and variable ALP concentration at (A) different temperatures, (B) different final volumes, (C) variable ALP concentration at different range and (D) different TP incubation times.

Considering the above-mentioned experimental data, the following optimal parameters for the enzymatic generation of CdS were selected: room temperature, 50  $\mu L$  final volume and 60 min of TP reaction time.

### 3.2.2. Immunoassay

Sandwich immunoassays were performed following the protocol of the ELISA kit for detection of human serum albumin (HSA) at room temperature. In order to improve the immunoassay process we studied the effect of reducing the number of steps and the incubation time of the

assay. First, we evaluated the pre-incubation time of the antigen and the detection antibody prior to the interaction with the capture antibody immobilised on the aminated plate (Figure 4A). The detection antibody was mixed with the antigen and let react for a selected time. Next, the detection part of the ELISA protocol was followed which consisted in the determination of the biotinylated detection antibody using labelling with biotinylated HRP through streptavidin. The conversion of reduced form of TMB into oxidised blue form of TMB was followed by UV-vis spectroscopy. Various pre-incubation times were used with no significant differences with respect to the time recommended by the kit provider (2 h). Therefore, we established 5 min as the best pre-incubation time which showed similar results to the normal procedure of the kit but in 5 min instead of 2 h of step.

Then, the effect of the incubation time with the capture antibody on the performance of the assay was studied (Figure 4B). First, the enzyme ALP labelled with avidin was mixed with the biotinylated detection antibody to ensure the antibody modification. Afterwards, the antigen was added and let react for 5 minutes (step previously optimized). In order to detect the activity of ALP immobilised on the surface of the microplates, the fluorogenic substrate pNPP was employed. A decrease in the signal height was obtained when reducing the incubation time from 2 h (kit recommendation) to 5 min due to the rate of the biorecognition reaction. Despite the decrease in the signal, the slope didn't change dramatically which means that the system maintains the sensitivity even at incubation time of 5 min with the capture antibody. Thus, the incubation time of 30 min with the capture antibody was selected for the further development of the immunoassay in order to ensure a suitable sensitivity.

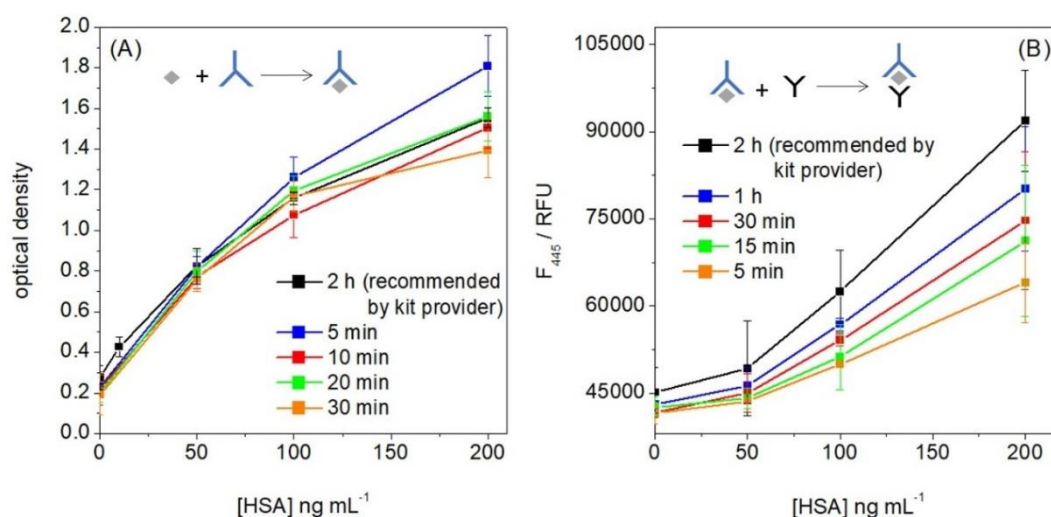


**Figure 4.** (A) Calibration plot from HSA ELISA assay at different pre-incubation times. (B) Calibration plot from HSA ELISA assay at different incubation times.

From the results of this section it can be concluded that the regular standard ELISA kit can be easily adapted to perform analysis at lower incubation times. The new protocol allows reducing volume and incubation time, two important features for designing a lab-on-a-chip, with the performance similar to that of the commercial kit.

### 3.2.3. Analytical performance

We evaluated the analytical performance of the system with the optimised parameters using standard polystyrene microplates. The capture antibody was immobilised on the surface of aminated polystyrene microplates, then, the analyte was added and detected with the biotinylated detection antibody labelled with avidin-ALP conjugate. The enzymatic reaction to form CdS QDs was carried out in a final volume was of 50  $\mu\text{L}$ , at room temperature and above-mentioned pre-incubation times of HSA with antibodies. PEC detection was conducted using a UV lamp emitting at 365 nm in presence of TG 20 mM using home-made SPCEs modified with osmium polymer.

The photocurrent response corresponding to varying HSA concentrations (from 0 to 200  $\text{ng mL}^{-1}$ ) is depicted in Figure 5A. The increase in the amount of HSA results in the growth of the detected photocurrent. Figure 5B shows the calibration plot corresponding to different HSA concentrations. The curve demonstrated a linear response up to 10  $\text{ng mL}^{-1}$ . The lowest amount of HSA that could be detected by this system was found to be 1.68  $\text{ng mL}^{-1}$  (S/N=3). This value is lower than that of the commercial kit (2  $\text{ng mL}^{-1}$ ) so it was confirmed that the photoelectrochemical process is suitable for the development of a photoelectrochemical immunosensor.

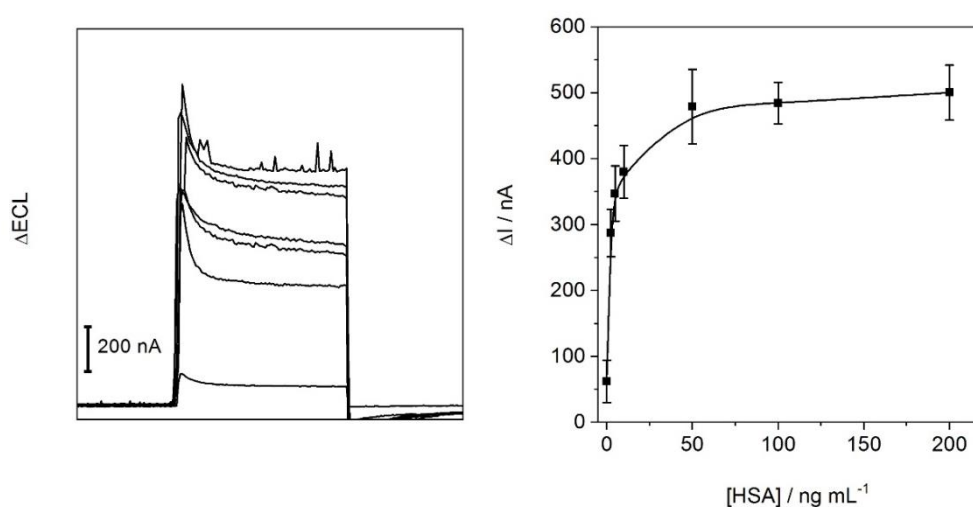


**Figure 5.** Photocurrent responses and calibration plot from the of CdS QDs in the system containing TP (0.5 mM),  $\text{Cd}(\text{NO}_3)_2$  (2.5 mM), TG (20 mM) and variable HSA concentration with PS film SPCE.

### 3.3. Chip design and fabrication

The design of the microfluidic device was done considering the steps of the assay and the selection of the different optimised parameters mentioned above. As shown before, the assay is divided into two processes: an ELISA immunoassay and the PEC detection. For this reason, the chip contains two chambers separated physically by a connector (Figure 6). The chamber for the ELISA immunoassay presents an elongated shape to ensure the maximum reactive surface available during the assay with a standard width for the connectors. This design is important when working with microfluidics because the increase in the surface area to volume ratio allows make material transport more efficient.<sup>32</sup>

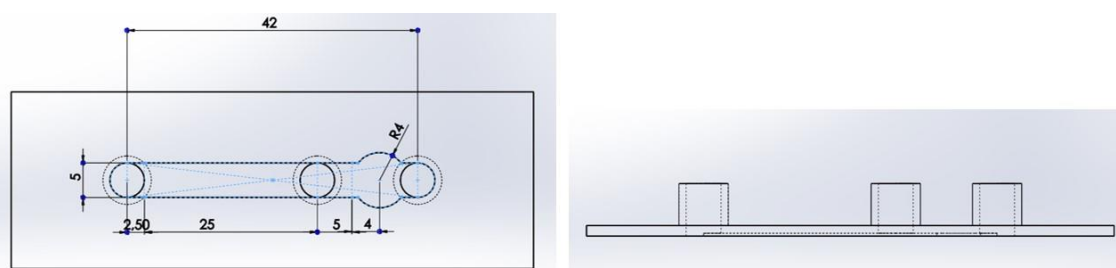


**Figure 6.** Top view of the design and dimensions of immunoassay (rectangle) and PEC (round) chambers. Lateral view of the inlets and outlets.

On the other hand, the chamber for PEC detection was round in order to cover the whole surface of the SPCE. In both cases the liquids are introduced and took out manually with a syringe and the final volume was selected as 50  $\mu\text{L}$  so the height and width of the channels were calculated to meet all the requirements. The final microfluidic design pattern was drawn using SolidWorks modelling software. The dimensions of the channel for the immunoassay were 5x0.4x25 mm for width, height, and length, respectively and the chamber for PEC detection has a diameter of 8 mm and 0.4 mm height. A volume of 100  $\mu\text{L}$  was selected for the reservoir which was also acting as the inlet. The microfluidic channel was fabricated by ChipShop in polystyrene.

The fabrication of the bottom part was carried out taking into consideration the design of the microfluidic channels. The electrodes were printed on aminated PS as substrate following the procedure described above. The SPCEs consisted of a round working carbon electrode with a diameter of 4 mm surrounded by a counter (carbon) and a reference (Ag/AgCl) electrodes. The width of the electrode presented is 8 mm (Figure 7).



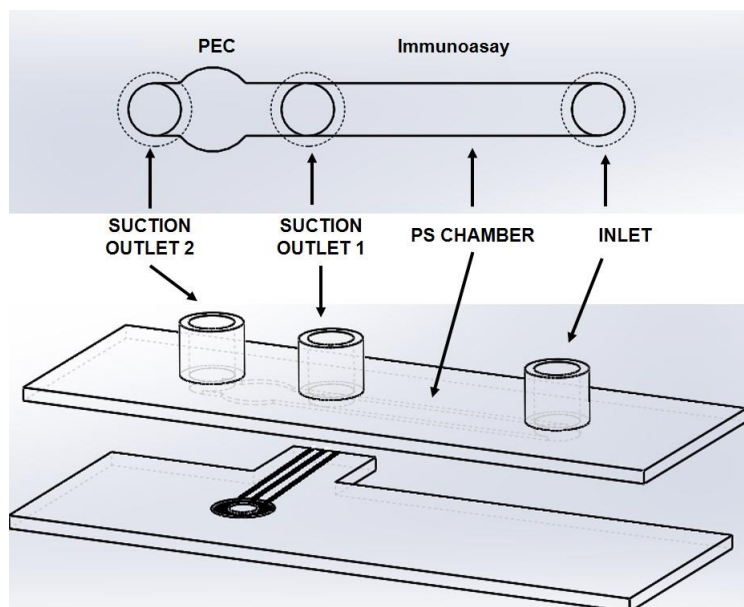


**Figure 7.** PS microfluidic layout consisting of a PS cover including the channel and the inlets/outlets and a bottom side made of aminated PS with the SPCE integrated.

A picture of the integrated device is shown in Figure 8. The sealing of the channels to the electrode was achieved with a suitable adhesive (KIWOPRINT® TC 2500). This is a high-quality pressure sensitive adhesive that is screen-printed on top of the polystyrene substrate allowing the sticking of both parts with high strength and stability.

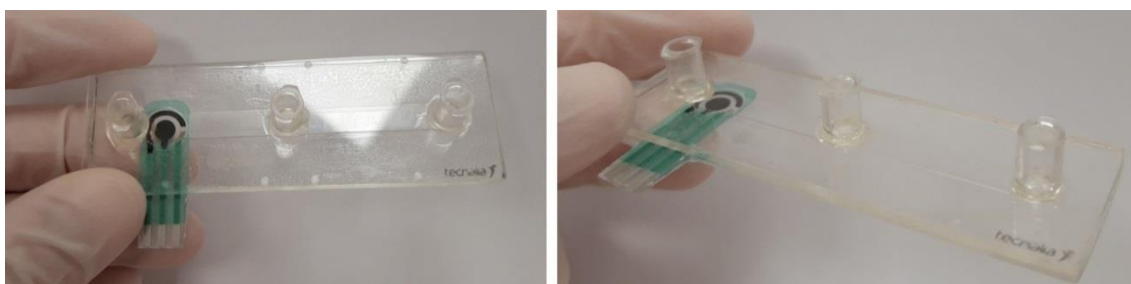


**Figure 8.** Assembled microfluidic device used as a biosensor module. The device consists of an aminated PS substrate sealed with the PS microchannels that provide a connection to the mac-world (1 inlet port and 2 outlet ports).

### 3.4. Analytical performance

The validation of the final prototype was assessed by measuring the photocurrent response to increasing concentrations of HSA. Regarding the chip design (Figure 7) the immunoassay is carried out in the aminated PS chamber, modified with antibodies, by injecting and removing the reagents through the inlet and outlet 1, respectively. During this process the outlet 2 is kept closed. Second, the enzymatic growth of CdS QDs is carried out in the PS chamber. Last, the outlet 1 is closed and outlet 2 is left free in order to take the CdS QDs from the PS chamber to the PEC chamber. The latter serves for PEC detection of enzymatically produced CdS QDs. The procedure is described in Figure 9.

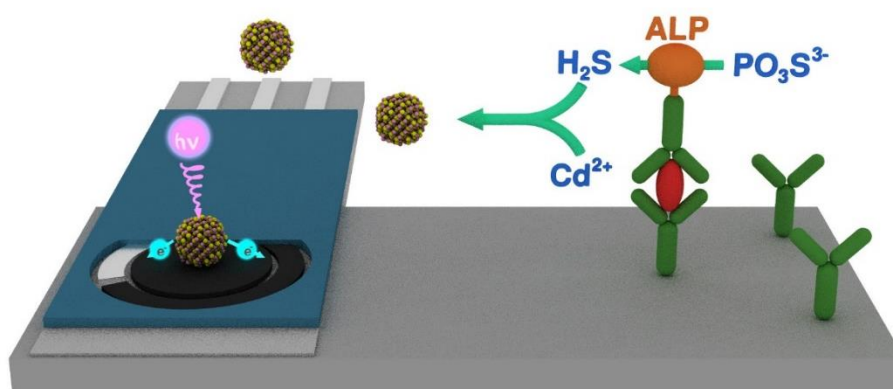


**Figure 9.** Operation for the photoelectrochemical immunoassay based on the microfluidic device.

Improved parameters from previous studies were used to perform this experiment: incubation at room temperature, 50  $\mu\text{L}$  of sample solution, antibody labelling with ALP, pre-incubation with antigen and reduced assay time. The new protocol can be described as follows. First, capture antibody was immobilized on aminated PS surface overnight at room temperature. After that, the surface was blocked with BSA 1% in PBS for 1 h. Subsequently, detection antibody was labelled with ALP during 1 h prior to the incubation with the antigen (5 min). Afterwards, the antibody-antigen complex was incubated in the channels with the capture antibody immobilized on the surface properly blocked to avoid non-specific interactions. Finally, the  $\text{S}^{2-}$  generated enzymatically by ALP from  $\text{Na}_3\text{O}_3\text{PS}$  interacted with  $\text{Cd}^{2+}$  to form CdS QDs. The photoelectrochemical signal was measured during irradiation the electrode with a UV LED of 365 nm in presence of TG 20 mM.

The calibration plot of the process is depicted in Figure 10. It can be seen that PEC signal increases gradually with HSA concentrations from 0 to 100  $\text{ng mL}^{-1}$  due to the increased enzymatic growth of CdS QDs in situ. The curve exhibited a linear response in the range studied with  $R^2$  of 0.996. Moreover, the detection limit was found to be of 1.97  $\text{ng mL}^{-1}$ , comparable to that of the optical commercial kit (2  $\text{ng mL}^{-1}$ ). The standard ELISA kit required around 6 h per measurement while our device required only 2.5 h per measurement. Thus, this prototype demonstrated its feasibility for the development of a lab-on-a-chip device based on photoelectrochemical detection system.

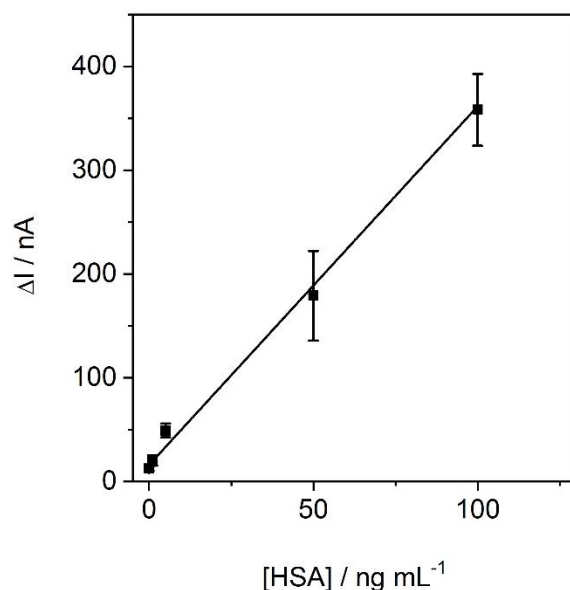


**Figure 10.** Photocurrent calibration plot from the of CdS QDs in the system containing TP (0.5 mM), Cd(NO<sub>3</sub>)<sub>2</sub> (2.5 mM), TG (20 mM) and variable HSA concentration with SPCE on PS 1.2 mm and new microfluidic system,  $\Delta I = 3.46 \cdot [HSA] + 15.93$ .

#### 4. Conclusion

In summary, we presented a new promising platform for photoelectrochemical immunosensor lab-on-a-chip (LOC). Polystyrene substrates were modified to improve the antibody orientation and the sandwich immunoassay was coupled to the enzymatic growth of CdS QDs in situ for the subsequent measurement of the PEC response using home-made screen-printed carbon electrodes. The method showed an enhanced performance due to the improvement of the immunoassay and the signal amplification achieved with the enzymatic reaction. The miniaturization of the device comprised the design, optimization, characterization and validation of the system with a model analyte. The resulting platform showed an improved detection time and detection limit in comparison with those of the commercial ELISA kit for Human Serum Albumin. The system developed in this study could be an attractive candidate for the use with a wide range of analytes due to the versatility of the enzymatic signal amplification process and the broad range of possible functional groups that can be introduced on PS substrates for the antibody immobilization. Moreover, the optimized protocol is fast, easy to use and convenient for point-of-care applications.

## References

- (1) Andreescu, S.; Sadik, O. A. Trends and Challenges in Biochemical Sensors for Clinical and Environmental Monitoring. *Pure Appl. Chem.* **2004**, *76* (4), 861–878.
- (2) Luka, G.; Ahmadi, A.; Najjaran, H.; Alocilja, E.; Derosa, M.; Wolthers, K.; Malki, A.; Aziz, H.; Althani, A.; Hoorfar, M. Microfluidics Integrated Biosensors: A Leading Technology towards Lab-on-A-Chip and Sensing Applications. *Sensors (Switzerland)* **2015**, *15* (12), 30011–30031.
- (3) Yamanaka, K.; Vestergaard, M. C.; Tamiya, E. Printable Electrochemical Biosensors: A Focus on Screen-Printed Electrodes and Their Application. *Sensors (Switzerland)* **2016**, *16* (10), 1–16.
- (4) 1993, 3, 85-92 Immunosenors Ppes and Apps.Pdf.
- (5) Lippa, P. B.; Sokoll, L. J.; Chan, D. W. Immunosenors - Principles and Applications to Clinical Chemistry. *Clin. Chim. Acta* **2001**, *314* (1–2), 1–26.
- (6) Felix, F. S.; Angnes, L. Electrochemical Immunosenors – A Powerful Tool for Analytical Applications. *Biosens. Bioelectron.* **2018**, *102* (November 2017), 470–478.
- (7) Bahadir, E. B.; Sezginürk, M. K. Applications of Commercial Biosensors in Clinical, Food, Environmental, and Biothreat/Biowarfare Analyses. *Anal. Biochem.* **2015**, *478*, 107–120.
- (8) Yang, C.; Huang, Y.; Hassler, B. L.; Worden, R. M.; Mason, A. J. Amperometric Electrochemical Microsystem for a Miniaturized Protein Biosensor Array. *IEEE Trans. Biomed. Circuits Syst.* **2009**, *3* (3), 160–168.
- (9) Devadoss, A.; Sudhagar, P.; Terashima, C.; Nakata, K.; Fujishima, A. Photoelectrochemical Biosensors: New Insights into Promising Photoelectrodes and Signal Amplification Strategies. *J. Photochem. Photobiol. C Photochem. Rev.* **2015**, *24*, 43–63.
- (10) Zhao, W. W.; Xu, J. J.; Chen, H. Y. Photoelectrochemical Bioanalysis: The State of the Art. *Chem. Soc. Rev.* **2015**, *44* (3), 729–741.
- (11) Zhao, W. W.; Ma, Z. Y.; Yu, P. P.; Dong, X. Y.; Xu, J. J.; Chen, H. Y. Highly Sensitive Photoelectrochemical Immunoassay with Enhanced Amplification Using Horseradish Peroxidase Induced Biocatalytic Precipitation on a CdS Quantum Dots Multilayer Electrode. *Anal. Chem.* **2012**, *84* (2), 917–923.
- (12) Zhao, W. W.; Han, Y. M.; Zhu, Y. C.; Zhang, N.; Xu, J. J.; Chen, H. Y. DNA Labeling Generates a Unique Amplification Probe for Sensitive Photoelectrochemical Immunoassay of HIV-1 P24 Antigen. *Anal. Chem.* **2015**, *87* (11), 5496–5499.
- (13) Zhang, X.; Liu, M.; Mao, Y.; Xu, Y.; Niu, S. Ultrasensitive Photoelectrochemical Immunoassay of Antibody against Tumor-Associated Carbohydrate Antigen Amplified by Functionalized Graphene Derivates and Enzymatic Biocatalytic Precipitation. *Biosens. Bioelectron.* **2014**, *59*, 21–27.
- (14) Zhao, W. W.; Dong, X. Y.; Wang, J.; Kong, F. Y.; Xu, J. J.; Chen, H. Y. Immunogold Labeling-Induced Synergy Effect for Amplified Photoelectrochemical Immunoassay of Prostate-Specific Antigen. *Chem. Commun.* **2012**, *48* (43), 5253–5255.
- (15) Sun, B.; Qiao, F.; Chen, L.; Zhao, Z.; Yin, H.; Ai, S. Effective Signal-on Photoelectrochemical Immunoassay of Subgroup J Avian Leukosis Virus Based on Bi2S3 Nanorods as Photosensitizer and in Situ Generated Ascorbic Acid for Electron Donating. *Biosens. Bioelectron.* **2014**, *54*, 237–243.
- (16) Malic, L.; Brassard, D.; Veres, T.; Tabrizian, M. Integration and Detection of Biochemical Assays in Digital Microfluidic LOC Devices. *Lab Chip* **2010**, *10* (4), 418–431.
- (17) Lee, C.-Y.; Chang, C.-L.; Wang, Y.-N.; Fu, L.-M. Microfluidic Mixing: A Review. *Int. J. Mol. Sci.* **2011**, *12* (5), 3263–3287.
- (18) Disch, A.; Mueller, C.; Reinecke, H. Low Cost Production of Disposable Microfluidics by Blister Packaging Technology. In *2007 29th Annual International Conference of the IEEE*

- Engineering in Medicine and Biology Society*; 2007; pp 6322–6325.
- (19) Dong, H.; Li, C.-M.; Zhang, Y.-F.; Cao, X.-D.; Gan, Y. Screen-Printed Microfluidic Device for Electrochemical Immunoassay. *Lab Chip* **2007**, *7* (12), 1752–1758.
  - (20) Godino, N.; Gorkin, R.; Bourke, K.; Ducr ee, J. Fabricating Electrodes for Amperometric Detection in Hybrid Paper/Polymer Lab-on-a-Chip Devices. *Lab Chip* **2012**, *12* (18), 3281–3284.
  - (21) Zang, D.; Ge, L.; Yan, M.; Song, X.; Yu, J. Electrochemical Immunoassay on a 3D Microfluidic Paper-Based Device. *Chem. Commun.* **2012**, *48* (39), 4683–4685.
  - (22) Katakis, I.; Ye, L.; Heller, A. Electrostatic Control of the Electron-Transfer Enabling Binding of Recombinant Glucose Oxidase and Redox Polyelectrolytes. *J. Am. Chem. Soc.* **1994**, *116* (8), 3617–3618.
  - (23) Barroso, J.; Saa, L.; Grinyte, R.; Pavlov, V. Photoelectrochemical Detection of Enzymatically Generated CdS Nanoparticles: Application to Development of Immunoassay. *Biosens. Bioelectron.* **2016**, *77*, 323–329.
  - (24) Del Prado, A.; Briz, N.; Navarro, R.; P erez, M.; Gallardo, A.; Reinecke, H. Transparent Polystyrene Substrates with Controllable Surface Chlorosulfonation: Stable, Versatile, and Water-Compatible Precursors for Functionalization. *Macromolecules* **2012**, *45* (6), 2648–2653.
  - (25) Del Prado, A.; Briz, N.; Navarro, R.; P erez, M.; Gallardo, A.; Reinecke, H. Chlorosulfonation of Polystyrene Substrates for Bioanalytical Assays: Distribution of Activated Groups at the Surface. *Analyst* **2012**, *137* (23), 5666–5671.
  - (26) Del Prado, A.; Briz, N.; Navarro, R.; P erez, M.; Gallardo, A.; Reinecke, H. Distribution of Chlorosulfonyl Groups in the Subsurface of Polystyrene Substrates. Analysis by Means of Vibrational Spectroscopy. *Vib. Spectrosc.* **2013**, *66*, 14–18.
  - (27) Barroso, J.; D iez-Buitrago, B.; Saa, L.; M oller, M.; Briz, N.; Pavlov, V. Specific Bioanalytical Optical and Photoelectrochemical Assays for Detection of Methanol in Alcoholic Beverages. *Biosens. Bioelectron.* **2018**, *101*, 116–122.
  - (28) Mistry, K. K.; Sagarika Deepthy, T.; Chaudhuri, C. R.; Saha, H. Electrochemical Characterization of Some Commercial Screen-Printed Electrodes in Different Redox Substrates. *Curr. Sci.* **2015**, *109* (8), 1427–1436.
  - (29) Yan, M.; Zang, D.; Ge, S.; Ge, L.; Yu, J. A Disposable Electrochemical Immunosensor Based on Carbon Screen-Printed Electrodes for the Detection of Prostate Specific Antigen. *Biosens. Bioelectron.* **2012**, *38* (1), 355–361.
  - (30) Iqbal, J. An Enzyme Immobilized Microassay in Capillary Electrophoresis for Characterization and Inhibition Studies of Alkaline Phosphatases. *Anal. Biochem.* **2011**, *414* (2), 226–231.
  - (31) Malashikhina, N.; Garai-Ibabe, G.; Pavlov, V. Unconventional Application of Conventional Enzymatic Substrate: First Fluorogenic Immunoassay Based on Enzymatic Formation of Quantum Dots. *Anal. Chem.* **2013**, *85* (14), 6866–6870.
  - (32) Bange, A.; Halsall, H. B.; Heineman, W. R. Microfluidic Immunosensor Systems. *Biosens. Bioelectron.* **2005**, *20* (12), 2488–2503.



## **CHAPTER 5: GENERAL CONCLUSIONS**

---





## General conclusions

This PhD thesis presents the advancements in bioanalysis based on the use of the enzymatic modulation of nanomaterials for analytical applications which can be employed for detection and signal amplification. The use of enzymes for nanoparticles and quantum dots growth in situ with applications in optical and electrochemical biosensors offers great advantages due to the wide range of possibilities in terms of substrates and analytes which potentially can be employed in bioanalytical analysis. Moreover, this approach has opened new strategies for signal amplification in electrochemical sensors and has proven its effectiveness in the performance of a photoelectrochemical immunosensor lab-on-a-chip platform.

The main conclusions of the work conducted during this PhD thesis are summarized below:

1. It was found that a wide range of enzymes and substrates can be employed the formation of several nanomaterials with varied characteristics such as Ag/Ag<sub>2</sub>S and CdS NPs and QDs with optical and electrochemical properties. This innovative strategy for the enzymatic growth and modification of metal containing nanoparticles and quantum dots was developed and applied to the detection of various analytes of interest.
2. The biocatalytic process involving alcohol oxidase, methanol and cysteine can inhibit the formation of semiconductor CdS QDs. This occurs because oxidation of methanol catalysed with alcohol oxidase results in the formation of H<sub>2</sub>O<sub>2</sub>. The latter is able to convert two molecules of cysteine into one molecule of cystine. This molecule is unable to stabilize the growth of CdS QDs in situ and thus, the concentration of CdS QDs decreases with increasing amounts of the analyte (methanol). This enzymatic process can be applied for the sensitive detection of methanol in real samples by fluorescence spectroscopy and photoelectrochemical methods. Both procedures exhibited higher sensitivities than previous bioassays and can be applied to the detection of methanol in vodka and cider. Moreover, **photoelectrochemical methodology** proved to be a convenient choice for the design of portable, miniaturized and disposable biosensors.
3. Enzymatic activity of glucose oxidase was employed to produce Ag/Ag<sub>2</sub>S NPs in the presence of citric acid as the capping agent. Glucose oxidase is able to catalyse formation of H<sub>2</sub>S resulting from the biocatalytic oxidation of 1-thio-D-glucose with oxygen. H<sub>2</sub>S interacts with silver ions almost instantly and, in presence of the capping agent citric acid, Ag/Ag<sub>2</sub>S NPs are formed. This **colorimetric method** can be used for

## General conclusions

the study of the competitive reaction between the 1-thio-D-glucose and the natural glucose, which doesn't produce H<sub>2</sub>S decreasing the amount of Ag/Ag<sub>2</sub>S NPs. Hence, the concentration of glucose can be determined in human serum with high precision and no pre-treatment of the sample.

4. The products of enzymatic reactions can block the surface of NPs modifying the **electrochemiluminescence** properties. CdS QDs were chemically synthesized for subsequent modification of carbon electrodes. Thiol-compounds such as thiocholine produced by acetylcholinesterase blocks CdS QDs immobilised on the electrode surface decreasing the ECL signal. On the other hand, some enzymes like glucose oxidase can release H<sub>2</sub>O<sub>2</sub> that act as the cofactor needed for the production of ECL signal. These strategies were applied to the detection of acetylcholinesterase in human serum and methanol in vodka with promising results.
5. The antibody immobilization strategy affects the specific antigen-binding event because the apparent affinity constant depends on the orientation of biomolecules on the surface of the solid support. Proper orientation of antibodies is preferable to increase the sensitivity of immunosensors. **Polystyrene modification** by a wet-chemical treatment with chlorosulfonic acid and posterior washing with sulfuric acid can provide reactive chlorosulfonyl groups on the surface. This procedure gives transparent polystyrene substrates stable at room temperature under normal atmosphere for at least one year. This modification can be used for posterior introduction of any functional group through the interaction between a primary aliphatic amine and the chlorosulfonyl groups (creating sulphonamide groups) in soft conditions (aqueous solutions, room temperature). An appropriate screening of those surfaces allows to find the chemical group on the surface that results in the better orientation of the antibody studied, improving the detection limit and being a critical knowledge to immobilize the antibody in a plastic cartridge for lab-on-a-chip manufacturing.
6. The **combination** of enzymatic signal amplification strategy and polystyrene modification for well-orientation of antibodies has proven to give promising results in the designing of a **photoelectrochemical immunosensor lab-on-a-chip**. The first prototype fabricated and developed in this PhD thesis showed good analytical performance and improvement of a commercial ELISA kit for a standard analyte. Although much remains unexplored, these results have opened new possibilities in the design of next generation of biosensors for point of care applications.





## **PUBLICATIONS**

---




- (1) **Díez-Buitrago, B.**; Fernández-SanArgimiro, F. J.; Lorenzo, L.; Bijelic, G.; Briz, N.; Pavlov, V. Design of a photoelectrochemical Lab-on-a-Chip immunosensor. *under edition*
- (2) **Díez-Buitrago, B.**; Saa, L.; Briz, N.; Pavlov, V. Development of portable CdS screen printed carbon electrode platform for electrochemiluminescence measurements and bioanalytical applications. *Submitted*
- (3) **Díez-Buitrago, B.**; Fernández-SanArgimiro; F.J., Lorenzo, J; Nerea Briz; Pavlov, V. Modification of chlorosulfonated polystyrene substrates for bioanalytical applications. *under review*
- (4) Saa, L.; **Díez-Buitrago, B.**; Briz, N.; Pavlov, V. CdS Quantum Dots Generated In-Situ for Fluorometric Determination of Thrombin Activity. *Microchim. Acta* **2019**, *186* (9), 657.
- (5) **Díez-Buitrago, B.**; Barroso, J.; Saa, L.; Briz, N.; Pavlov, V. Facile Synthesis and Characterization of Ag/Ag<sub>2</sub>S Nanoparticles Enzymatically Grown In Situ and Their Application to the Colorimetric Detection of Glucose Oxidase. *ChemistrySelect* **2019**, *4* (28), 8212.
- (6) Kumar, J.; López-Martínez, E.; Cortajarena, A. L.; Solís, D. M.; Taboada, J. M.; **Díez-Buitrago, B.**; Pavlov, V.; Liz-Marzán, L. M. Charge-Induced Shifts in Chiral Surface Plasmon Modes in Gold Nanorod Assemblies. *Part. Part. Syst. Charact.* **2019**, *36* (5).
- (7) **Díez-Buitrago, B.**; Briz, N.; Liz-Marzán, L. M.; Pavlov, V. Biosensing Strategies Based on Enzymatic Reactions and Nanoparticles. *Analyst* **2018**, *143* (8), 1727–1734.
- (8) Barroso, J.; **Díez-Buitrago, B.**; Saa, L.; Möller, M.; Briz, N.; Pavlov, V. Specific Bioanalytical Optical and Photoelectrochemical Assays for Detection of Methanol in Alcoholic Beverages. *Biosens. Bioelectron.* **2018**, *101* (October 2017), 116–122.
- (9) Grinyte, R.; Barroso, J.; **Díez-Buitrago, B.**; Saa, L.; Möller, M.; Pavlov, V. Photoelectrochemical Detection of Copper Ions by Modulating the Growth of CdS Quantum Dots. *Anal. Chim. Acta* **2017**, *986*, 42–47.





## BEATRIZ DÍEZ BUITRAGO

 +34 666150726

 beatrizdibu@hotmail.com

### ACADEMIC BACKGROUND

- 2013 Sept – 2014 Oct**      **Autonoma University of Madrid, Spain.**  
*M.S., Applied Chemistry*  
Thesis Development of electrochemiluminescent sensors based on ruthenium complexes. Study of the immobilization of reagents on screen-printed electrodes
- 2009 Sep – 2013 July**      **Complutense University of Madrid, Spain.**  
*B.S., Chemistry*  
Thesis Electrochemiluminescence applications in Analytical Chemistry: determination of pollutants in environmental samples.

### WORK EXPERIENCE

- 2019 Aug - present**      **Tecnalia**, Parque Científico y Tecnológico de Guipúzcoa (Spain)  
*Graduate researcher*
- 2016 Feb – 2019 Aug**      **CIC biomaGUNE - Tecnalia**, Parque Científico y Tecnológico de Guipúzcoa (Spain)  
*Graduate researcher*
- 2014 Oct – 2015 July**      **Polytechnic Institute of Bordeaux**, ENSCBP, Institut des Sciences Moléculaires, groupe Nanosystèmes Analytiques (France)  
*Undergraduate researcher*
- 2012 Aug – 2012 Oct**      **Central Laboratory of the Army**, Villaverde Alto (Spain)  
*Research assistant*

### LANGUAJE SKILLS

<b>Spanish</b>	Native
<b>English</b>	B2 (FCE 2008)
<b>French</b>	Basic

### FELLOWSHIPS AND GRANTS

- 2014 Oct – 2015 Jul**      **Erasmus+ practices**  
NanoSystèmes Analytiques (NSysA) group at the University of Bordeaux and is located at the Graduate School of Chemistry, Biology and Physics (ENSCBP).

## a. Refereed Full Papers

1. L. Saa, B. Díez-Buitrago, N. Briz, V. Pavlov, **"CdS Quantum Dots Generated In-Situ for Fluorometric Determination of Thrombin Activity"**, *Microchimica Acta* 2019, 186 (9), 657.
2. B. Díez-Buitrago, J. Barroso, L. Saa, N. Briz, V. Pavlov, **"Facile Synthesis and Characterization of Ag/Ag<sub>2</sub>S Nanoparticles Enzymatically Grown In Situ and their Application to the Colorimetric Detection of Glucose Oxidase"**, *Chemistryselect* 2019, 4 (28). 8212
3. J. Kumar, E. López-Martínez, A. L. Cortajarena, D. M. Solís, J. M. Taboada, B. Díez-Buitrago, V. Pavlov, L. M. Liz-Marzán, **"Charge-Induced Shifts in Chiral Surface Plasmon Modes in Gold Nanorod Assemblies"**, *Particle & Particle Systems Characterization* 2019, 36 (5).
4. B. Díez-Buitrago, N. Briz, L. M. Liz-Marzán, V. Pavlov, **"Biosensing strategies based on enzymatic reactions and nanoparticles"**, *Analyst* 2018,143, 1727-1734.
5. J. Barroso, B. Díez-Buitrago, L. Saa, M. Möller, N. Briz, V. Pavlov, **"Specific bioanalytical optical and photoelectrochemical assays for detection of methanol in alcoholic beverages"**, *Biosensors and Bioelectronics* 2018, 101, 116-122.
6. R. Grinyte, J. Barroso, B. Díez-Buitrago, L. Saa, M. Möller, V. Pavlov, **"Photoelectrochemical detection of copper ions by modulating the growth of CdS quantum dots"**, *Analytica Chimica Acta* 2017, 986, 42-47.
7. A. de Poulpiquet, B. Díez-Buitrago, M. Dumont Milutinovic, M. Sentic, S. Arbault, L. Bouffier, A. Kuhn, N. Sojic, **"Dual Enzymatic Detection by Bulk Electrogenerated Chemiluminescence"**, *Anal. Chem.* 2016, 88 (12).
8. A. De Poulpiquet, B. Díez-Buitrago, M. Milutinovic, B. Goudeau, L. Bouffier, S. Arbault, A. Kuhn, N. Sojic, **"Dual-colour electrogenerated chemiluminescence from dispersion of conductive micro-beads addressed by bipolar electrochemistry,"** *ChemElectroChem*, 2016, 3, 404.

## b. Refereed Conference Publications

1. B. Díez-Buitrago; F.J. Fernández-SanArgimiro; N. Briz, V. Pavlov, **"PHOTOELECTROCHEMICAL IMMUNOSENSOR BASED ON ENZYMATIC GROWTH OF QDS ON-SITE"**, *International Congress on Analytical Nanoscience and Nanotechnology*, July 2019, Zaragoza (Spain), poster 079.
2. B. Díez-Buitrago; N. Briz, V. Pavlov, **"PHOTOELECTROCHEMICAL IMMUNOSENSOR BASED ON ENZYMATIC GROWTH OF QDS"**, *XXXVII Bienal de la RSEQ 2019*, San Sebastián (Spain), May 2019, poster 75.
3. B. Díez-Buitrago; N. Briz, V. Pavlov, **"INNOVATIVE PHOTOELECTROCHEMICAL BIOSENSOR BASED ON QUANTUM DOTS"**, *NanoBiosensors*, September 2017, Dresden (Germany), oral presentation.
4. M. Luaces; B. Díez-Buitrago; C. Pérez-Conde; A. M. Gutiérrez; A. B. Descalzo; G. Orellana; M. C. Moreno-Bondi, **"Antibiotic sensing with electrochemiluminescent sensors,".XXIV National Meeting of Spectroscopy-VII Iberian Congress of Spectroscopy**, July 2014, La Rioja (Spain), poster 049.
5. L. Carranza; B. Díez-Buitrago; M. Luaces; C. Valdés; C. Pérez-Conde; A. M. Gutiérrez; M.C. Moreno-Bondi, **"Determination of enrofloxacin in natural water by EQL of ruthenium complexes"**, *XVIII Meeting of the Spanish Society of Analytical Chemistry*, June 2013, Jaén (Spain), Book of abstracts p. 251.





## Acknowledgements

First of all, I would like to express my gratitude to Dr. Nerea Briz and Dr. Valery Pavlov for giving me the opportunity to develop this PhD thesis under their supervision. Thank you for your help and motivation, for guiding me and showing me the way when I was lost, and especially, for your support and dedication of these four years. Despite the challenging of the project and the stones on the road, it is only thanks to you that I have been able to get where I am today.

I would also like to thank CIC biomaGUNE and TecNALIA for allowing me to conduct the experimental work of this thesis at their centres of international excellence including direction, administration, maintenance, technological platforms and cleaning staff.

I acknowledge the University of the Basque Country for providing the chance to perform the PhD and the financial support from the Spanish Ministry of Science, Innovation and Universities and the Basque Government.

I give special thanks to my colleagues from Biosensing Lab. To Dr. Javier Barroso for helping me when I started at CIC biomaGUNE, thank you for your advice and your day to day tricks. To Dr. Laura Saa and Dr. Ruta Grinyte for introducing me to the fascinating world of enzymes and nanomaterials, thank you for giving me a hand with the “bio” part. To Verónica, for the good moments, your comprehension, your support, your olivas negras, but most of all, for your friendship.

Big thanks to the people of Biomaterials groups, you have always made me feel at home. To Carol, Iratxe, Leire, Ainhoa, María, Anetxu, Garbi and Noelia. To Goran, for sharing with me your immense knowledge and for your guide in the scientific field. To Nerea García for your palmeritas de chocolate, lenguas de gato and all kinds of sweets to cheer me up. To Xabi, for your unlimited conversation inside and outside the lab. To my namesake Bea, for helping me with the technical part and showing me how cool the mirrors are. Thanks a lot to Jaione, you have been my great support here, thank you for being there when I needed a reactive, a pattern for a skirt or a cake recipe. Once again, to my mentor Nerea Briz, thank you for believing in me and supporting me in every decision.

To all my friends in Donosti. Thank you Elena, Dani and Idoia for the moments in the cafeteria, the dinners and all the experiences together. To the paddle people for that great moments of stress relief. To Susu, my beloved Mexican friend, thank you for your unconditional support no matter what. To my dearest half, Anabel. From the beginning of this adventure you have been

there giving me your help and love, and I hope it will never change. To Alex, David and Remei, for taking part of this amazing experience. To former people from CIC biomaGUNE, Ane, Silvia, Manu, María and the rest from the student's (Marta, Edu, Lucia, Antonio...).

A mi familia, para los que las palabras se quedan cortas. Gracias mamá y papá por darme todo en esta vida, por vuestro amor y confianza, por ser mi ejemplo a seguir y, en definitiva, por todo lo que soy. A mis hermanos, sin los que no sabría con quién guerrear y los que hacen de cada instante un momento único. A mis abuelas, prim@s y ti@s por su cariño y apoyo. A Maribe, por su amor infinito. A Sandra y Patri, mis mosqueteras, y a Chus, mi hermana adoptiva, gracias por aguantarme todos estos años.

Por último, a ti, Juan, o al destino que te puso en mi camino, o a tu empeño por no querer irte. Gracias por estar a mi lado, por quererme, apoyarme, cuidarme y hacer que me levante cada día con una sonrisa en la cara. Gracias también por ser mi ancla, mi red y mis alas, por llenar mi vida de locura y amor. Gracias por elegirme para pasar junto a ti el resto de tu vida.

*Vive,  
y que te quiten lo bailao*

